NAL TR-1191T

ISSN 0389-4010
UDC 533. 6. 07

TECHNICAL REPORT OF NATIONAL AEROSPACE LABORATORY

TR-1191T

A Comparative Study of BGK No.1 Airfoil Data in High Reynolds Number Transonic Wind Tunnels

Norikazu SUDANI, Kenichi MATSUNO,
Hiroshi KANDA, Mamoru SATO,
Hitoshi MIWA, Iwao KAWAMOTO

January 1993

NATIONAL AEROSPACE LABORATORY

CHŌFU, TOKYO, JAPAN

A Comparative Study of BGK No. 1 Airfoil Data in High Reynolds Number Transonic Wind Tunnels*

Norikazu SUDANI*1, Kenichi MATSUNO*1, Hiroshi KANDA*1,
Mamoru SATO*1 Hitoshi MIWA*1 and Iwao KAWAMOTO*1

ABSTRACT

A comparative study of BGK No. 1 airfoil data in the NAL (Japan) and IAR (Canada) high Reynolds number transonic wind tunnels was performed to evaluate the techniques and the accuracy of airfoil testing. Tests were conducted from a low subsonic speed over the design speed of the airfoil mainly at a Reynolds number of 21 million based on airfoil chord at both facilities. Pressure distributions and aerodynamic characteristics measured in both wind tunnels are compared and discussed. The results of the comparisons reveal slight differences in shock position and suction peak level ahead of the shock, suggesting the necessity of a correction for sidewall boundary-layer effects. Application of sidewall interference correction to both sets of wind tunnel data improves agreement between the two sets of data. The results also raise new issues on drag measurement and flow two-dimensionality at a high angle of attack and/or a high Mach number. The results of this study will lead to improvements in the accuracy of airfoil testing.

Key Words: Airfoil Data, Transonic Flow, BGK No. 1, High Reynolds Number Testing, Wall Interference Correction

概　　要

BGK No.1翼型に関する対応風洞試験が航空宇宙技術研究所とカナダ国立航空研究所（IAR，旧NAE）の高レイノルズ数遷音速翼型試験設備において実施された。試験はレイノルズ数（翼弦長基準）21×10^6を中心として低亜音速域から設計点を越える速度域まで実施され，圧力分布や空力係数の比較検討を行った。その結果，衝撃波の位置や衝撃波上流での圧力係数値に微妙な相違が認められ，側壁干渉効果補正の必要性が示唆された。そこで，ある側壁干渉補正法を適用したところ両者の測定結果は良好な一致を示すことが確認された。また，この試験により大仰角あるいは高マッハ数での抵抗測定の精度向上や流れの二次元性の確保等の新たな問題点が浮き彫りにされ，高精度の翼型試験の実現のための有益な資料を得ることができた。

Nomenclature

b	airfoil span
C, c	airfoil chord
C_D, C_d, $C_{d\ wake}$	section drag coefficient from wake measurement
C_{Dp}	section pressure drag coefficient
C_L, C_l	section lift coefficient
C_p	pressure coefficient
$C_{p,c}$	corrected pressure coefficient
C_p^*	critical pressure coefficient
M	Mach number

* received 6 November 1992

*1 Aircraft Aerodynamics Division

ΔM deviation between the corrected and setting Mach number ($=M_c-M_s$)
Re Reynolds number based on the airfoil chord
X, x streamwise coordinate
y spanwise coordinate
α angle of attack
subscripts:
c corrected value
g geometric value
s setting value
u uncorrected value

1. Introduction

Today extremely high accurate wind tunnel measurement is strongly required, and its demand at the high Reynolds number regime has become an inevitable item in order to develop a high performance commercial airplane at a transonic speed.

Various types of effort have been done in order to get the high order accurate data. One of the most efficient and reliable methods to accomplish this higher accuracy of the measurement is to compare measured data with those of other wind tunnels, analyze the difference, estimate the characteristics of the wind tunnel itself, and obtain the cause of the uncertainty of the measurement. Many comparative studies have been conducted in the world.

The two-dimensional transonic wind tunnel of the National Aerospace Laboratory (abbrev. NAL), Japan, can operate at the Reynolds number range from 5.5 million to 40 million and the Mach number range from 0.2 to 1.15. This wind tunnel is specially designed for the airfoil analysis[1]. While, the two-dimensional test facility of the Institute for Aerospace Research (abbrev. IAR, formerly the National Aeronautical Establishment; abbrev. NAE), National Research Council, Canada, is the wind tunnel that is designed to test an airfoil at transonic speeds under the high Reynolds number condition[2]. These two two-dimensional wind tunnels have the close wind tunnel characteristics.

A comparative study has been performed on the high-Reynolds-number two-dimensional wind tunnel testing between the National Aerospace Laboratory and the Institute for Aerospace Research. The purpose of the present project is to develop the wind tunnel testing method and accomplish the measurement as accurate as possible by means of the comparative study on the wind tunnel tests of a two-dimensional transonic airfoil. The typical transonic airfoil, BGK No.1 airfoil, is chosen as the testing airfoil.

The comparison was done mainly on pressure distribution and aerodynamic parameters such as lift coefficients and drag coefficients. The flow visualization was also conducted in order to investigate the flow physics. More than couples of hunderd runs were conducted. A half of those were pressure measurements, and the other half were flow visualization mainly by the oilflow method.

This paper presents the results of the comparative studies mainly on pressure distributions on the airfoil surface and aerodynamic parameters C_l and C_d. Results of flow visualization studies are to be presented separately.

2. Apparatus

2.1 Wind Tunnel

Tests of the BGK No.1 airfoil were conducted in the NAL Two-Dimensional Transonic Wind Tunnel[1]. The wind tunnel is of the blowdown type. The tunnel is capable of operating at stagnation pressures ranging from 196kPa up to 1176kPa at an atmospheric temperature. Reynolds number based on the airfoil chord length (250mm) can be varied from 5.5 million to 40 million according to the variation of the stagnation pressure. Mach number can be varied from about 0.2 to 1.15.

The test section of the wind tunnel is 1m

in height and 0.3m in width. The facility is equipped with a pressure scanning system, a wake traverse system, a schlieren photograph system, and a surface flow visualization system for application of the oilflow method or the liquid crystal method. The top and bottom walls each have four full slots and two half-slots at the sides. Width of the slots can be varied to obtain an open area ratio (OAR) from 0% to a maximum of 10%. The ratio is normally fixed at 3% on the basis of the results of initial calibration tests. Pressure rails are installed on the top and bottom walls for a wall interference correction.

The tunnel is equipped with a sidewall boundary-layer removal system to minimize the sidewall effects. Recent calibration tests showed, however, that the sidewall boundary-layer suction in the vicinity of the model caused Mach number nonuniformity in the flow direction[3]. As part of this study, the sidewall boundary-layer suction only behind of the 75% chord location of the model was tried in order to remove the corner separation region near the sidewall. The suction, however, cannot affect the pressure distribution at the mid-span and improvement of the flow two-dimensionality cannot be recognized (see Figure 10). The removal system is therefore not activated in the present tests.

2.2 Model

A BGK No.1 airfoil was selected in this study. This airfoil is of the supercritical type and designed for shockless flow at a Mach number of 0.75 and a lift coefficient of 0.63[4]. On the design condition the supersonic region extends over about 60% of the upper surface. It has a maximum thickness-to-chord ratio of 0.118 with a blunt trailing edge of 0.1% chord thickness.

The model had a chord of 250mm and a span of 300mm (the width of the tunnel), and was constructed of stainless steel. The airfoil shape and pressure orifice layout are illustrated in Figure 1. The model is designed to have 61 orifices on the upper surface and 20 orifices on the lower surface. These orifices are located along the mid-span except around the leading edge and the trailing edge for manufactural reasons. In addition, there are 11 spanwise orifices on the upper surface in order to check the two-dimensionality of the flow over the model. All the orifices are 0.5mm in inside diameter.

3. Test Program

The comparative study contains three phases of pressure measurements. In the first phase, comparisons of pressure distributions at the same geometric (uncorrected) angles of attack as those of the IAR tests[5] were performed in order to obtain basic information for the purpose of detecting differences in data between the NAL and the IAR wind tunnels. In the second phase, pressure distributions were measured at the same lift coefficients as those of the IAR tests, and both sets of data were compared. Moreover, in the third phase, supplementary pressure measurements were conducted in order to investigate the applicability of a sidewall interference correction to both sets of data.

As shown in Table 1, the tests were made at Mach numbers from about 0.5 to 0.8 and at lift coefficients from about -0.25 to 1.2, and mainly at a Reynolds number (based on the airfoil chord) of 21×10^6. No attempt was made to fix the transition on the model in any of the cases.

4. Comparison of Data

As previously mentioned, these tests were carried out in three phases. In this report, results from the second and the third phases are discussed. An outline of the pressure measurements in the second phase is shown in Table 2. The tests in the NAL wind tunnel were conducted at the same Mach numbers as those of the IAR data corrected

for the top and bottom wall effects only.

Drag coefficients are measured with a wake rake in both wind tunnels. In the NAL tunnel, the rake is positioned at $y/(b/2) = 0.2$. In the IAR tunnel, the drag measurements are usually performed using the rake with four pitot probes, which are positioned at $y/(b/2) = 0.0$, 0.233, 0.467, and 0.700[2]. In this study, data of the probe at $y/(b/2) = 0.233$ are only selected and compared with the NAL data because the probe is located at the closest spanwise position to that of the rake in the NAL tunnel.

On these conditions, pressure distributions and aerodynamic characteristics measured in each wind tunnel are compared.

5. Wall Interference Corrections

Wall interference corrections were applied to the sets of the NAL data. With respect to the correction for the top and bottom wall effects, the Sawada method[6] was used. Although the method corrects a free-stream Mach number and an angle of attack, the Mach number correction is only discussed in this study because it is difficult to evaluate the validity of the corrected angle of attack accurately. With respect to the correction for the sidewall effects, the Murthy method[7, 8] was used. The method is based on the transonic similarity rule and corrects a free-stream Mach number and a pressure coefficient. Combination of the top and bottom wall correction and the sidewall correction for a free-stream Mach number is therefore necessary. The detailed procedure of the Mach number correction is mentioned in Appendix C.

6. Results and Discussion

6.1 Comparison of Pressure Distributions

Typical pressure distributions in subcritical flow are shown in Figure 2. The upper figure shows chordwise distributions at the mid-span and the lower figure shows a spanwise distribution at the location of 90% airfoil chord. Open circles represent the NAL data and solid triangles denote the IAR (NAE) data. Both the NAL and the IAR data are in good agreement on pressure distribution and drag coefficient. In the subcritical flow, both data are in good agreement over a wide range of lift coefficients. Furthermore, satisfactory results are obtained with respect to the spanwise pressure distribution. It is noted that the flow over the airfoil maintains good two-dimensionality, judging from the fact that the spanwise pressure is almost constant.

Figure 3 shows pressure distributions nearly at the design Mach number. In this case, there exsists a relatively weak shock wave on the upper surface. Slight differences in shock position and suction peak level ahead of the shock are recognized. This result suggests that there exists a discrepancy in effective Mach number due to the sidewall boundary-layer displacement effect in each wind tunnel test. Both drag coefficients are in good agreement in spite of the difference in shock position because the component of the pressure drag due to the shock wave in the drag coefficient is still small. The spanwise pressure distribution reveals that the flow over the airfoil accelerates near the sidewalls. This is attributed to the displacement effect of the sidewall boundary layers. In the central region, on the other hand, the pressure distribution is nearly two-dimensional unless the flow separates near the trailing edge. It is shown that at a relatively low angle of attack the flow acceleration near the sidewalls cannot affect the chordwise pressure measurements in the central region. Another comparison of pressure distributions is shown in Figure 4. In this case, disagreement in pressure distribution behind the shock becomes noticeable in addition to the differences in shock position and pressure level ahead of the shock. This is believed to be due to the formation of a separation bubble behind the shock, but no conclu-

sive evidence has been obtained.

Figure 5 shows a comparison of pressure distributions nearly at the design Mach number when a strong shock wave impinges on the upper surface. Both the NAL and the IAR data are in good agreement on shock position. The agreement is accounted for by the fact that the position of the strong shock impinging on this airfoil upper surface tends to be insensitive to Mach number and fix nearly at the 50% chord location. The same differences, however, in suction peak level ahead of the shock and pressure distribution behind it as those indicated in Figures 3 and 4 are recognized. There remains therefore room for doubt about the free-stream Mach number. The chordwise and spanwise pressure distributions near the trailing edge reveal that trailing edge separation does not occur and the flow behind the shock can maintain good two-dimensionality except the slight acceleration near the sidewalls. Disagreement between both drag coefficients, however, becomes remarkable. It is unclear whether this is due to the discrepancy in free-stream Mach number caused by the sidewall boudary-layer effects, or not.

Figure 6 shows a comparison of pressure distributions over the design Mach number. In this case, there rise some problems. One of the problems is that there exists slight pressure rise near the mid-chord. The pressure rise can be observed also in some pressure distributions on another airfoil measured in the NAL wind tunnel, and leads to disagreement on shock position, moreover drag coefficient. This is believed to be due to a very weak compression wave emanating from the leading edge near the sidewall. Flow visualization data with the oilflow or liquid crystal method, which indicate the existence of the wave, have been obtained[9]. This result shows that the sidewall effects extend to the central region, and suggests the necessity of a high aspect ratio model for airfoil testing. Another problem is that the spanwise pressure distribution becomes three-dimensional when the flow separates near the trailing edge. Pressure distributions and drag coefficients measured at high Mach numbers and/or angles of attack must be dealt with in consideration of the flow three-dimensionality.

6.2 Comparison of Aerodynamic Characteristics

Comparison of the aerodynamic characteristics of the BGK No.1 airfoil has been made. Figure 7 shows a lift curve and a drag polar curve nearly at the design Mach number. The NAL data were measured at an uncorrected Mach number of 0.745, while the IAR data were at the corrected (for the top and bottom wall effects only) Mach number of 0.745. Both lift curve slopes to geometric (uncorrected) angle of attack are in good agreement. The NAL lift curve slope to corrected angle of attack is, however, slightly larger than that of IAR. Since application of both the NAL and IAR corrections to the same data leads to no difference in correction value, an account for the slight discrepancy in curve slope has been unclear. With respect to the drag polar curve, both data are in good agreement over a wide range of angles of attack. In another case, however, the result that both drag coefficients disagree at a high angle of attack has been obtained. The disagreement is deeply connected with the three-dimensionality of the wake caused by the sidewall effects. Improvement of drag measurement at a high angle of attack is one of the most important tasks in the NAL wind tunnel in order to conduct more accurate and reliable tests.

Figure 8 shows the effect of Mach number on lift coefficient at constant angles of attack. The IAR data are taken from the primary test results in Reference 4. The comparison of both data for the same lift coefficient at the design Mach number shows that the NAL data at an angle of attack of 1.7° correspond to the IAR data at an angle of attack of 1.0° Nearly shockless flow could be observed at an uncorrected Mach number

of 0.765 in the IAR wind tunnel as shown in Reference 4, while at an uncorrected Mach number of 0.772 in the NAL wind tunnel. The lift coefficient increases gradually up to the design Mach number (the nearly shockless condition), and falls sharply over this Mach number. Although the lift divergence Mach numbers and lift coefficients around the design Mach number measured in both tunnels are in good agreement, below the design Mach number the NAL data tend to be higher than the IAR data.

Figure 9 shows the effect of Mach number on drag coefficient at constant angles of attack. Also in this figure, the NAL data at $\alpha = 1.7^\circ$ are compared with the IAR data at $\alpha = 1.0^\circ$. Although both drag divergence Mach numbers are in good agreement, there is a slight difference in drag value below this Mach number. The drag coefficient of NAL is almost constant up to the design Mach number, while that of IAR increases gradually. This discrepancy may be explained by the fact that both data are uncorrected for wall interference because of some uncertainties.

6.3 Investigation on Sidewall Boundary-Layer Effects

The comparisons of pressure distribution data between NAL and IAR suggest that there exist sidewall boundary-layer effects on pressure measurements in the form of the variation in effective Mach number. As one of the reform measures, using a sidewall boundary-layer removal system is considered, and this system has been employed in most wind tunnels for airfoil testing[2, 10]. The NAL wind tunnel is also equipped with the removal system. When the system is activated, the sidewall boundary-layer suction is made through the Rigimesh only in the vicinity of a model using the pressure difference between the static pressure on the test section sidewall and atmospheric pressure. Recent calibration tests showed, however, that the suction induced axial Mach number nonuniformity with a maximum deviation of 0.015[3]. The effects of the local suction just at the region where there exist strong viscous effects of the sidewall boundary layer threrfore have been examined.

A comparison of pressure distributions, with and without the suction, is shown in Figure 10. The suction is made at the region behind the location of 75% airfoil chord. No noticeable change in pressure distribution with the suction, however, can be recognized. Furthermore, the spanwise pressure distribution does not change significantly. If the sidewall boudary-layer removal system is applied to airfoil testing, detailed examination on suction region, quantity of suction flow, and quality of the free stream are required.

As another reform measure, the Murthy method is applied to both the NAL and IAR data in order to assess the applicability of sidewall inteference correction. The application of the method to NACA0012 airfoil data has already led to significant results in the NAL wind tunnel[8]. Figure 11 shows a comparison of pressure distributions corrected for the four wall effects. Both data are corrected for the top and bottom wall effects and furthermore for the sidewall effects by the Murthy method. To apply the Murthy method, values of displacement thickness and shape factor of the sidewall boundary layer are necessary. The values measured in the empty tunnel calibration tests are used for correction of the NAL data. With respect to the IAR data the maximum value taken from Reference 11 for the sidewall boundary-layer displacement thickness and the typical value of 1.5 for the shape factor in transonic turbulent boundary layer are used. Although the IAR data contain the sidewall boundary-layer suction, its effects are ignored in this investigation. Figure 11 reveals that applying the correction eliminates the slight difference in shock position and suction peak level ahead of the shock, and that it improves agreement drastically in comparison with

Figure 3. Another comparison is shown Figure 12. Although the difference in pressure distribution behind the shock still exists, the other disagreement is removed by applying the method as compared with Figure 4. The comparisons suggest that it is very promising to apply the Murthy correction to both sets of tunnel data. There still remains, however, some difficult problems, such as the validity of the corrected Mach number. Furthermore, how the effect of the suction should be dealt with in the procedure of the correction is one of the most important problems. In order to conduct reliable two-dimensional tests, comprehensive research on the combination of the best experimental technique and the most suitable wall correction will be required.

7. Conclusions

A comparative study of the BGK No.1 airfoil data between NAL and IAR were carried out. The results can be summarized as follows:

1) The NAL uncorrected data on the pressure distributions and drag coefficients were in agreement with the IAR data corrected for the top and bottom wall interference, especially at low subsonic speeds.

2) There were slight differences in shock wave position and suction peak level ahead of the shock when a weak shock impinges on the upper surface. This result showed that there existed a discrepancy in effective Mach number due to sidewall boundary-layer displacement effect in each wind tunnel test.

3) Over the design Mach number, both data were in disagreement in shock position, pressure distribution ahead of and/or behind the shock, and drag coefficient. Furthermore, the spanwise pressure distribution indicated the three-dimensionality of the separated flow behind the shock.

4) The lift curves and drag polar curves nearly at the design Mach number, which were obtained in both tunnels, were in good agreement except at high angles of attack.

5) Applying a sidewall correction removed discrepancies between data of the two wind tunnels in shock position and suction peak level ahead of the shock and led to satisfactory agreement between the two sets of data.

One of the most important tasks in future development of aircraft is to conduct more reliable two-dimensional airfoil tests with higher accuracy, clarifying uncertainties which still remain in wind tunnel testing. For this objective, comprehensive research including investigations on model aspect ratio, sidewall boundary-layer suction technique, and wall interference correction will be required. This comparative study is expected to be benefit of both wind tunnels because it raised new tasks for improvement of measurement accuracy in transonic airfoil testing.

Appendix A
Comparison of Pressure Distributions at the Same Lift Coefficient

A set of pressure distribution data on the BGK No.1 airfoil in the NAL and the IAR wind tunnel are shown in Figures A-1 to A-38. The Mach numbers of the NAL data are not corrected, while those of the IAR data are corrected for the top and bottom wall effects only. Both data were measured at the same lift coefficient and Reynolds number based on airfoil chord. No attempt was made to fix the trasition on both models. The IAR data were measured with sidewall boundary-layer suction, while the NAL data were without the suction.

Appendix B
Data Corrected for the Top and Bottom Wall Effects

A set of the NAL data corrected for the top and bottom wall effects by the Sawada method is shown in Figures B-1 to B-38. These figures contain wall pressure data measured with pressure rails installed on the top and

bottom walls, free-stream axial velocity distributions in the vicinity of the model, and aerodynamic characteristics corrected by the method.

Appendix C
Data Corrected for the Four Wall Effects

A set of the NAL data corrected for the four wall effects is shown in Figures C-1 to C-38. In these figures, pressure coefficients and lift coefficients are corrected because the Murthy method is based on the transonic similarity rule. With respect to the angle of attack and drag coefficient, uncorrected values are shown because it is very difficult to evaluate the validity of the corrected values accurately.

The corrected values of the free-stream Mach numbers are determined according to the following procedure. The first stage of the correction is the calculation of the deviation between the free-steam Mach number and the corrected Mach number for sidewall effects by the Murthy method (ΔM_1). In the same way, the second stage is the calculation of the Mach number deviation corrected for top and bottom wall effects from the free-stream Mach number (ΔM_2). Finally, the corrected Mach number for four wall effects is derived from these deviations according to the following equation:

$$M_c = M_u + \Delta M_1 + \Delta M_2 \qquad \text{(C1)}$$

In the strict sense, the procedure includes slight errors in simple summation, but they can be negligible. The reasons for it are that the deviation by the Murthy correction is almost constant at transonic speeds, and that the deviation by the Sawade method is insensitive to the slight variation in the uncorrected free-stream Mach number.

Acknowledgments

The authors express their sincere thanks to Dr. Y.Y. Chan and his staff of IAR High Speed Aerodynamics Laboratory, Canada, for helpful discussions, especially to Dr. M. Mokry for technical advice in conducting this work, and to the staff of NAL Aircraft Aerodynamic Division for support in conducting these wind tunnel tests.

References

1) The Staff of the Second Aerodynamics Division. "Construction and Performance of NAL Two-Dimensional Transonic Wind Tunnel", NAL TR-647T, Tokyo, Japan, Feb. 1982.
2) Galway, R.D., "The IAR High Reynolds Number Two-Dimensional Test Facility —A Description of Equipment and Procedures Common to Most 2-D Airfoil Tests," NRC, IAR-AN-66, Ottawa, Canada, Jun. 1990.
3) Kawamoto, I., Miwa, H., Baba, S., Sato, M., Kanda, H., and Sudani, N., "Recent Airfoil Tests in NAL 2D High Reynolds Number Wind Tunnel," *Proceedings of the 28th Aircraft Symposium*, Tokyo, Japan, 1990.
4) Kacprzynski, J.J., Ohman, L.H., Garabedian, P.R., and Korn, D.G., "Analysis of the Flow past a Shockless Lifting Airfoil in Design and Off-Design Conditions", NRC, LR-554, Ottawa, Canada, Nov. 1971.
5) Plosenski, M.J., Jones, D.J., Mokry, M., and Ohman, L.H., "Supplementary Investigation of the BGK No.1 Airfoil; Wall Interference Study, ADDENDUM; Tabulated Data Corrected for Wall Interference," NRC, LTR-HA-5×5/0127, Ottawa, Canada, Aug. 1981.
6) Sawada, H., Sakakibara, S., Sato, M., and Kanda, H., "Wall Interference Estimation of the NAL's Two-Dimensional Wind Tunnel," NAL TR-829, Tokyo, Japan, Aug. 1984 (in Japanese).
7) Murthy, A.V., "Effects of Aspect Ratio and Sidewall Boundary-Layer in Airfoil Testing", *Journal of Aircraft*, Vol.25, No.3, 1988, pp.244–249.

8) Sudani, N., Kanda, H., Sato, M., Miwa, H., Matsuno, K., and Takanashi, S., "Evaluation of NACA0012 Airfoil Test Results in the NAL Two-Dimensional Transonic Wind Tunnel," NAL TR-1109T, Tokyo, Japan, May 1991.

9) Sudani, N., Sato, M., Kanda, H., and Matsuno, K., " Flow Visualization Studies on Sidewall Effects in Two-Dimensional Transonic Airfoil Testing," AIAA Paper 93-0090, 1993.

10) Murthy, A.V., Johnson, C.B., Ray, E.J., and Stanewsky, E., "Investigation of Sidewall Boundary Layer Removal Effects on Two Different Chord Airfoil Models in the Langley 0.3-Meter Trasonic Cryogenic Tunnel", AIAA Paper 84-0598, 1984.

11) Ohman, L.H. and Brown, D. "The NAE High Reynolds Number 15in. × 60in. Two-Dimensional Test Facility, Part II. Results of Initial Calibration," NRC, LTR-HA-4, Ottawa, Canada, Sept. 1970.

Table 1 Test conditions of the comparative study between NAL and IAR.

			NAL		NAE		NAL_u &	NAL corrected data	
Mach	Re	C_l	Run	Scan	Run	Scan	NAE_c data	T&B walls	Four walls
0.500	21×10^6	-0.124	7339	2	20908	1	Fig. A-1	Fig. B-1	Fig. C-1
0.500	21×10^6	0.237	7134	3	20908	2	Fig. A-2	Fig. B-2	Fig. C-2
0.498	21×10^6	0.548	7135	1	20908	3	Fig. A-3	Fig. B-3	Fig. C-3
0.496	21×10^6	0.906	7340	2	20909	1	Fig. A-4	Fig. B-4	Fig. C-4
0.494	21×10^6	1.172	7341	1	20909	2	Fig. A-5	Fig. B-5	Fig. C-5
0.494	21×10^6	1.176	7342	1	20909	3	Fig. A-6	Fig. B-6	Fig. C-6
0.701	21×10^6	-0.195	7343	2	20910	1	Fig. A-7	Fig. B-7	Fig. C-7
0.700	21×10^6	0.255	7132	3	20910	2	Fig. A-8	Fig. B-8	Fig. C-8
0.695	21×10^6	0.655	7133	3	20910	3	Fig. A-9	Fig. B-9	Fig. C-9
0.689	21×10^6	0.950	7344	1	20911	1	Fig. A-10	Fig. B-10	Fig. C-10
0.688	21×10^6	1.079	7346	2	20911	2	Fig. A-11	Fig. B-11	Fig. C-11
0.689	21×10^6	1.118	7346	1	20911	3	Fig. A-12	Fig. B-12	Fig. C-12
0.750	21×10^6	-0.202	7120	2	20912	1	Fig. A-13	Fig. B-13	Fig. C-13
0.748	21×10^6	0.283	7119	3	20912	2	Fig. A-14	Fig. B-14	Fig. C-14
0.745	21×10^6	0.565	7129	1	20912	3	Fig. A-15	Fig. B-15	Fig. C-15
0.743	21×10^6	0.734	7102	2	20912	4	Fig. A-16	Fig. B-16	Fig. C-16
0.738	21×10^6	0.896	7127	3	20912	5	Fig. A-17	Fig. B-17	Fig. C-17
0.736	21×10^6	0.974	7131	2	20912	6	Fig. A-18	Fig. B-18	Fig. C-18
0.769	21×10^6	-0.248	7348	2	20913	1	Fig. A-19	Fig. B-19	Fig. C-19
0.767	21×10^6	0.292	7115	3	20913	2	Fig. A-20	Fig. B-20	Fig. C-20
0.762	21×10^6	0.598	7107	1	20913	3	Fig. A-21	Fig. B-21	Fig. C-21
0.760	21×10^6	0.767	7116	2	20913	4	Fig. A-22	Fig. B-22	Fig. C-22
0.757	21×10^6	0.883	7117	3	20913	5	Fig. A-23	Fig. B-23	Fig. C-23
0.755	21×10^6	0.865	7349	3	20913	6	Fig. A-24	Fig. B-24	Fig. C-24
0.778	21×10^6	-0.213	7353	1	20914	1	Fig. A-25	Fig. B-25	Fig. C-25
0.777	21×10^6	0.297	7361	1	20914	2	Fig. A-26	Fig. B-26	Fig. C-26
0.772	21×10^6	0.612	7108	3	20914	3	Fig. A-27	Fig. B-27	Fig. C-27
0.769	21×10^6	0.775	7101	1	20914	4	Fig. A-28	Fig. B-28	Fig. C-28
0.768	21×10^6	0.815	7351	2	20914	5	Fig. A-29	Fig. B-29	Fig. C-29
0.767	21×10^6	0.815	7351	3	20914	6	Fig. A-30	Fig. B-30	Fig. C-30
0.796	21×10^6	-0.197	7357	1	20915	1	Fig. A-31	Fig. B-31	Fig. C-31
0.797	21×10^6	0.315	7359	1	20915	2	Fig. A-32	Fig. B-32	Fig. C-32
0.789	21×10^6	0.620	7144	1	20915	3	Fig. A-33	Fig. B-33	Fig. C-33
0.787	21×10^6	0.713	7113	2	20915	4	Fig. A-34	Fig. B-34	Fig. C-34
0.786	21×10^6	0.721	7364	2	20915	5	Fig. A-35	Fig. B-35	Fig. C-35
0.786	21×10^6	0.618	7363	2	20915	6	Fig. A-36	Fig. B-36	Fig. C-36
0.762	15×10^6	0.601	7137	2	20916	3	Fig. A-37	Fig. B-37	Fig. C-37
0.760	32×10^6	0.581	7141	1	20919	1	Fig. A-38	Fig. B-38	Fig. C-38

u : uncorrected data

c : data corrected for wall interference

T&B : top and bottom

Table 2 Outline of pressure measurements in the second phase.

	NAL		IAR(NAE)
Model chord	250mm		254mm(10in.)
Model span	300mm		381mm(15in.)
Aspect ratio	1.2		1.5
Correction	No		Top and bottom walls
Sidewall B.L. suction	Without		With
Mach number	uncorrected M	⇐ same ⇒	M corrected for for top and bottom walls
Lift coefficient	C_l calculated by the pressure integration	⇐ same ⇒	C_l calculated by the pressure integration
Drag coefficient	C_d measured by the wake rake at z/(b/2)=0.2	← comparison →	C_d measured by the wake rake at z/(b/2)=0.233

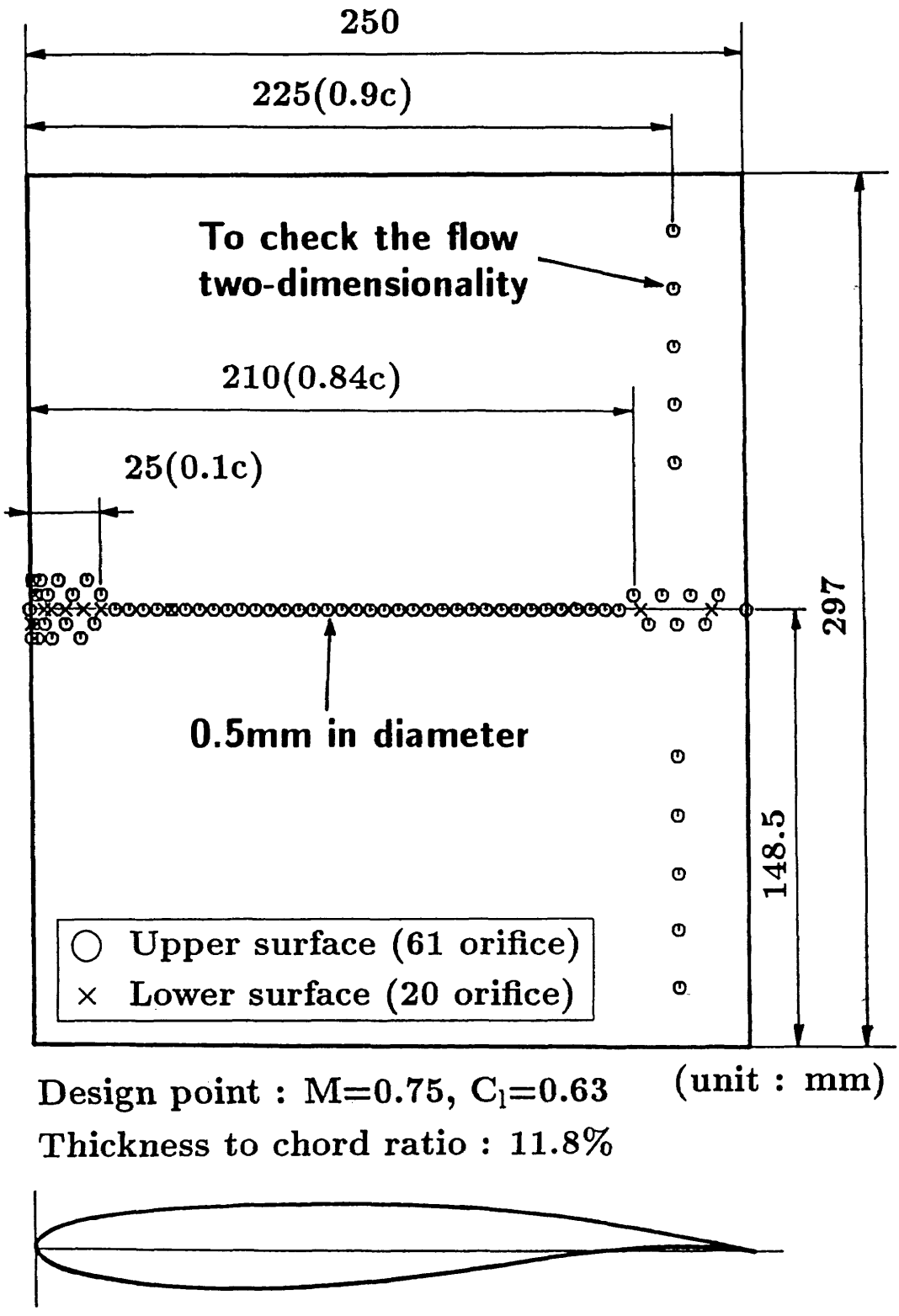

Figure 1 BGK No.1 airfoil shape and pressure orifice location.

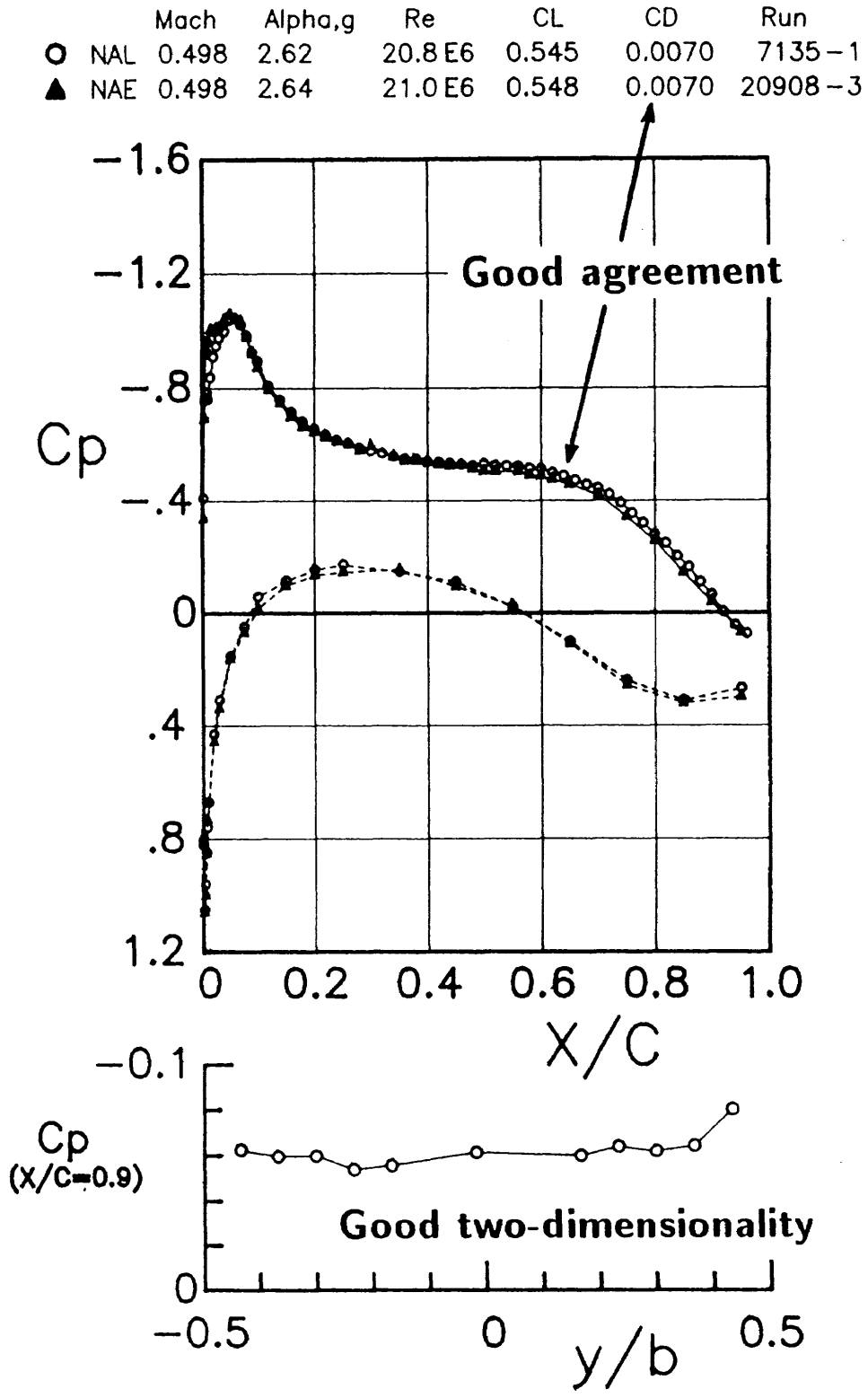

Figure 2 Comparison of pressure distribution data measured in the NAL and IAR wind tunnels with the same lift coefficient at a low subsonic speed; $M=0.498$, $Re=21\times10^6$, $C_l=0.548$.

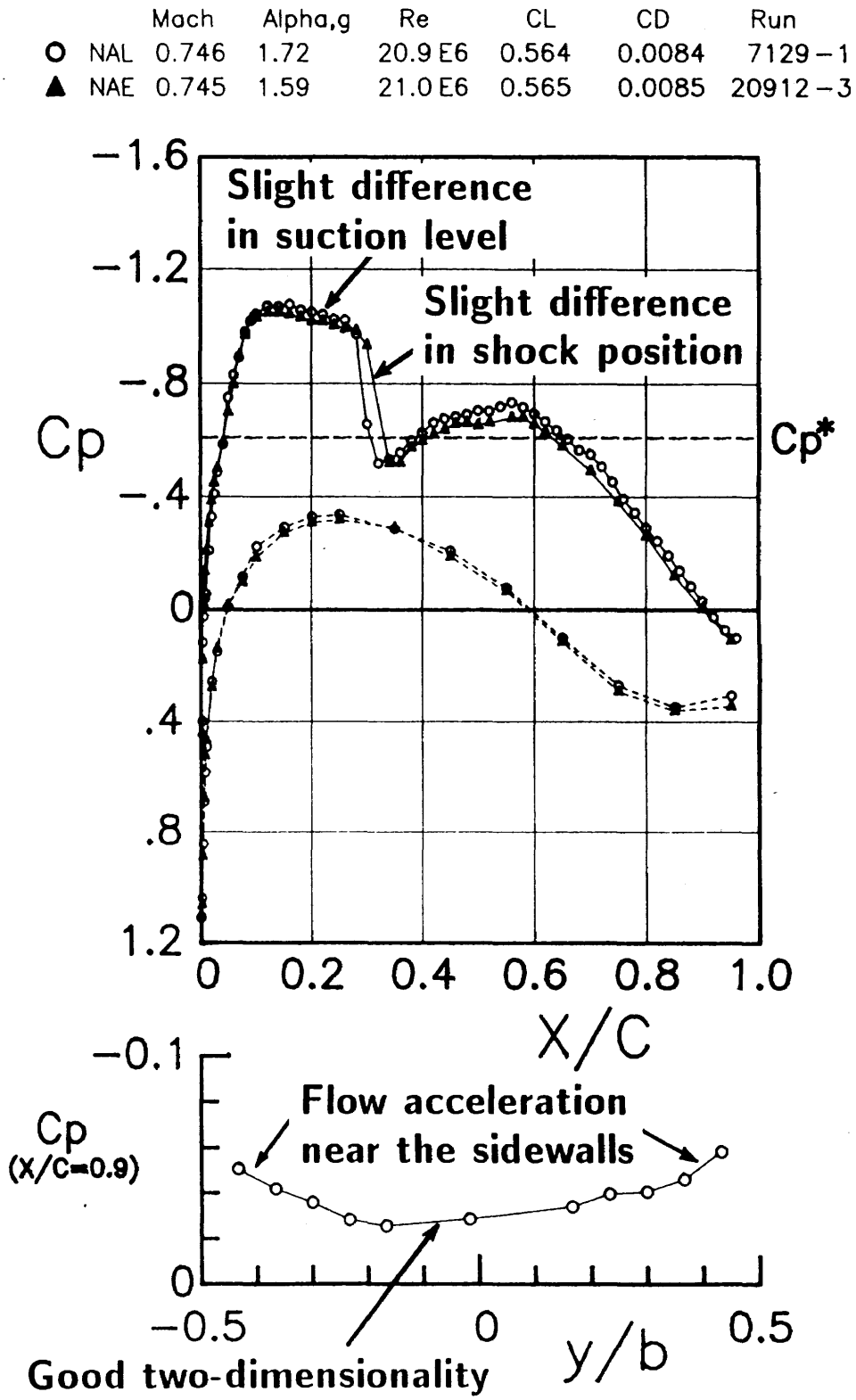

Figure 3 Comparison of pressure distribution data measured in the NAL and IAR wind tunnels with the same lift coefficient nearly at the design Mach number; $M=0.745$, $Re=21\times10^6$, $C_l=0.565$.

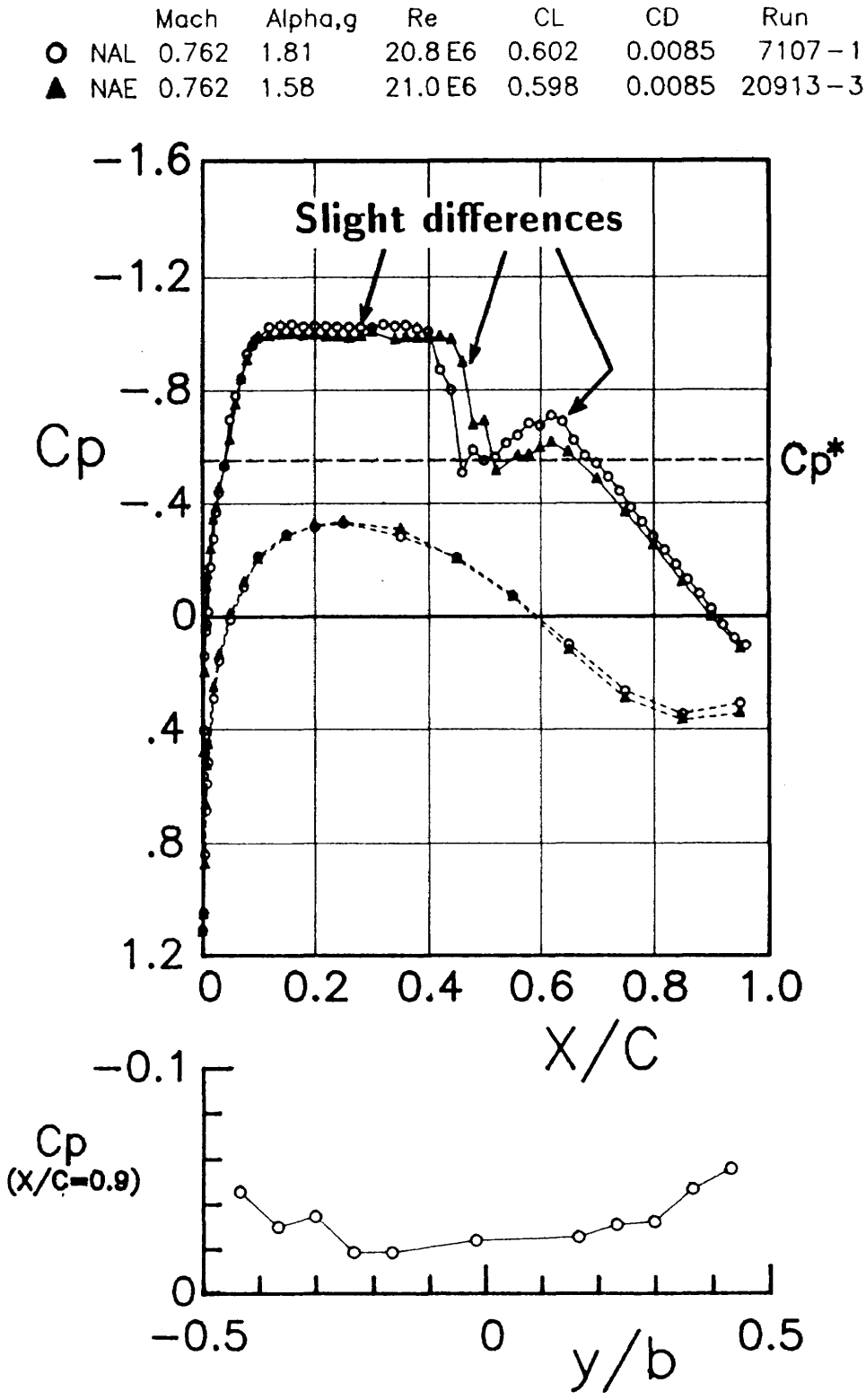

Figure 4 Comparison of pressure distribution data measured in the NAL and IAR wind tunnels with the same lift coefficient nearly at the design Mach number; $M=0.762$, $Re=21\times10^6$, $C_l=0.598$.

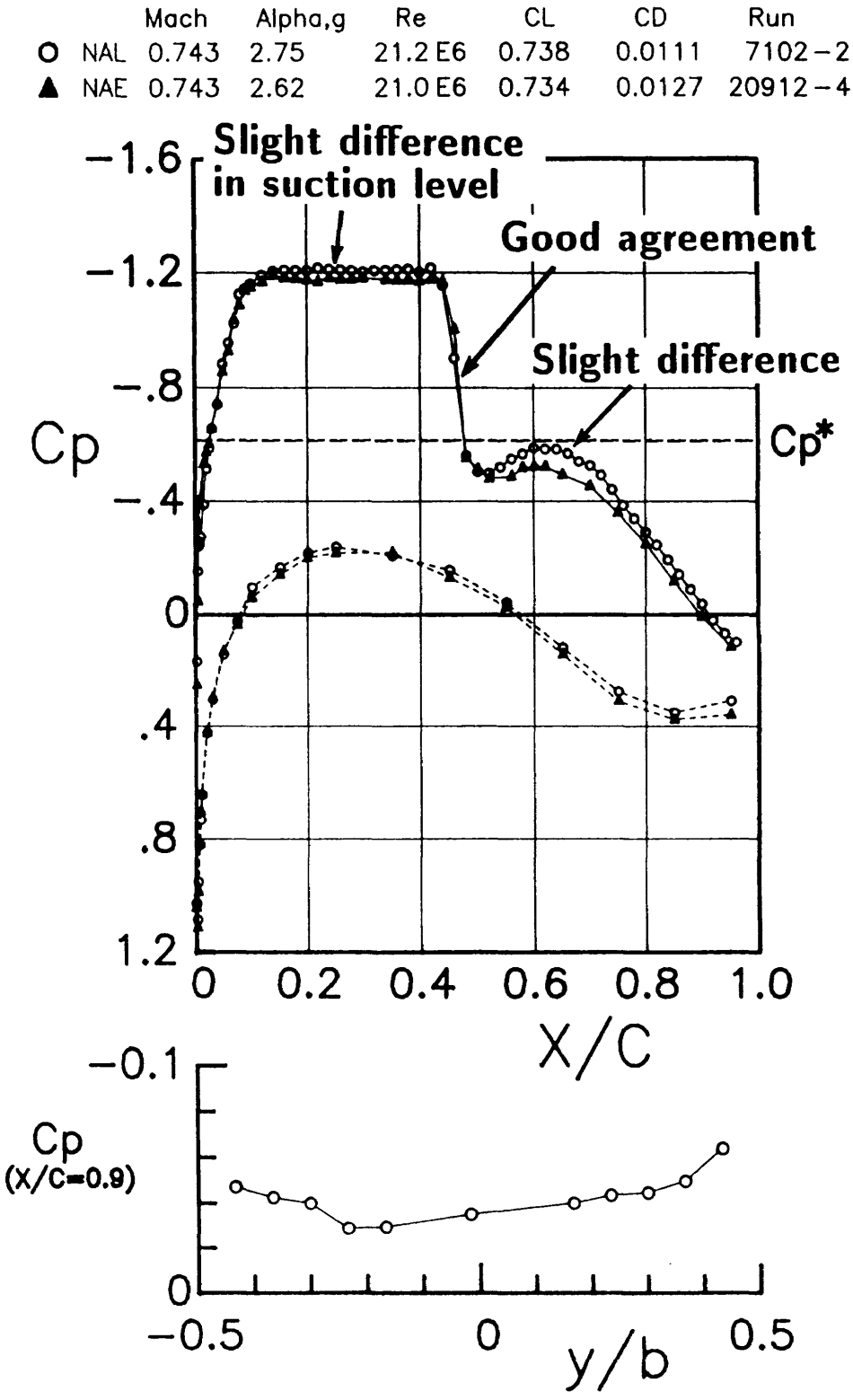

Figure 5 Comparison of pressure distribution data measured in the NAL and IAR wind tunnels with the same lift coefficient nearly at the design Mach number; $M=0.743$, $Re=21\times10^6$, $C_l=0.734$.

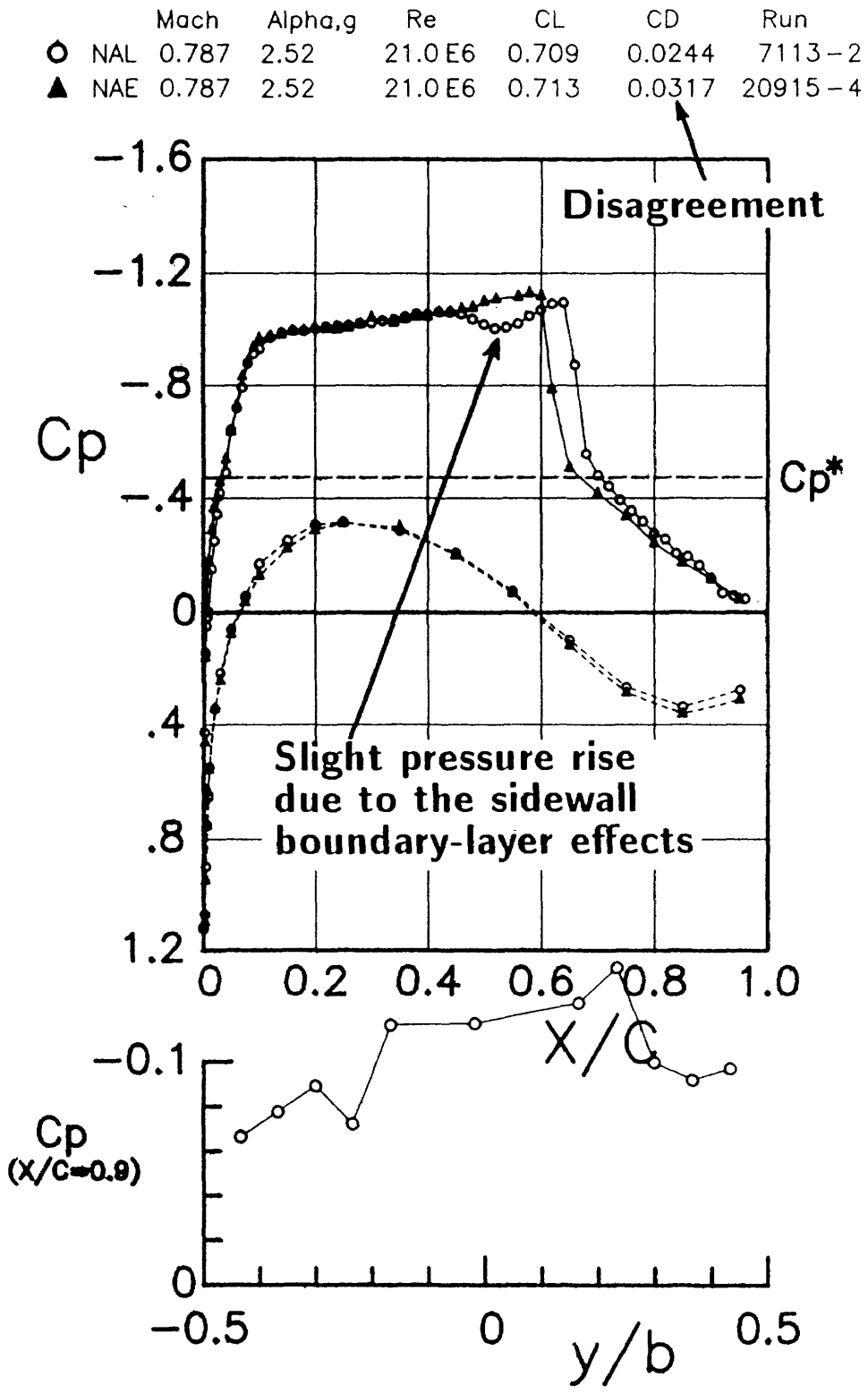

Figure 6 Comparison of pressure distribution data measured in the NAL and IAR wind tunnels with the same lift coefficient over the design Mach number; $M=0.787$, $Re=21\times10^6$, $C_l=0.713$.

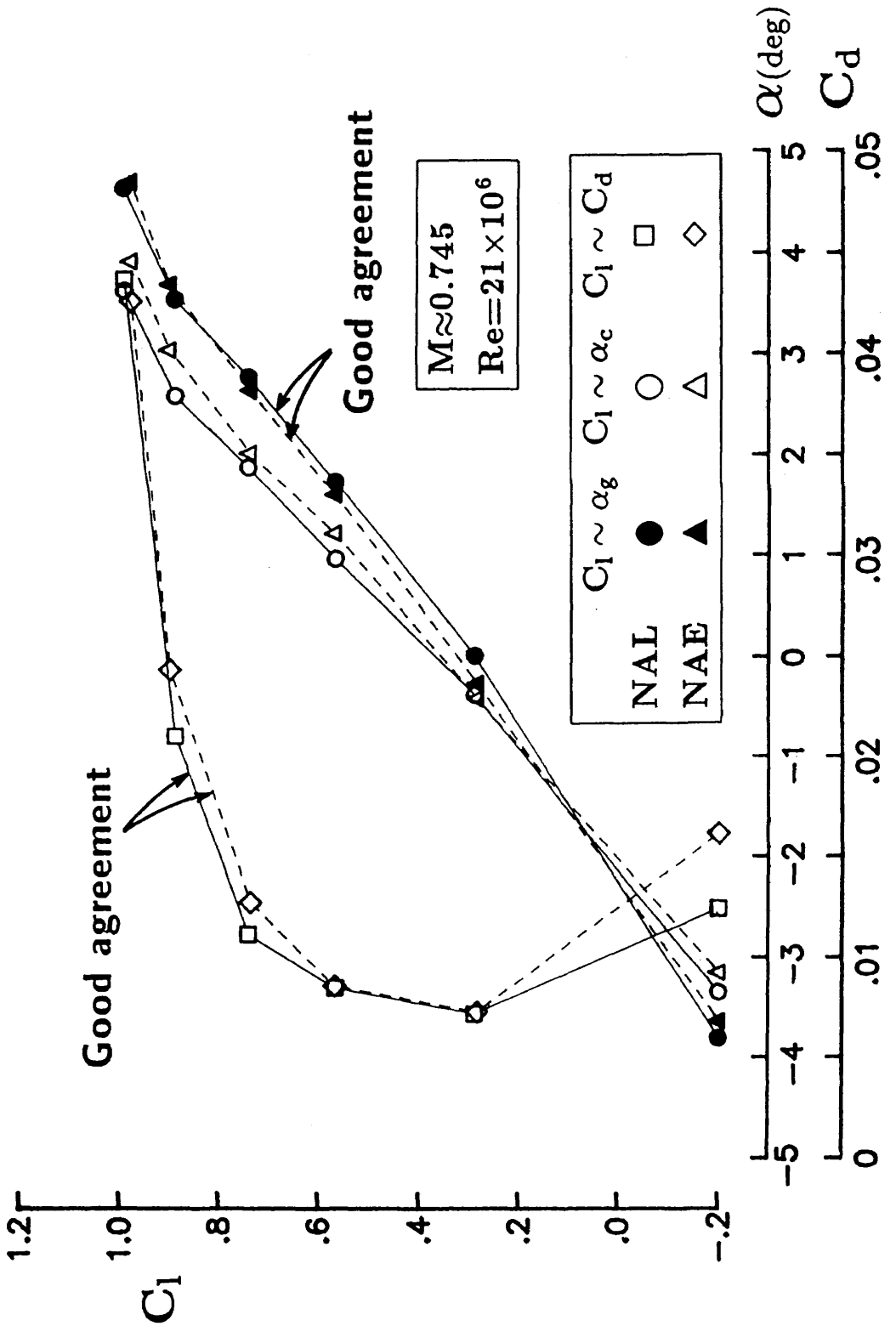

Figure 7 Effect of angle of attack or drag coefficient on lift coefficient; $M \simeq 0.745$, $Re = 21 \times 10^6$.

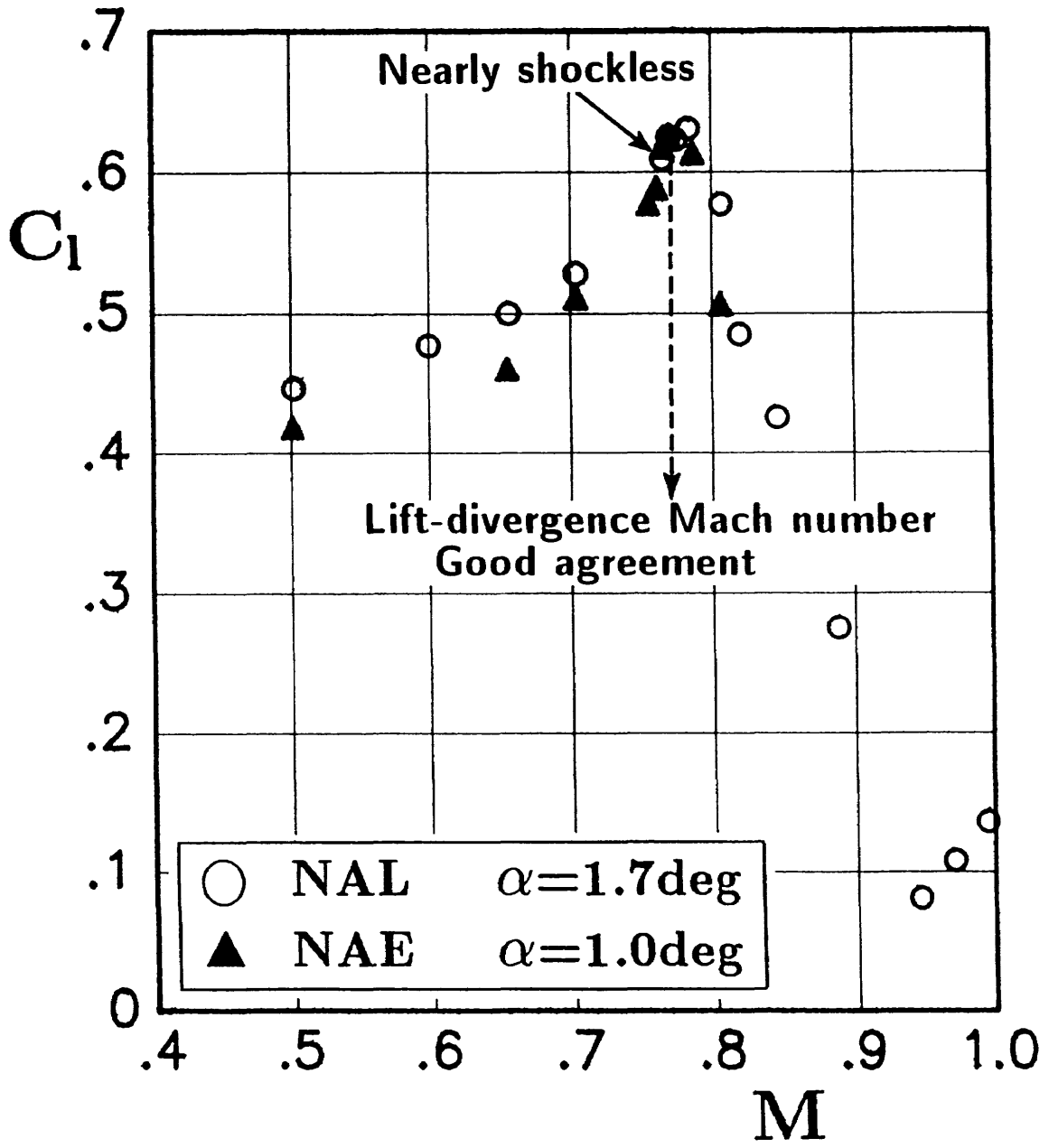

Figure 8 Effect of Mach number on lift coefficient at constant angles of attack.

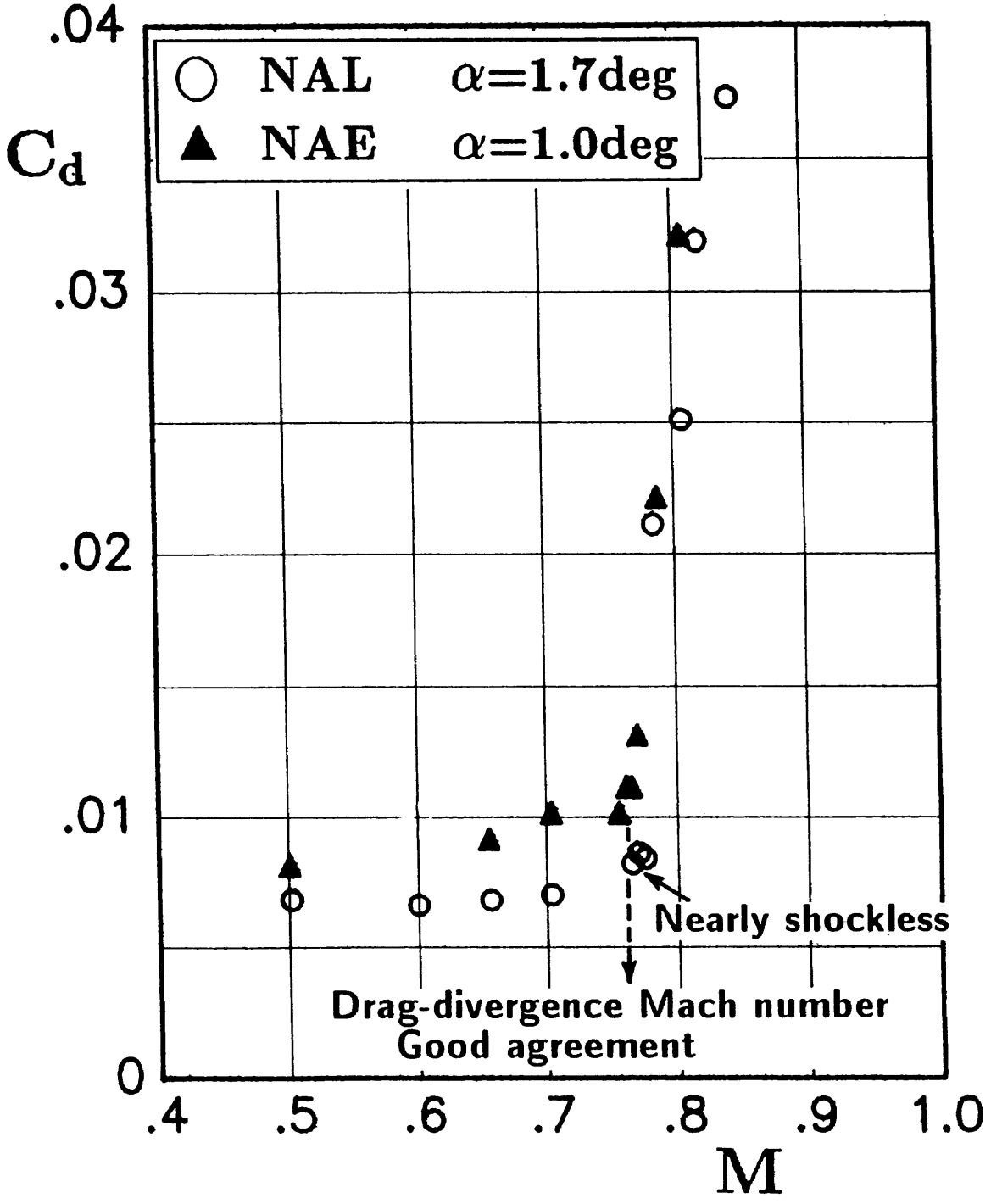

Figure 9 Effect of Mach number on drag coefficient at constant angles of attack.

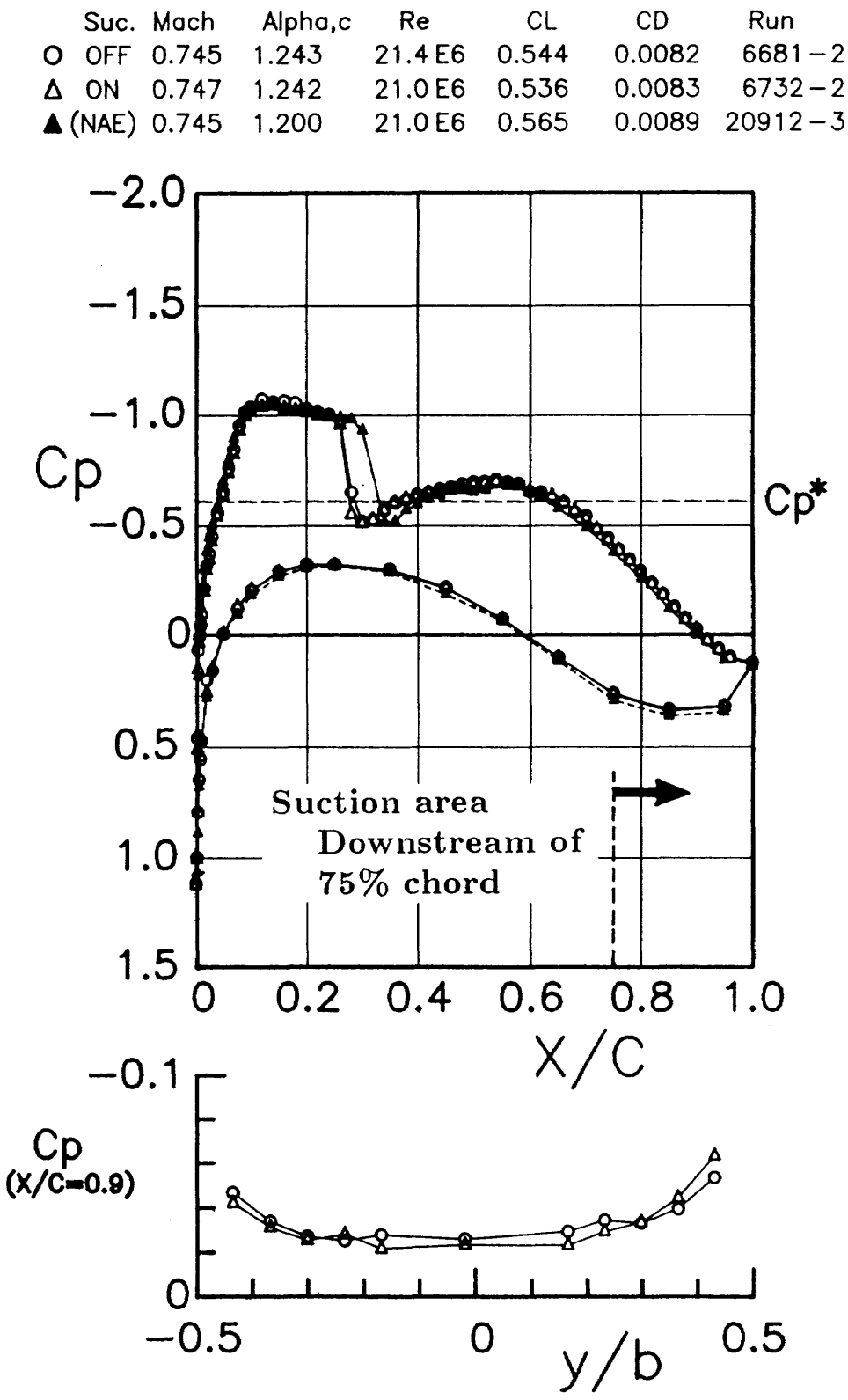

Figure 10 Effect of sidewall boundary-layer suction on pressure distribution; $M=0.745$, $Re=21\times10^6$.

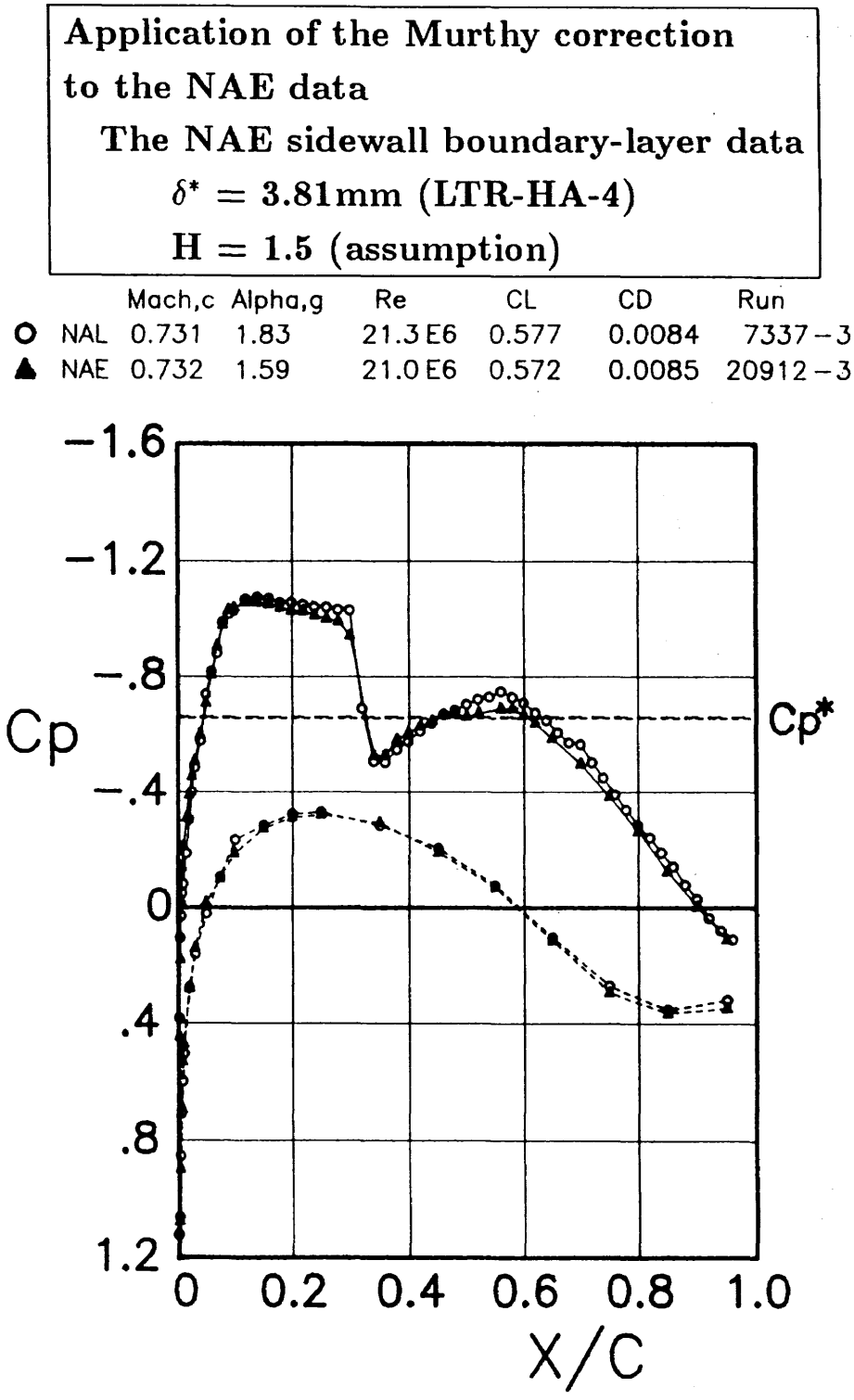

Figure 11 Comparison of corrected pressure distribution data for the four wall effects obtained in the NAL and IAR wind tunnels with the same lift coefficient; $M=0.732$, $Re=21\times10^6$, $C_l=0.572$.

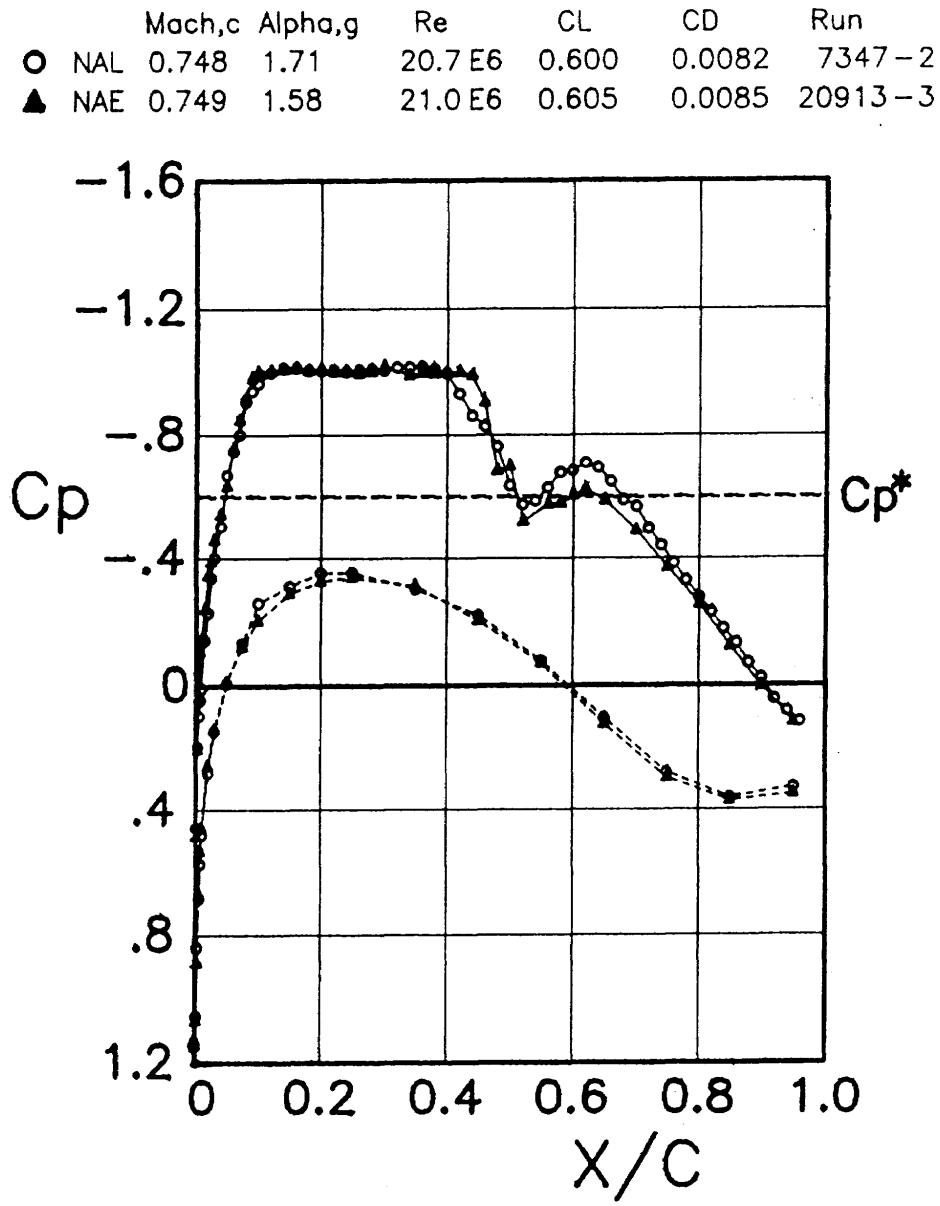

Figure 12 Comparison of corrected pressure distribution data for the four wall effects obtained in the NAL and IAR wind tunnels with the same lift coefficient; $M=0.749$, $Re=21\times10^6$, $C_l=0.605$.

	Mach	Alpha,g	Re	CL	CD	Run
○ NAL	0.500	−3.52	20.8 E6	−0.126	0.0069	7339−2
▲ NAE	0.500	−3.49	21.0 E6	−0.124	0.0066	20908−1

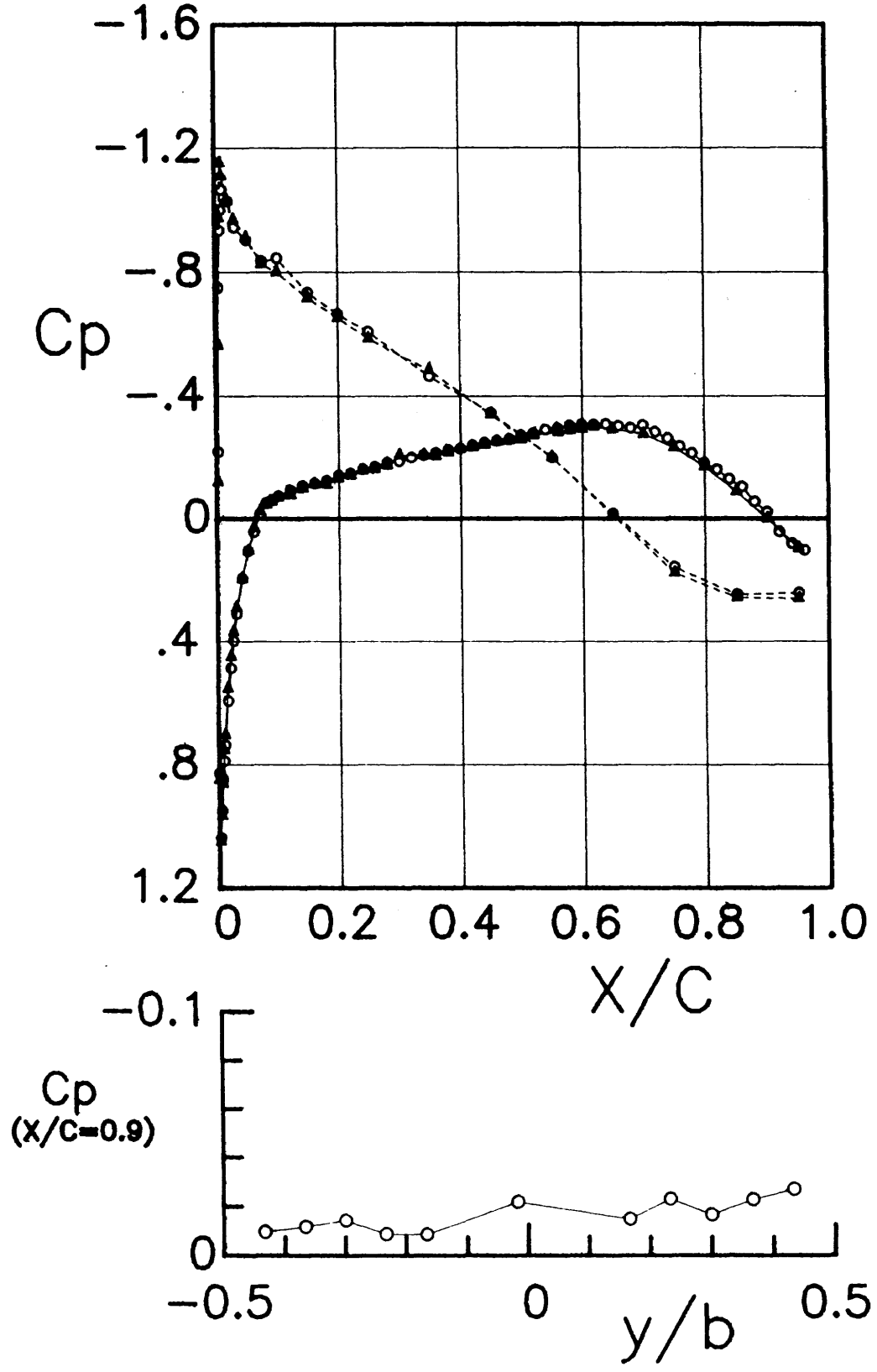

Figure A − 1 Comparison of pressure distribution data measured in the NAL and IAR wind tunnels with the same lift coefficient.

	Mach	Alpha,g	Re	CL	CD	Run
○ NAL	0.500	−0.10	20.9 E6	0.236	0.0067	7134−3
▲ NAE	0.500	−0.19	21.0 E6	0.237	0.0069	20908−2

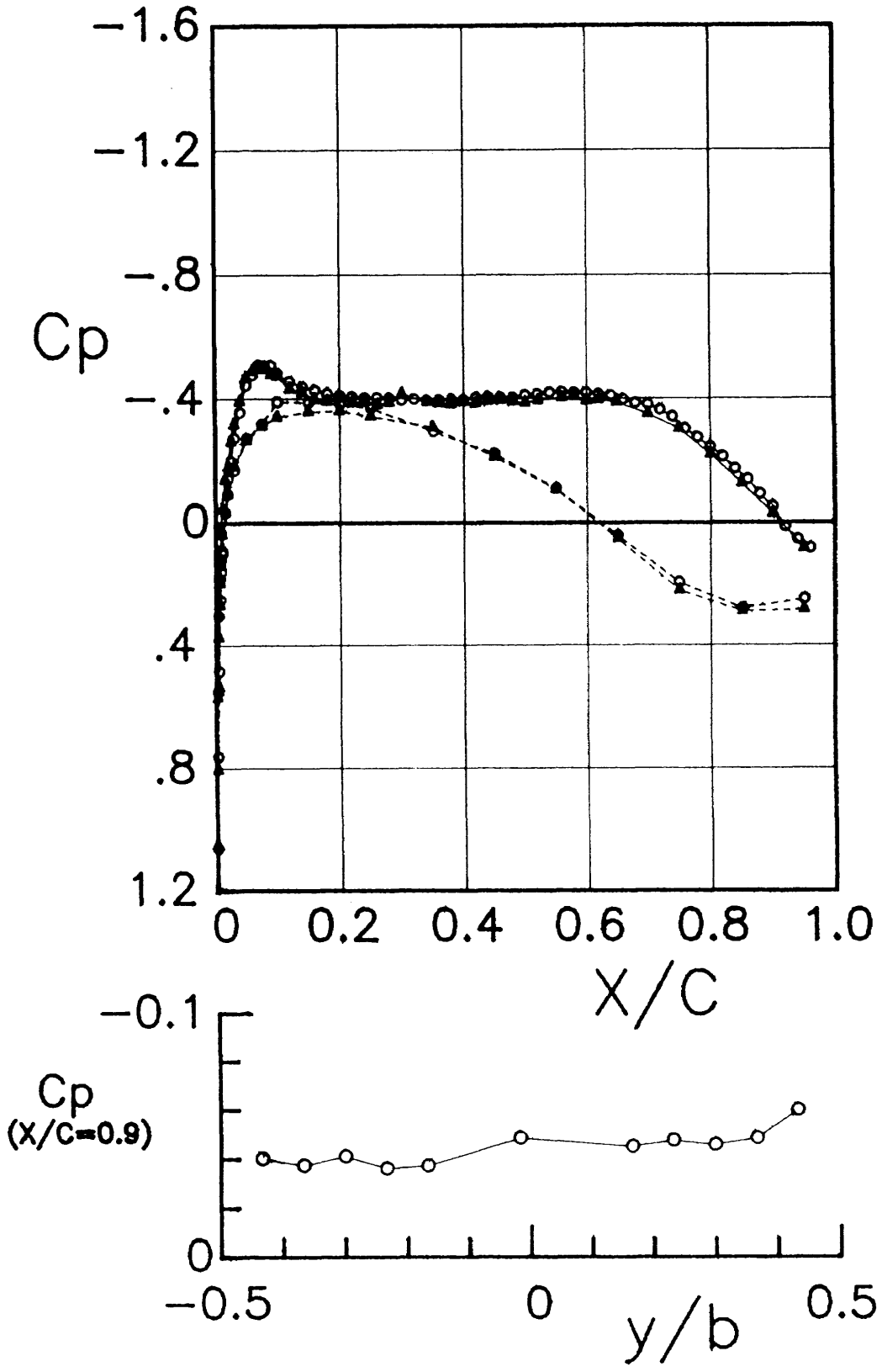

Figure A − 2 Comparison of pressure distribution data measured in the NAL and IAR wind tunnels with the same lift coefficient.

	Mach	Alpha,g	Re	CL	CD	Run
○ NAL	0.498	2.62	20.8 E6	0.545	0.0070	7135－1
▲ NAE	0.498	2.64	21.0 E6	0.548	0.0070	20908－3

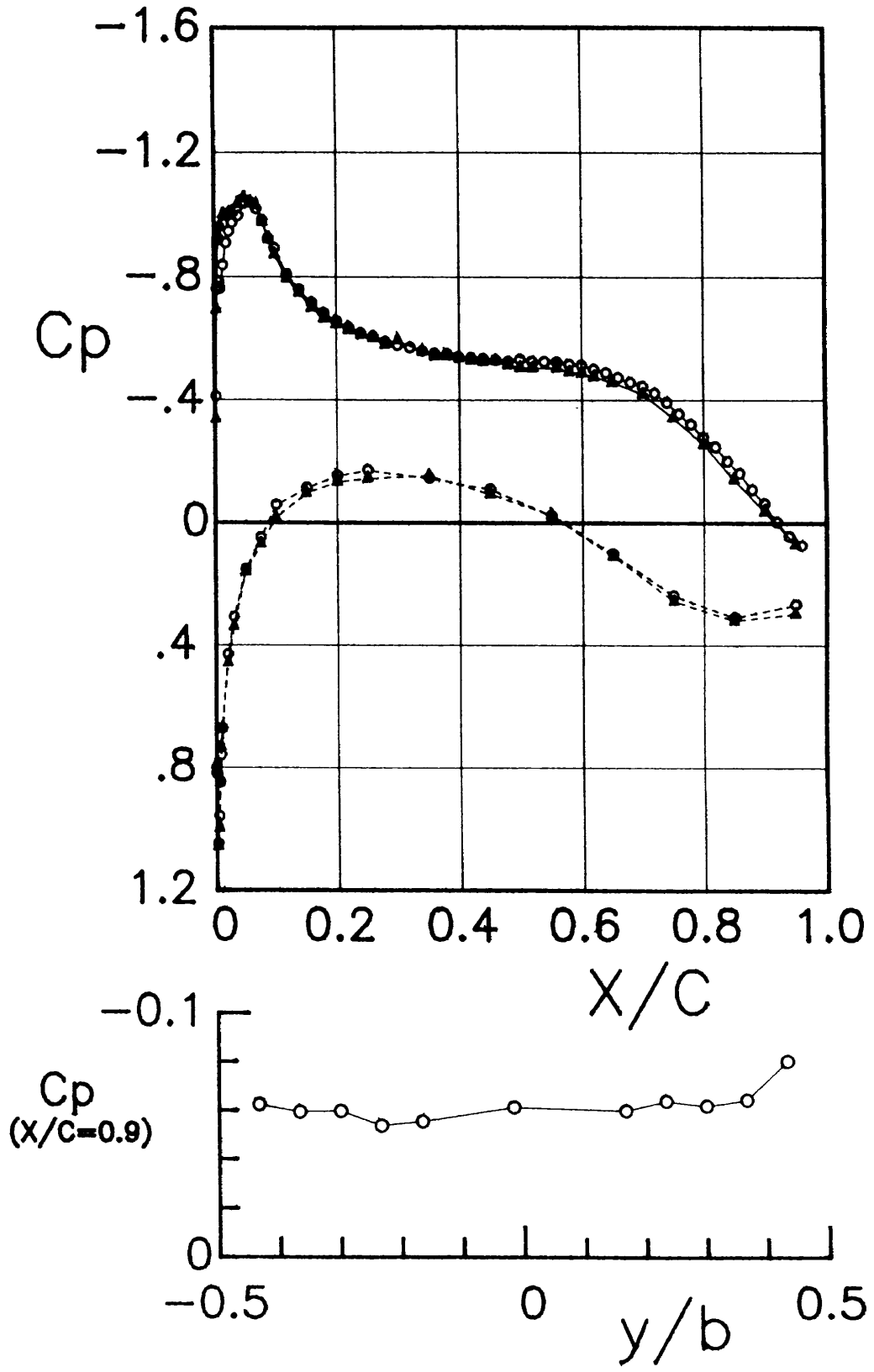

Figure A－3 Comparison of pressure distribution data measured in the NAL and IAR wind tunnels with the same lift coefficient.

		Mach	Alpha,g	Re	CL	CD	Run
O	NAL	0.496	5.73	20.7 E6	0.917	0.0079	7340−2
▲	NAE	0.496	5.76	21.0 E6	0.906	0.0079	20909−1

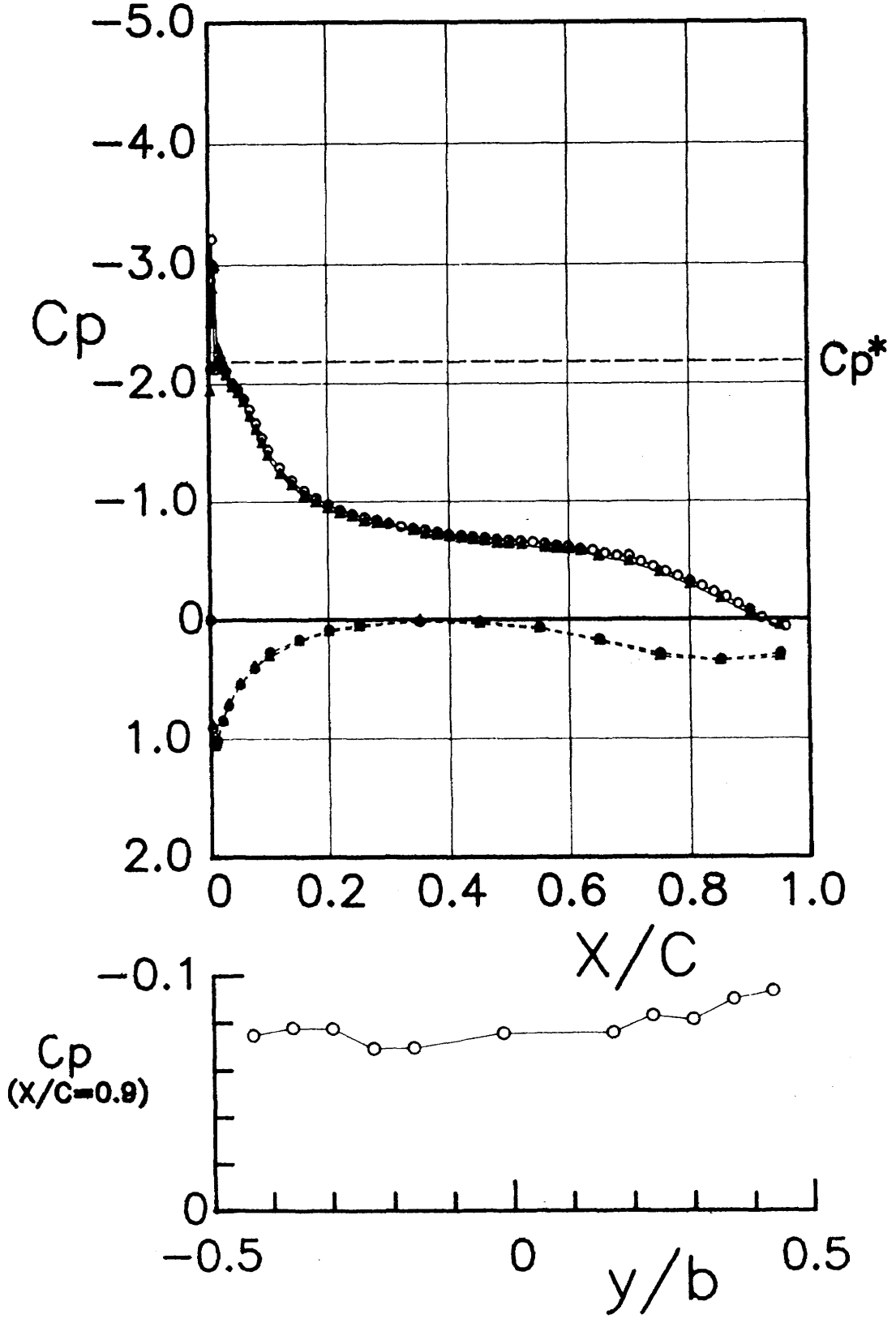

Figure A − 4 Comparison of pressure distribution data measured in the NAL and IAR wind tunnels with the same lift coefficient.

	Mach	Alpha,g	Re	CL	CD	Run
○ NAL	0.494	8.53	20.5 E6	1.174	0.0155	7341 − 1
▲ NAE	0.494	8.82	21.0 E6	1.172	0.0186	20909 − 2

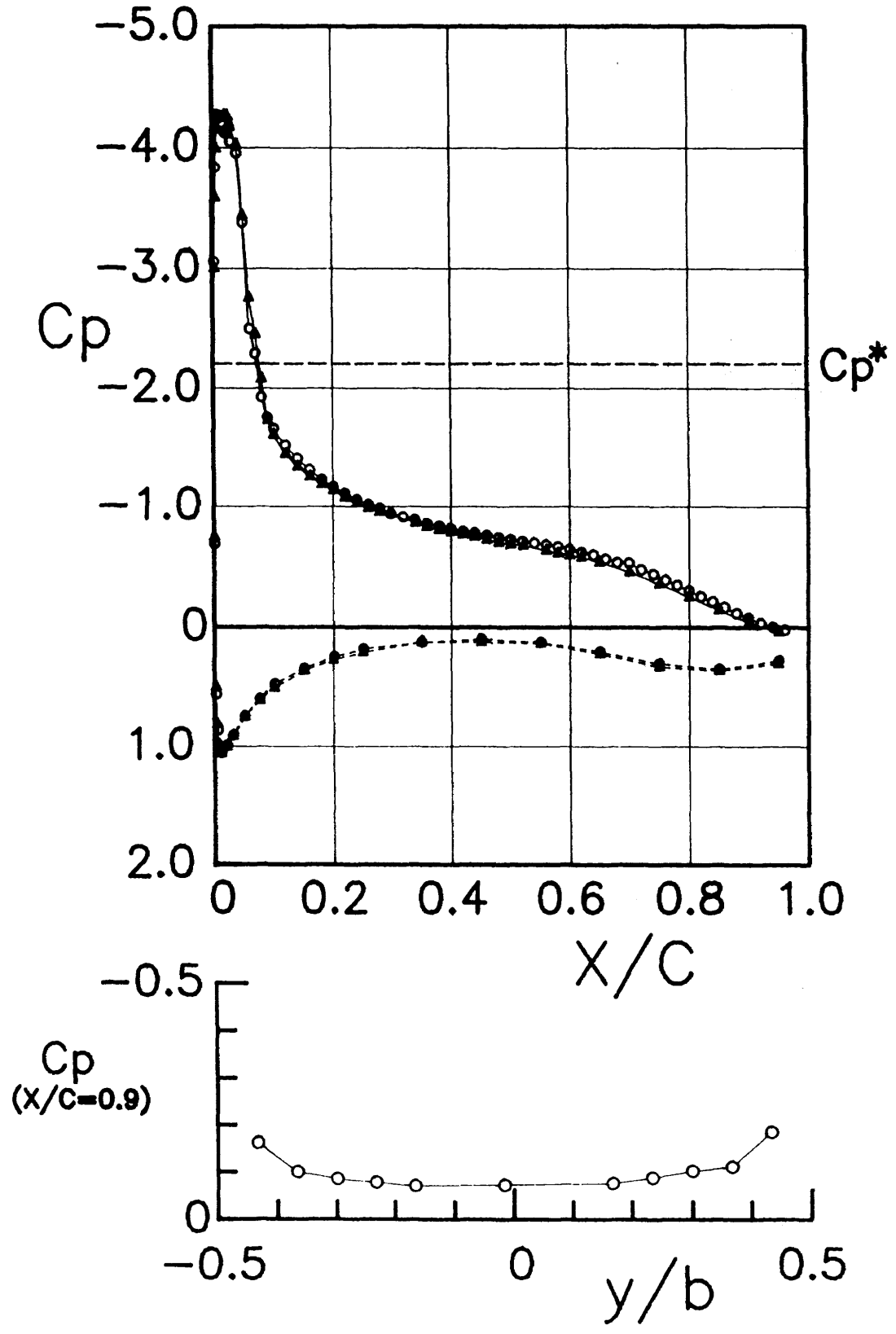

Figure A − 5 Comparison of pressure distribution data measured in the NAL and IAR wind tunnels with the same lift coefficient.

		Mach	Alpha,g	Re	CL	CD	Run
O	NAL	0.494	11.53	21.3 E6	1.174	0.0596	7342−1
▲	NAE	0.494	11.80	21.0 E6	1.176	0.0704	20909−3

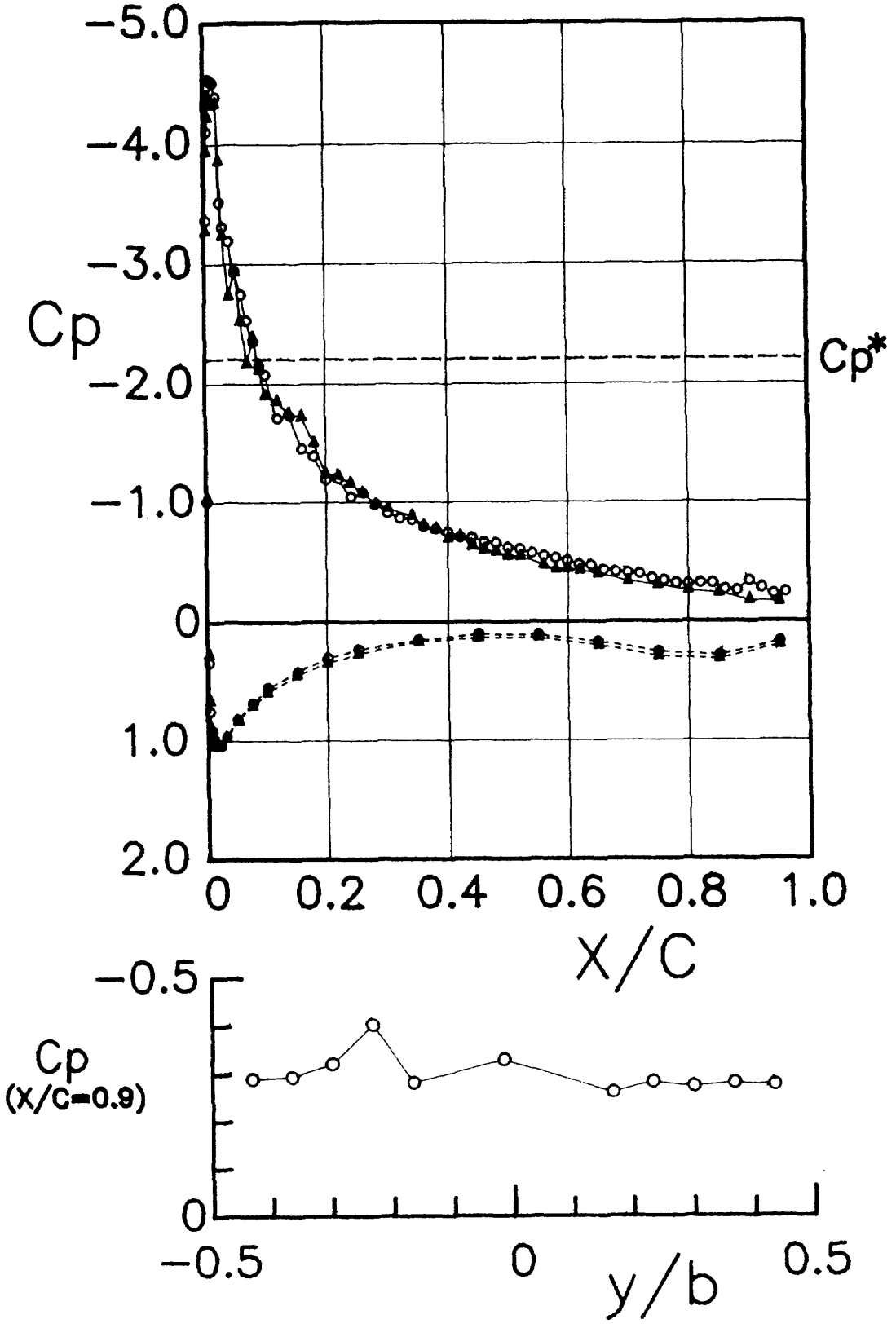

Figure A − 6 Comparison of pressure distribution data measured in the NAL and IAR wind tunnels with the same lift coefficient.

	Mach	Alpha,g	Re	CL	CD	Run
○ NAL	0.701	−3.72	21.3 E6	−0.184	0.0074	7343−2
▲ NAE	0.701	−3.62	21.0 E6	−0.195	0.0074	20910−1

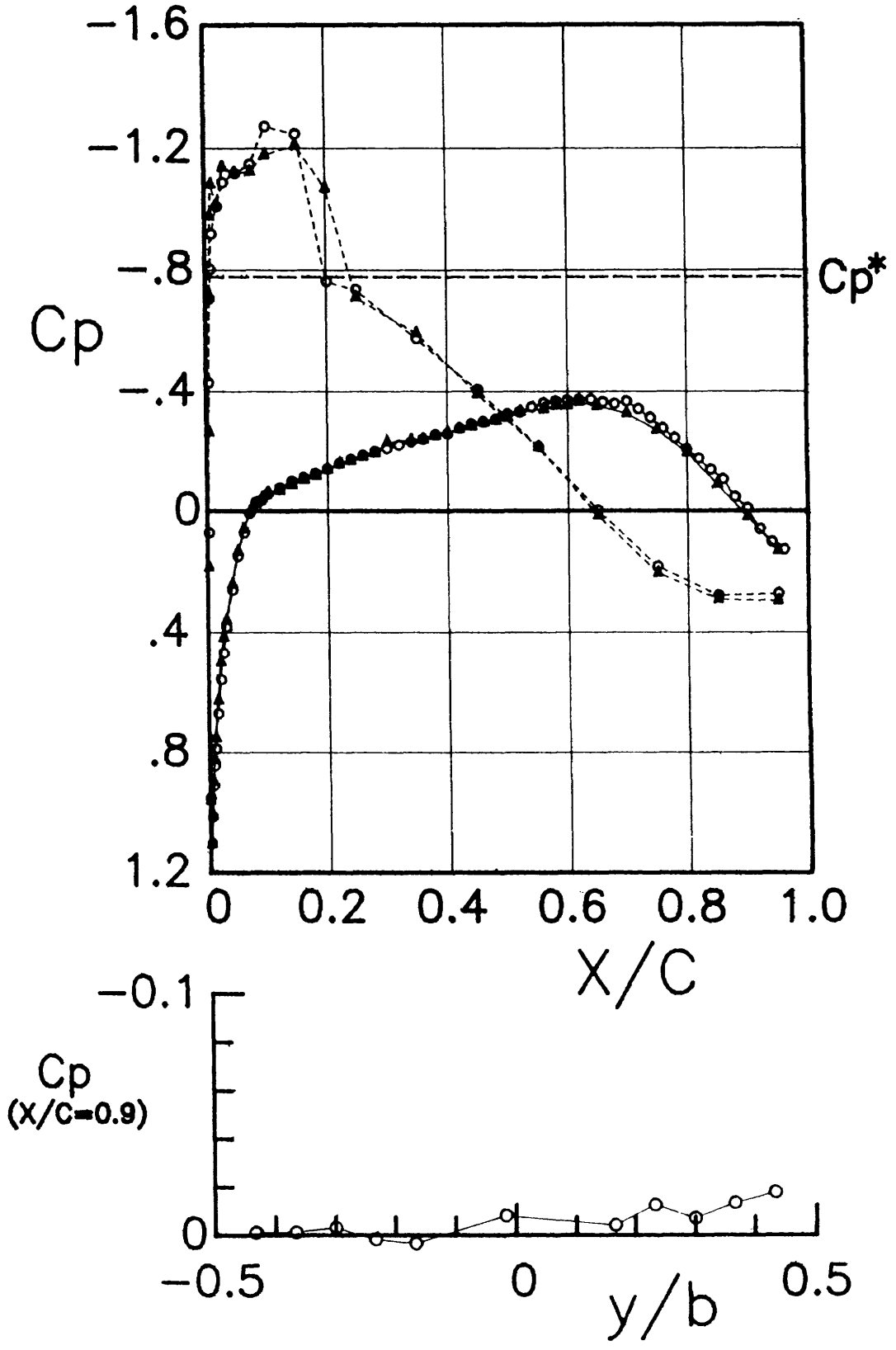

Figure A − 7 Comparison of pressure distribution data measured in the NAL and IAR wind tunnels with the same lift coefficient.

		Mach	Alpha,g	Re	CL	CD	Run
O	NAL	0.700	−0.20	21.1 E6	0.252	0.0068	7132−3
▲	NAE	0.700	−0.27	21.0 E6	0.255	0.0068	20910−2

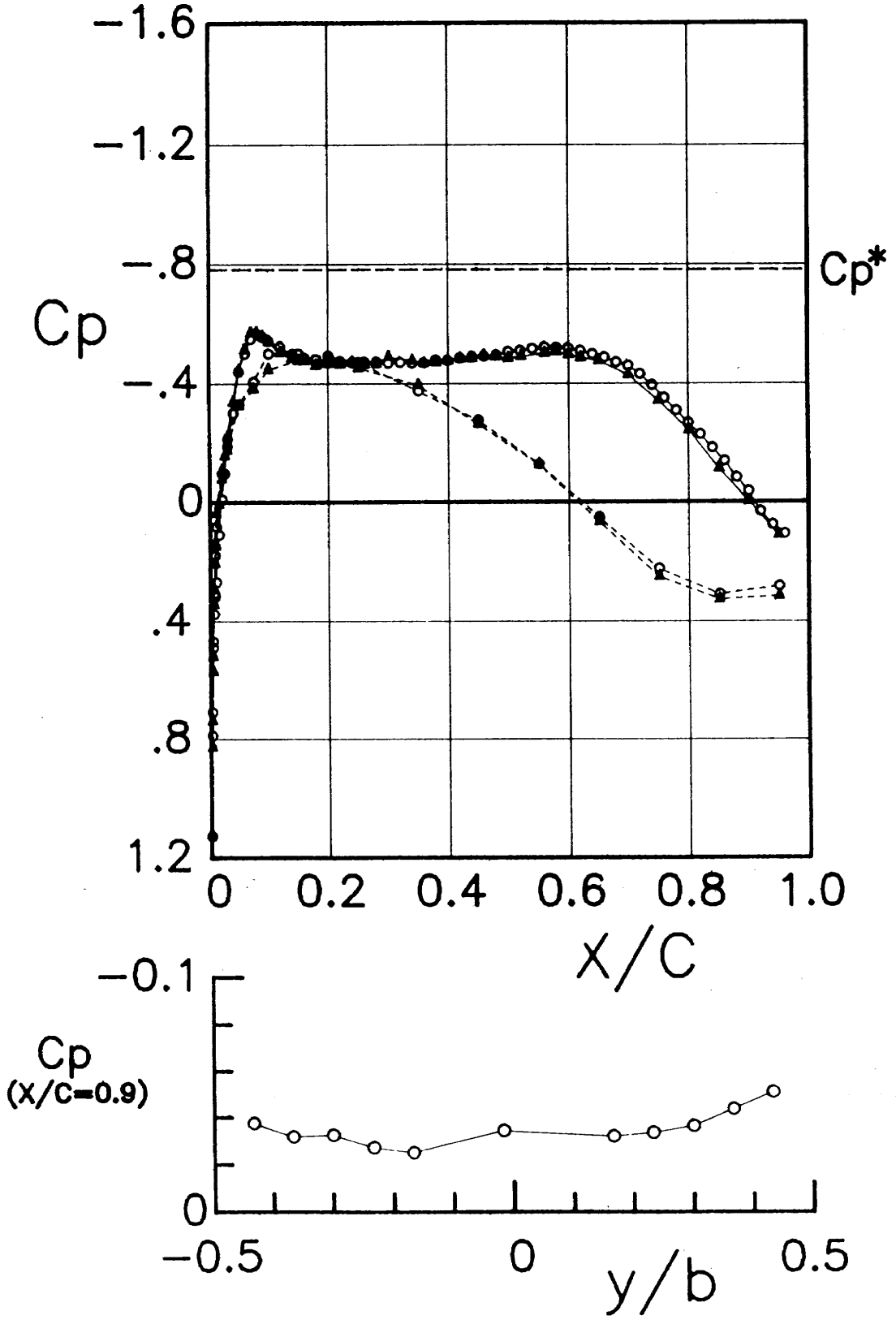

Figure A − 8 Comparison of pressure distribution data measured in the NAL and IAR wind tunnels with the same lift coefficient.

		Mach	Alpha,g	Re	CL	CD	Run
O	NAL	0.695	2.73	20.9 E6	0.659	0.0093	7133-3
▲	NAE	0.695	2.66	21.0 E6	0.655	0.0092	20910-3

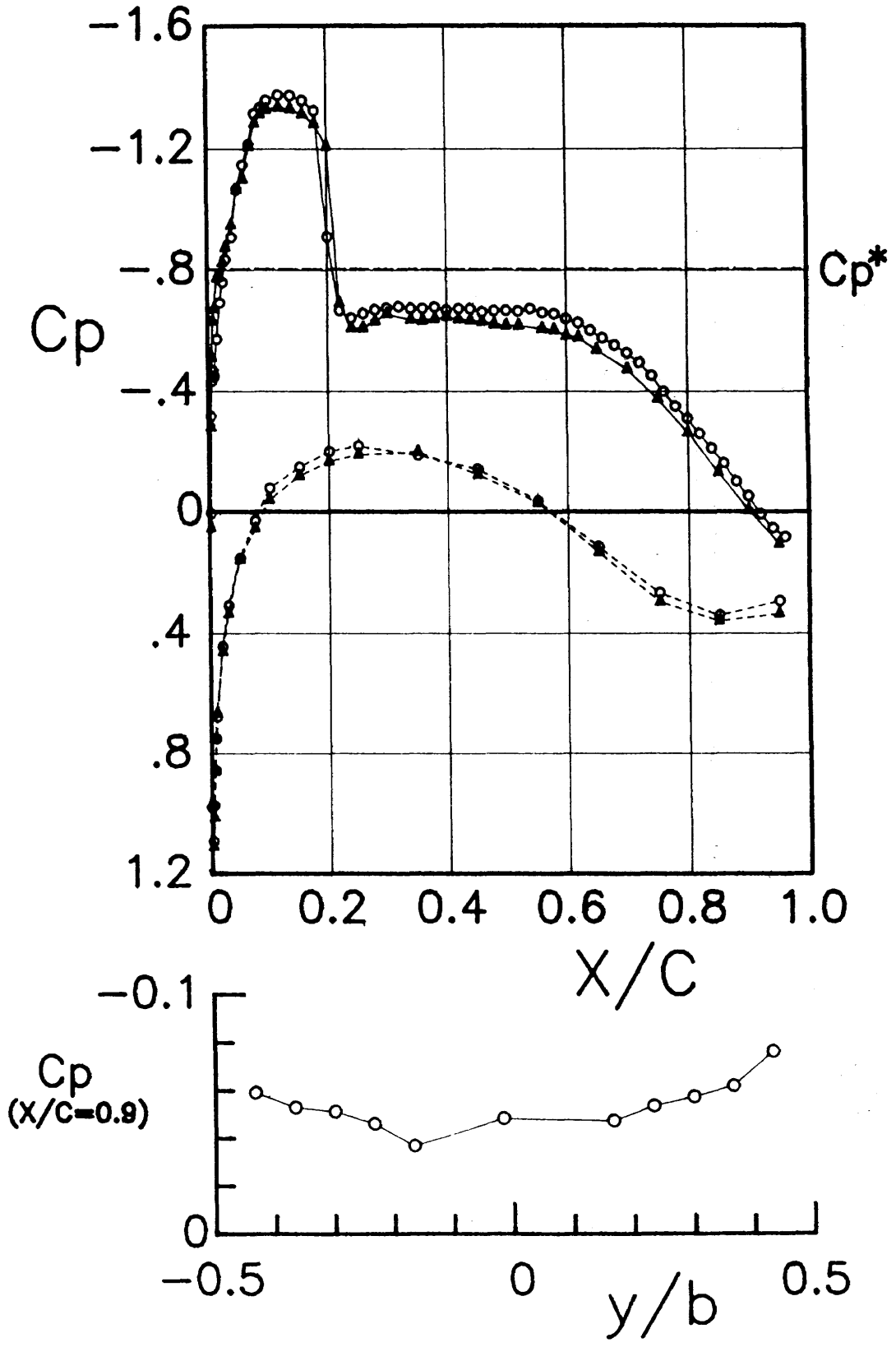

Figure A－9 Comparison of pressure distribution data measured in the NAL and IAR wind tunnels with the same lift coefficient.

		Mach	Alpha,g	Re	CL	CD	Run
O	NAL	0.689	4.52	21.0 E6	0.954	0.0222	7344−1
▲	NAE	0.689	4.76	21.0 E6	0.950	0.0236	20911−1

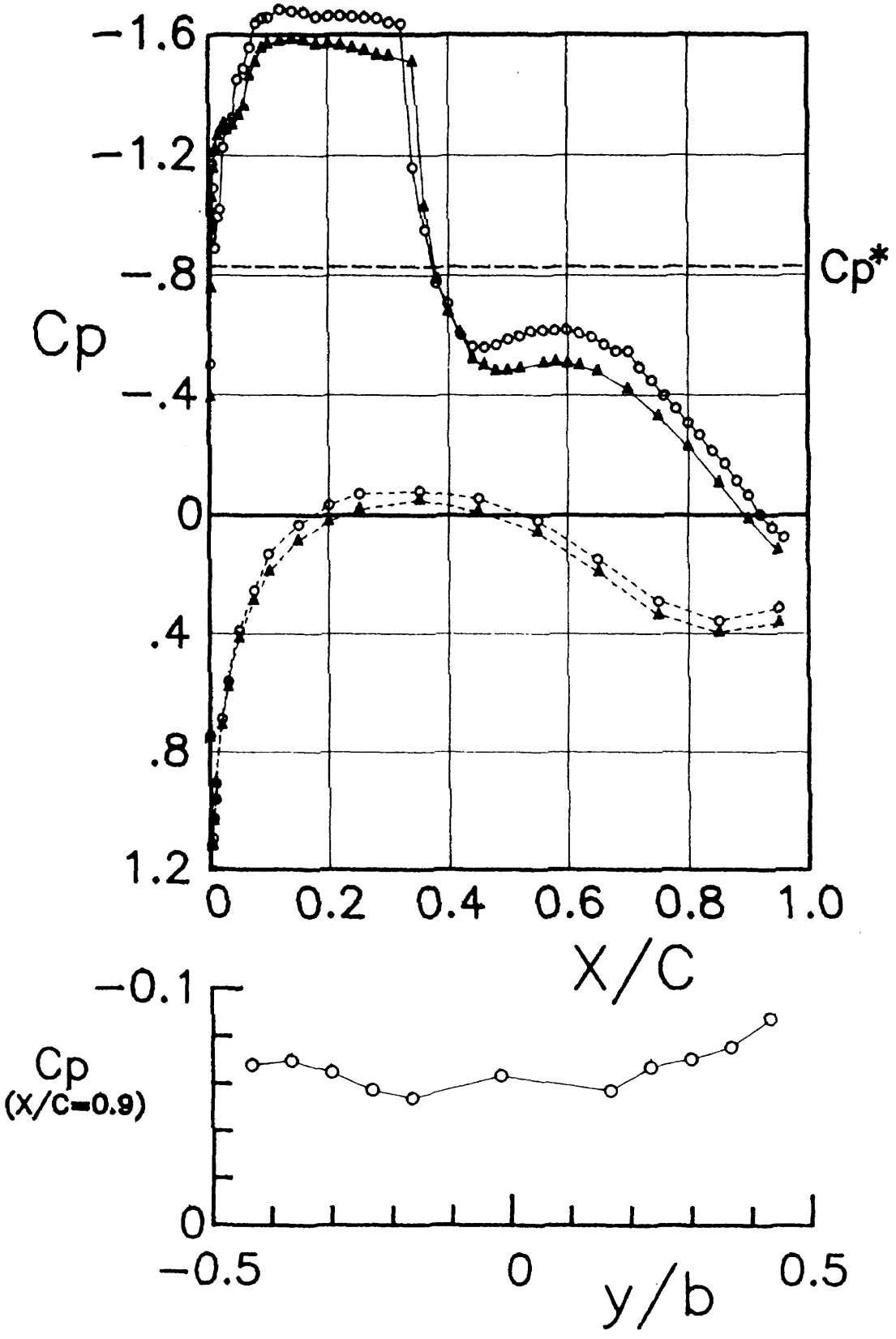

Figure A−10 Comparison of pressure distribution data measured in the NAL and IAR wind tunnels with the same lift coefficient.

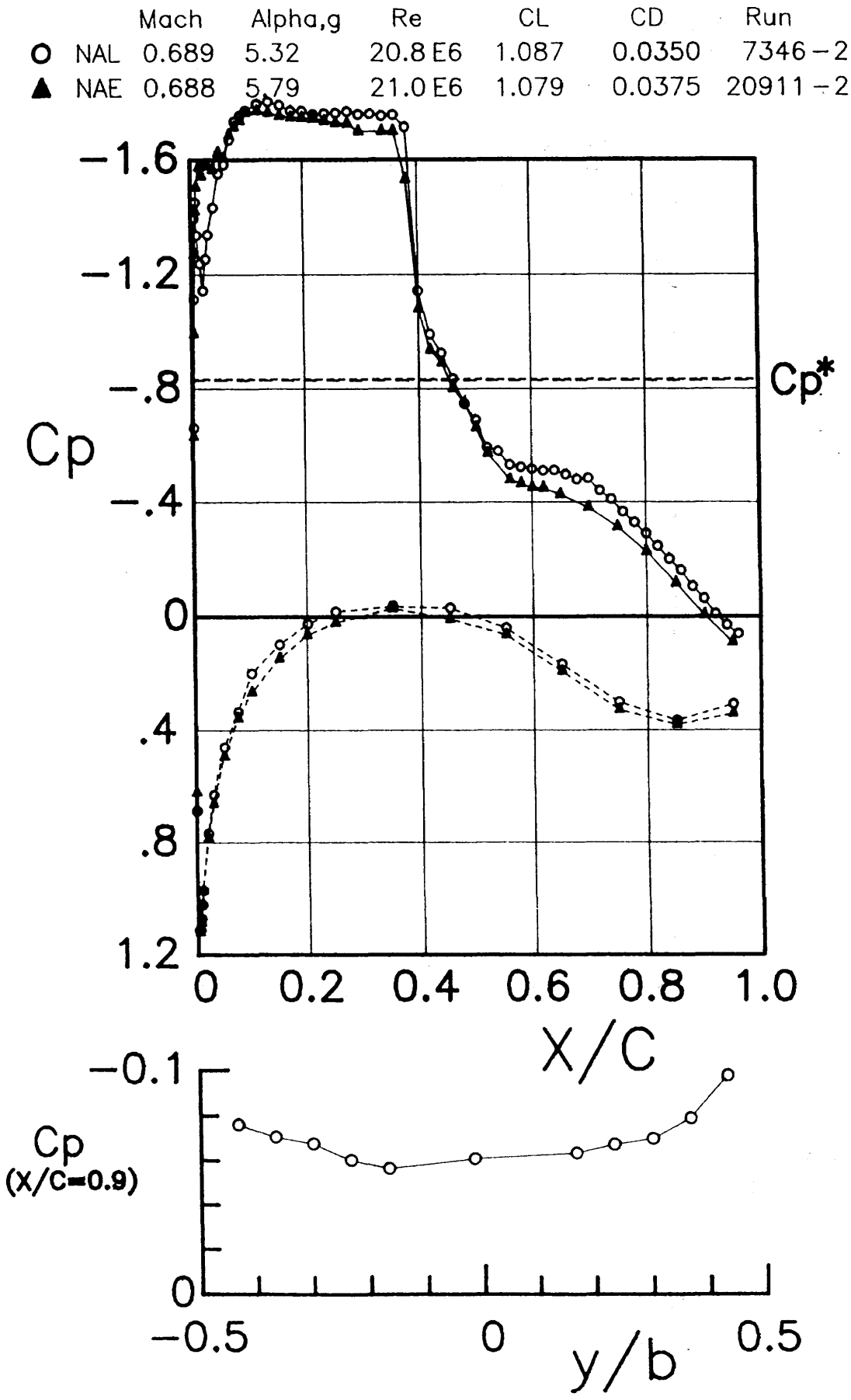

Figure A-11 Comparison of pressure distribution data measured in the NAL and IAR wind tunnels with the same lift coefficient.

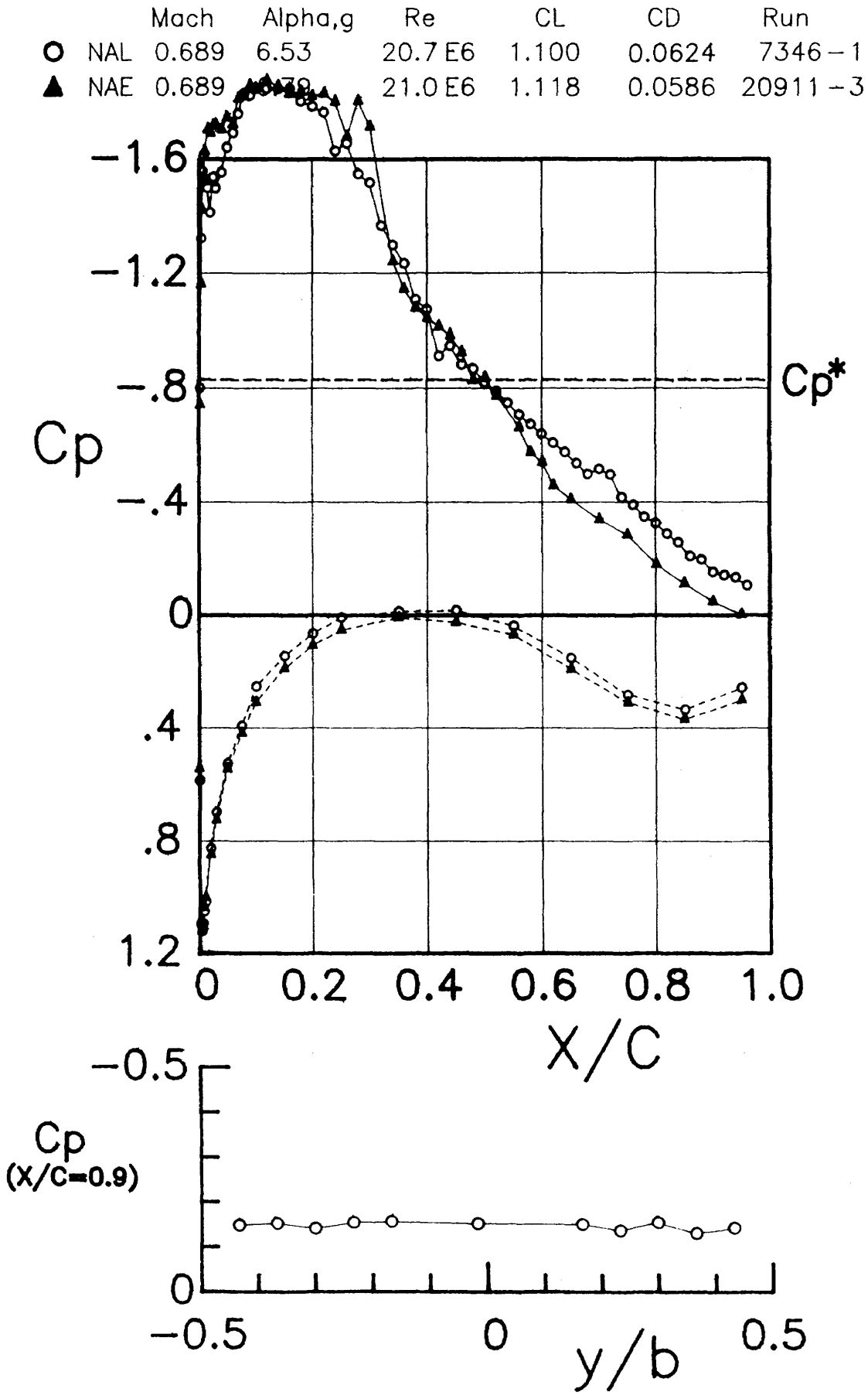

Figure A−12 Comparison of pressure distribution data measured in the NAL and IAR wind tunnels with the same lift coefficient.

	Mach	Alpha,g	Re	CL	CD	Run
○ NAL	0.751	−3.82	21.0 E6	−0.201	0.0124	7120−2
▲ NAE	0.750	−3.65	21.0 E6	−0.202	0.0161	20912−1

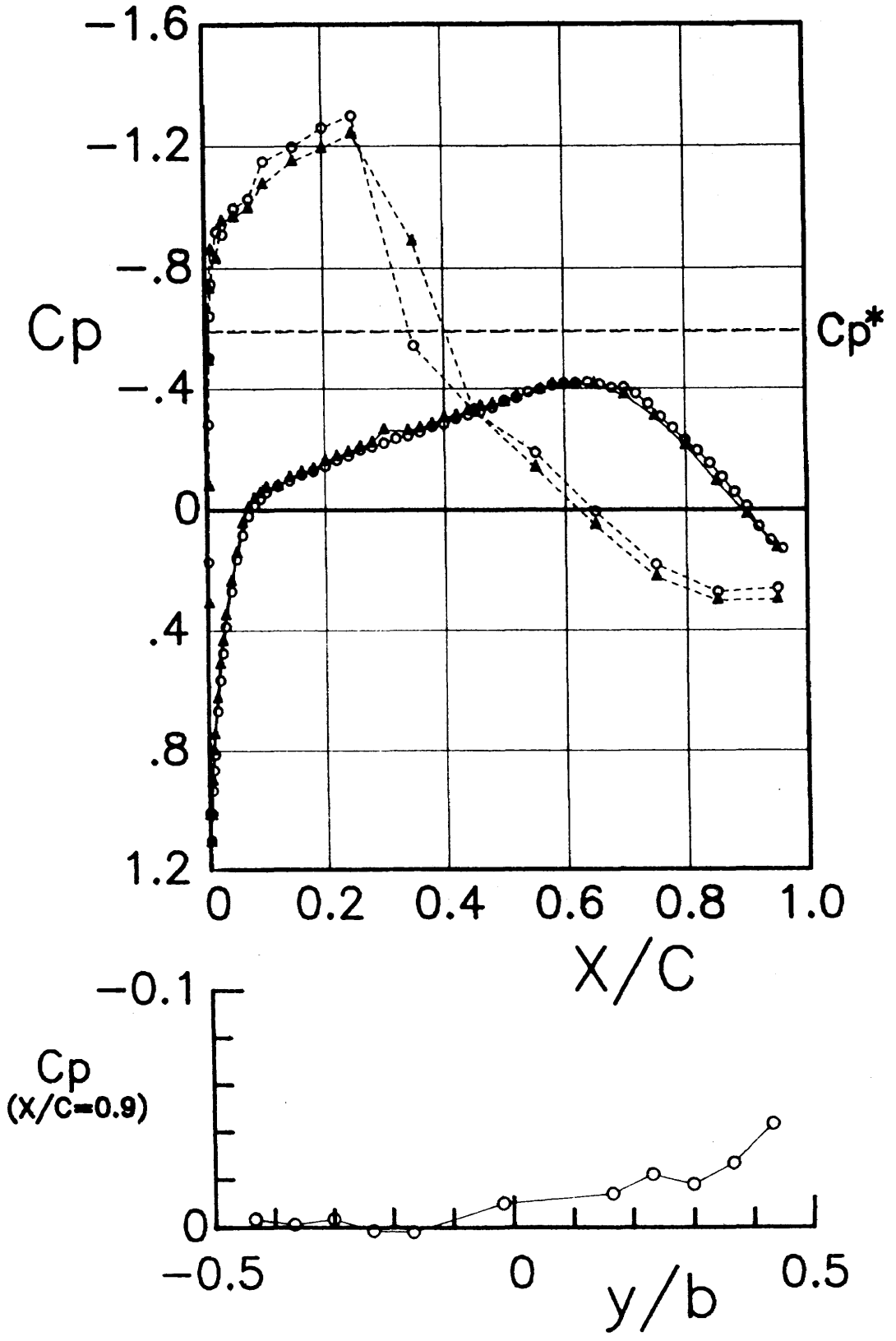

Figure A−13 Comparison of pressure distribution data measured in the NAL and IAR wind tunnels with the same lift coefficient.

		Mach	Alpha,g	Re	CL	CD	Run
O	NAL	0.748	0.00	21.1 E6	0.289	0.0071	7119−3
▲	NAE	0.748	−0.28	21.0 E6	0.283	0.0072	20912−2

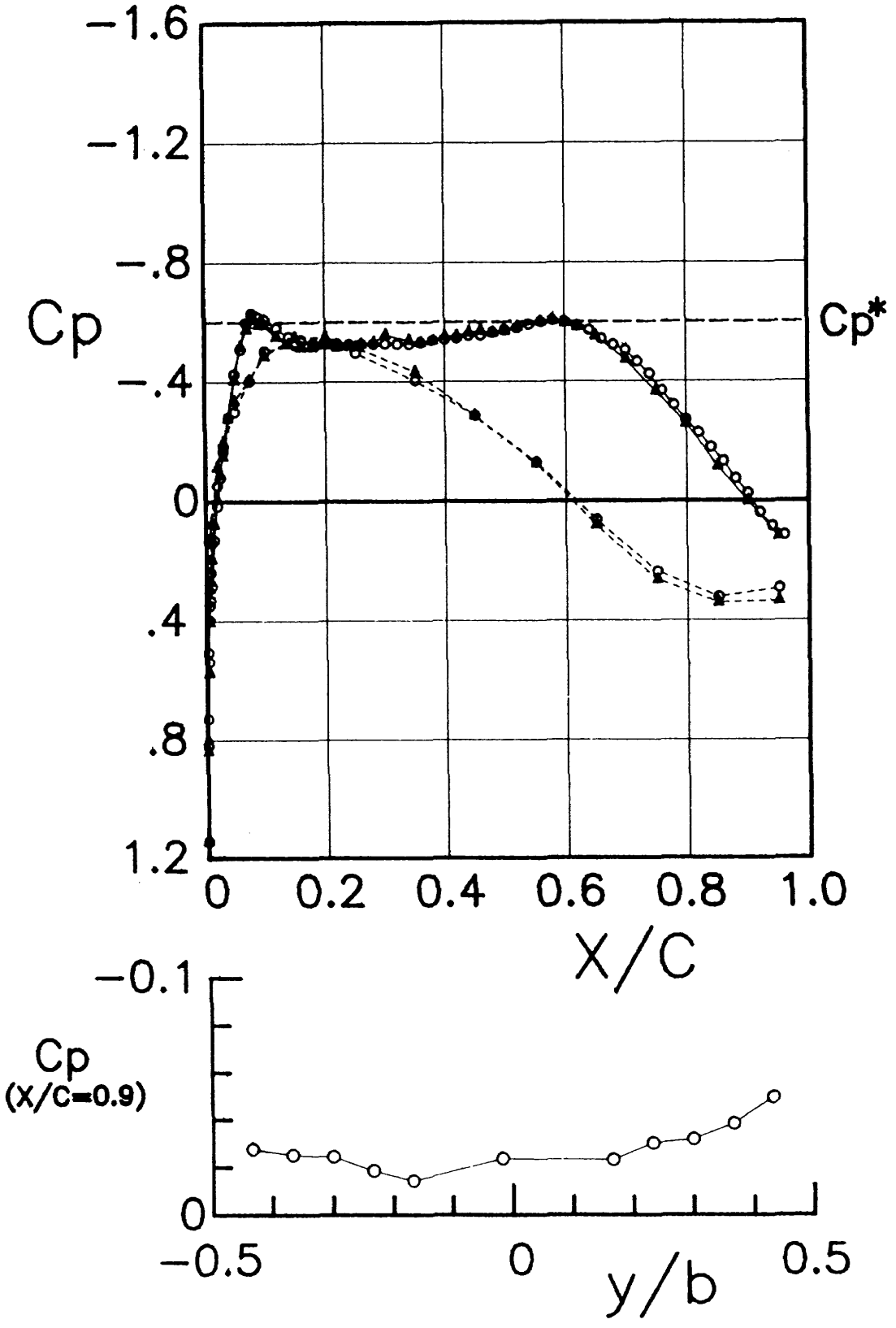

Figure A−14 Comparison of pressure distribution data measured in the NAL and IAR wind tunnels with the same lift coefficient.

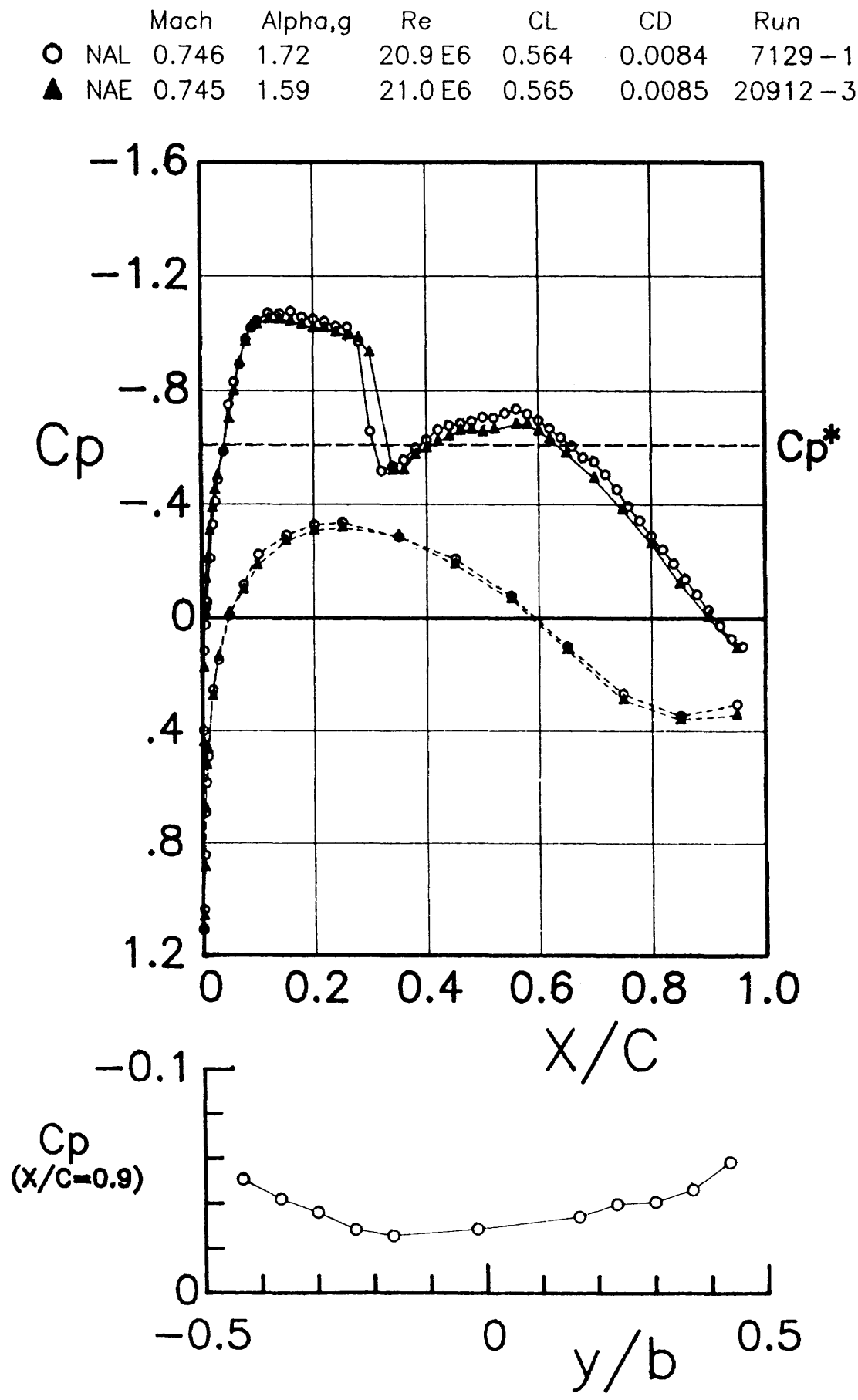

Figure A−15 Comparison of pressure distribution data measured in the NAL and IAR wind tunnels with the same lift coefficient.

		Mach	Alpha,g	Re	CL	CD	Run
O	NAL	0.743	2.75	21.2 E6	0.738	0.0111	7102−2
▲	NAE	0.743	2.62	21.0 E6	0.734	0.0127	20912−4

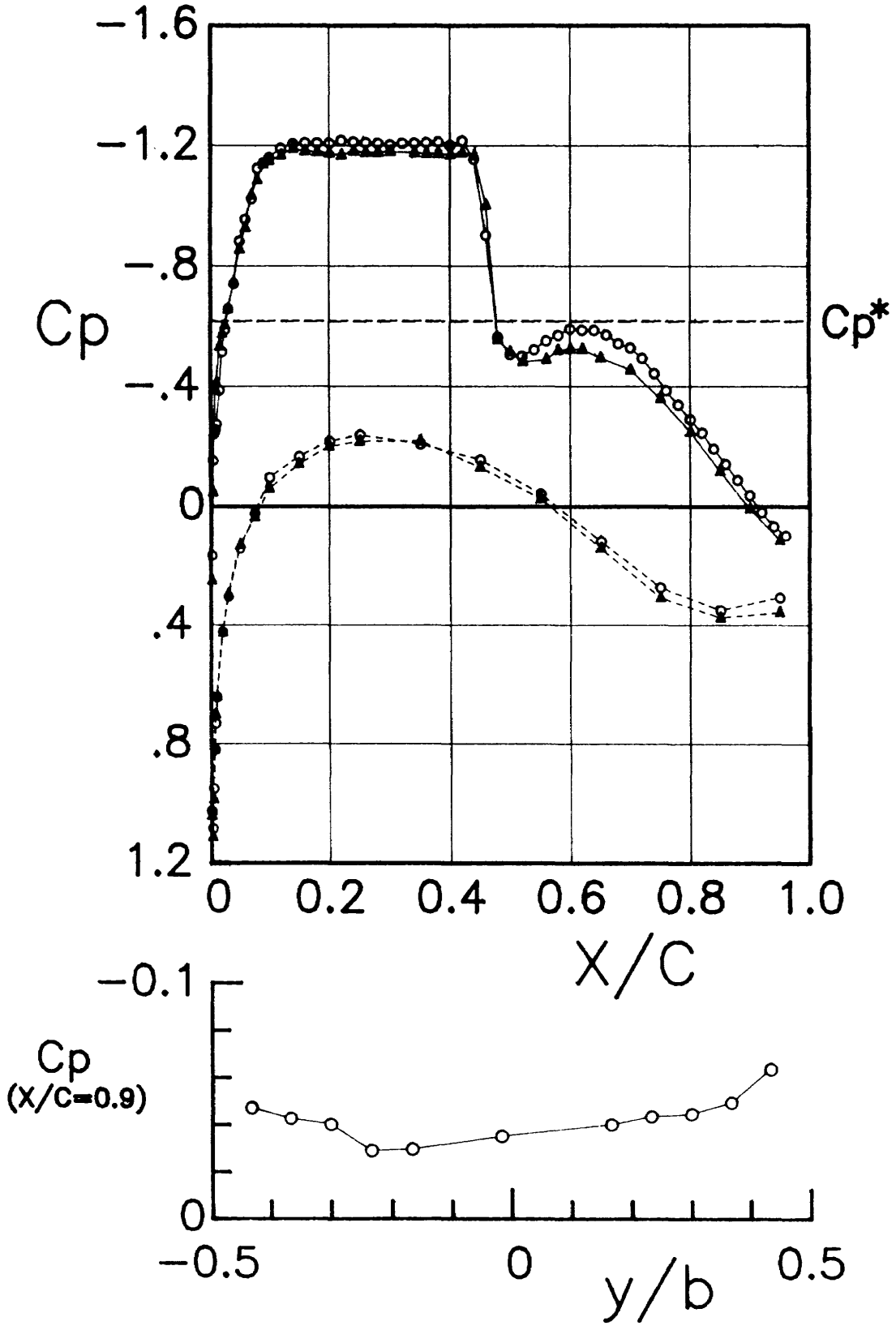

Figure A−16 Comparison of pressure distribution data measured in the NAL and IAR wind tunnels with the same lift coefficient.

	Mach	Alpha,g	Re	CL	CD	Run
O NAL	0.738	3.52	20.8 E6	0.886	0.0210	7127-3
▲ NAE	0.738	3.67	21.0 E6	0.896	0.0243	20912-5

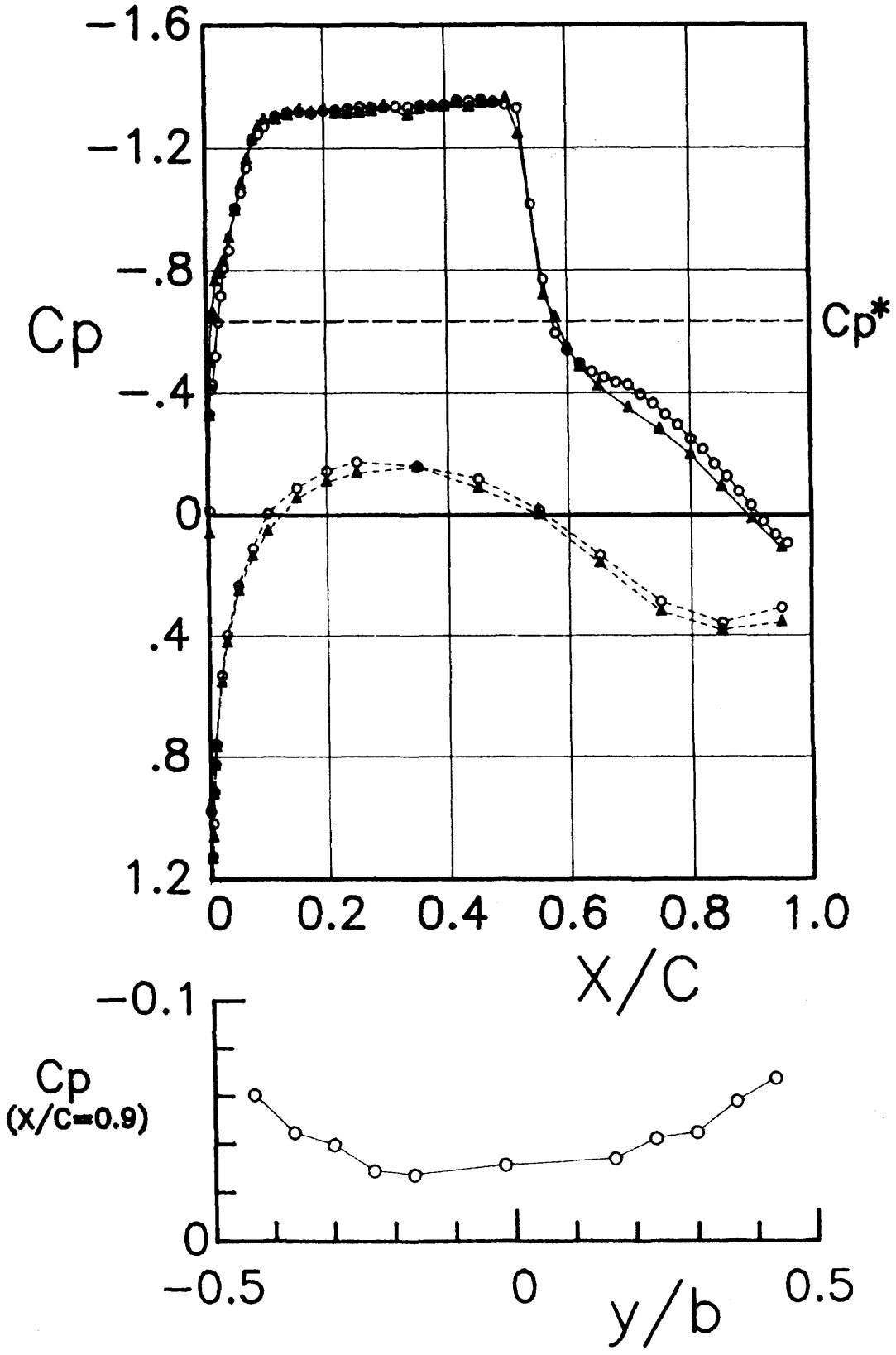

Figure A-17 Comparison of pressure distribution data measured in the NAL and IAR wind tunnels with the same lift coefficient.

		Mach	Alpha,g	Re	CL	CD	Run
O	NAL	0.736	4.62	21.0 E6	0.988	0.0436	7131−2
▲	NAE	0.736	4.68	21.0 E6	0.974	0.0425	20912−6

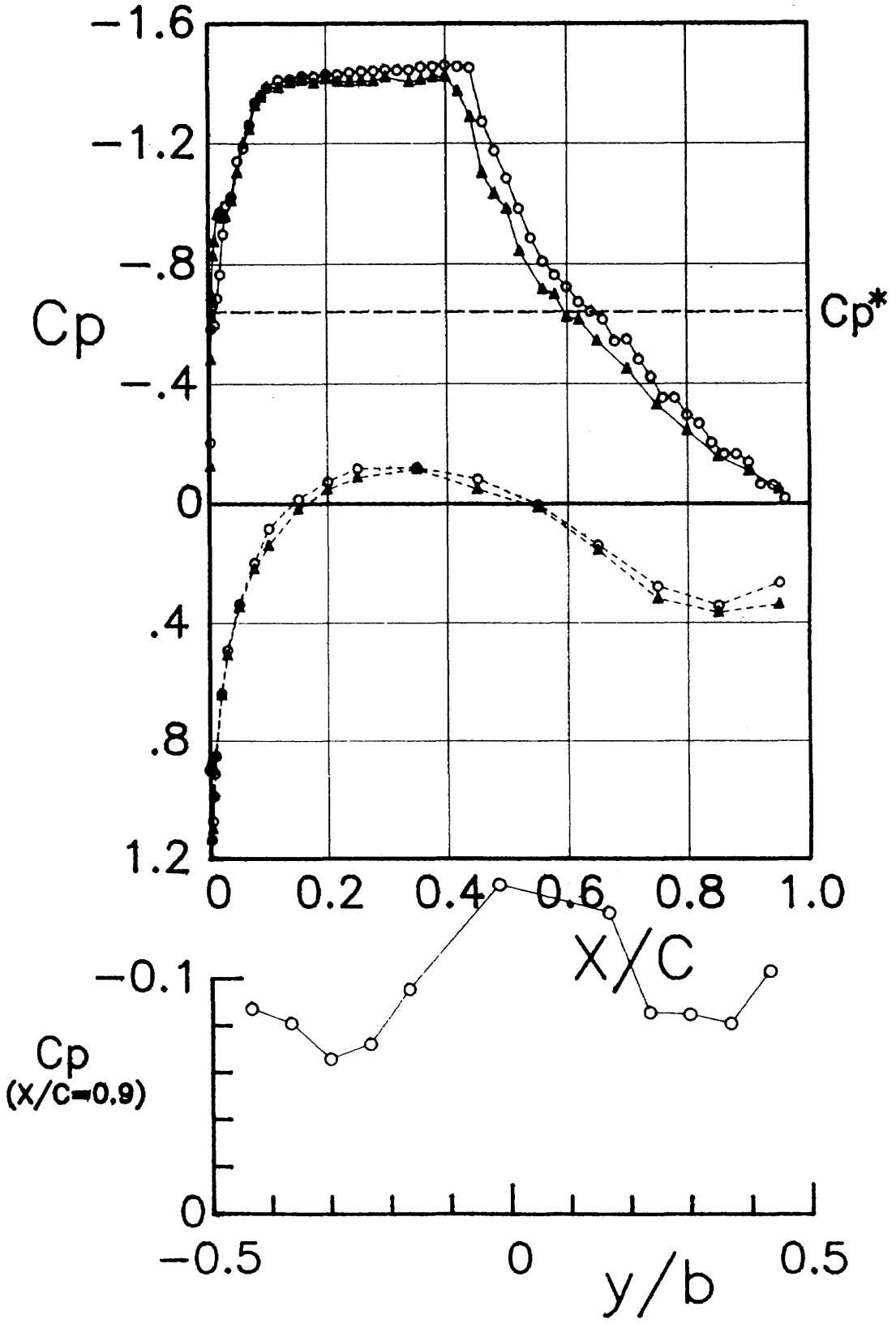

Figure A−18 Comparison of pressure distribution data measured in the NAL and IAR wind tunnels with the same lift coefficient.

	Mach	Alpha,g	Re	CL	CD	Run
○ NAL	0.769	−3.73	20.7 E6	−0.248	0.0199	7348−2
▲ NAE	0.769	−3.65	21.0 E6	−0.248	0.0236	20913−1

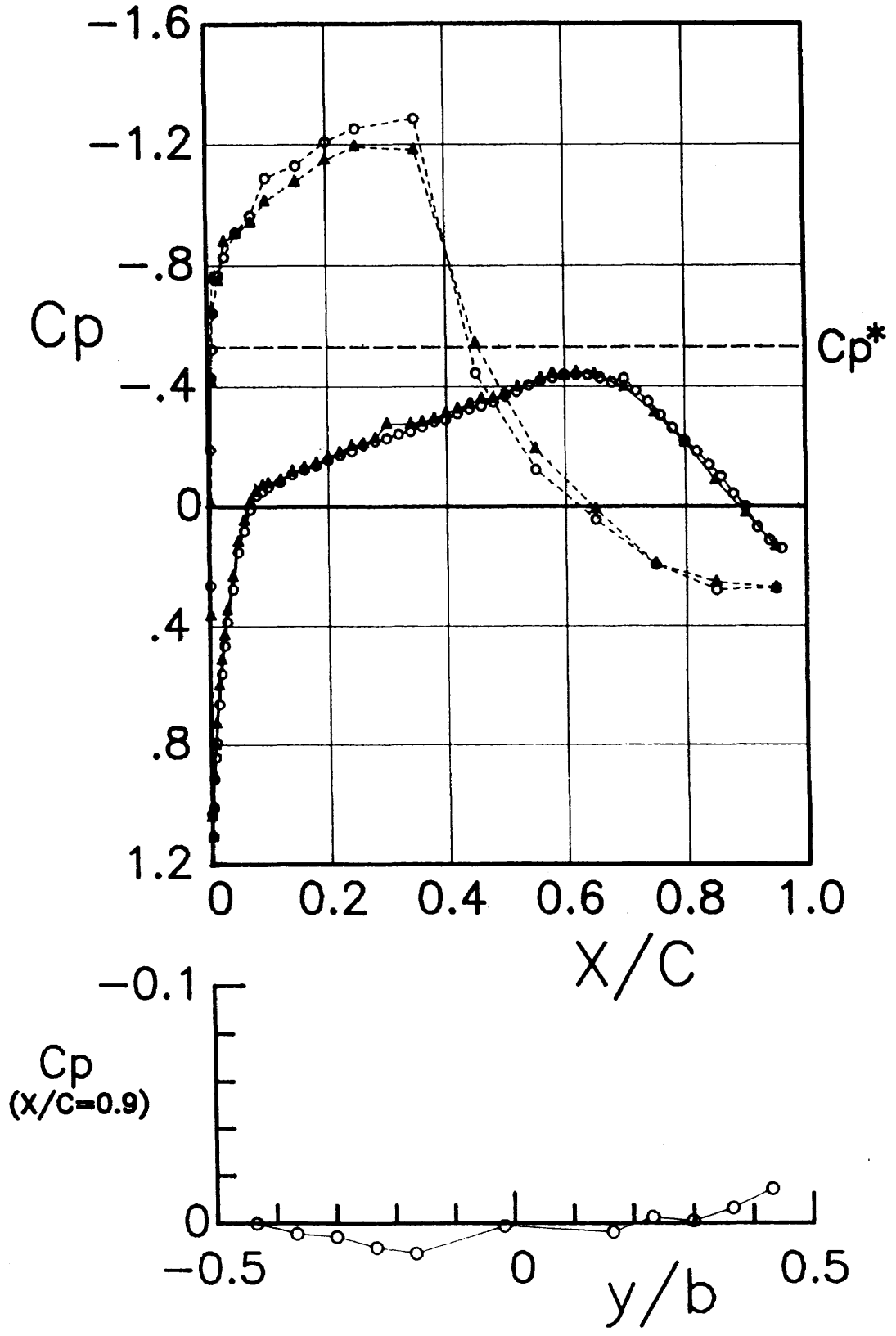

Figure A−19 Comparison of pressure distribution data measured in the NAL and IAR wind tunnels with the same lift coefficient.

	Mach	Alpha,g	Re	CL	CD	Run
○ NAL	0.767	0.01	21.2 E6	0.298	0.0074	7115−3
▲ NAE	0.767	−0.30	21.0 E6	0.292	0.0075	20913−2

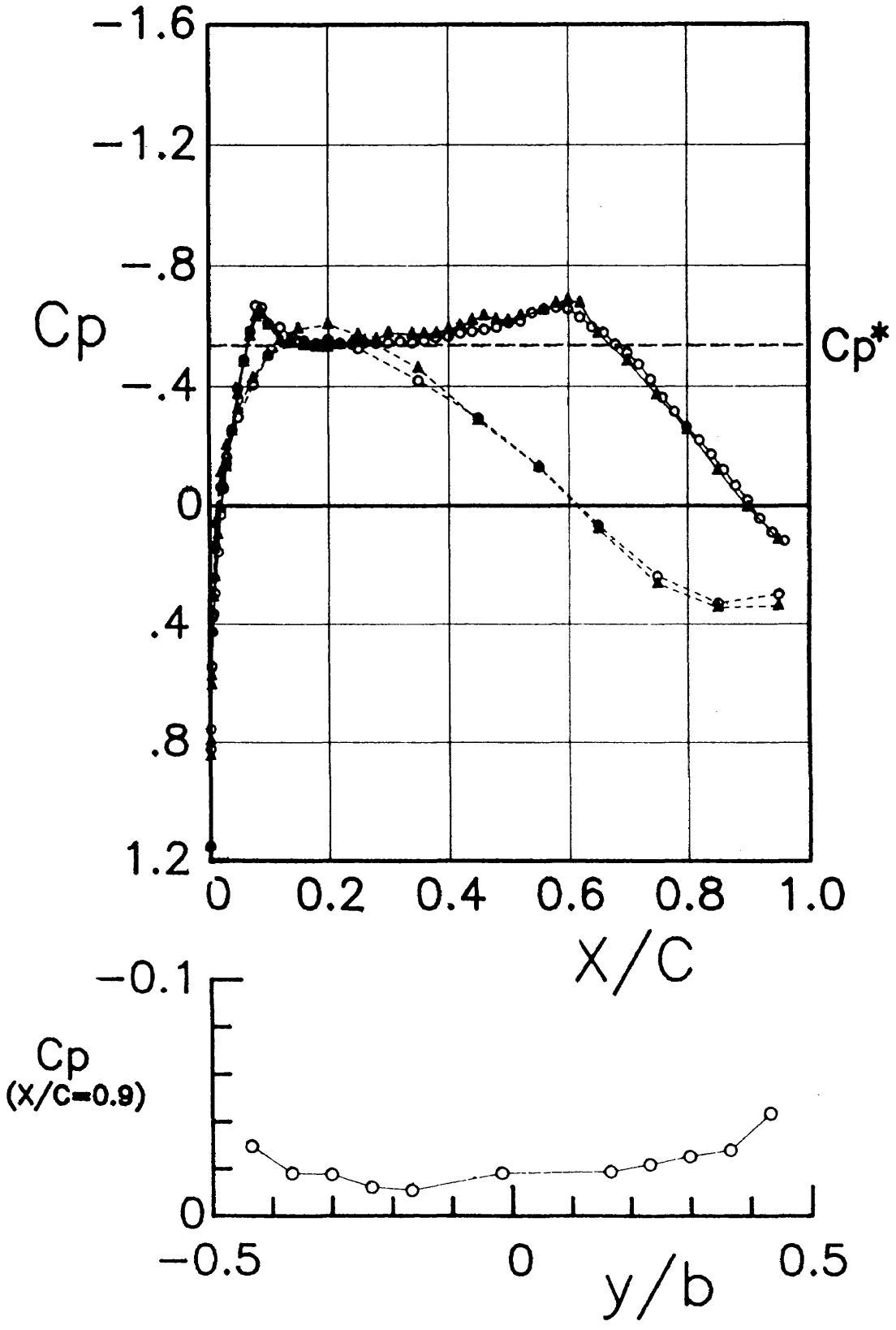

Figure A−20 Comparison of pressure distribution data measured in the NAL and IAR wind tunnels with the same lift coefficient.

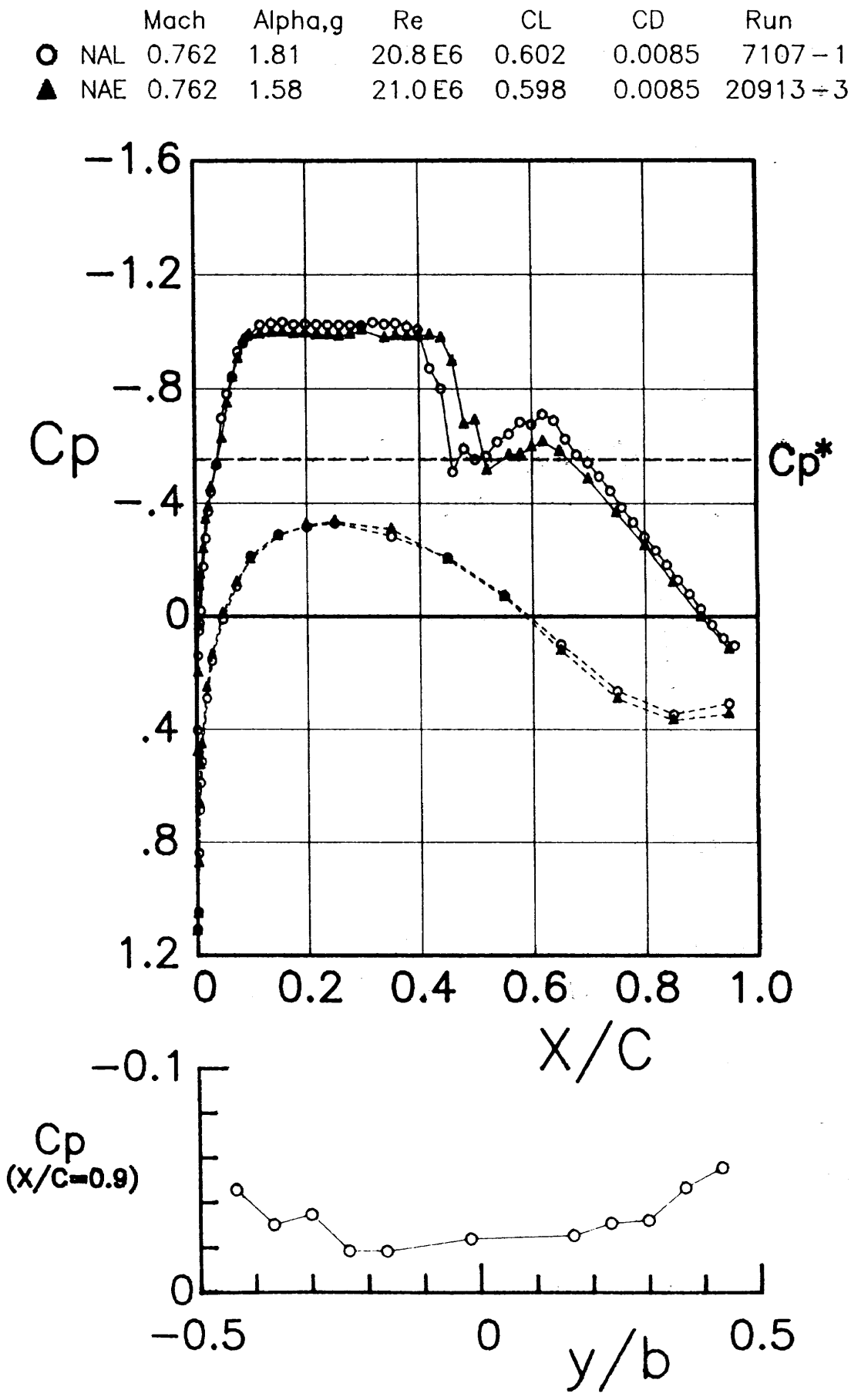

Figure A－21 Comparison of pressure distribution data measured in the NAL and IAR wind tunnels with the same lift coefficient.

	Mach	Alpha,g	Re	CL	CD	Run
○ NAL	0.760	2.62	21.1 E6	0.754	0.0130	7116−2
▲ NAE	0.760	2.58	21.0 E6	0.767	0.0162	20913−4

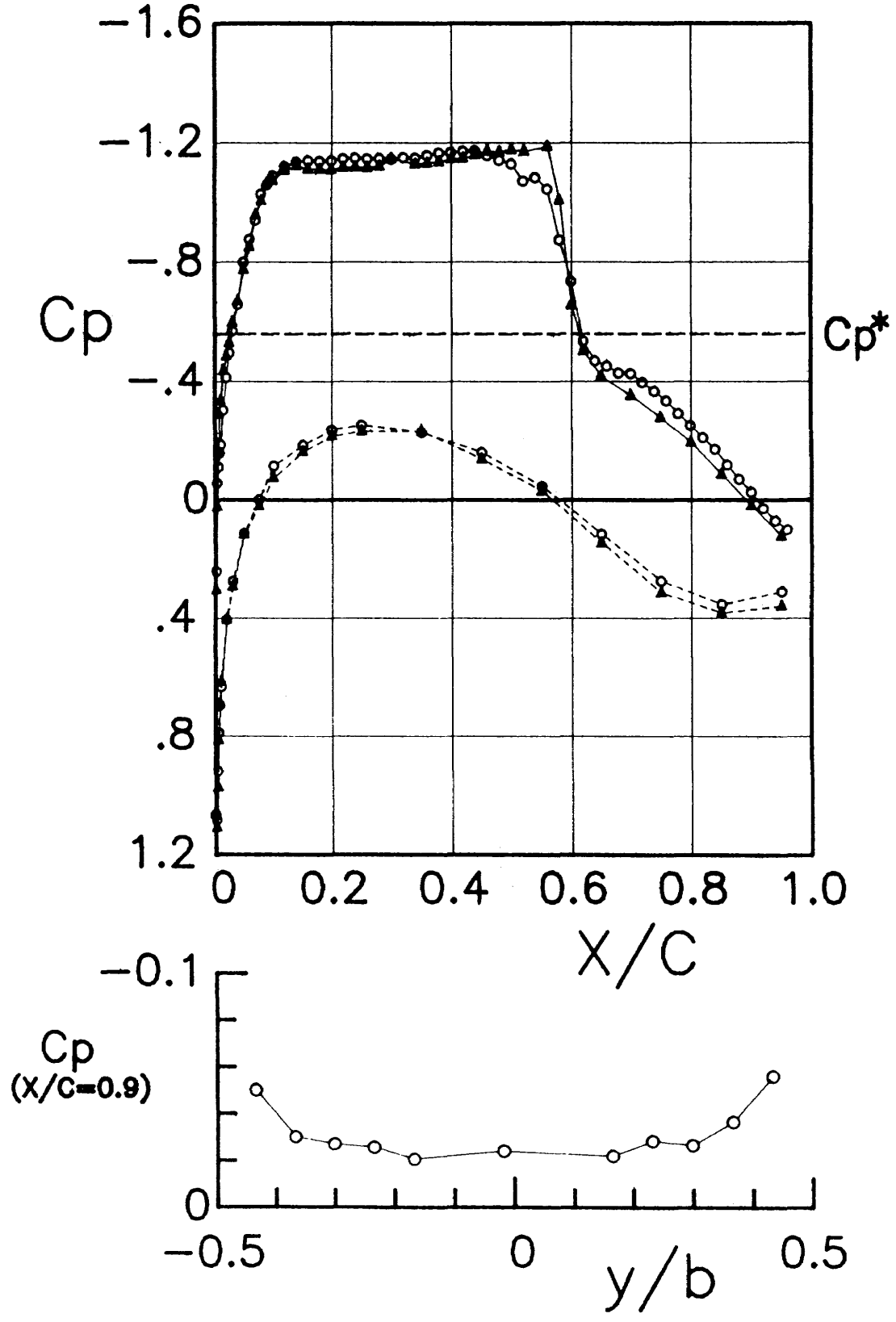

Figure A−22 Comparison of pressure distribution data measured in the NAL and IAR wind tunnels with the same lift coefficient.

	Mach	Alpha,g	Re	CL	CD	Run
○ NAL	0.758	3.51	21.1 E6	0.888	0.0302	7117−3
▲ NAE	0.757	3.60	21.0 E6	0.883	0.0312	20913−5

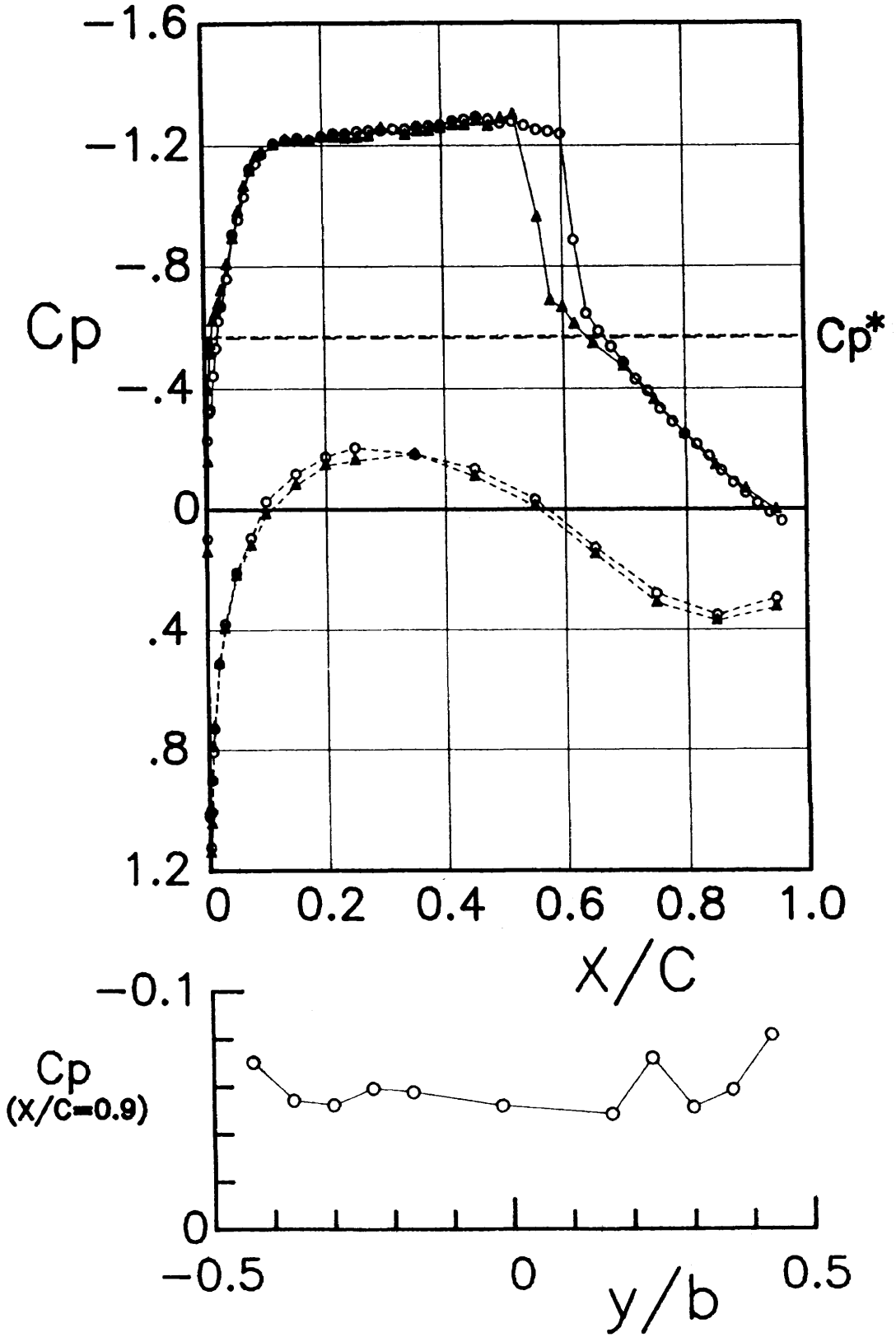

Figure A−23 Comparison of pressure distribution data measured in the NAL and IAR wind tunnels with the same lift coefficient.

	Mach	Alpha,g	Re	CL	CD	Run
○ NAL	0.755	4.72	20.7 E6	0.888	0.0609	7349−3
▲ NAE	0.755	4.63	21.0 E6	0.865	0.0513	20913−6

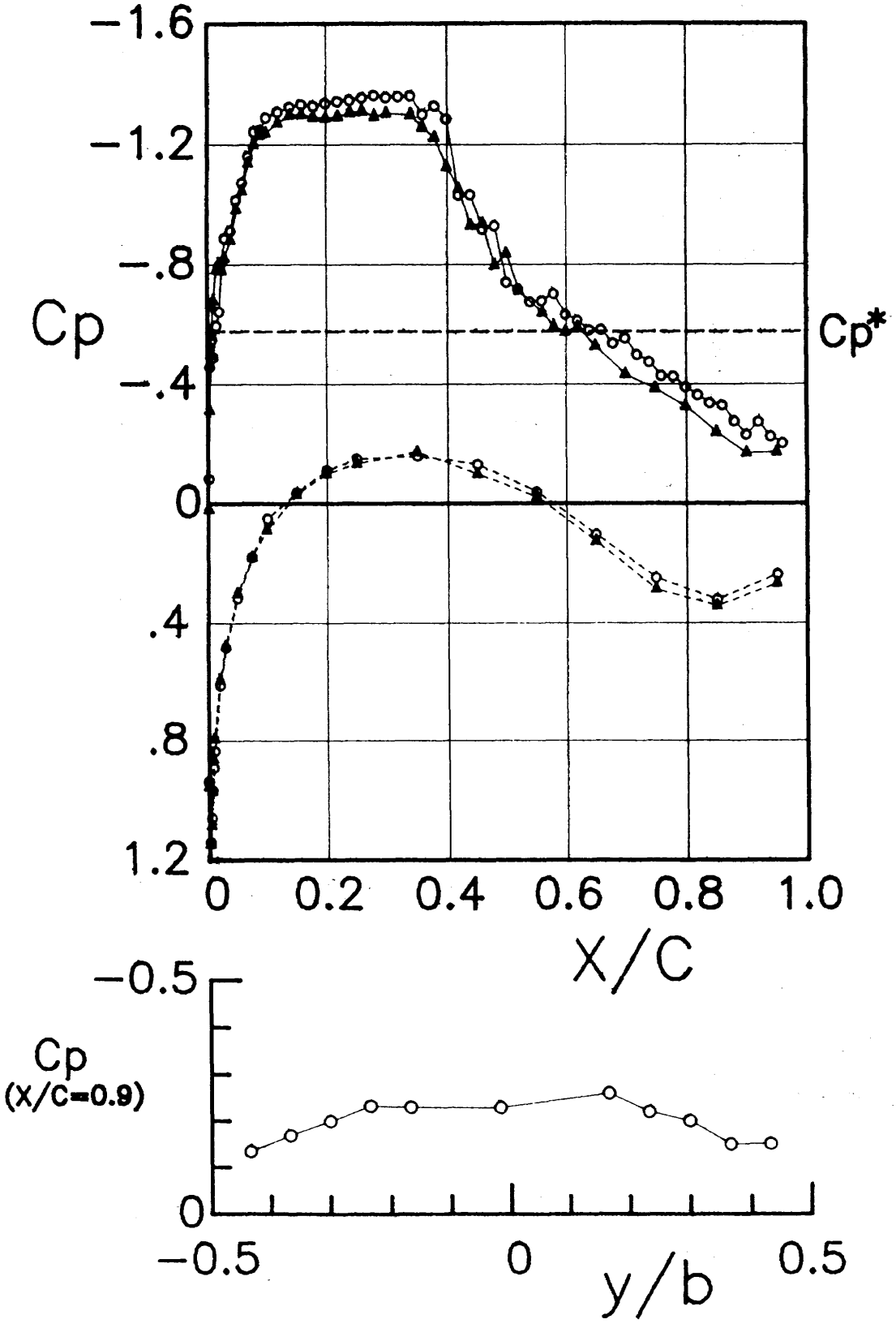

Figure A−24 Comparison of pressure distribution data measured in the NAL and IAR wind tunnels with the same lift coefficient.

	Mach	Alpha,g	Re	CL	CD	Run
○ NAL	0.778	−3.52	20.8 E6	−0.221	0.0208	7353−1
▲ NAE	0.778	−3.62	21.0 E6	−0.213	0.0304	20914−1

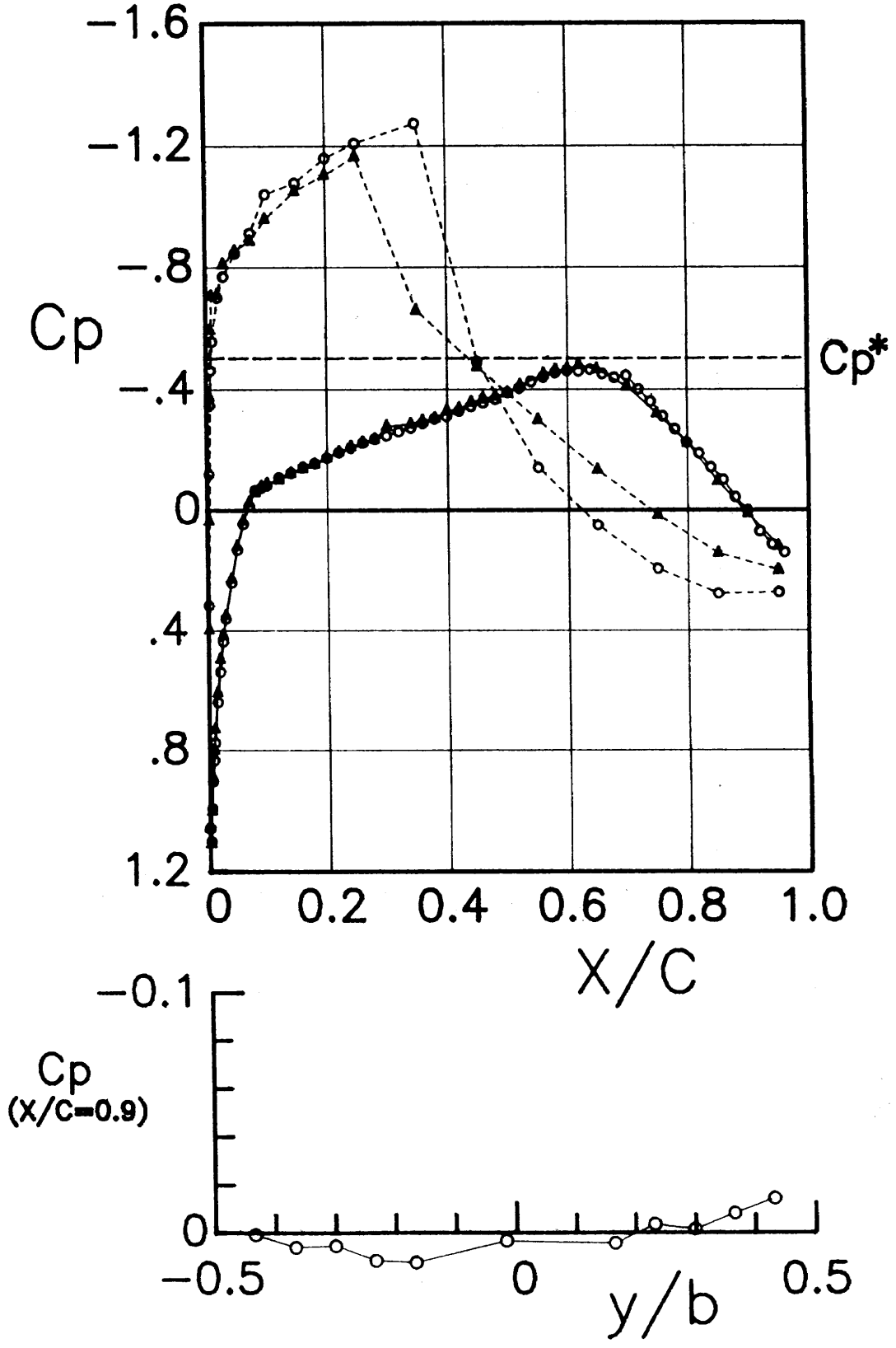

Figure A−25 Comparison of pressure distribution data measured in the NAL and IAR wind tunnels with the same lift coefficient.

	Mach	Alpha,g	Re	CL	CD	Run
○ NAL	0.777	−0.10	21.3 E6	0.299	0.0075	7361−1
▲ NAE	0.777	−0.30	21.0 E6	0.297	0.0076	20914−2

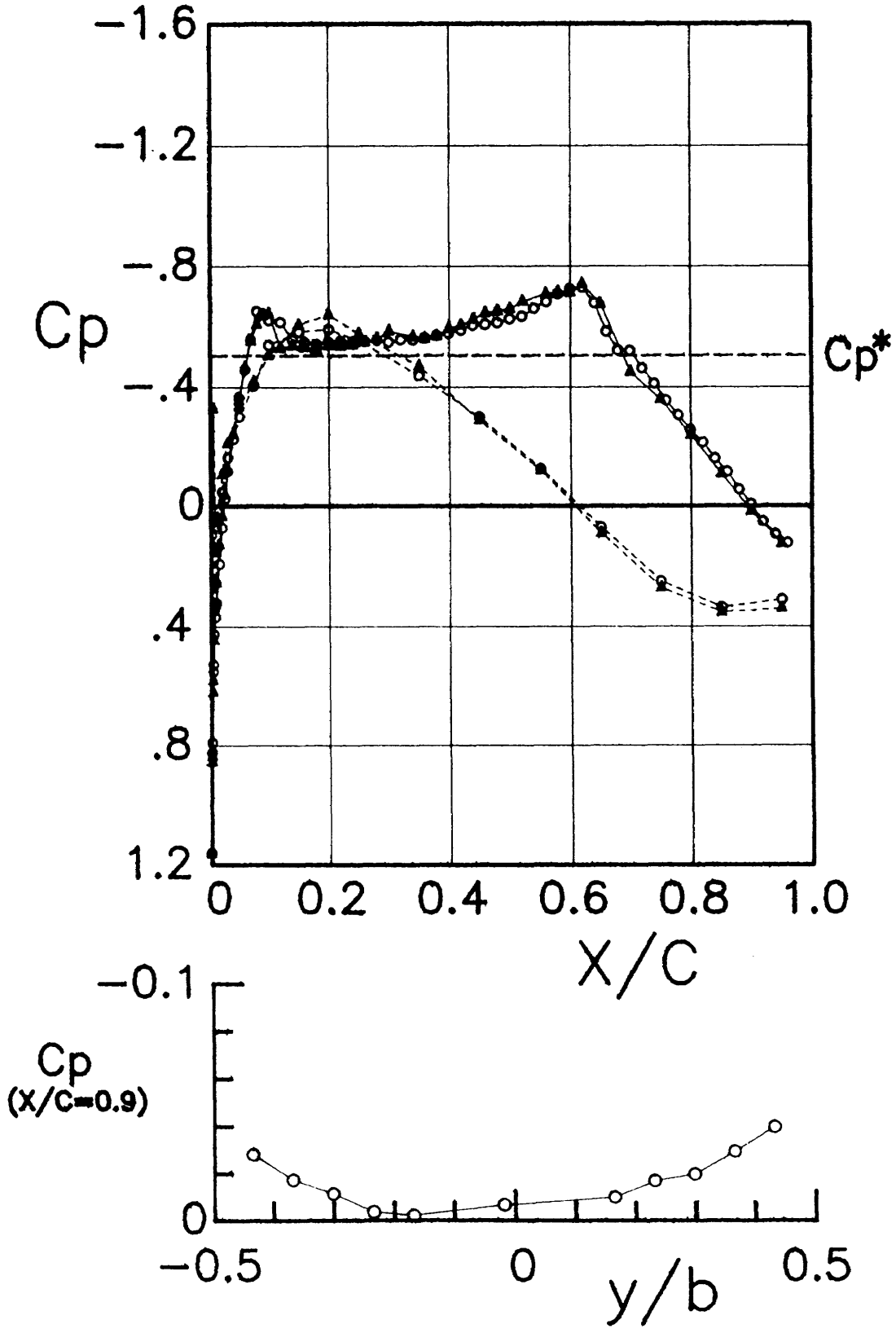

Figure A−26 Comparison of pressure distribution data measured in the NAL and IAR wind tunnels with the same lift coefficient.

	Mach	Alpha,g	Re	CL	CD	Run
○ NAL	0.772	1.81	21.1 E6	0.610	0.0083	7108−3
▲ NAE	0.772	1.57	21.0 E6	0.612	0.0093	20914−3

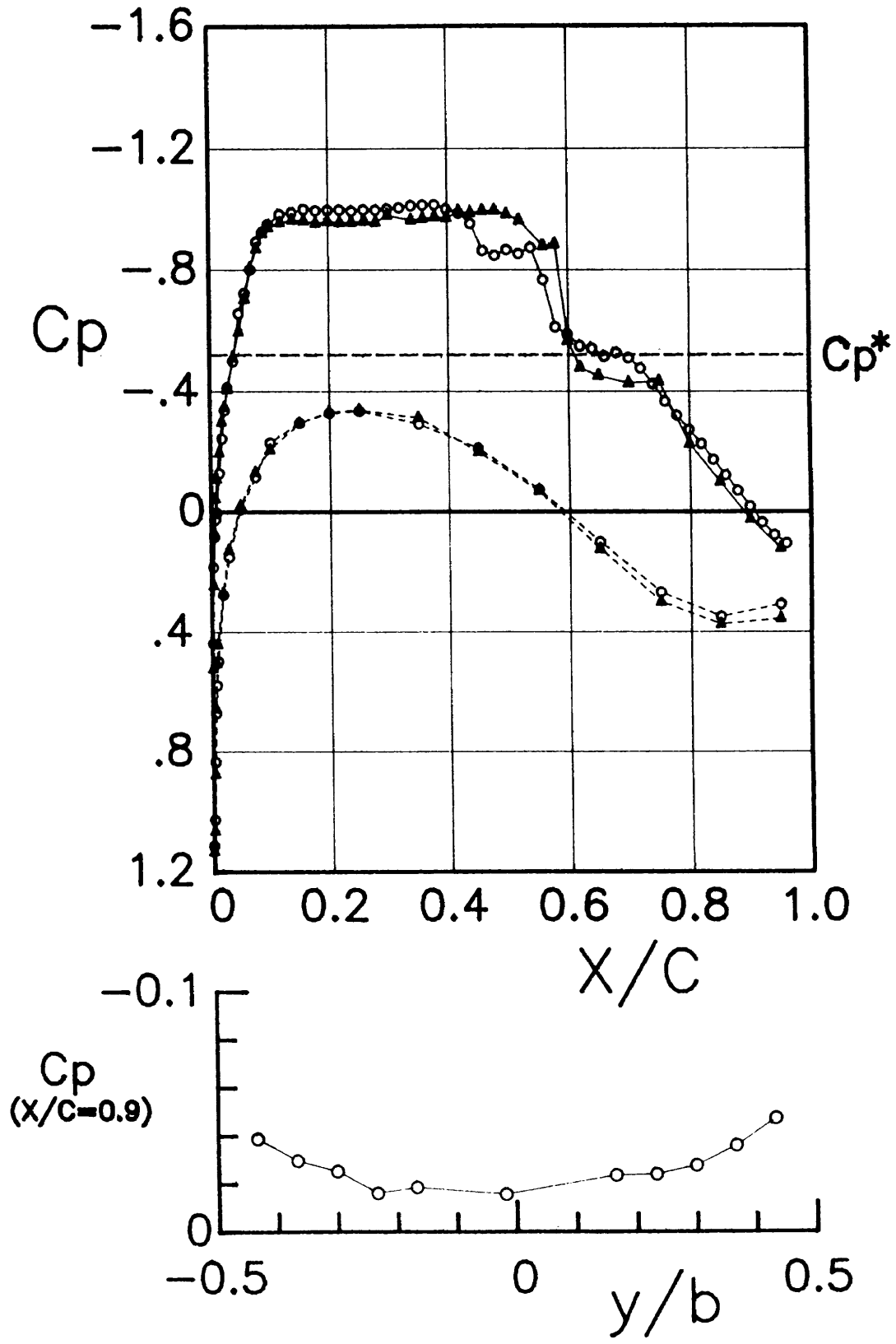

Figure A−27 Comparison of pressure distribution data measured in the NAL and IAR wind tunnels with the same lift coefficient.

		Mach	Alpha,g	Re	CL	CD	Run
O	NAL	0.769	2.62	21.3 E6	0.775	0.0165	7101 – 1
▲	NAE	0.769	2.56	21.0 E6	0.775	0.0197	20914 – 4

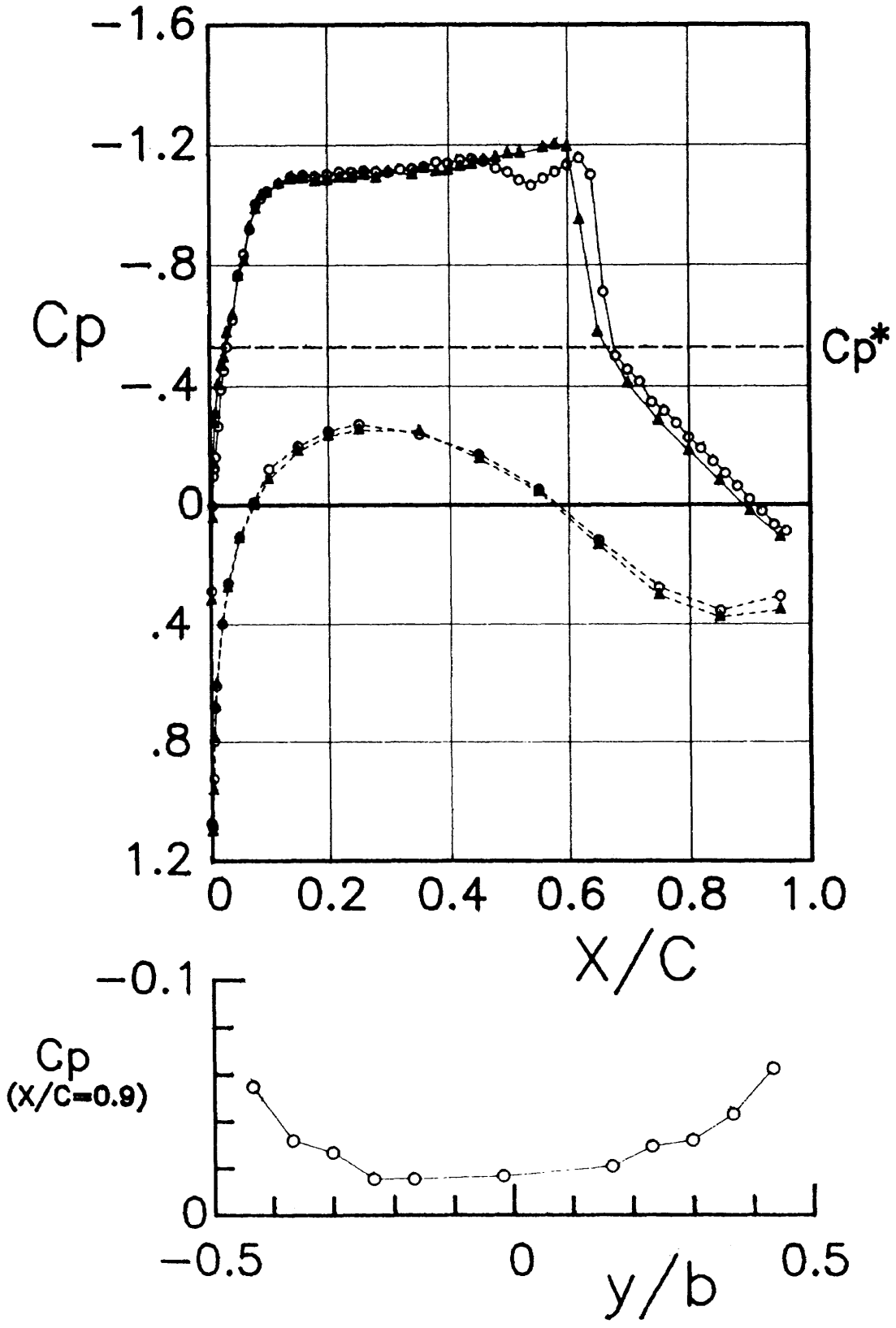

Figure A – 28 Comparison of pressure distribution data measured in the NAL and IAR wind tunnels with the same lift coefficient.

	Mach	Alpha,g	Re	CL	CD	Run
○ NAL	0.768	3.11	21.0 E6	0.831	0.0286	7351−2
▲ NAE	0.768	3.58	21.0 E6	0.815	0.0360	20914−5

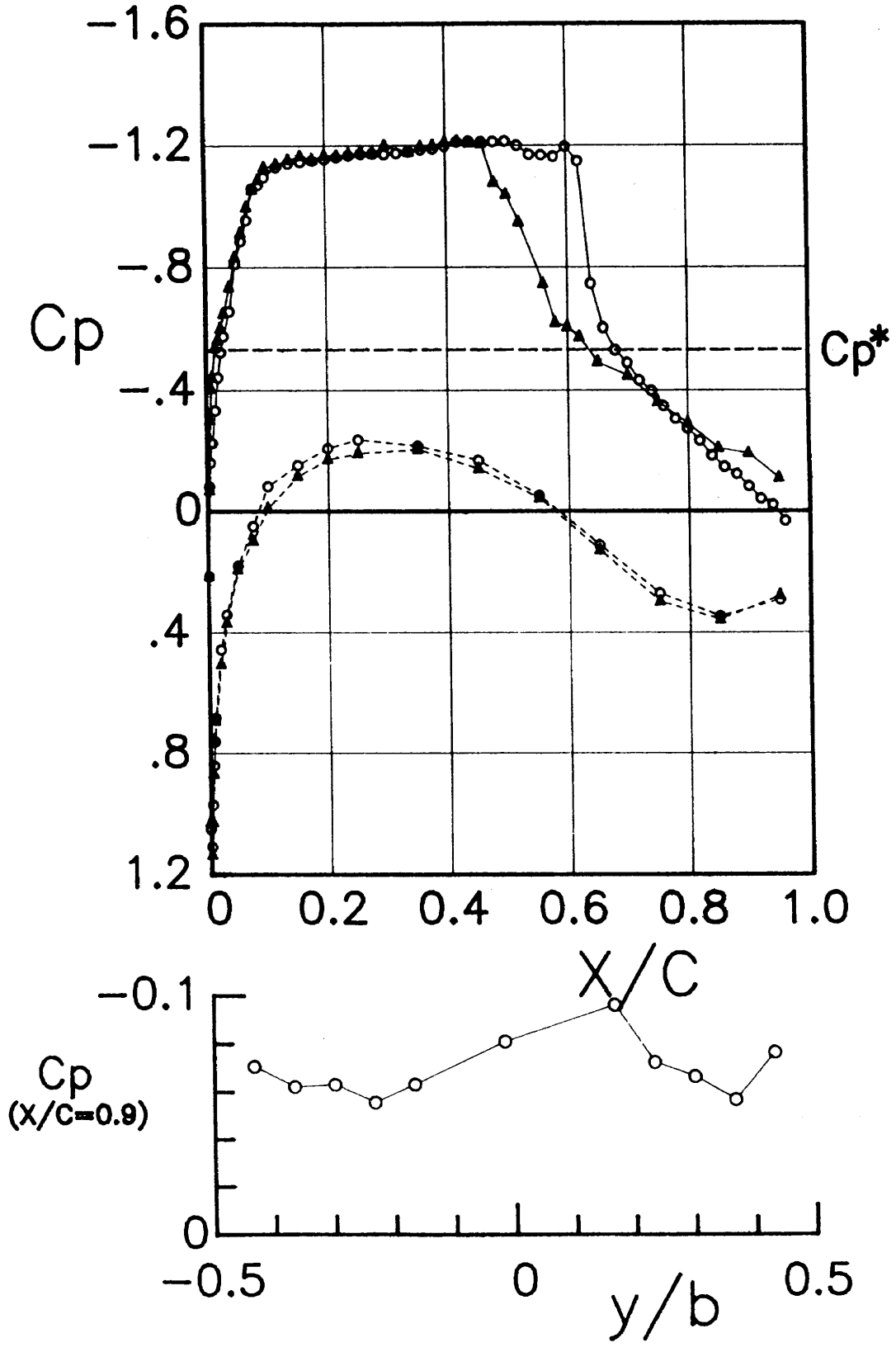

Figure A−29 Comparison of pressure distribution data measured in the NAL and IAR wind tunnels with the same lift coefficient.

		Mach	Alpha,g	Re	CL	CD	Run
O	NAL	0.768	4.52	21.1 E6	0.829	0.0654	7351−3
▲	NAE	0.767	4.60	21.0 E6	0.815	0.0563	20914−6

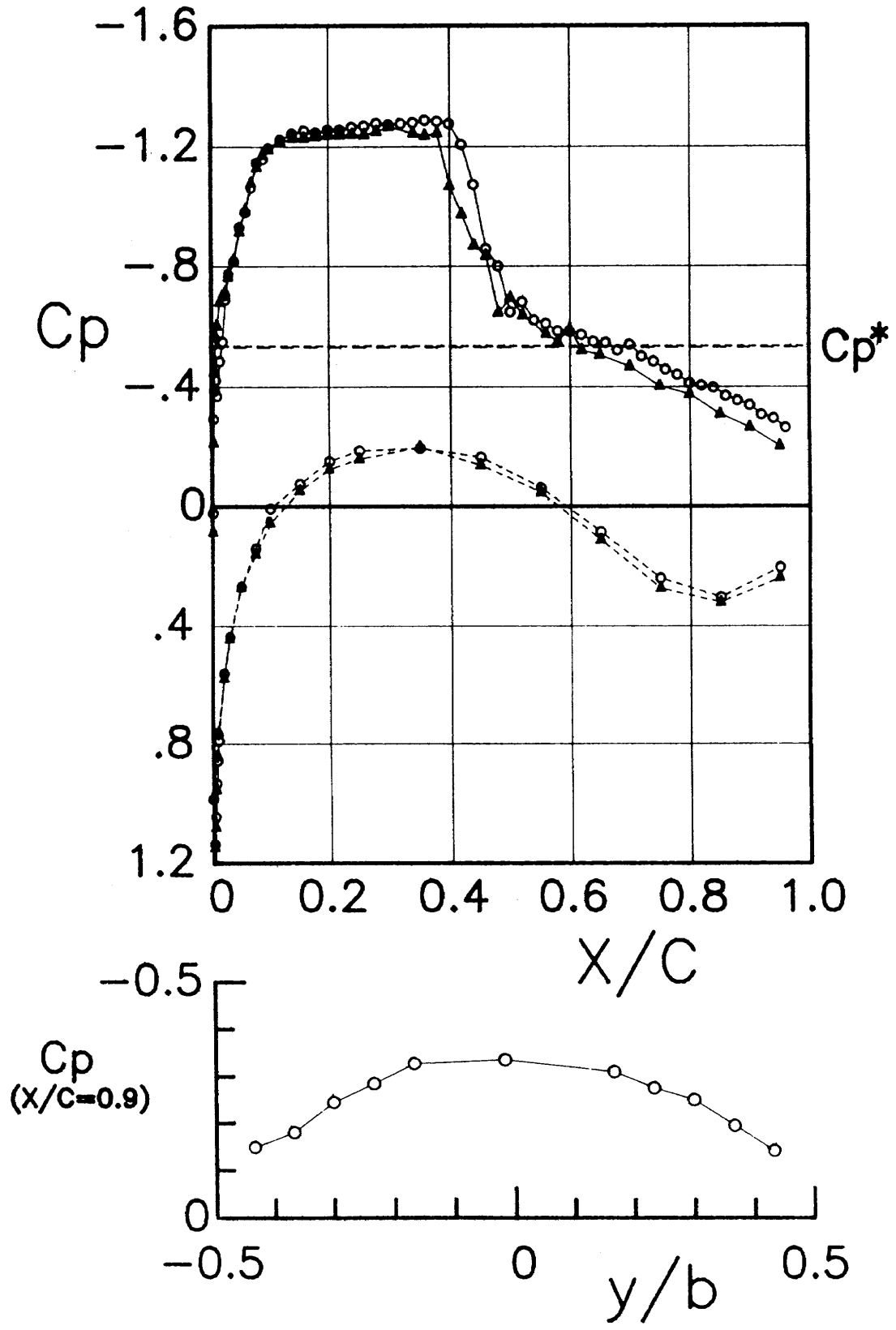

Figure A−30 Comparison of pressure distribution data measured in the NAL and IAR wind tunnels with the same lift coefficient.

	Mach	Alpha,g	Re	CL	CD	Run
○ NAL	0.795	−3.43	20.4 E6	−0.195	0.0344	7357−1
▲ NAE	0.796	−3.58	21.0 E6	−0.197	0.0426	20915−1

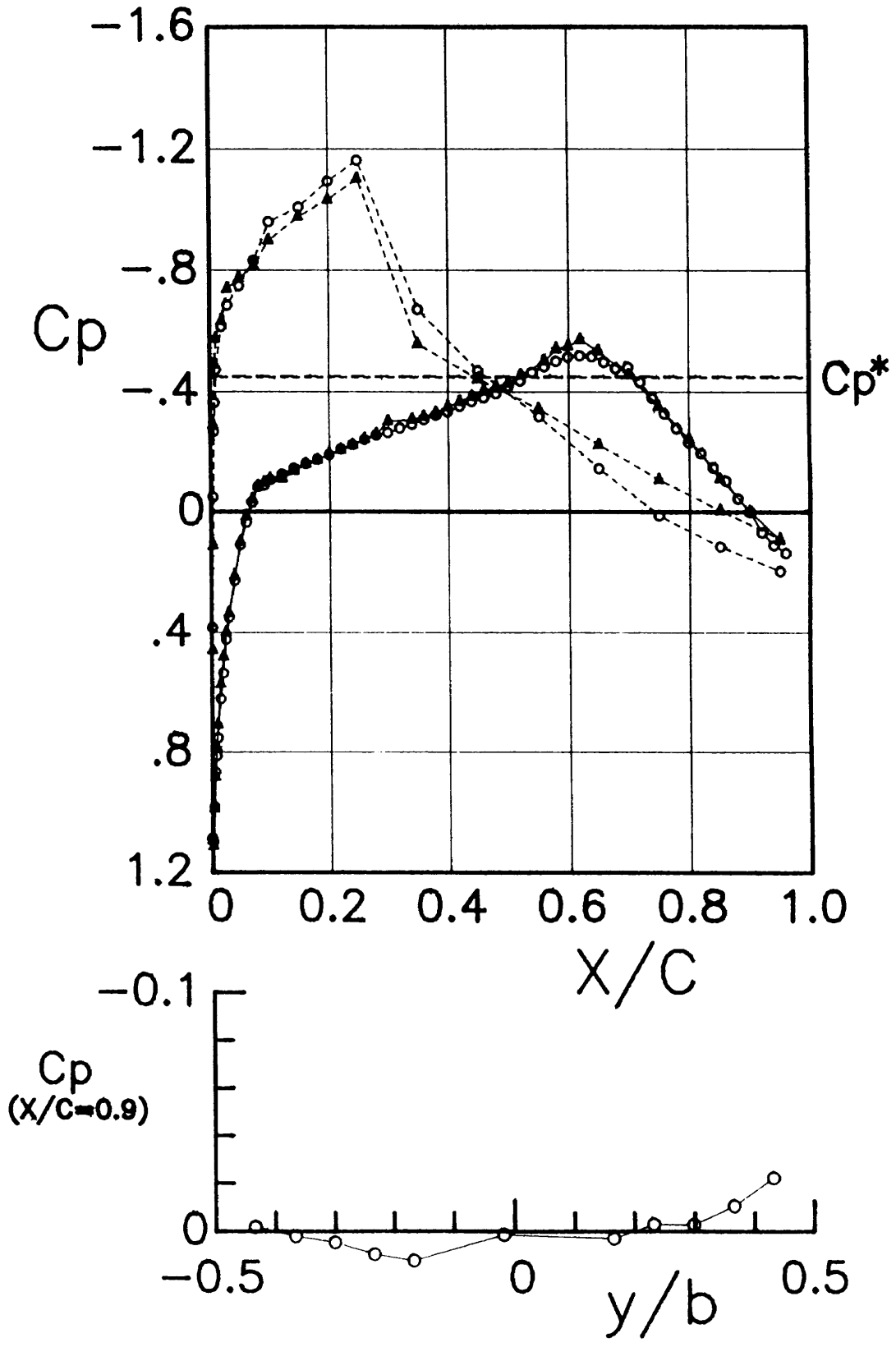

Figure A−31 Comparison of pressure distribution data measured in the NAL and IAR wind tunnels with the same lift coefficient.

		Mach	Alpha,g	Re	CL	CD	Run
O	NAL	0.798	0.00	20.4 E6	0.320	0.0091	7359−1
▲	NAE	0.797	−0.33	21.0 E6	0.315	0.0096	20915−2

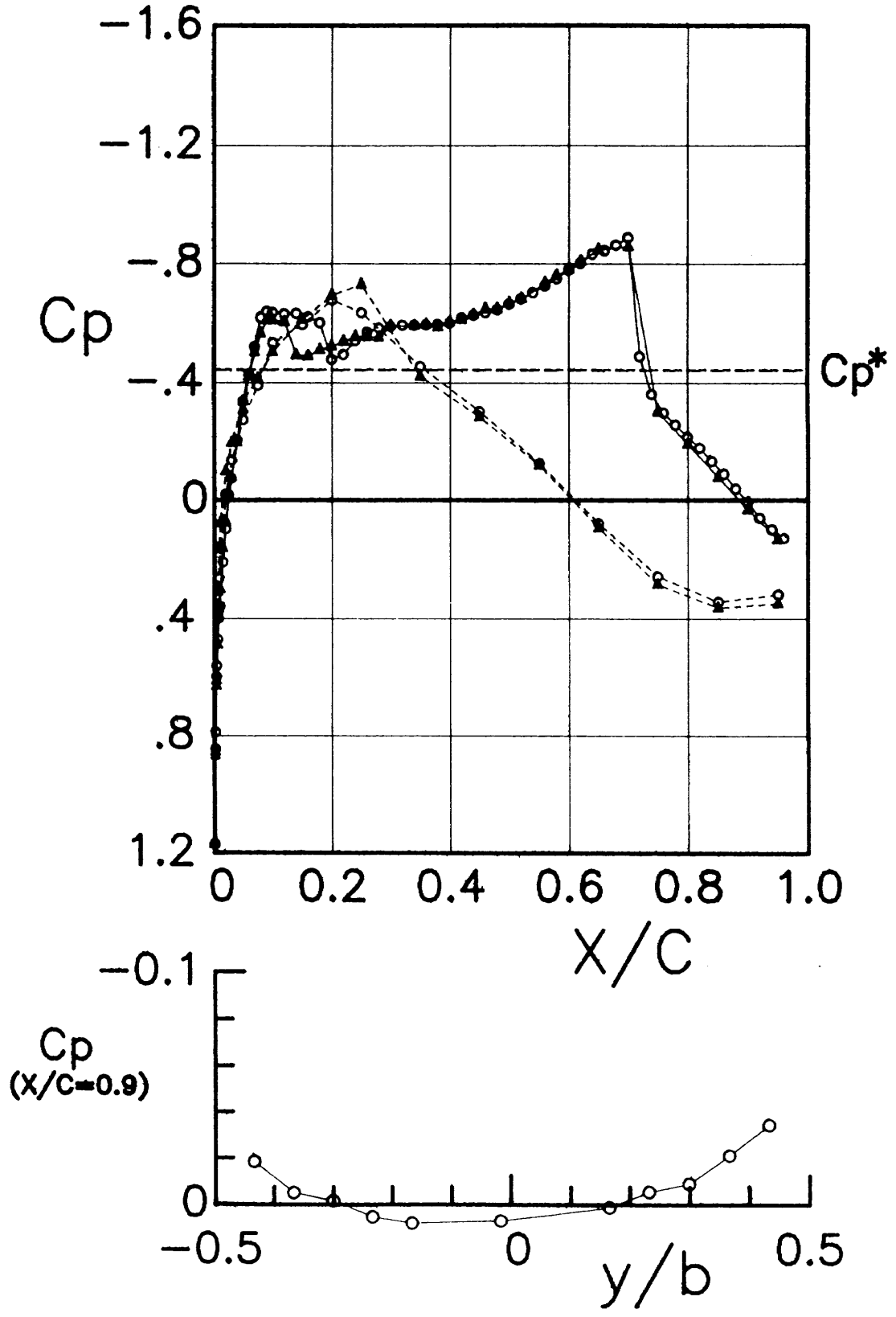

Figure A−32 Comparison of pressure distribution data measured in the NAL and IAR wind tunnels with the same lift coefficient.

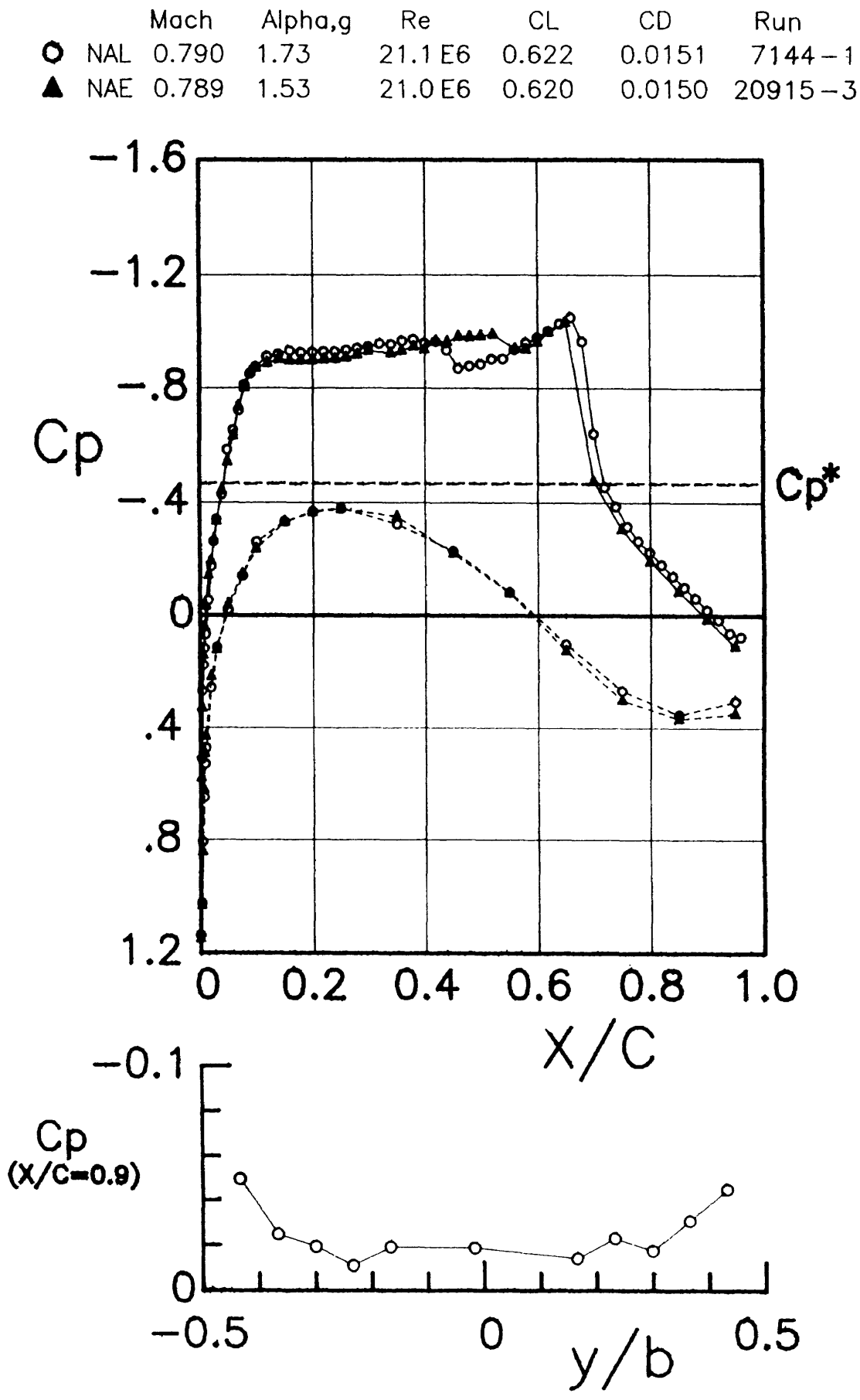

Figure A−33 Comparison of pressure distribution data measured in the NAL and IAR wind tunnels with the same lift coefficient.

		Mach	Alpha,g	Re	CL	CD	Run
○	NAL	0.787	2.52	21.0 E6	0.709	0.0244	7113−2
▲	NAE	0.787	2.52	21.0 E6	0.713	0.0317	20915−4

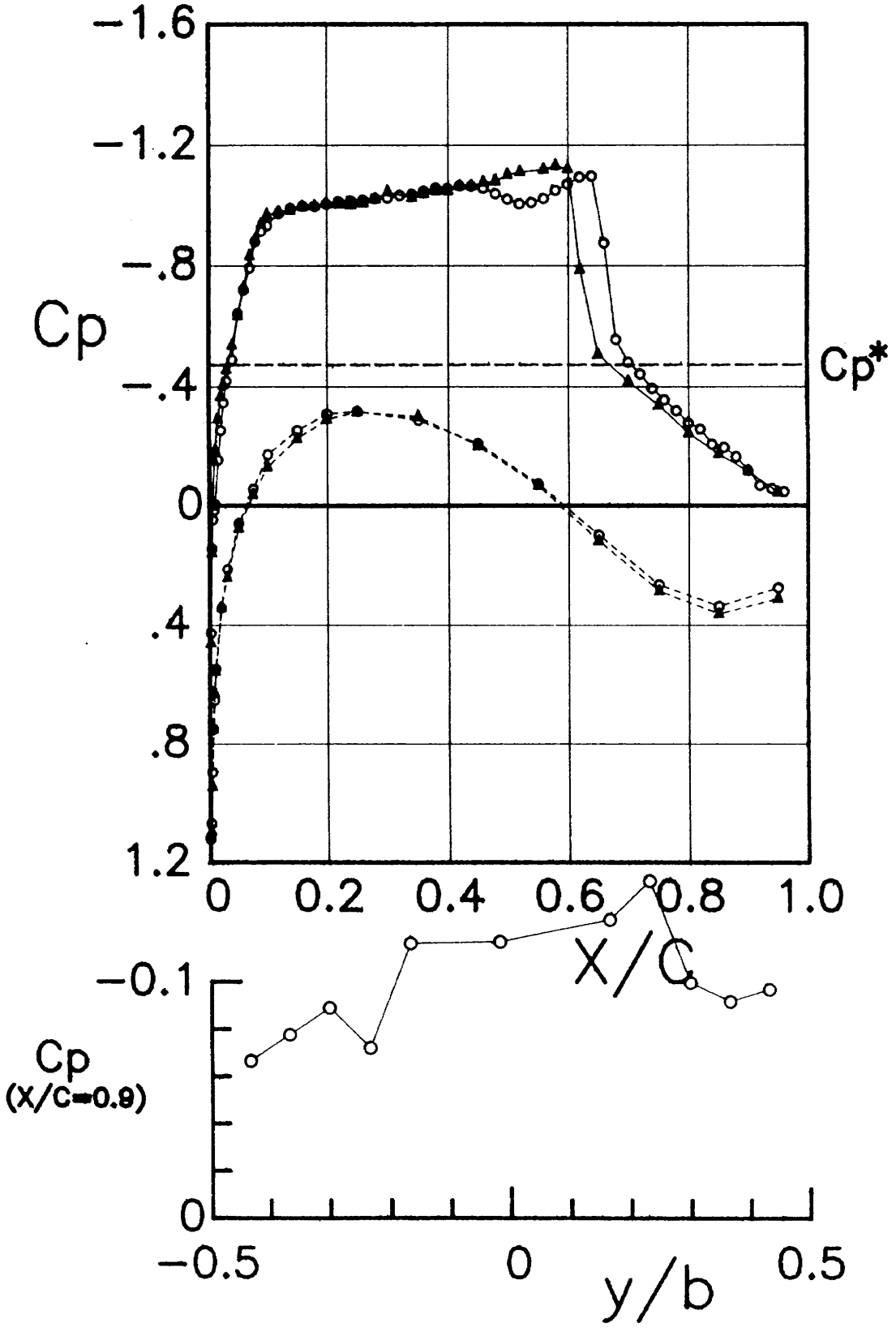

Figure A−34 Comparison of pressure distribution data measured in the NAL and IAR wind tunnels with the same lift coefficient.

	Mach	Alpha,g	Re	CL	CD	Run
○ NAL	0.786	2.91	21.2 E6	0.755	0.0312	7364−2
▲ NAE	0.786	3.54	21.0 E6	0.721	0.0448	20915−5

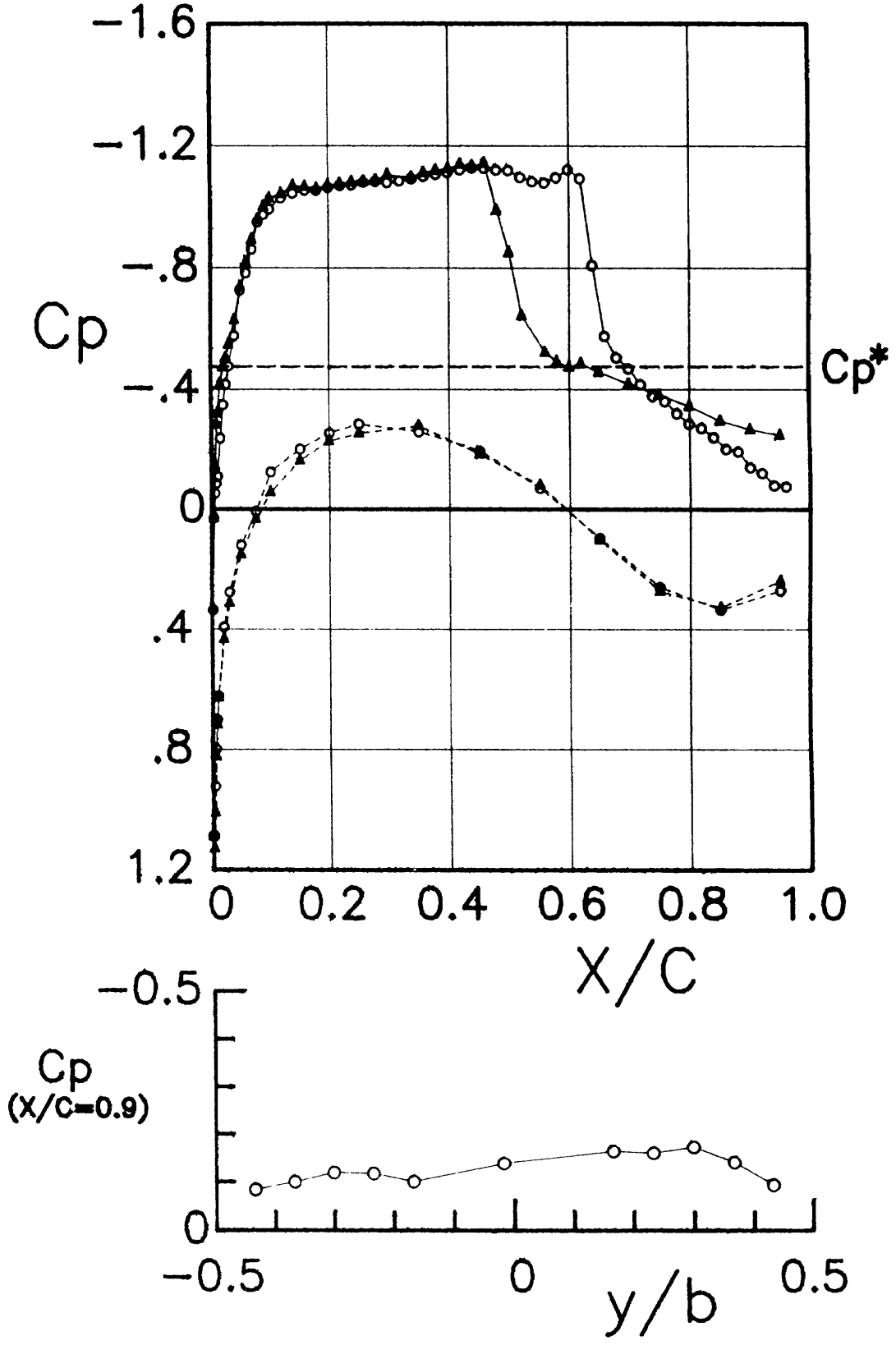

Figure A−35 Comparison of pressure distribution data measured in the NAL and IAR wind tunnels with the same lift coefficient.

	Mach	Alpha,g	Re	CL	CD	Run
○ NAL	0.786	4.42	21.2 E6	0.766	0.0672	7363−2
▲ NAE	0.786	4.55	21.0 E6	0.743	0.0618	20915−6

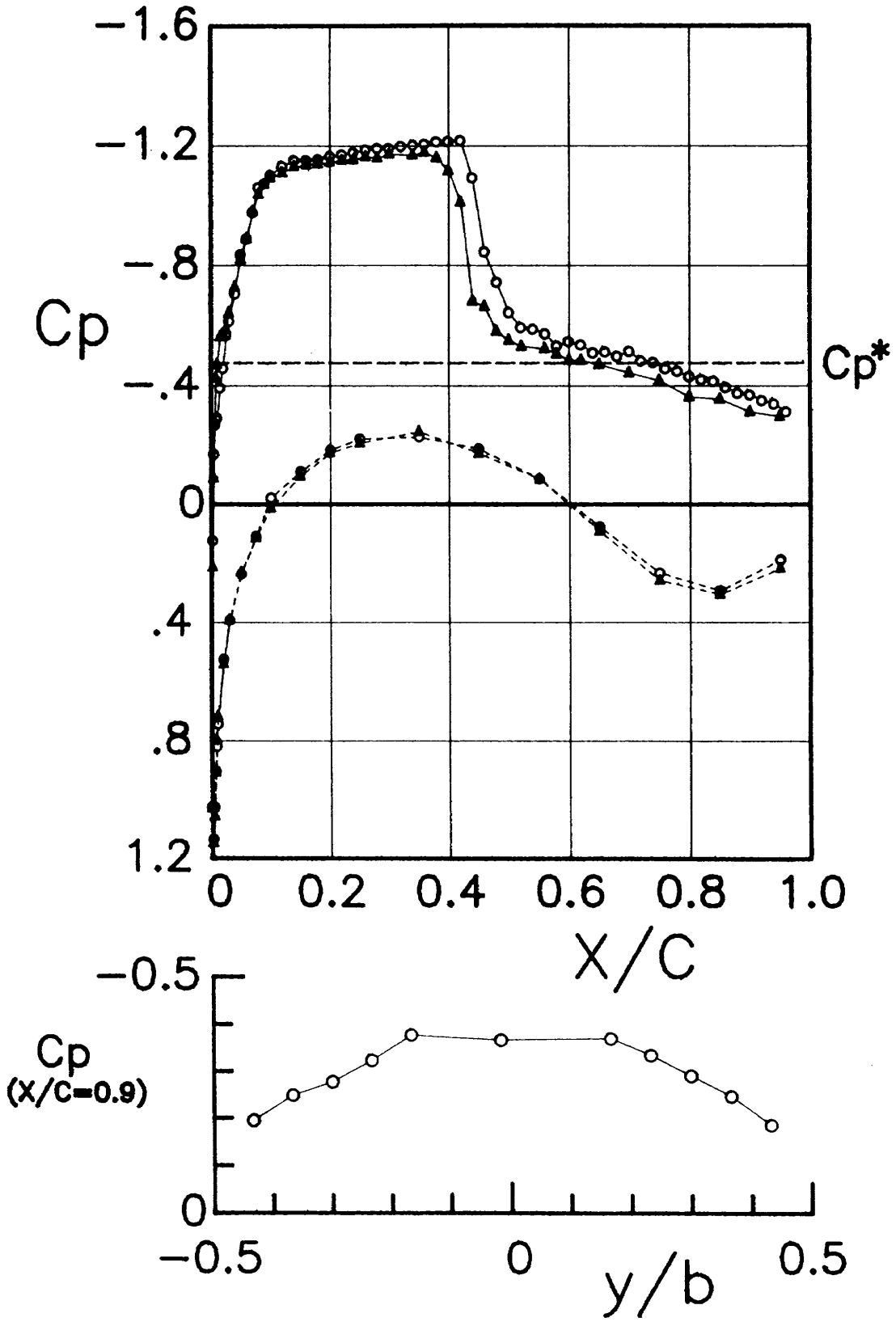

Figure A−36 Comparison of pressure distribution data measured in the NAL and IAR wind tunnels with the same lift coefficient.

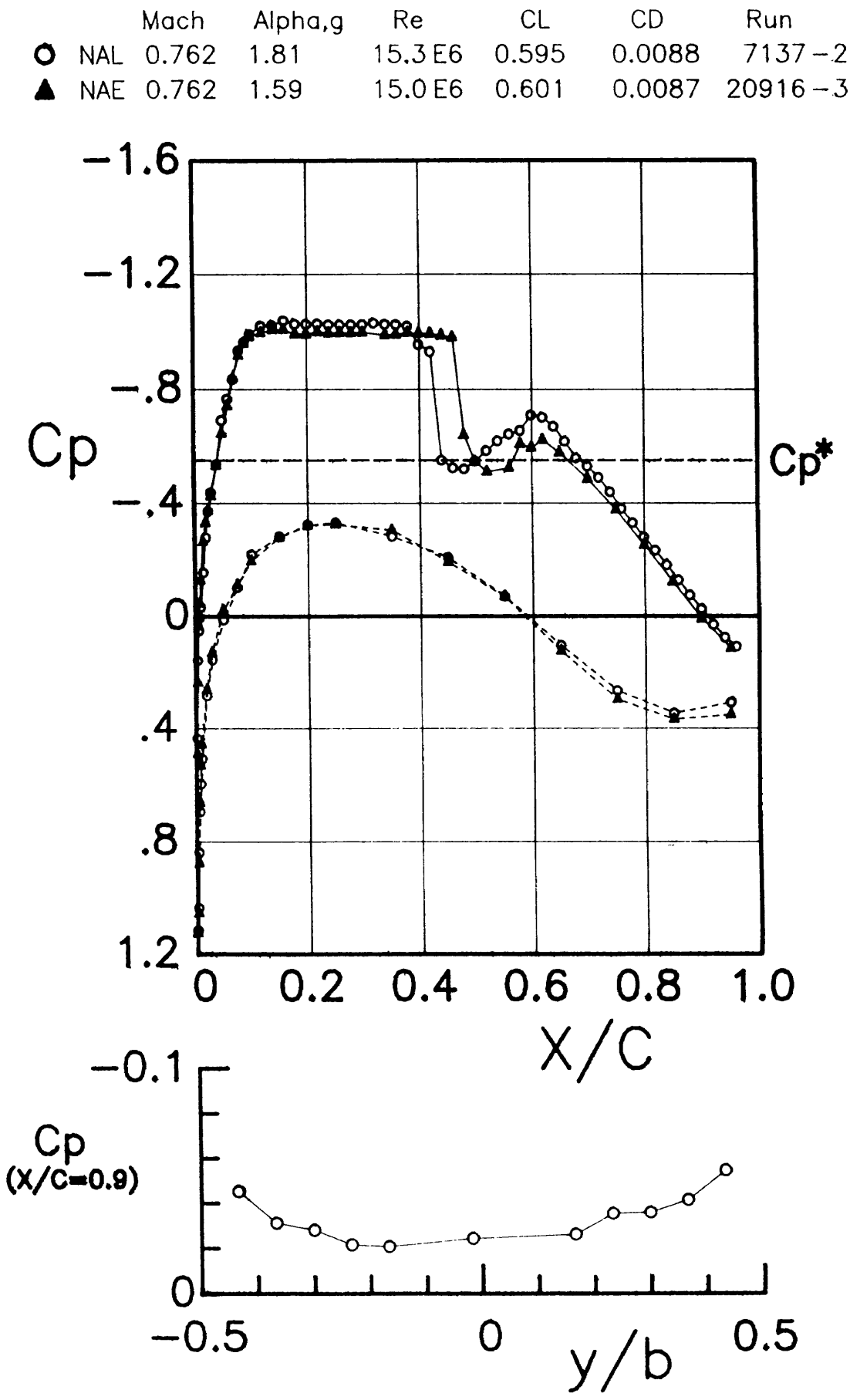

Figure A−37 Comparison of pressure distribution data measured in the NAL and IAR wind tunnels with the same lift coefficient.

		Mach	Alpha,g	Re	CL	CD	Run
O	NAL	0.760	1.75	30.0 E6	0.577	0.0081	7141−1
▲	NAE	0.760	1.51	32.0 E6	0.581	0.0076	20919−1

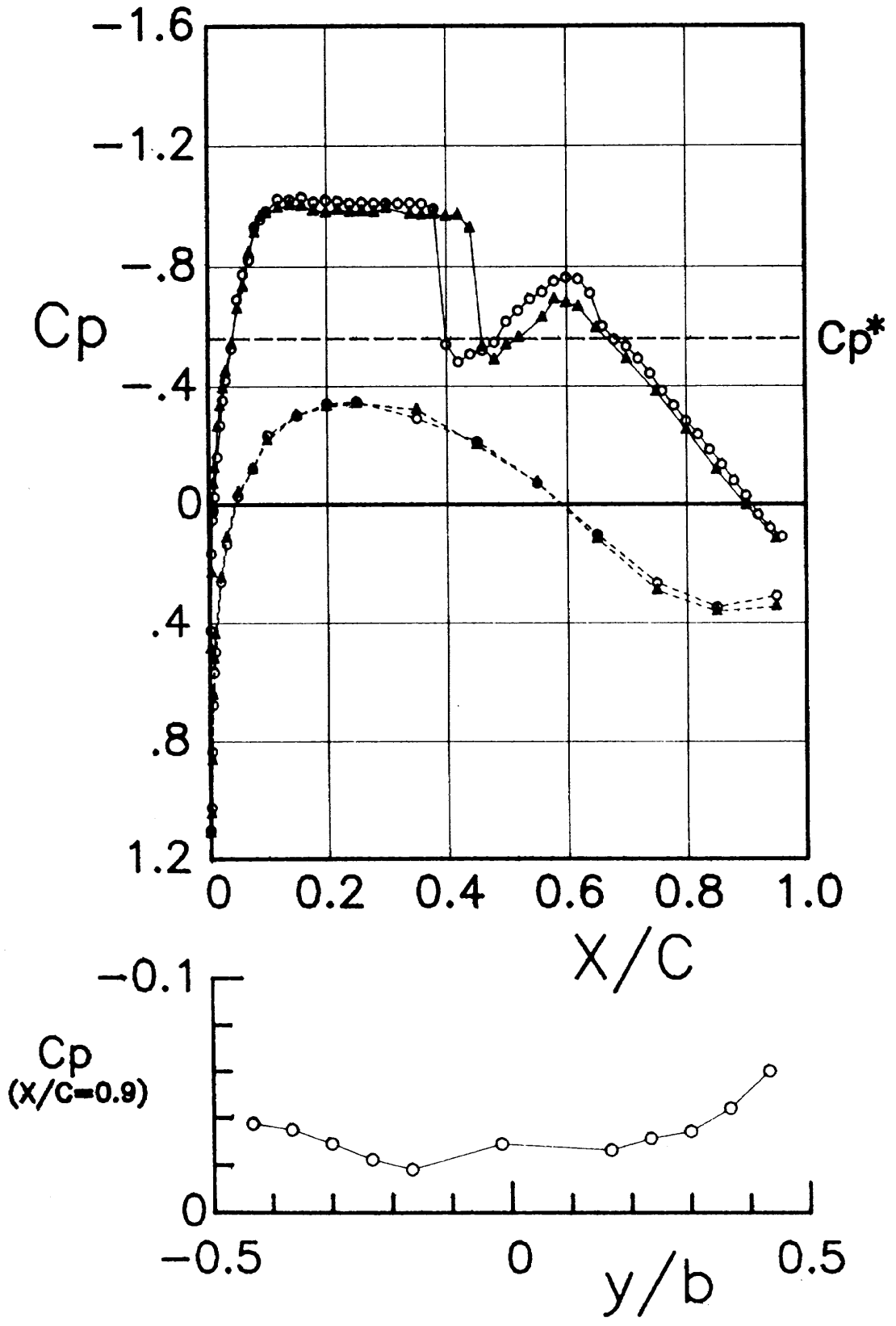

Figure A−38 Comparison of pressure distribution data measured in the NAL and IAR wind tunnels with the same lift coefficient.

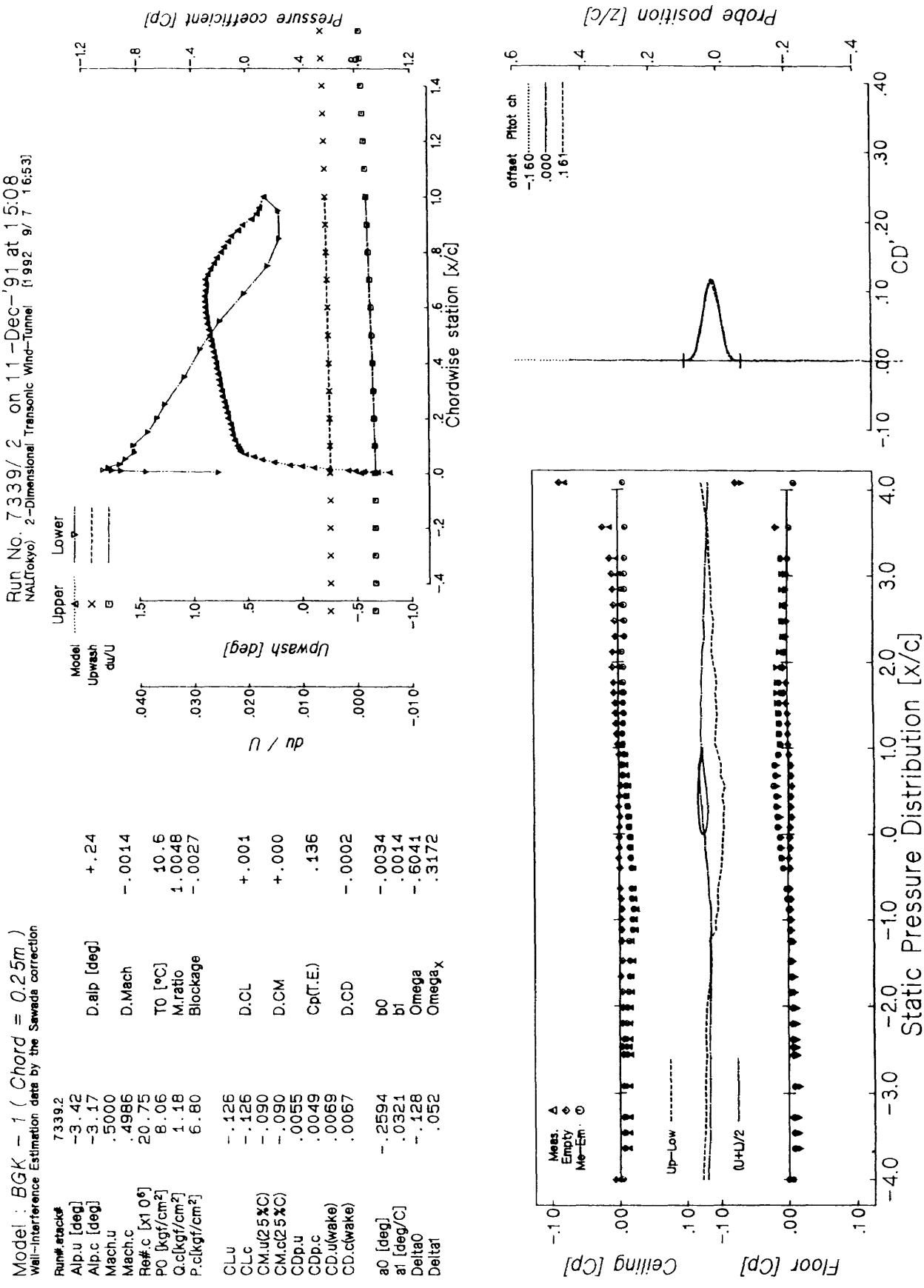

Run#.stack#	7339.2
Alp.u [deg]	-3.42
Alp.c [deg]	-3.17
Mach.u	.5000
Mach.c	.4986
Re#.c [x1 0^6]	20.75
P0 [kgf/cm^2]	8.06
Q.c[kgf/cm^2]	1.18
P.c[kgf/cm^2]	6.80
CLu	-.126
CLc	-.126
CM.u(25%C)	-.090
CM.c(25%C)	-.090
CDp.u	.0055
CDp.c	.0049
CD.u(wake)	.0069
CD.c(wake)	.0067
a0 [deg]	-.2594
a1 [deg/C]	.0321
Delta0	-.128
Delta1	.052
D.alp [deg]	+.24
D.Mach	-.0014
T0 [°C]	10.6
M.ratio	1.0048
Blockage	-.0027
D.CL	+.001
D.CM	+.000
Cp(T.E.)	.136
D.CD	-.0002
b0	-.0034
b1	.0014
Omega	-.6041
Omega$_x$	.3172

Figure B－1 The NAL data corrected for the top and bottom wall effects.

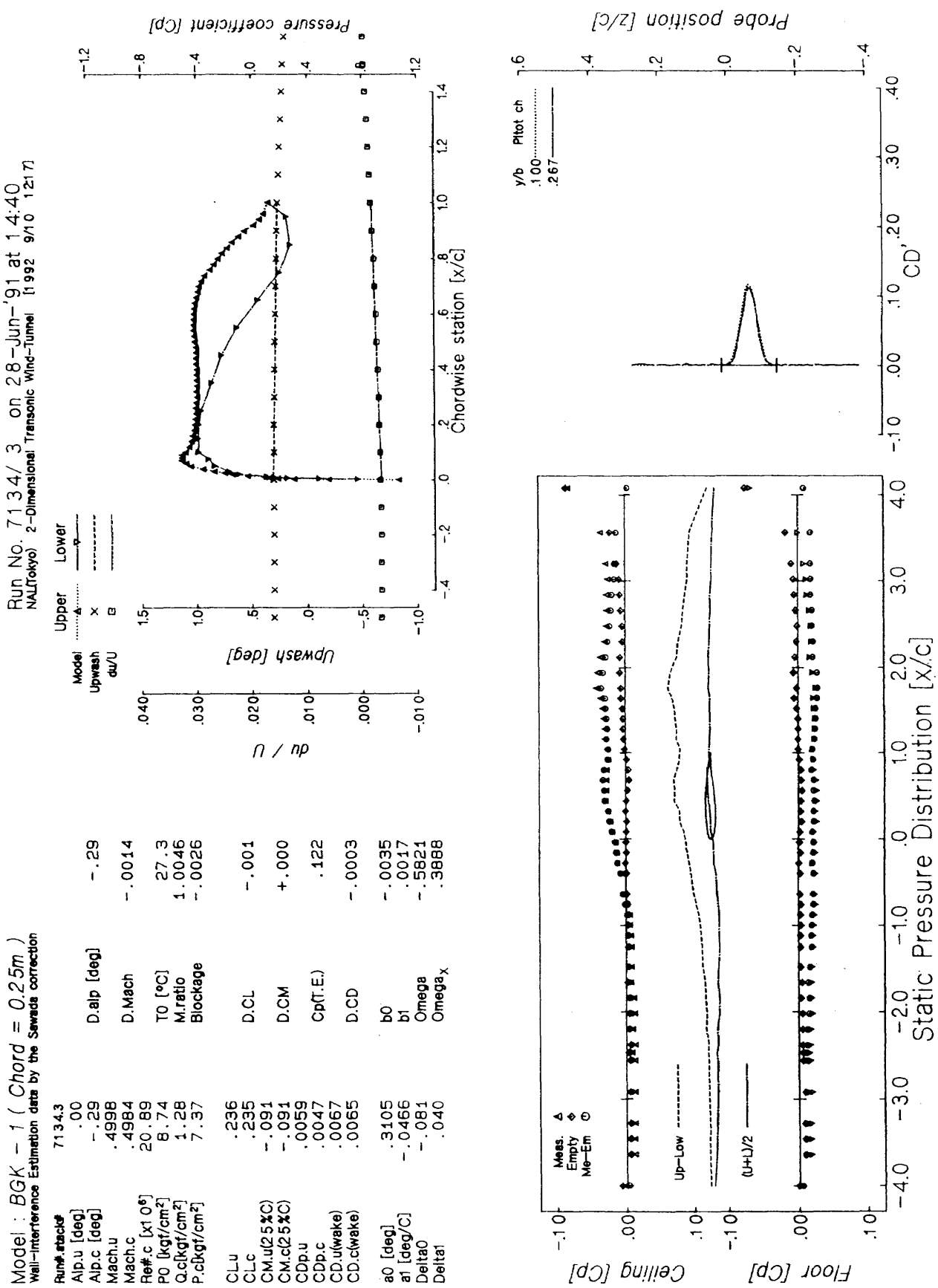

Figure B – 2 The NAL data corrected for the top and bottom wall effects.

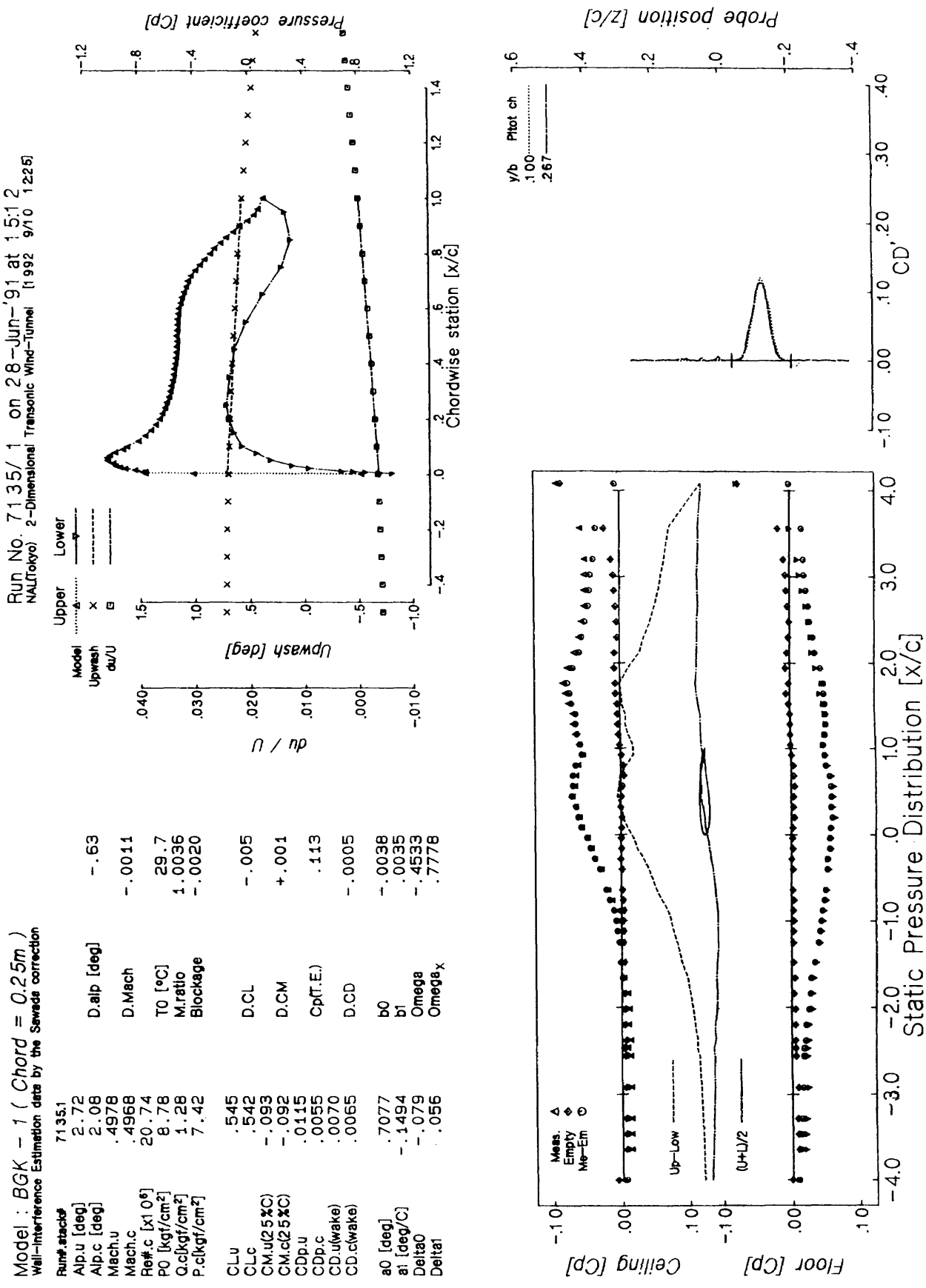

Figure B – 3 The NAL data corrected for the top and bottom wall effects.

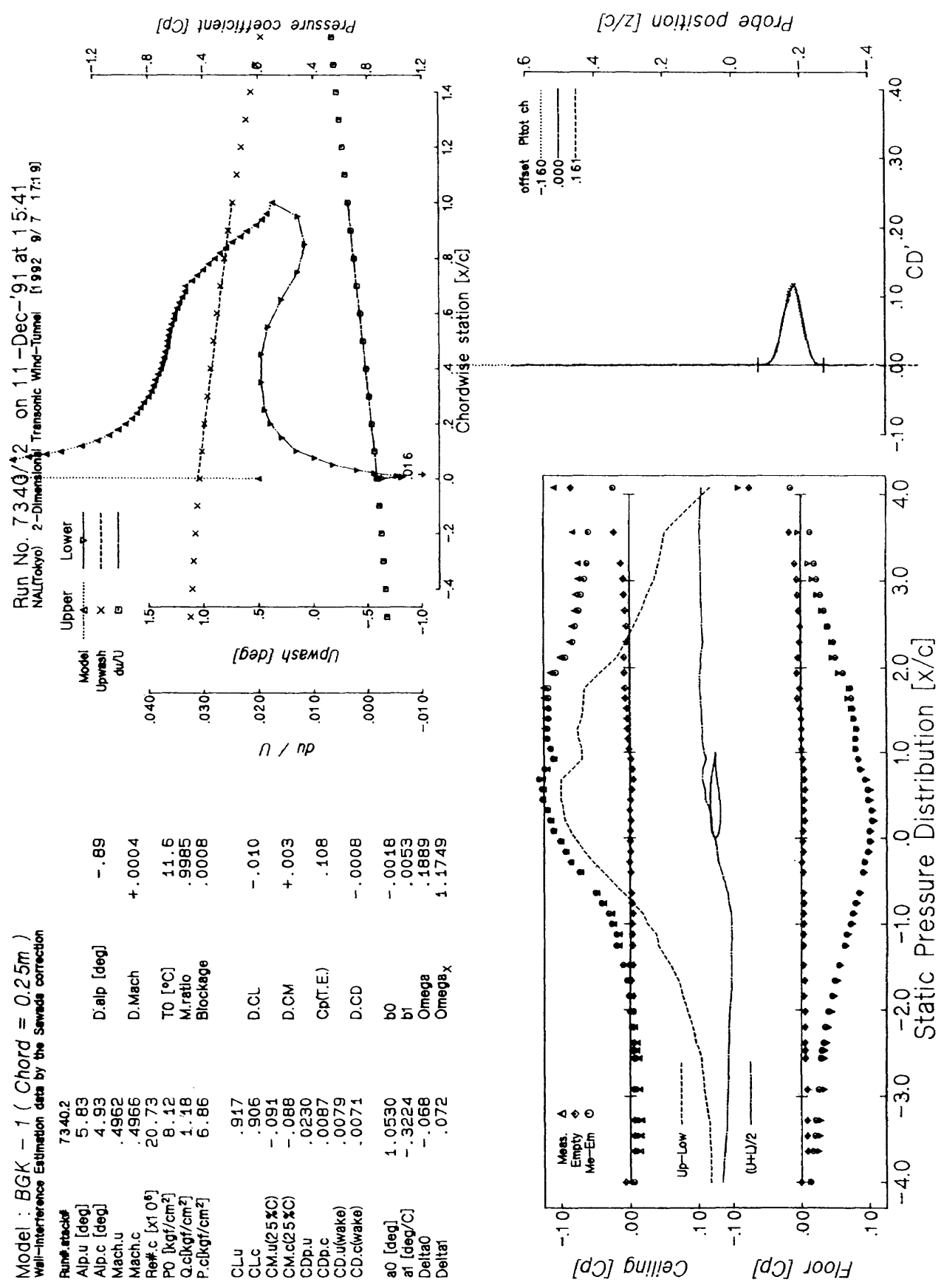

Figure B – 4 The NAL data corrected for the top and bottom wall effects.

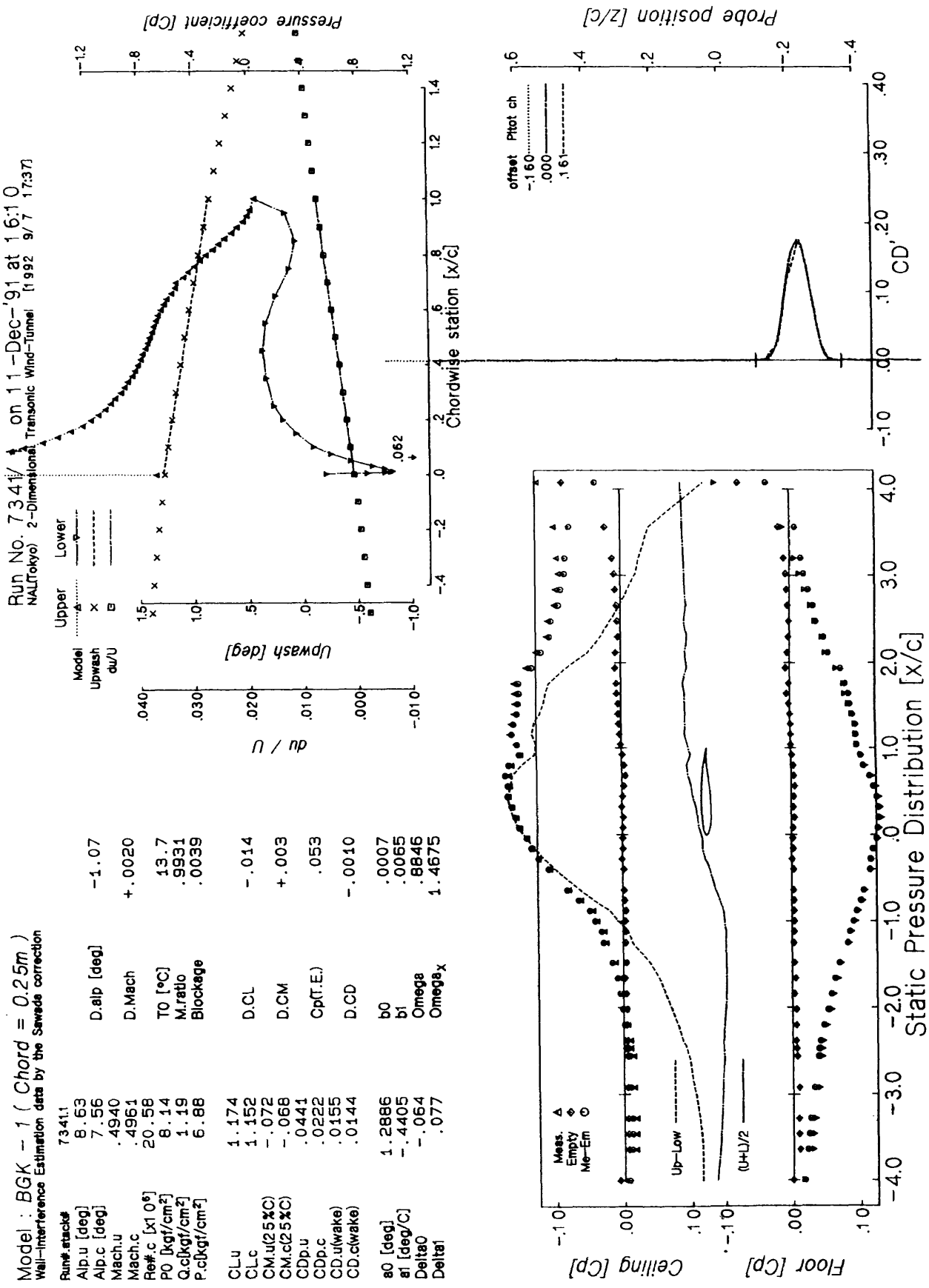

Figure B – 5 The NAL data corrected for the top and bottom wall effects.

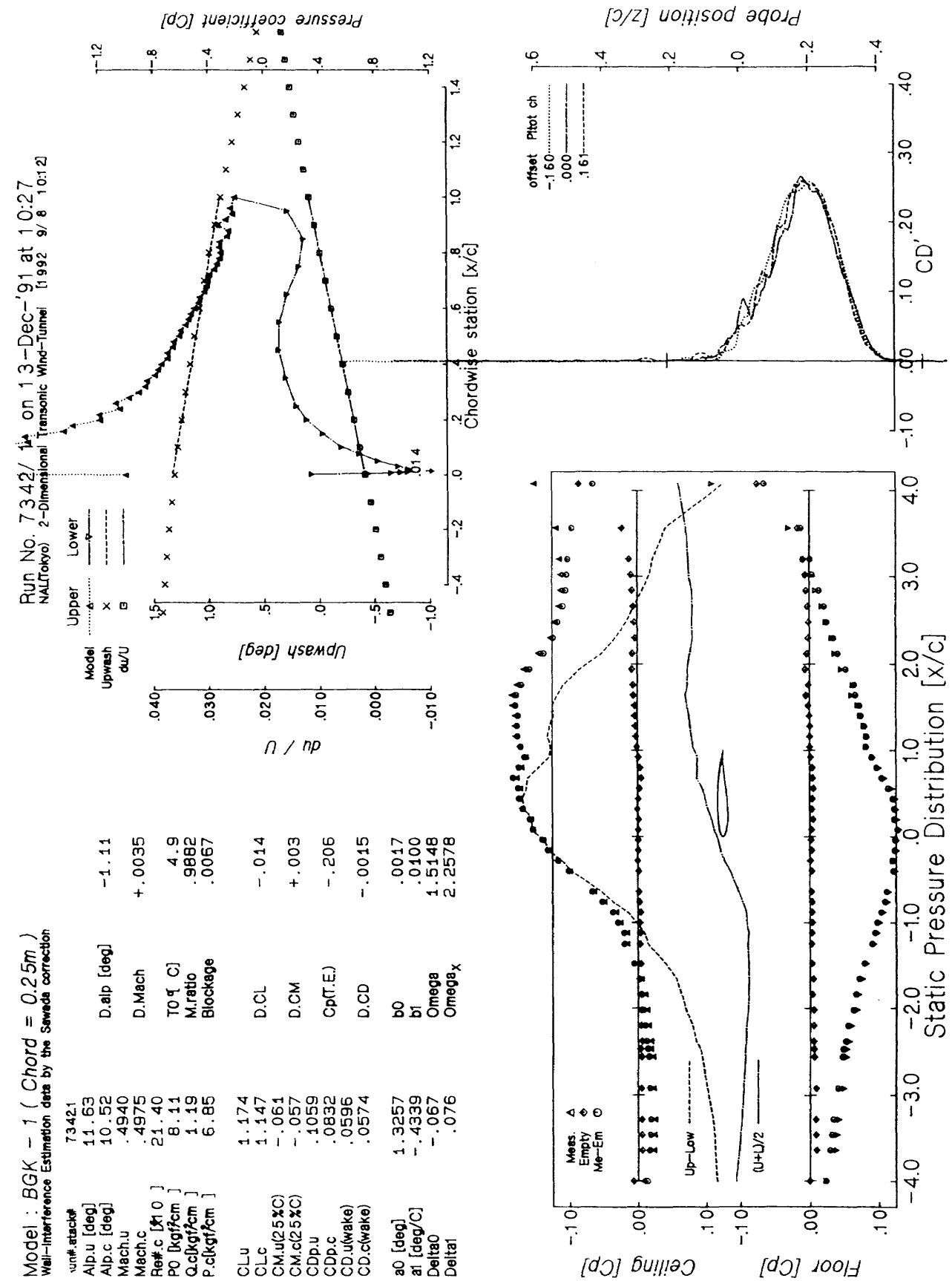

Figure B－6 The NAL data corrected for the top and bottom wall effects.

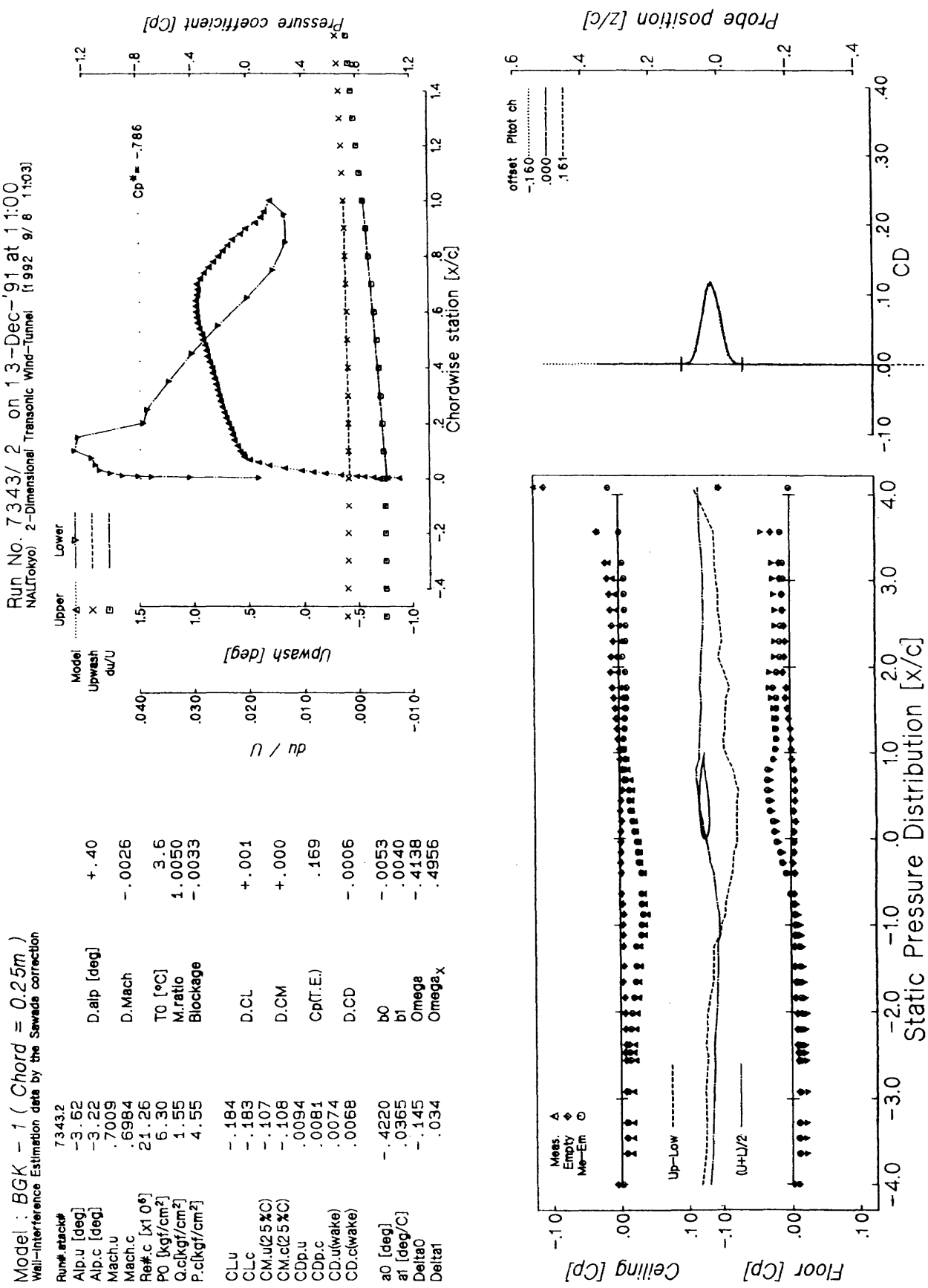

Figure B – 7 The NAL data corrected for the top and bottom wall effects.

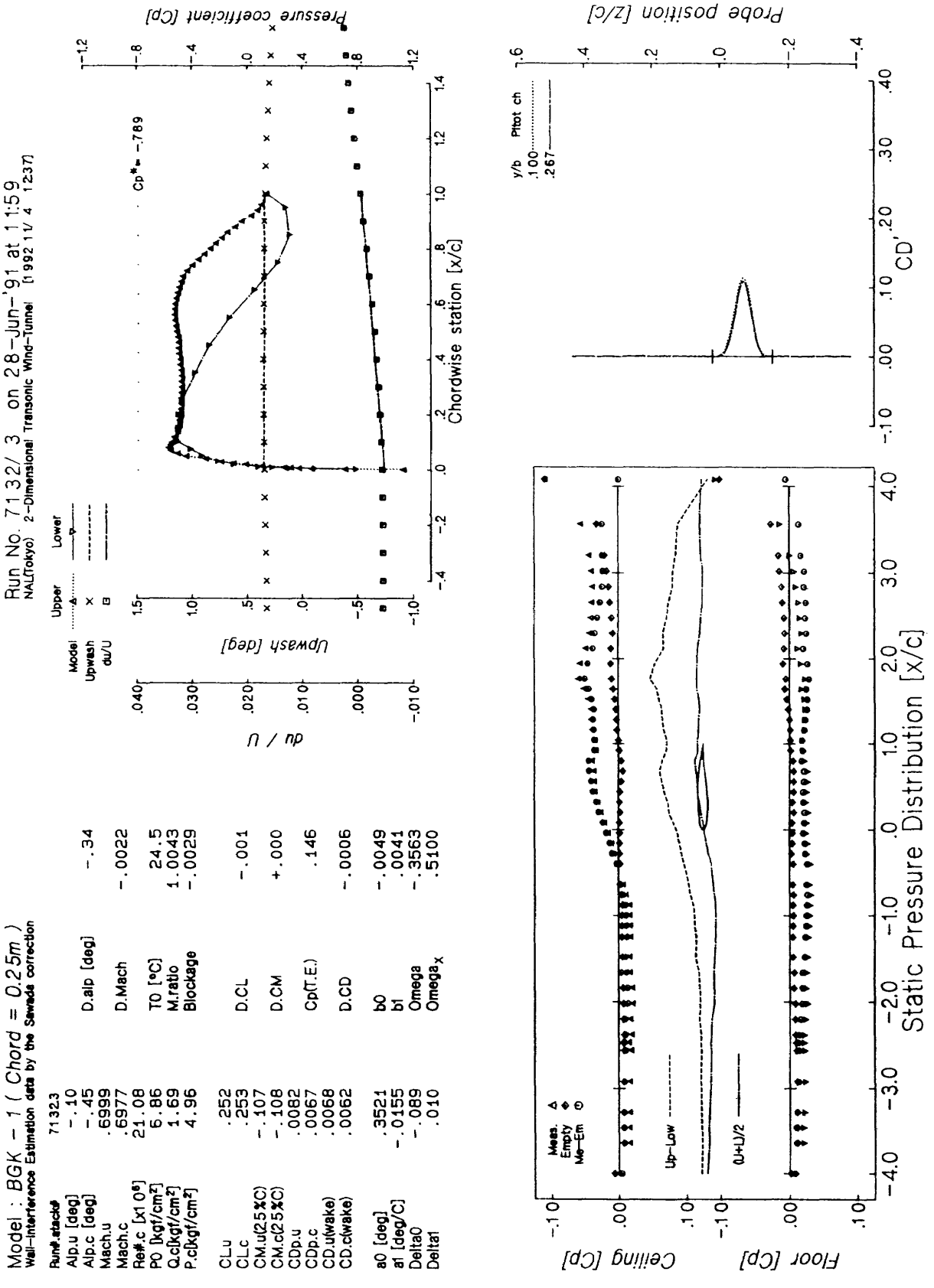

Figure B – 8 The NAL data corrected for the top and bottom wall effects.

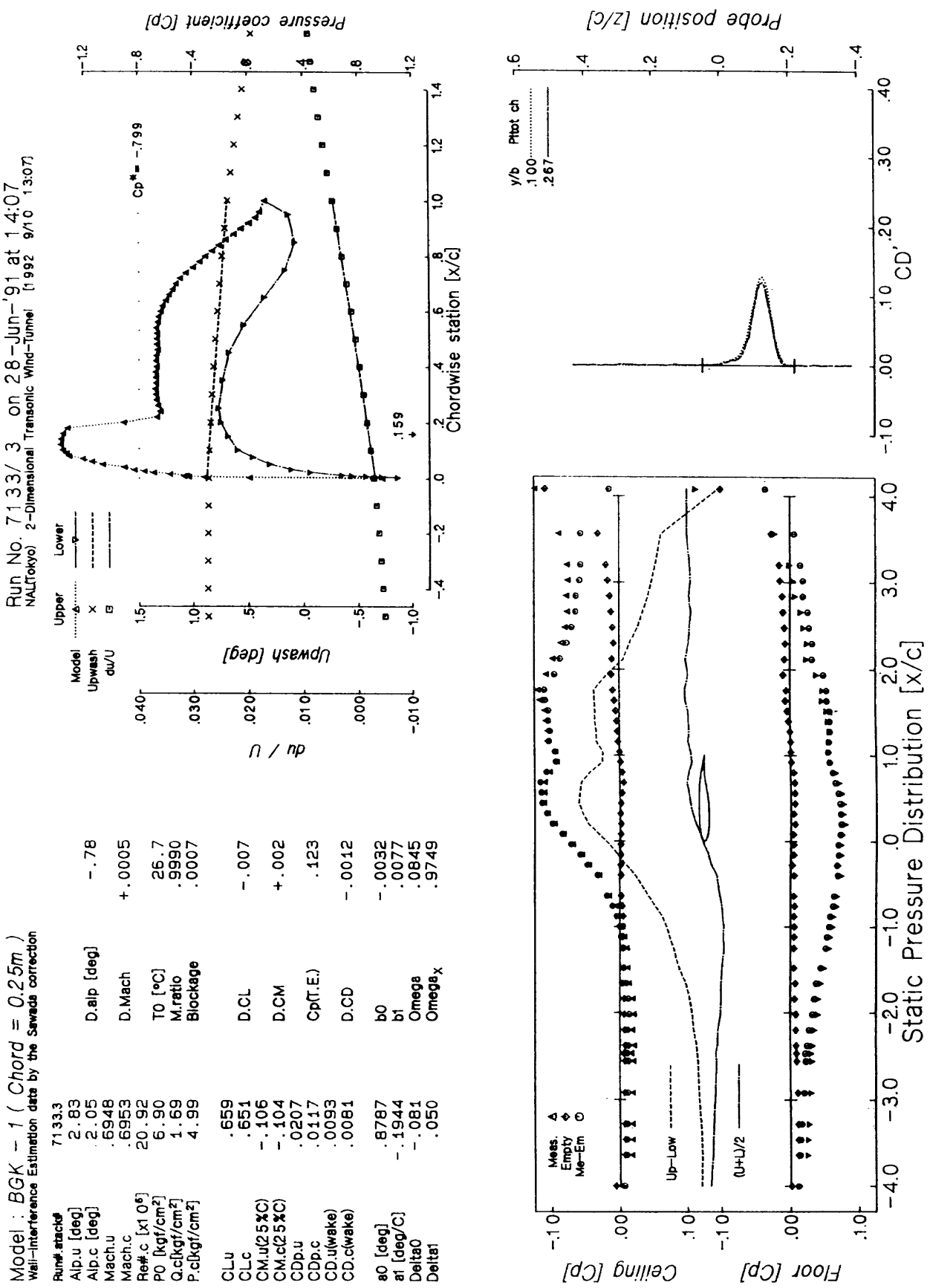

Figure B－9 The NAL data corrected for the top and bottom wall effects.

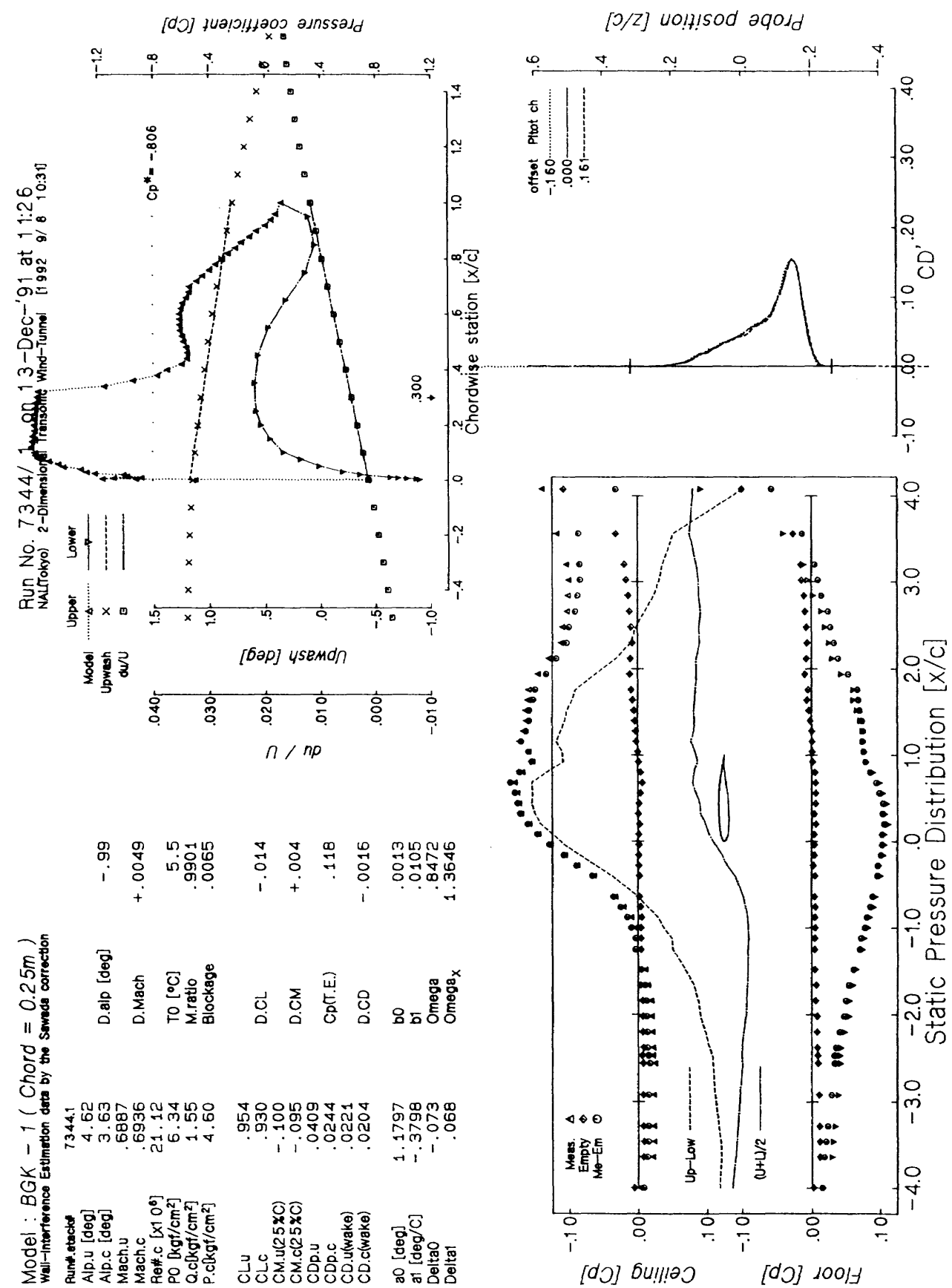

Figure B-10 The NAL data corrected for the top and bottom wall effects.

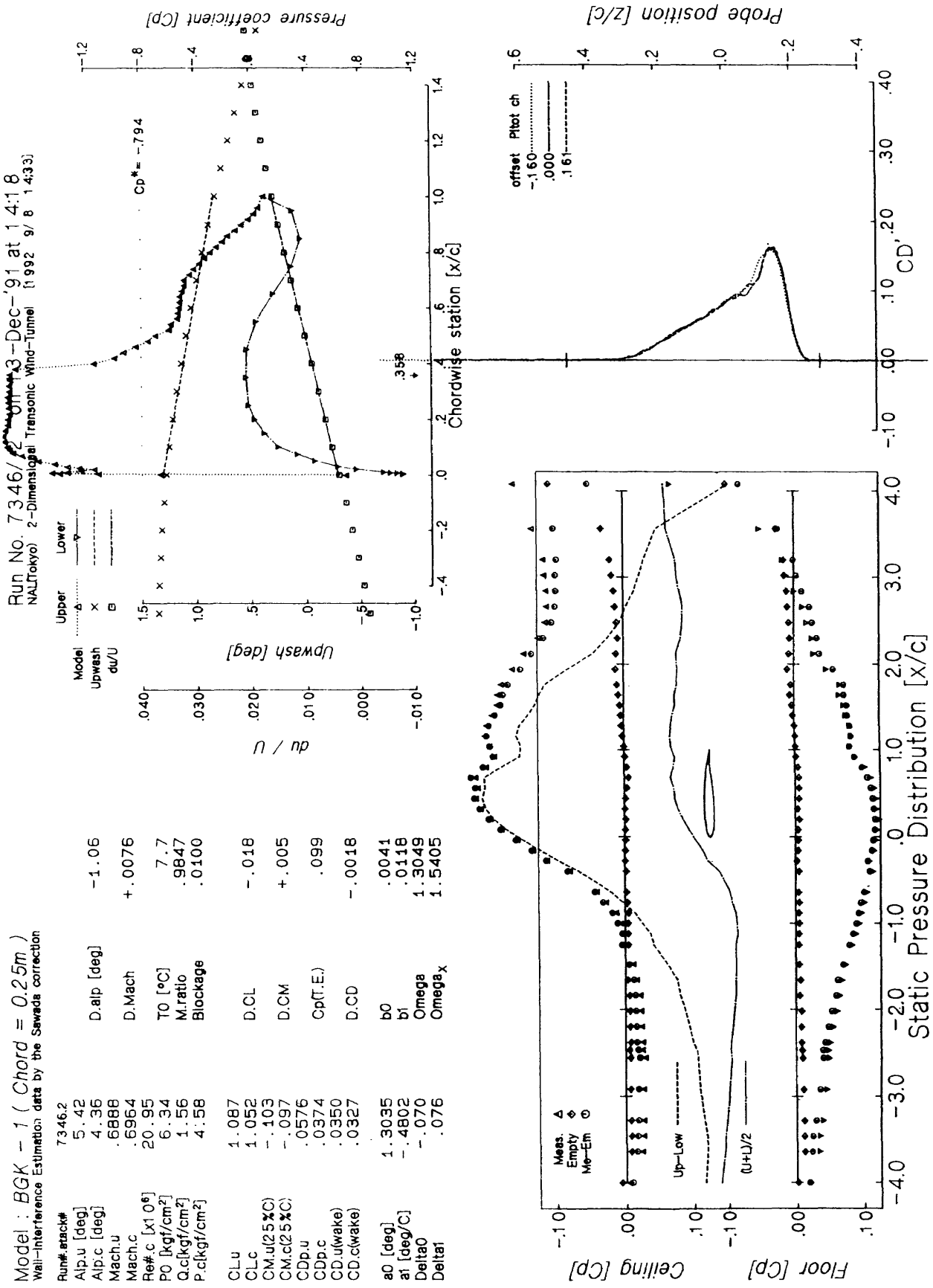

Figure B−11 The NAL data corrected for the top and bottom wall effects.

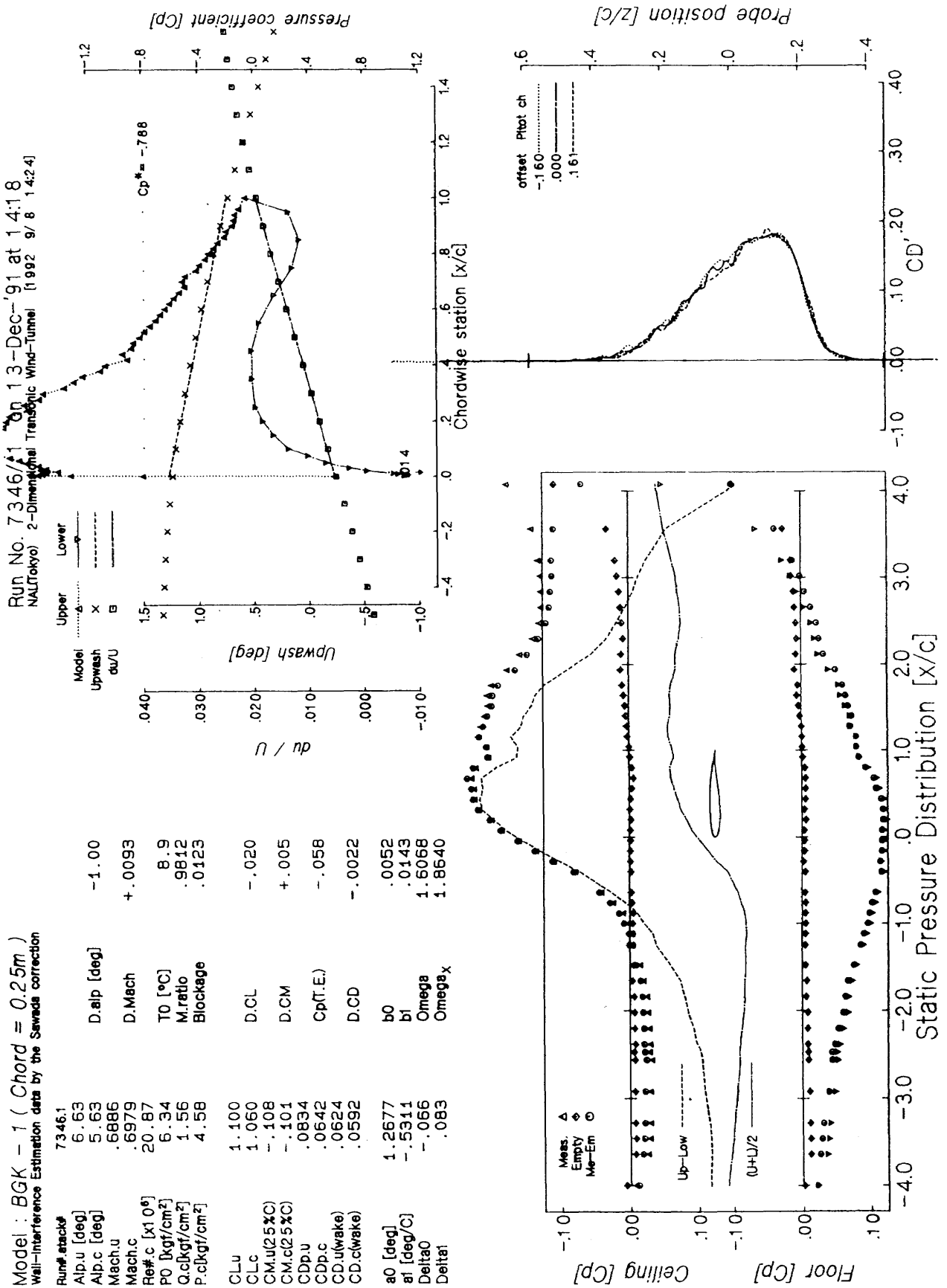

Figure B−12 The NAL data corrected for the top and bottom wall effects.

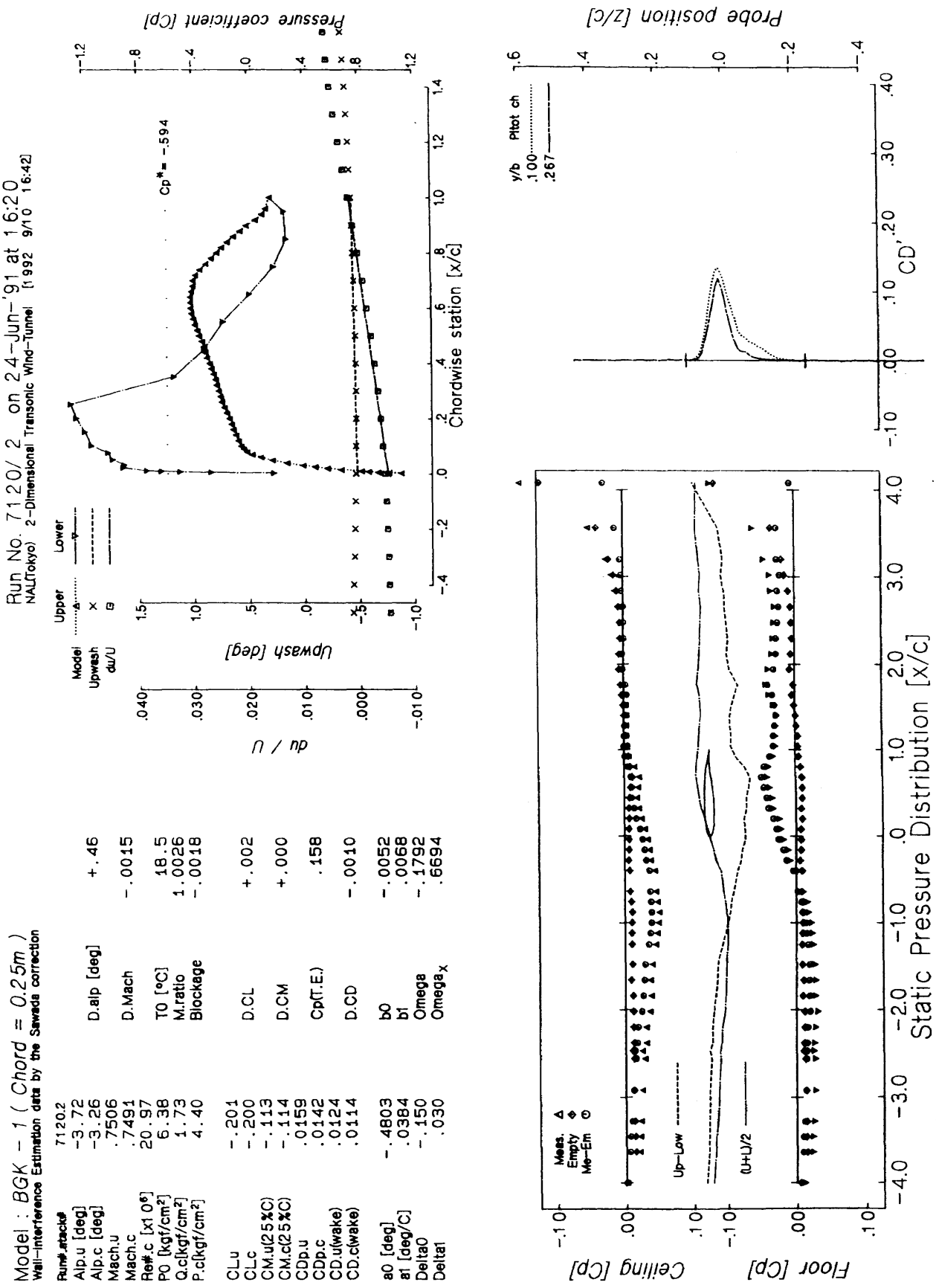

Figure B－13 The NAL data corrected for the top and bottom wall effects.

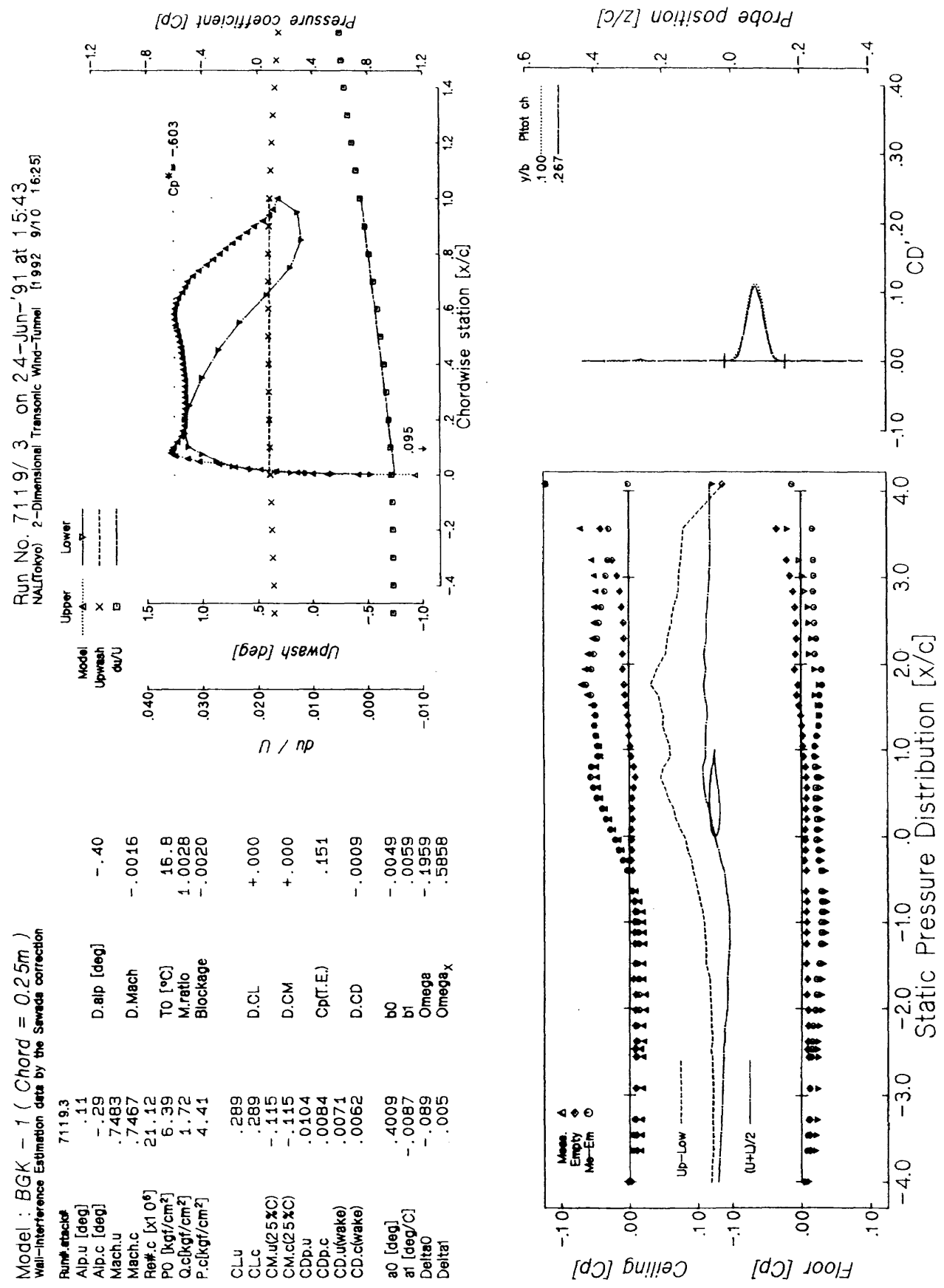

Figure B−14 The NAL data corrected for the top and bottom wall effects.

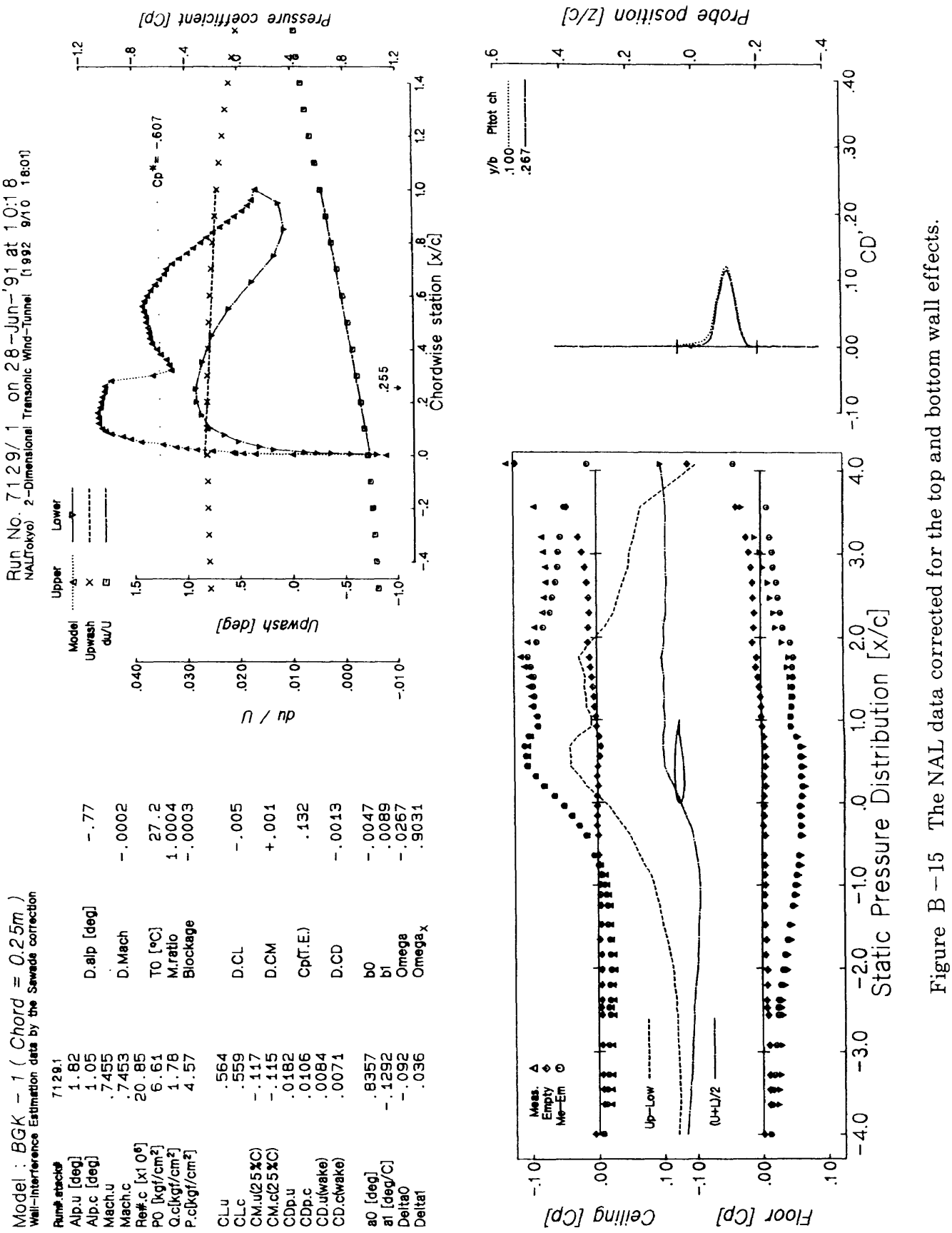

Figure B−15 The NAL data corrected for the top and bottom wall effects.

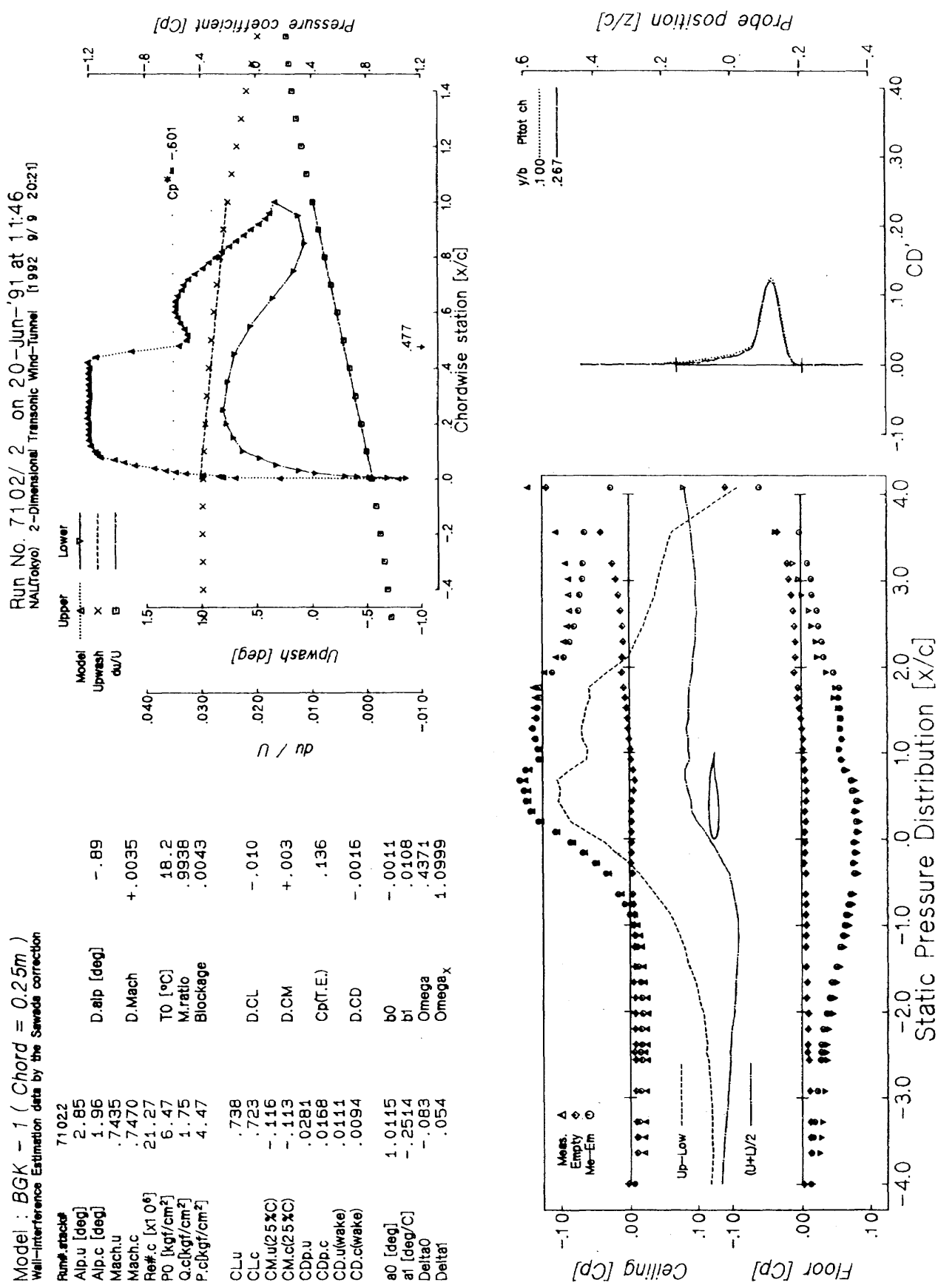

Figure B—16 The NAL data corrected for the top and bottom wall effects.

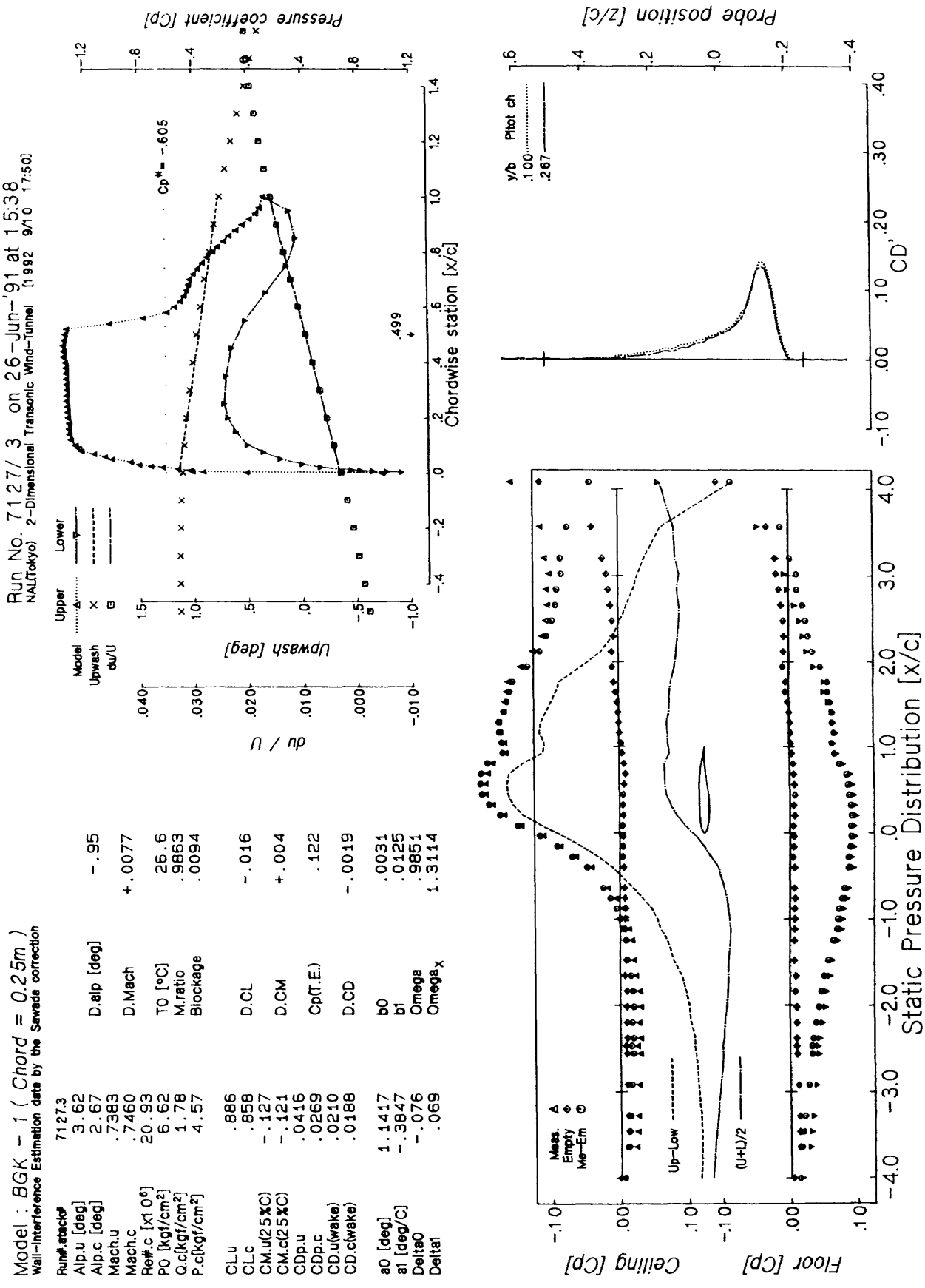

Figure B－17 The NAL data corrected for the top and bottom wall effects.

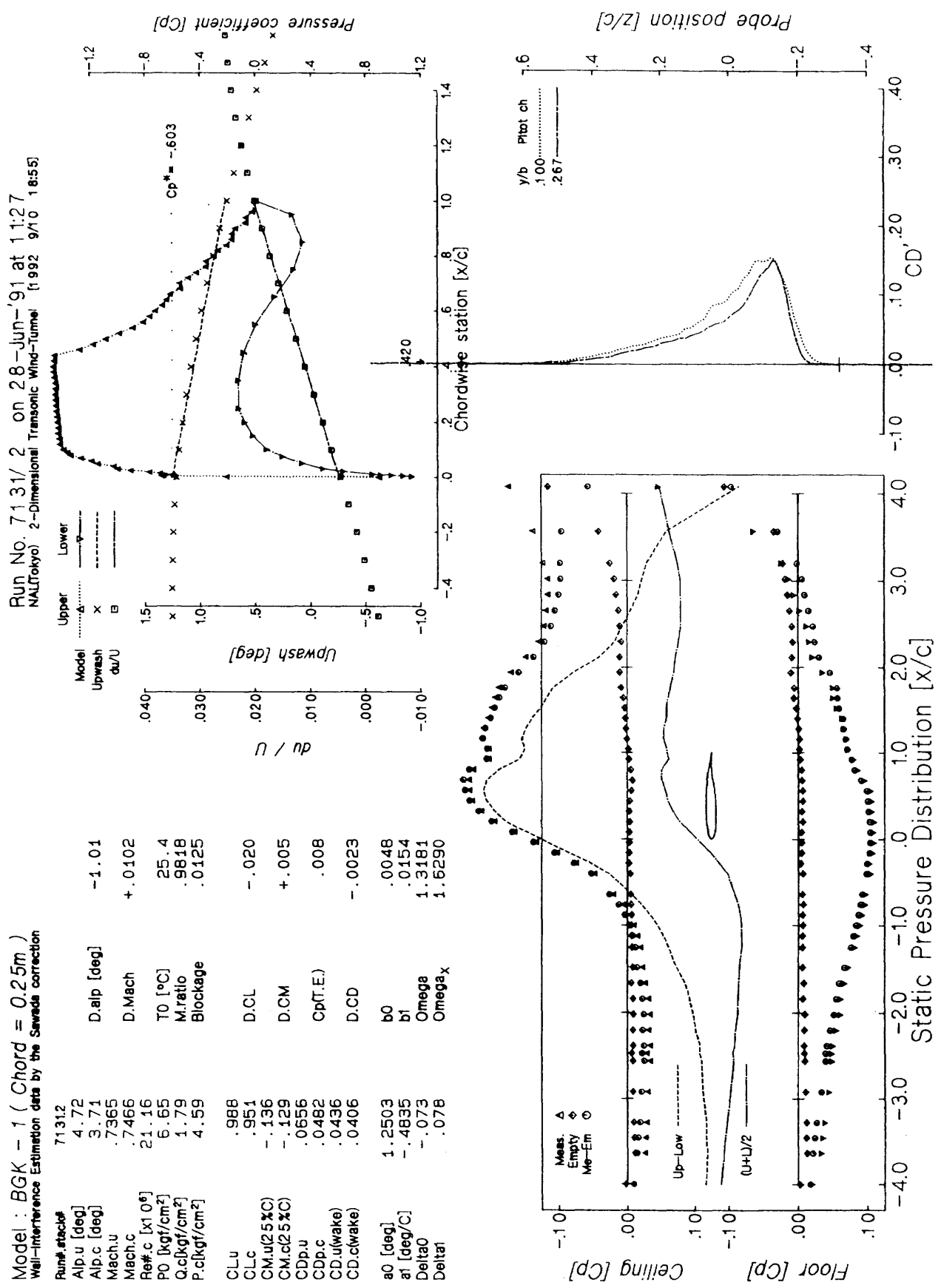

Figure B—18 The NAL data corrected for the top and bottom wall effects.

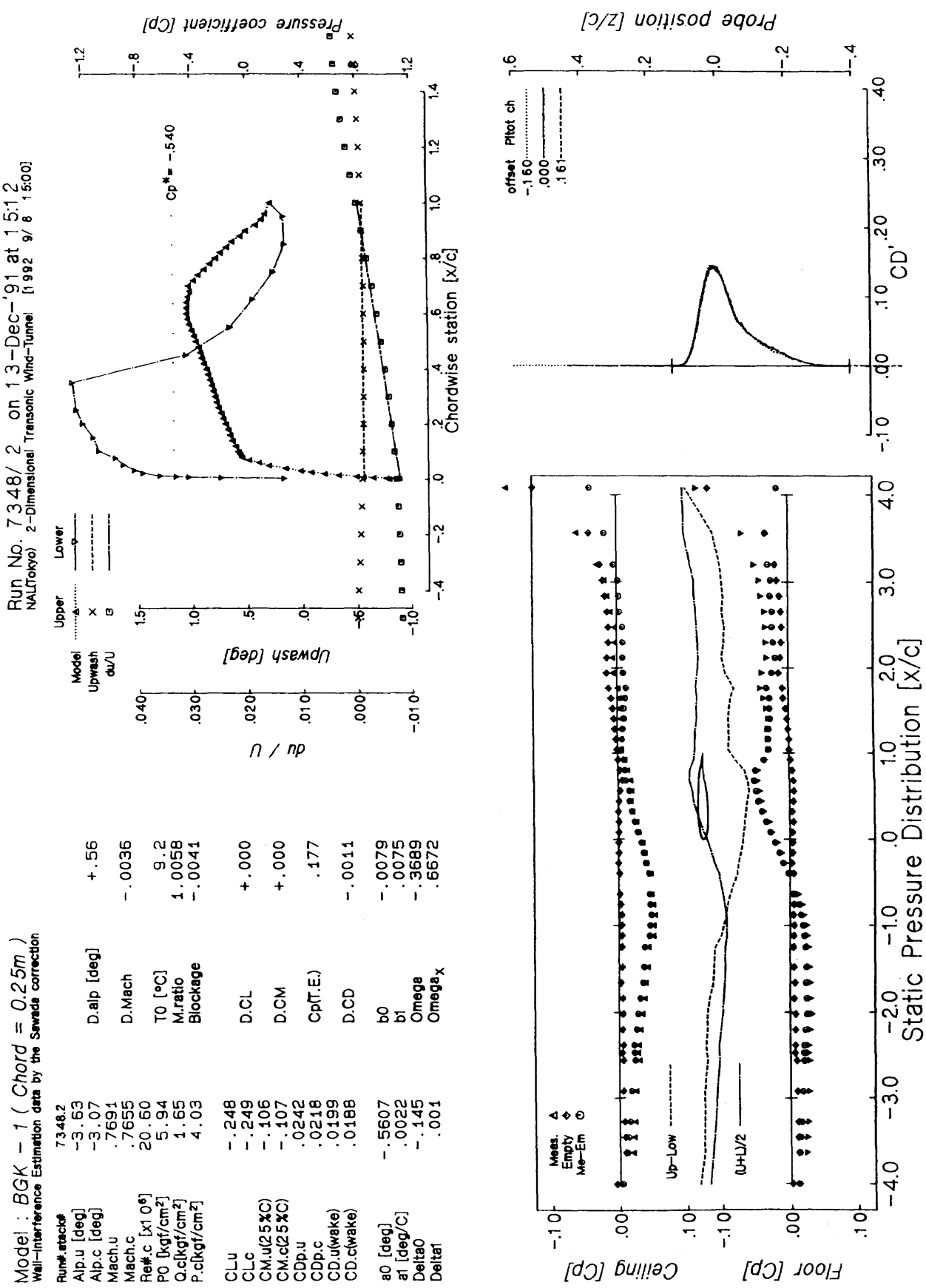

Figure B−19 The NAL data corrected for the top and bottom wall effects.

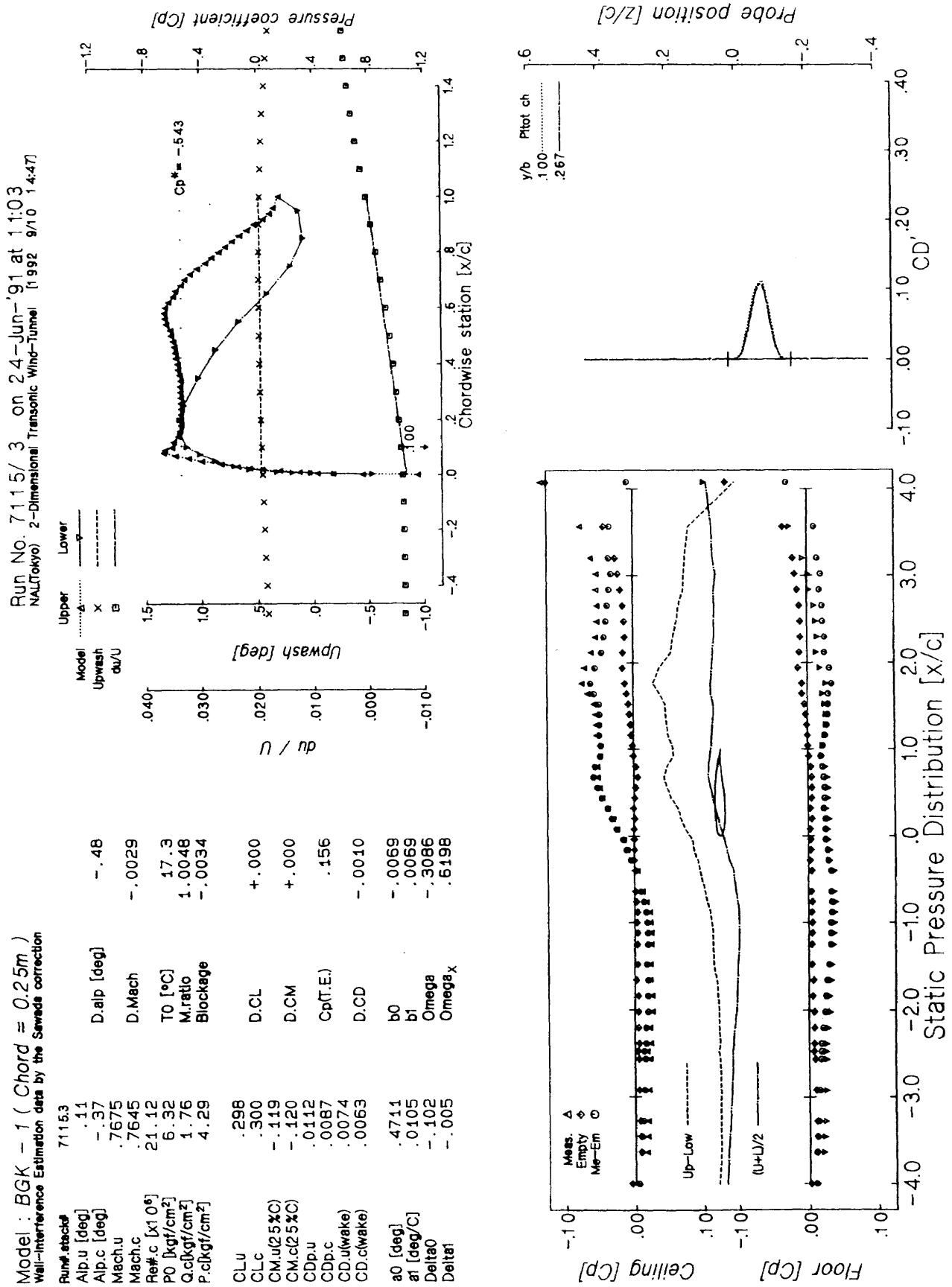

Figure B－20 The NAL data corrected for the top and bottom wall effects.

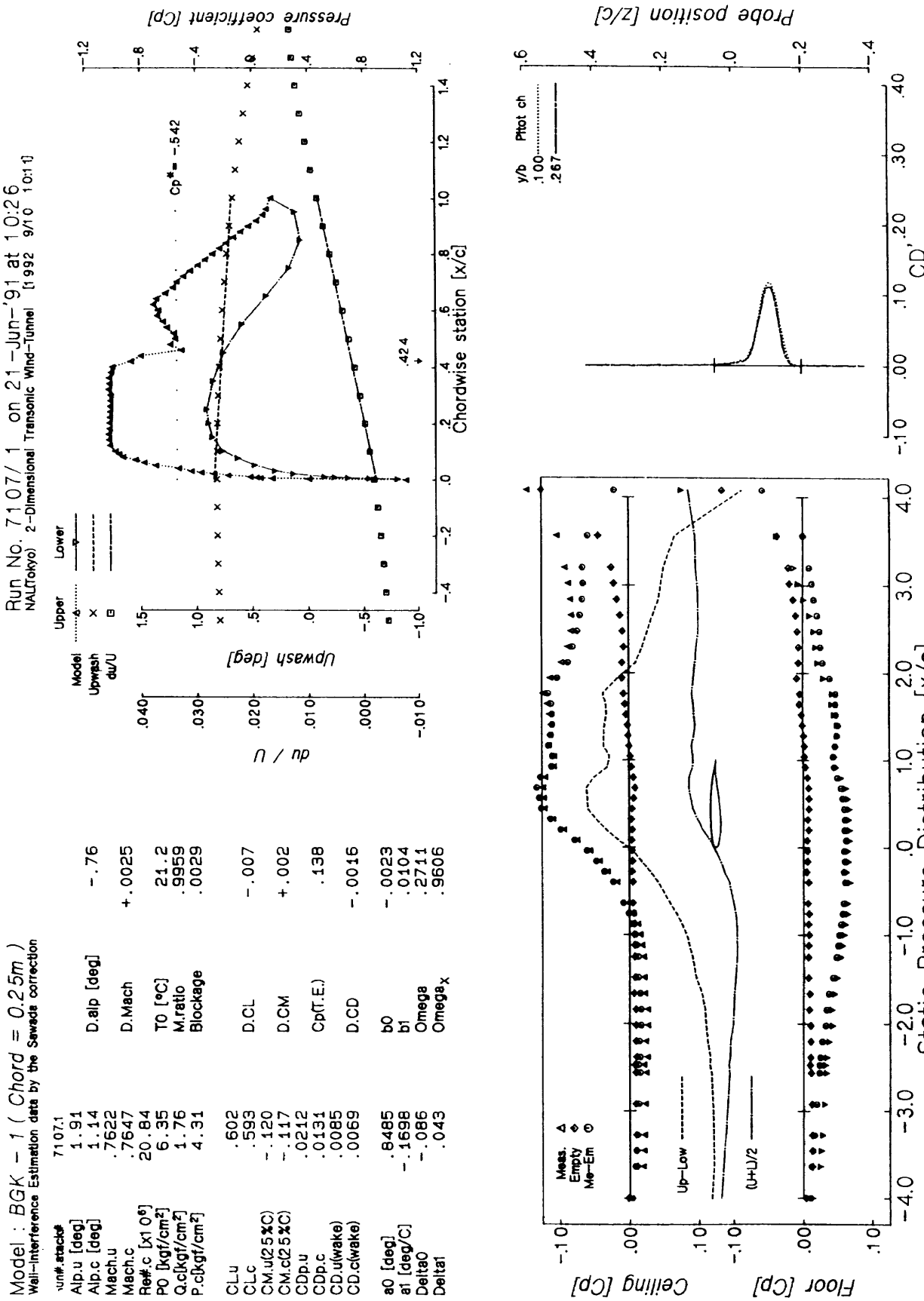

run#,stack#	7107.1		
Alp.u [deg]	1.91		
Alp.c [deg]	1.14	D.alp [deg]	-.76
Mach.u	.7622		
Mach.c	.7647	D.Mach	+.0025
Re#.c [x10^6]	20.84		
P0 [kgf/cm²]	6.35	T0 [°C]	21.2
Q.c[kgf/cm²]	1.76	M.ratio	.9959
P.c[kgf/cm²]	4.31	Blockage	.0029
CL.u	.602		
CL.c	.593	D.CL	-.007
CM.u(25%C)	-.120		
CM.c(25%C)	-.117	D.CM	+.002
CDp.u	.0212		
CDp.c	.0131	Cp(T.E.)	.138
CD.u(wake)	.0085		
CD.c(wake)	.0069	D.CD	-.0016
a0 [deg]	.8485	b0	-.0023
a1 [deg/C]	-.1698	b1	.0104
DeltaO	-.086	Omega	.2711
Delta1	.043	Omega$_x$	.9606

Figure B−21 The NAL data corrected for the top and bottom wall effects.

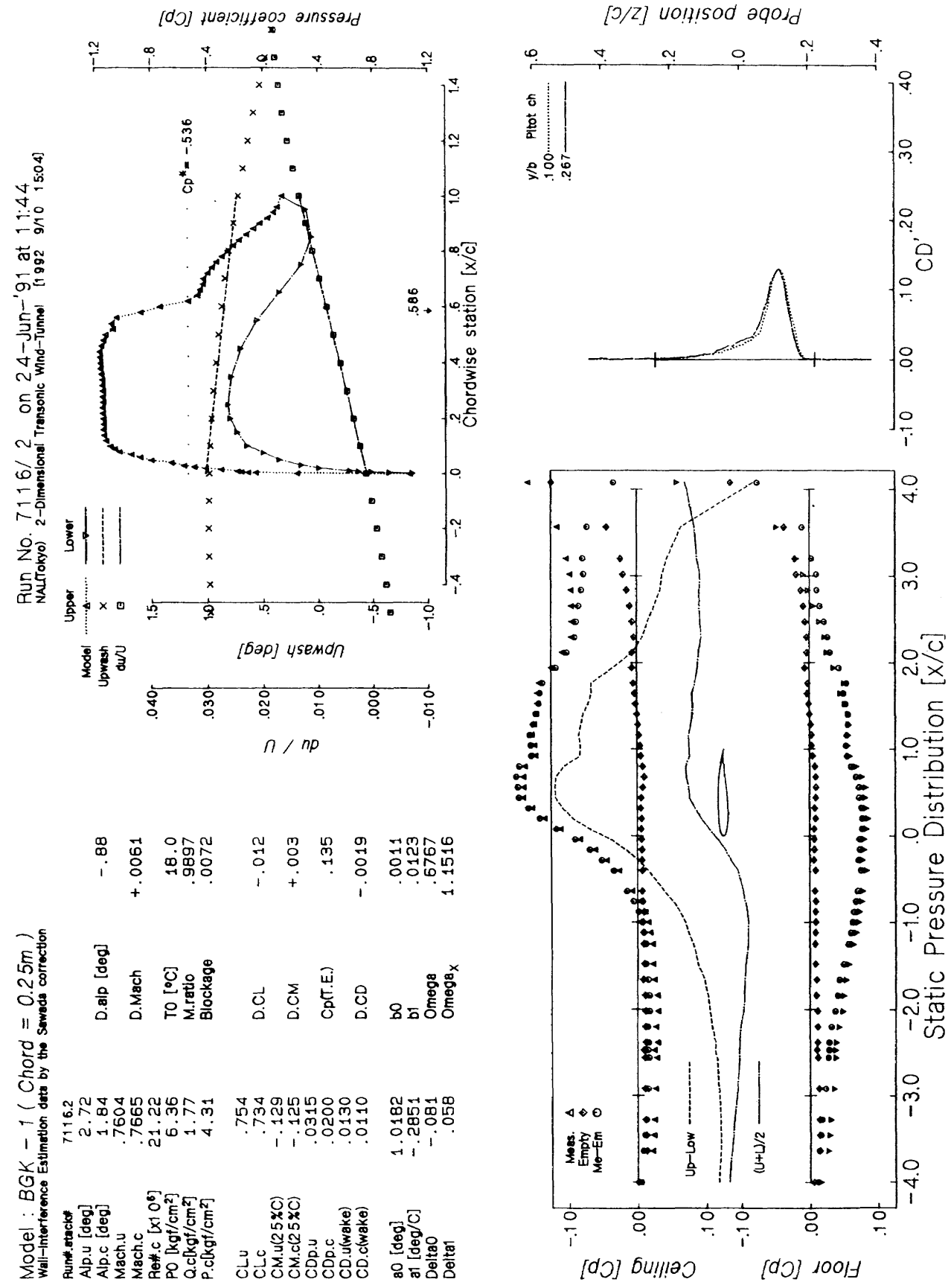

Figure B－22 The NAL data corrected for the top and bottom wall effects.

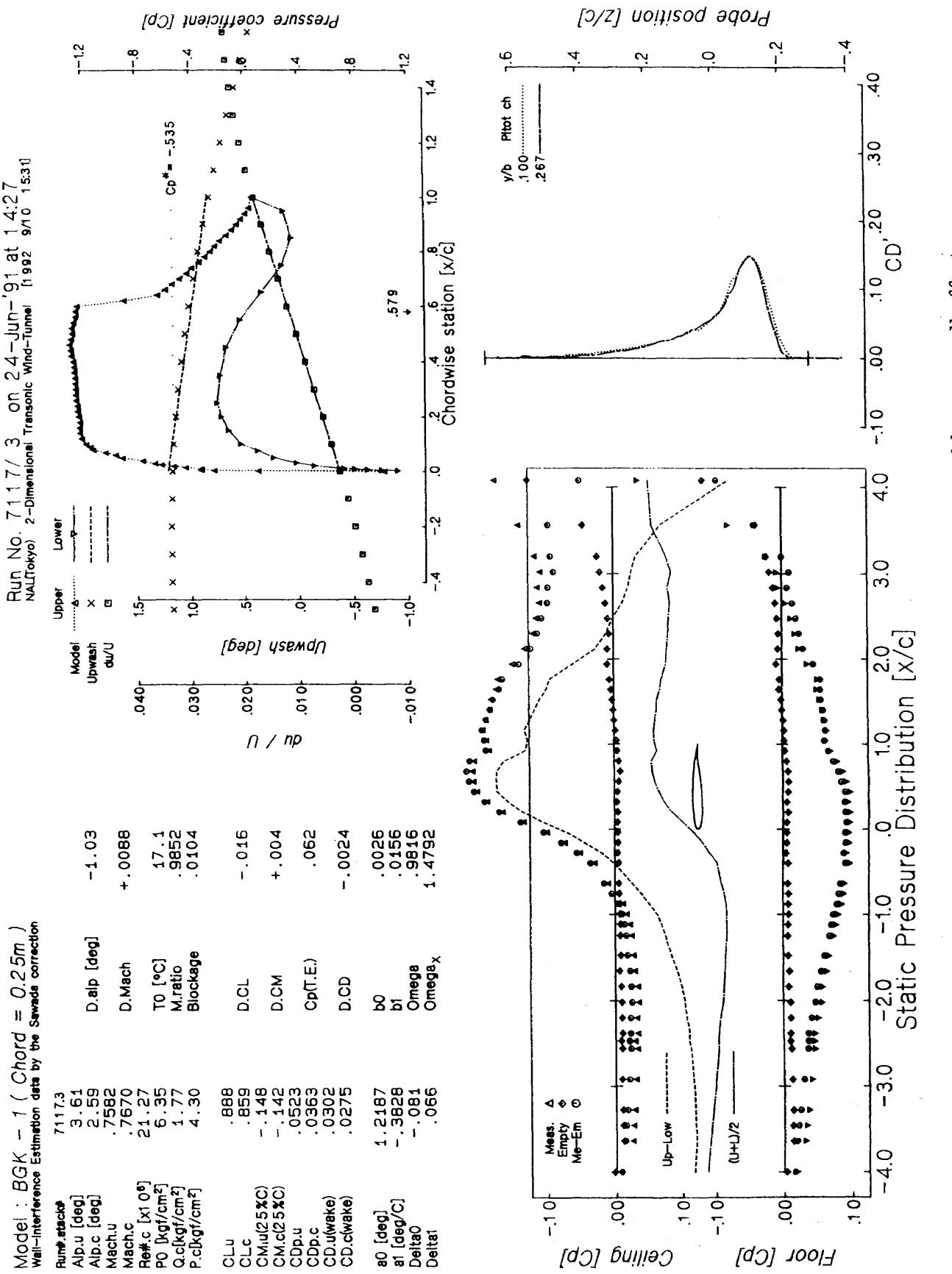

Figure B－23 The NAL data corrected for the top and bottom wall effects.

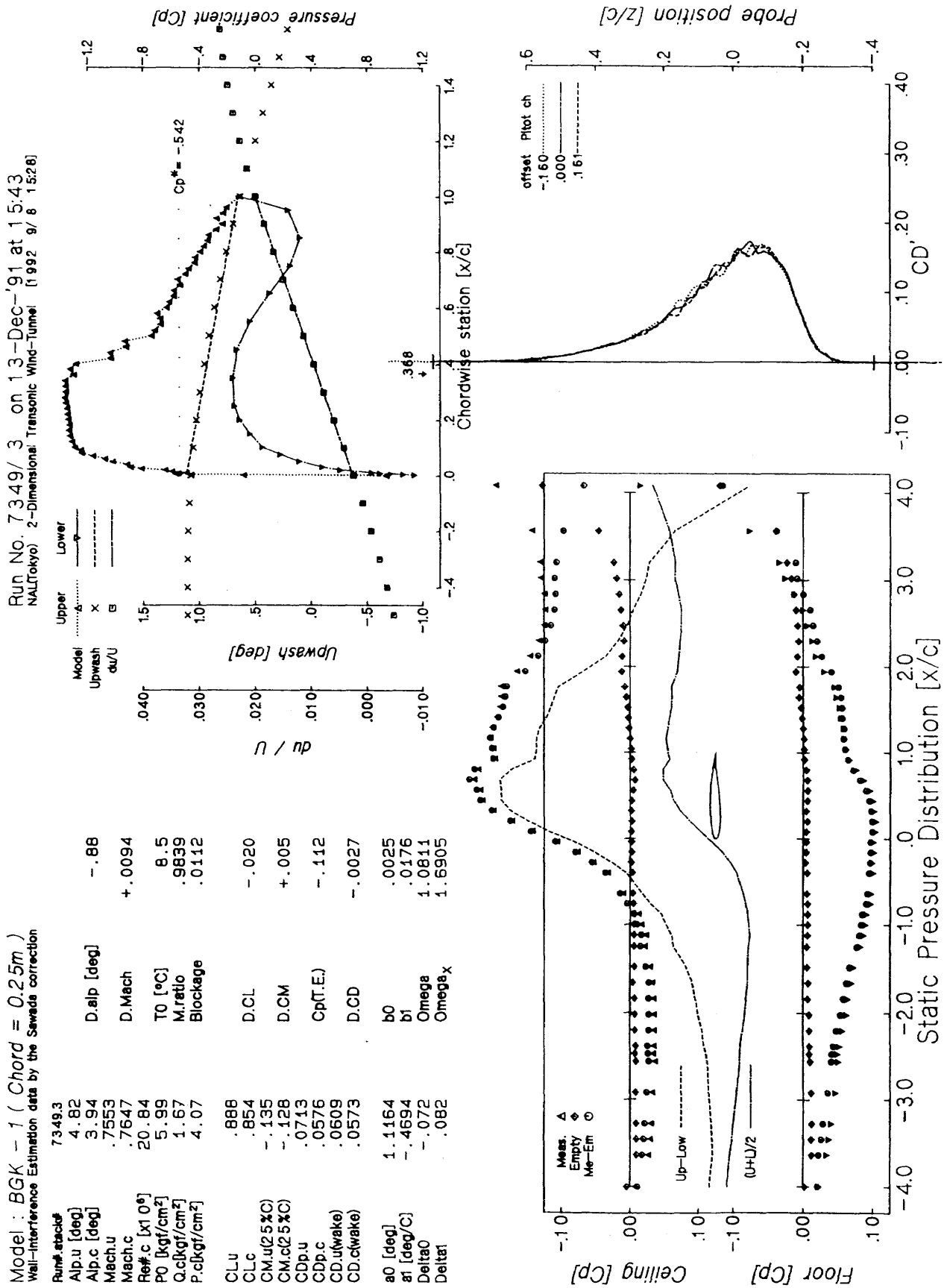

Figure B−24 The NAL data corrected for the top and bottom wall effects.

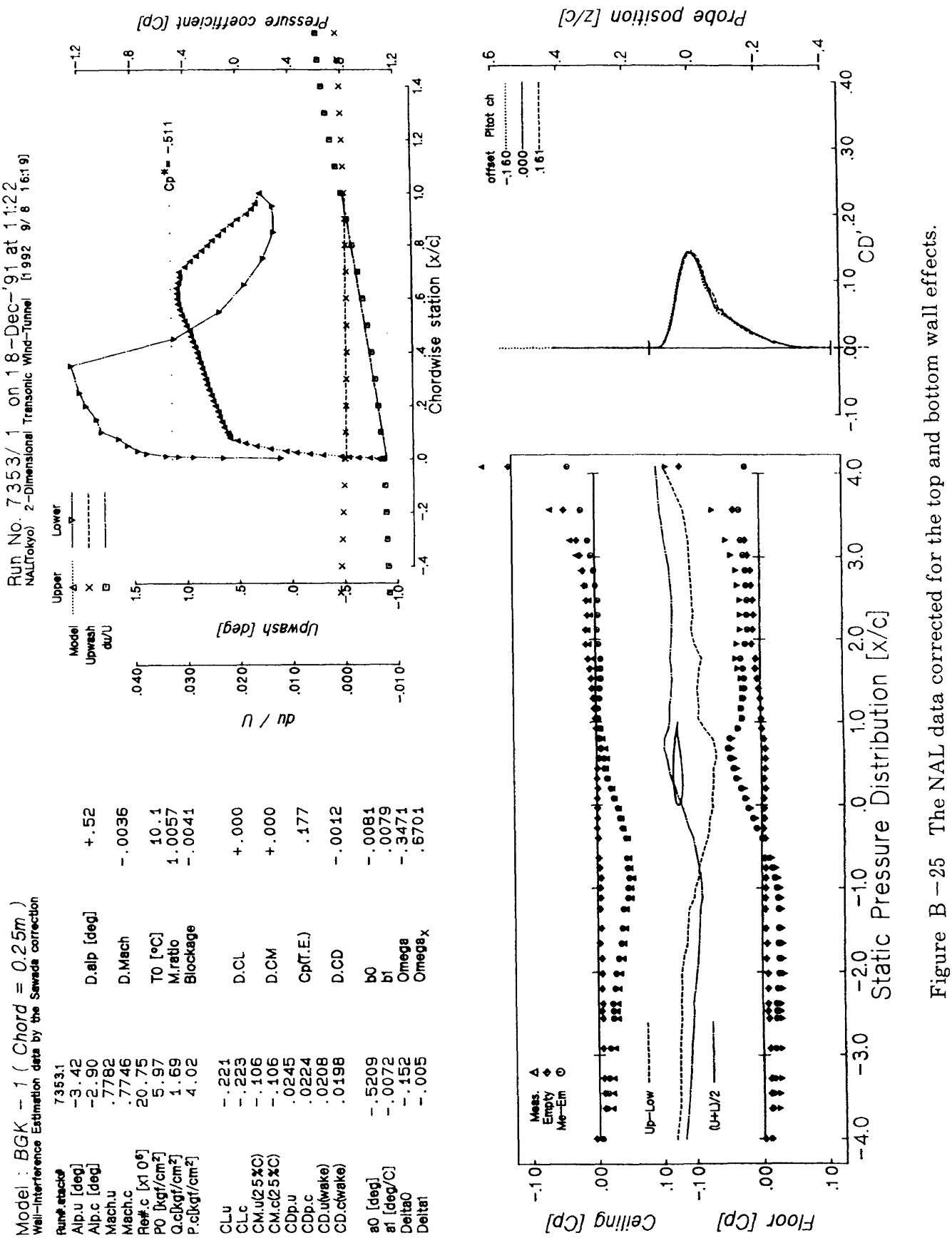

Figure B−25 The NAL data corrected for the top and bottom wall effects.

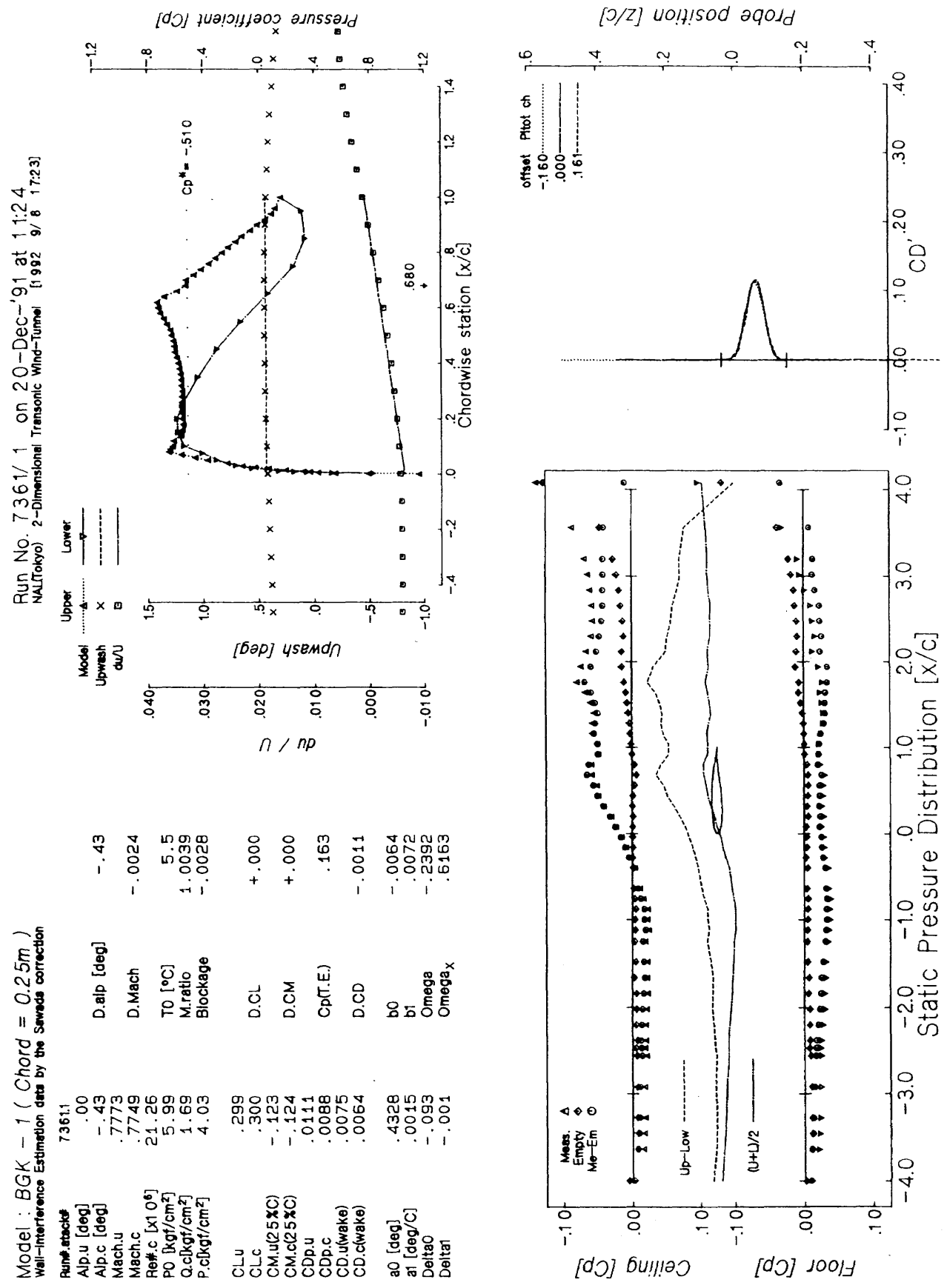

Figure B−26 The NAL data corrected for the top and bottom wall effects.

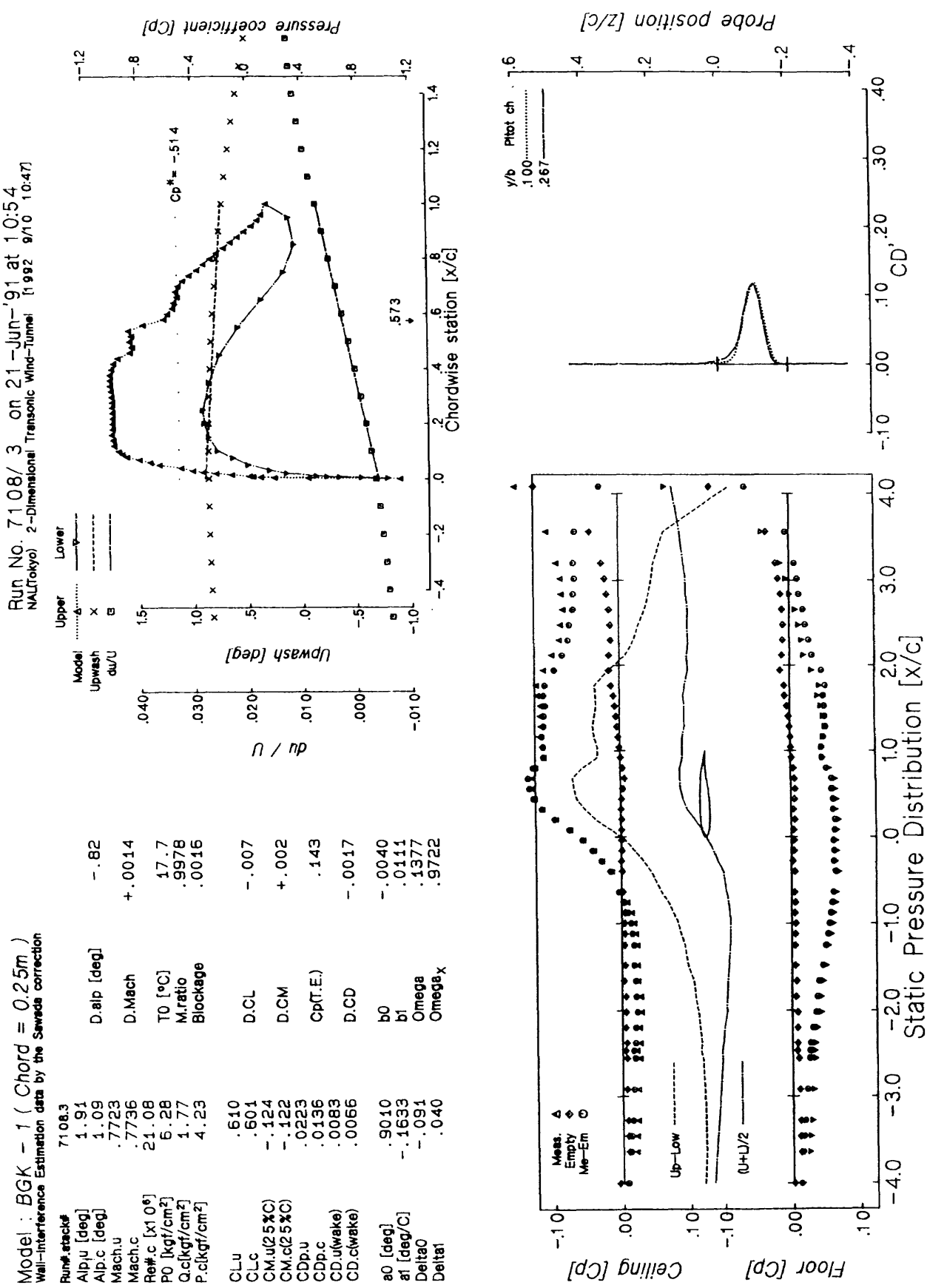

Figure B−27 The NAL data corrected for the top and bottom wall effects.

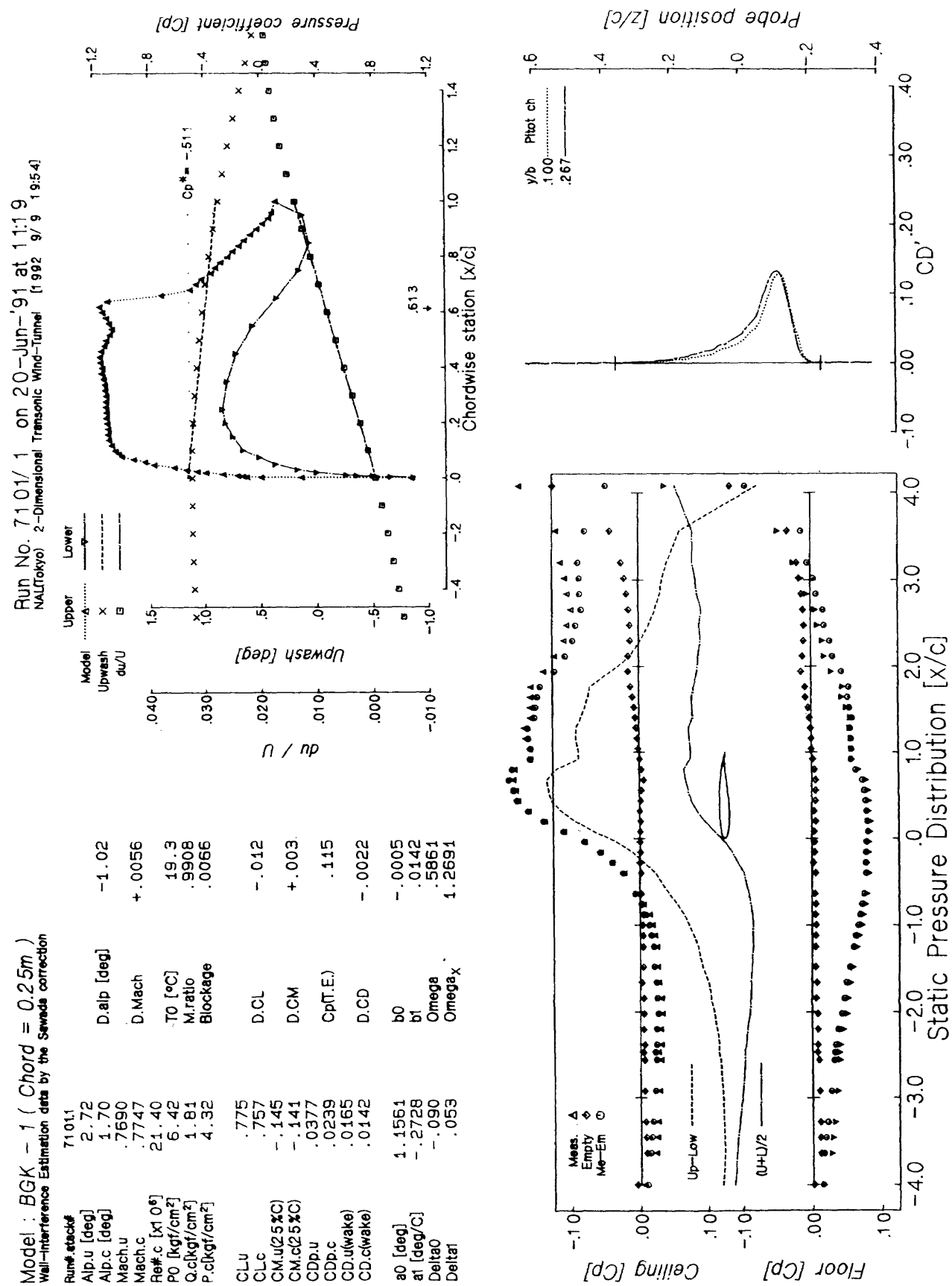

Figure B－28 The NAL data corrected for the top and bottom wall effects.

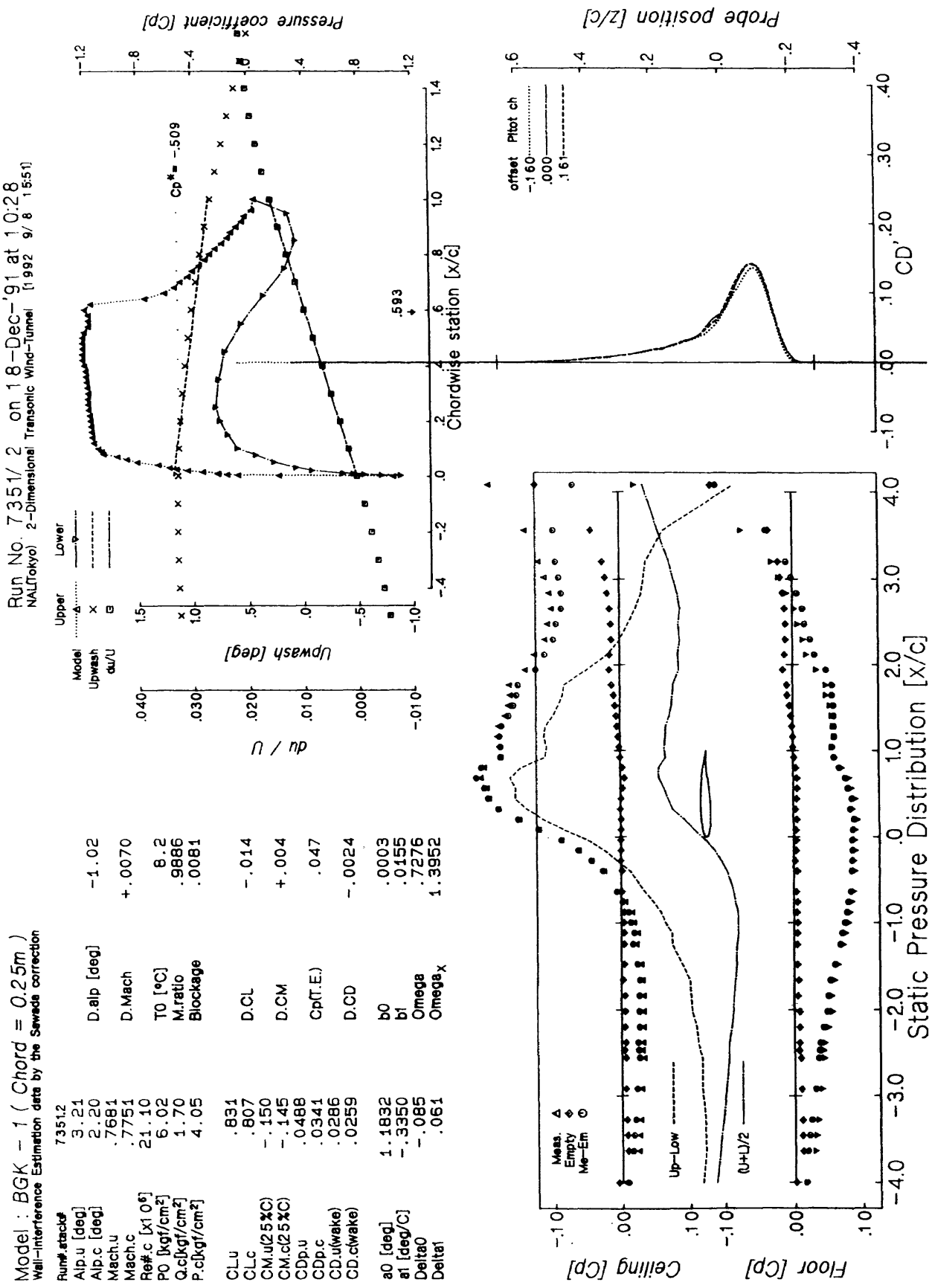

Figure B－29 The NAL data corrected for the top and bottom wall effects.

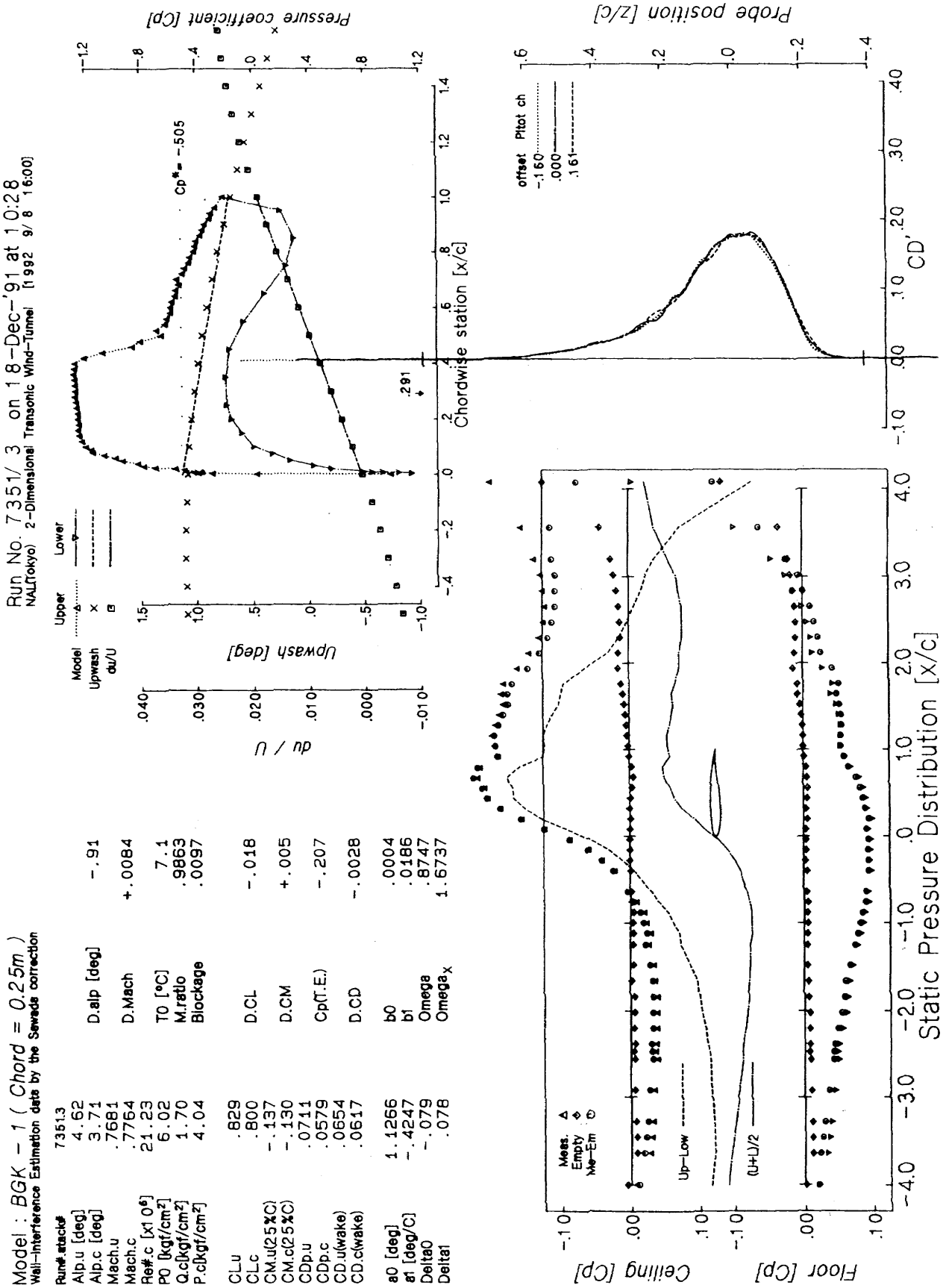

Figure B-30 The NAL data corrected for the top and bottom wall effects.

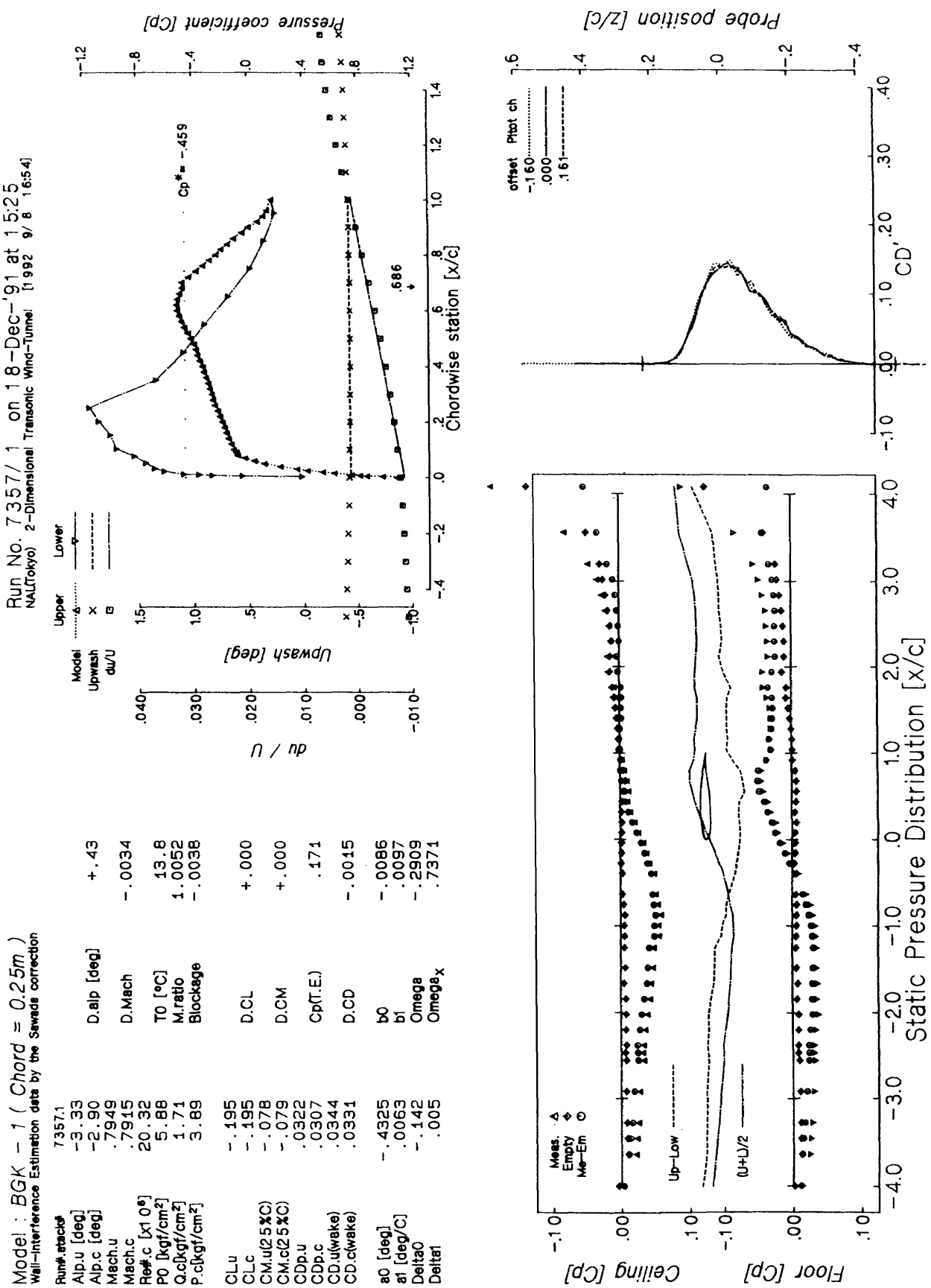

Figure B－31 The NAL data corrected for the top and bottom wall effects.

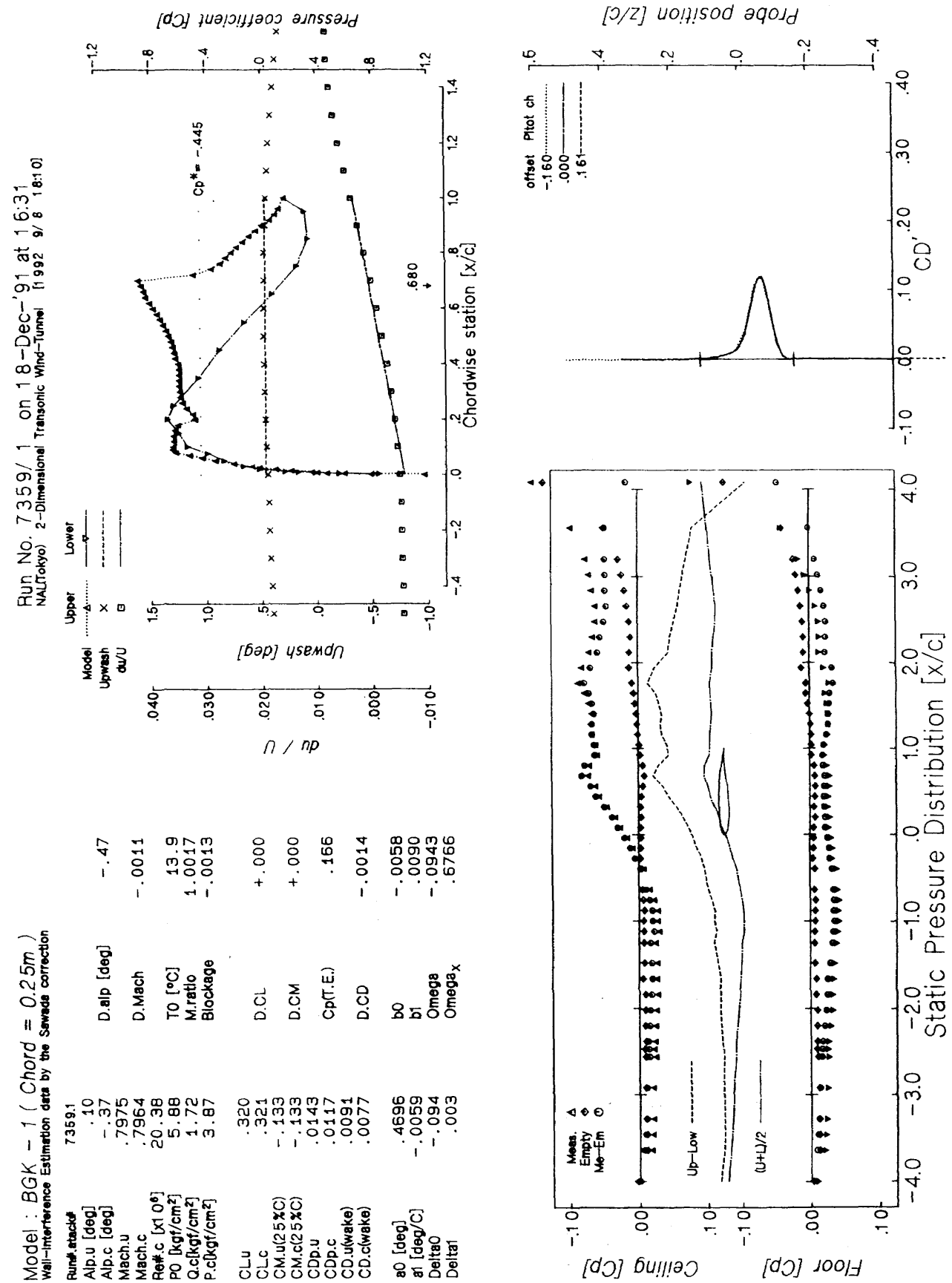

Figure B−32 The NAL data corrected for the top and bottom wall effects.

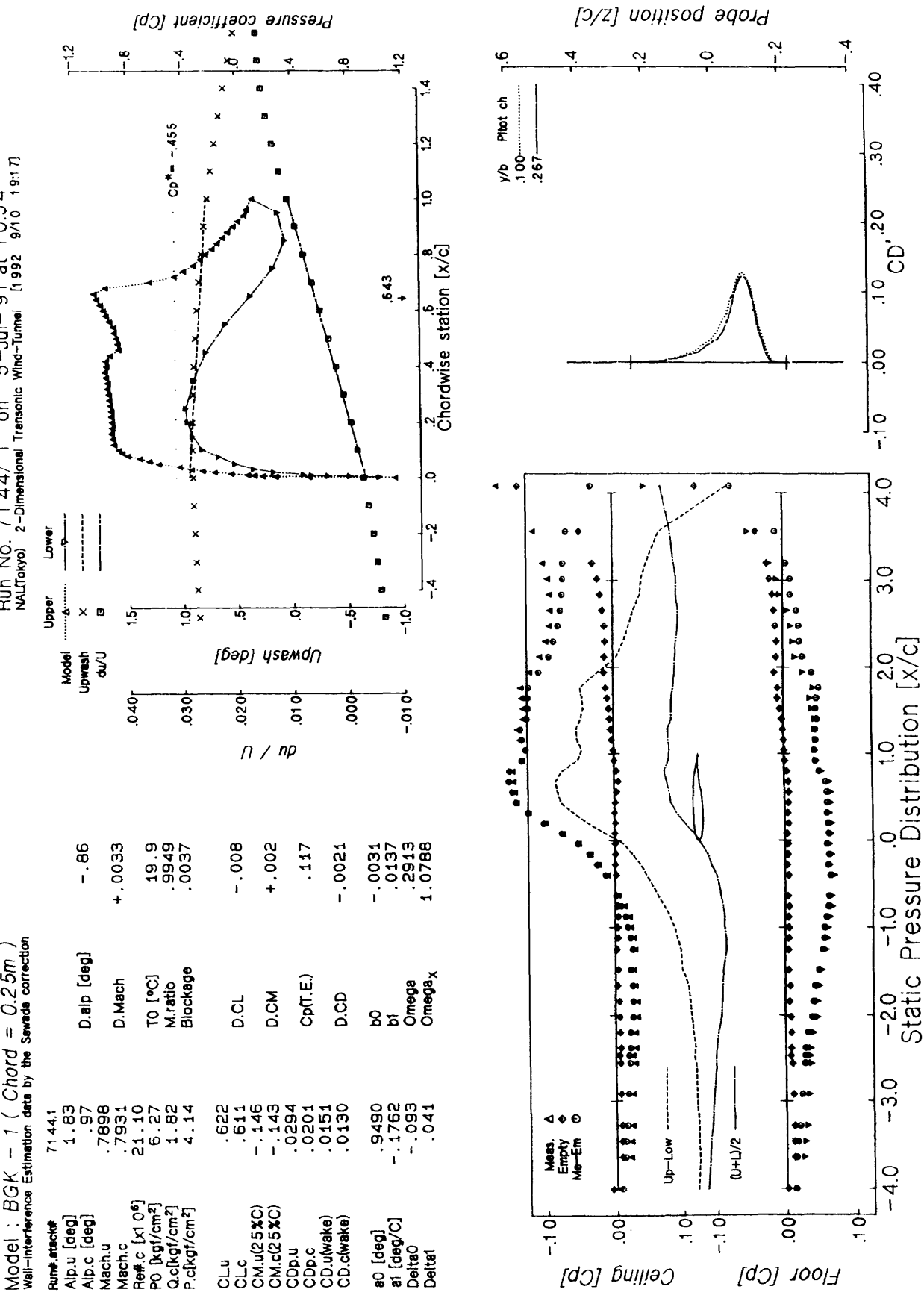

Figure B—33 The NAL data corrected for the top and bottom wall effects.

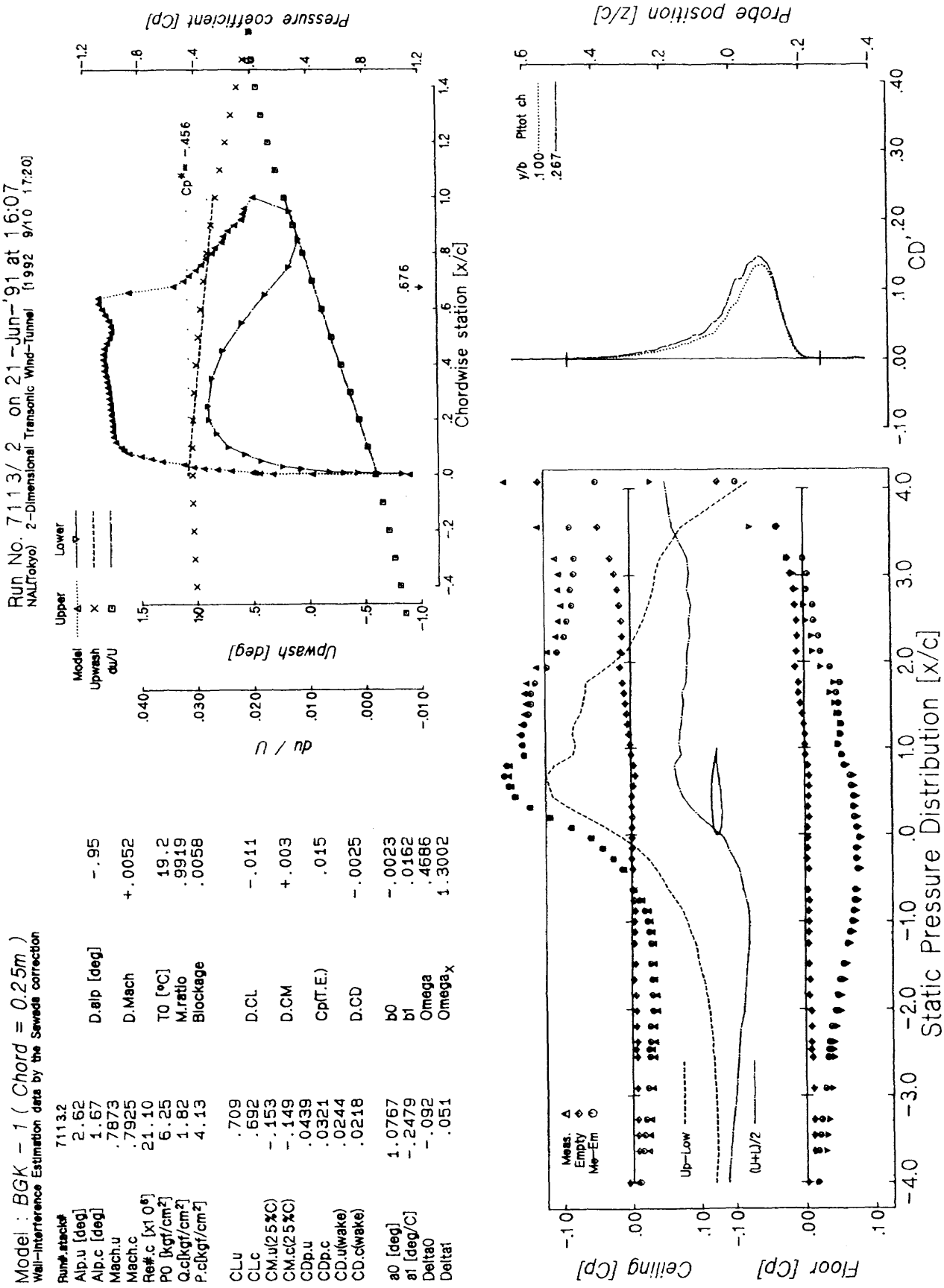

Figure B−34 The NAL data corrected for the top and bottom wall effects.

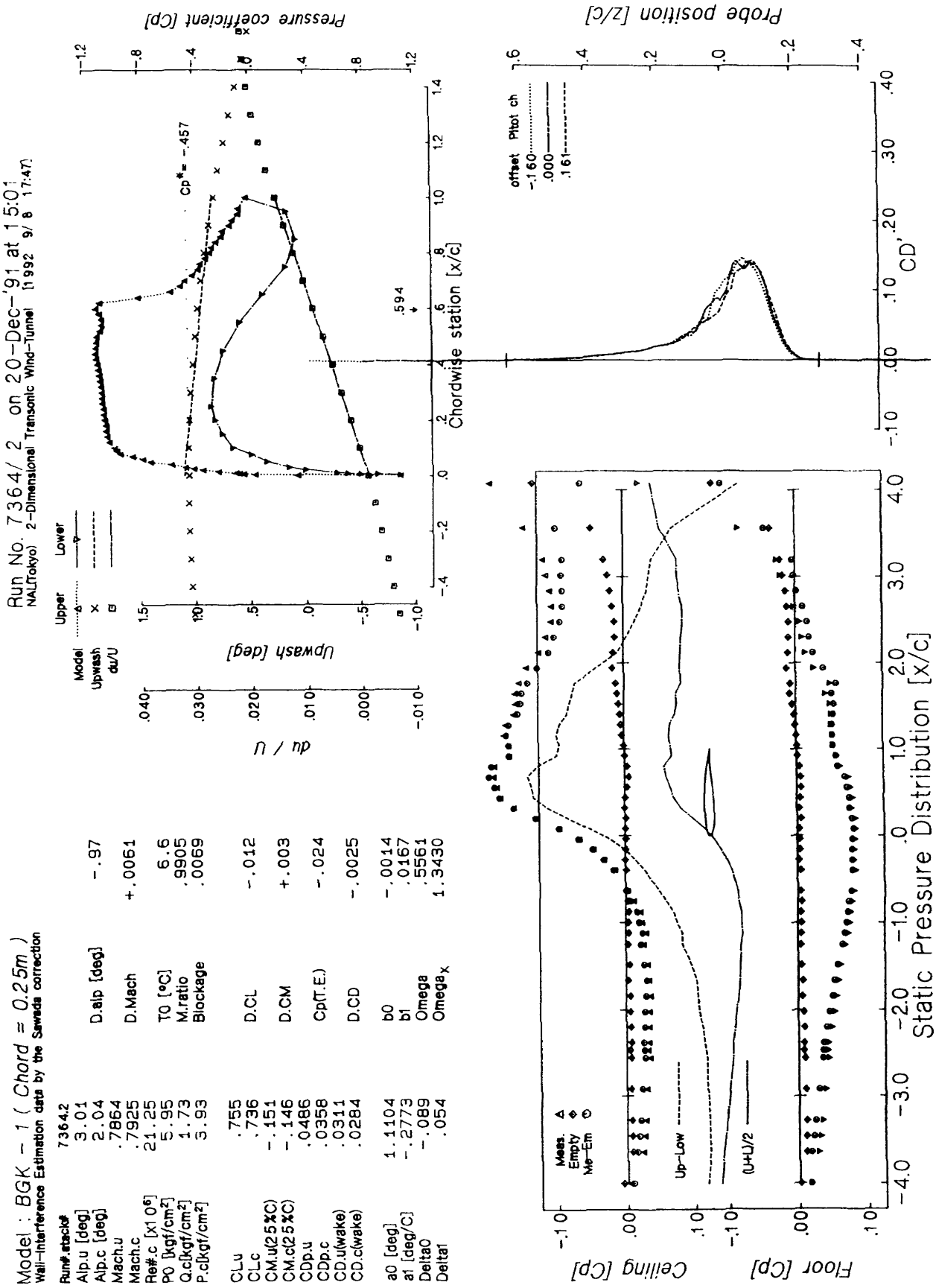

Figure B－35 The NAL data corrected for the top and bottom wall effects.

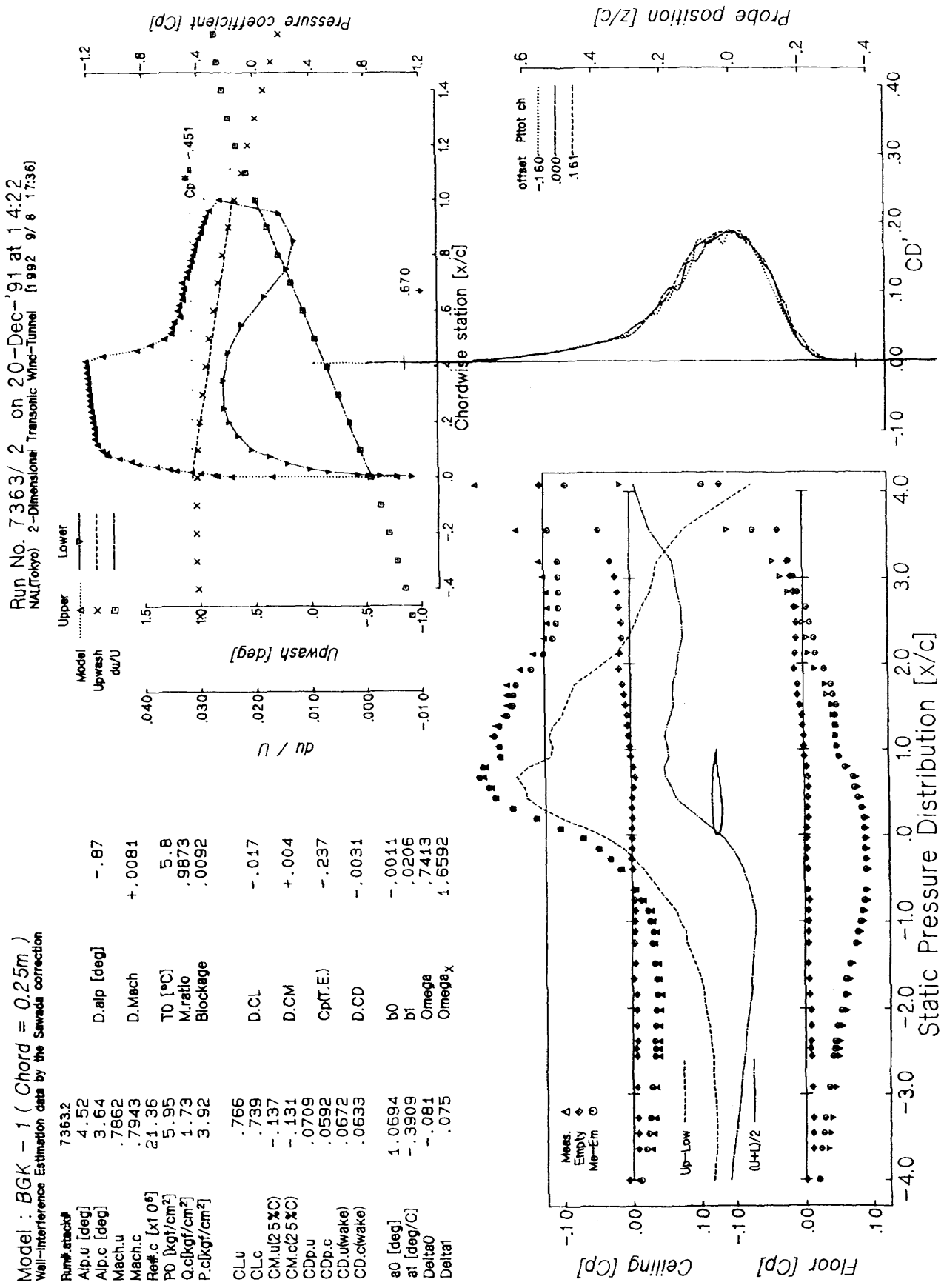

Figure B－36 The NAL data corrected for the top and bottom wall effects.

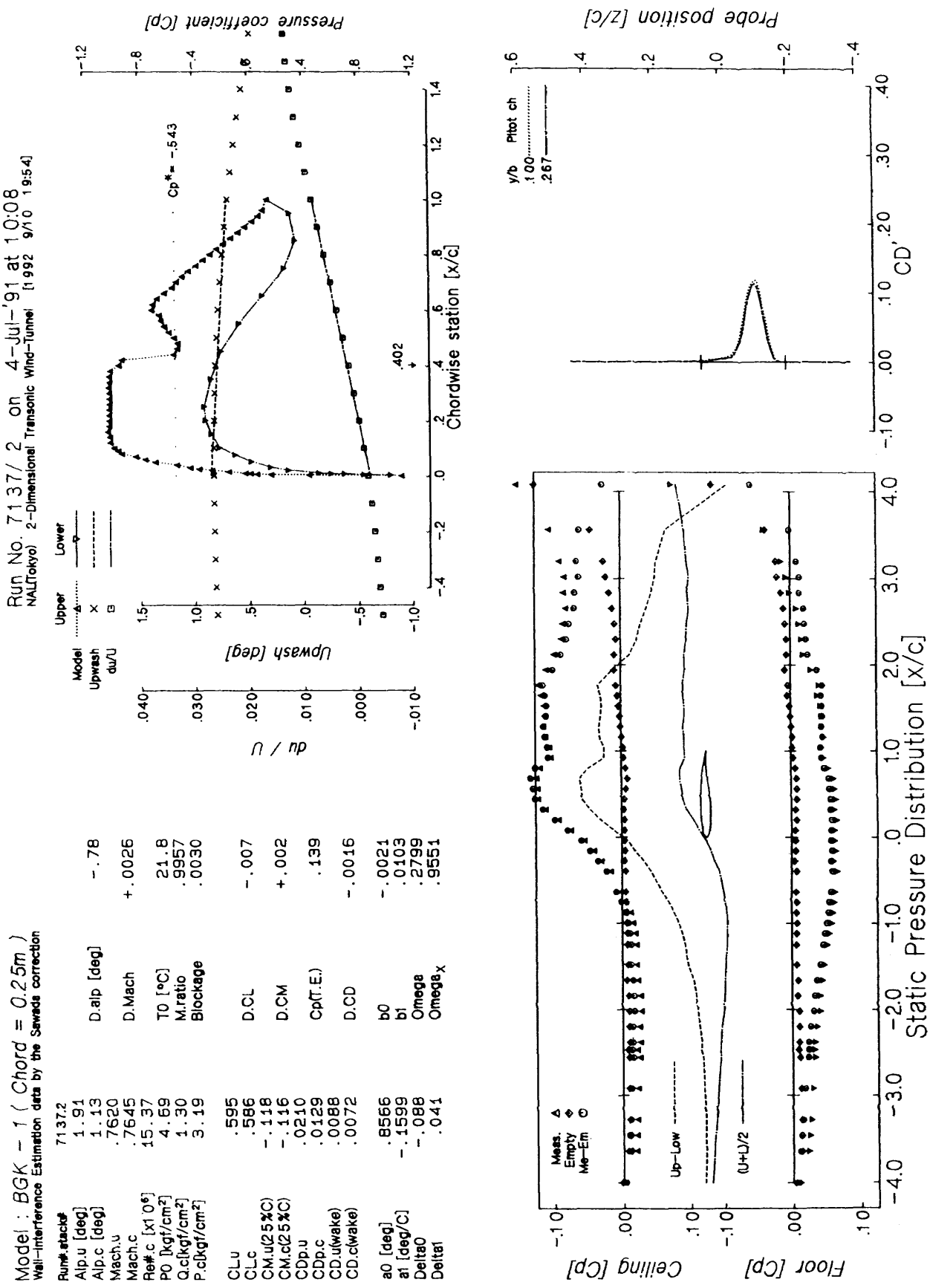

Figure B－37 The NAL data corrected for the top and bottom wall effects.

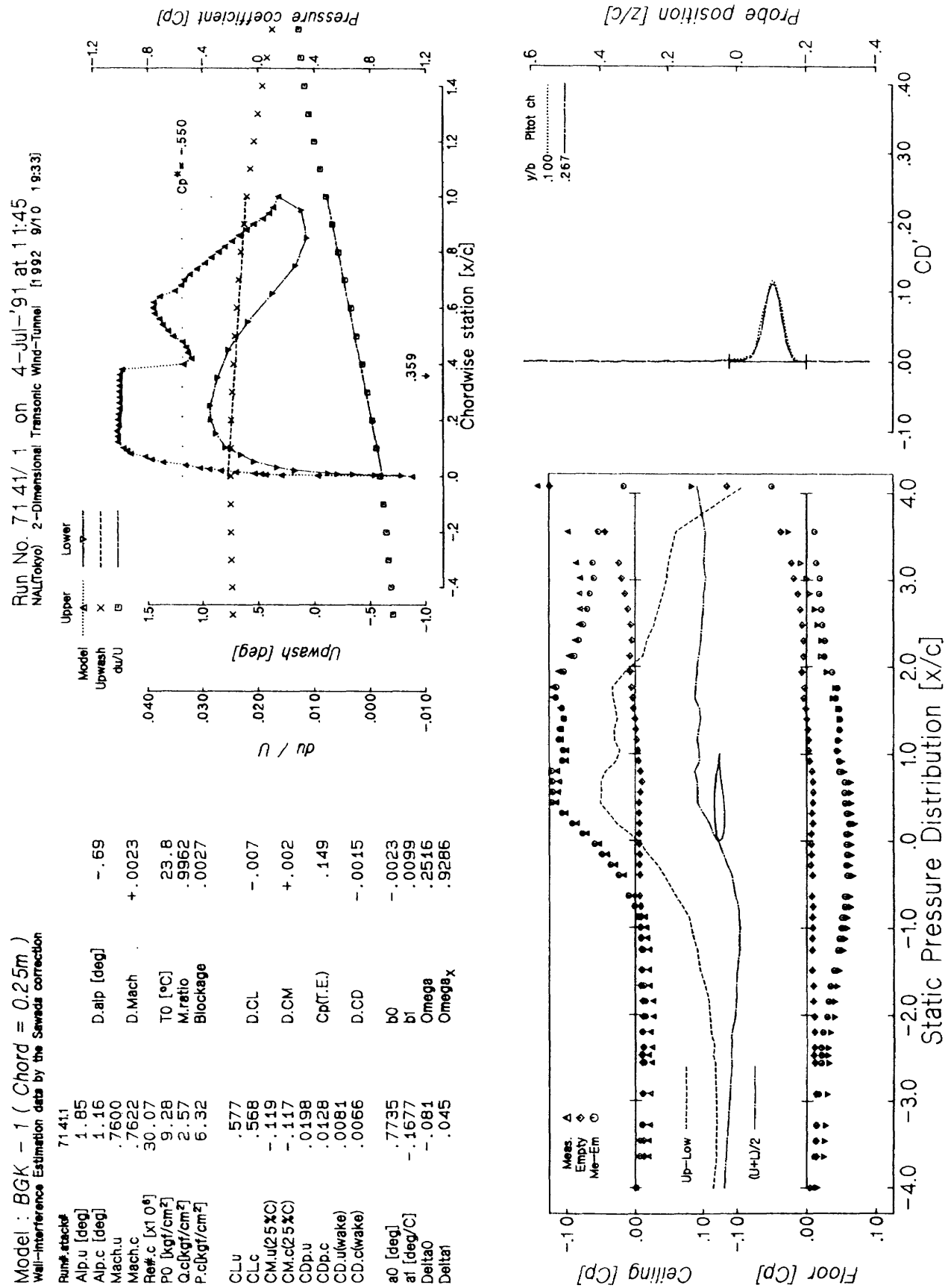

Figure B－38 The NAL data corrected for the top and bottom wall effects.

Run	Scan	M_s	M_c	α_g(deg)	Re	C_{l_u}	C_{l_c}	$C_{d_{wake}}$
7339	2	0.500	0.483	-3.52	20.8×10^6	-0.126	-0.129	0.0069

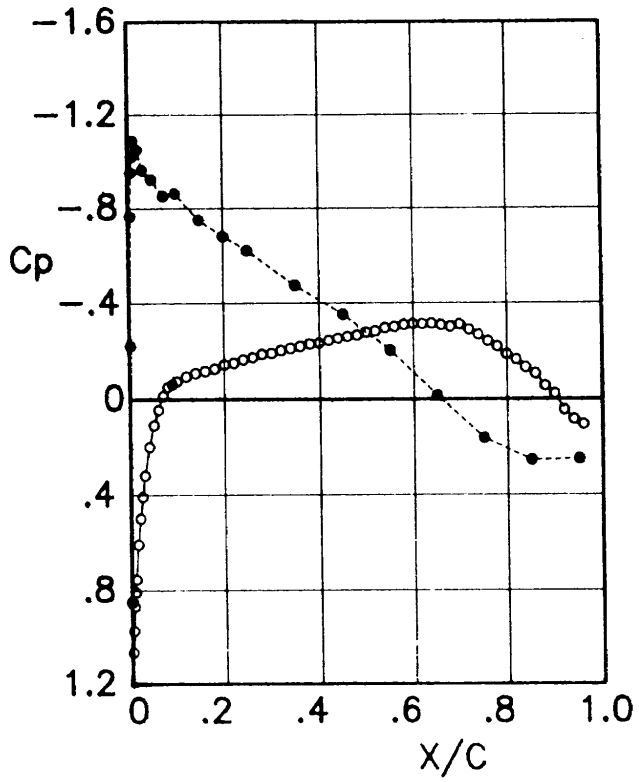

Corrected pressure distribution

Upper surface

x/c	Cp	C_{p_c}
0.000	0.829	0.849
0.002	1.040	1.064
0.004	0.950	0.972
0.006	0.848	0.868
0.008	0.789	0.807
0.010	0.736	0.754
0.015	0.594	0.608
0.020	0.488	0.499
0.025	0.398	0.408
0.030	0.311	0.318
0.040	0.194	0.199
0.050	0.105	0.108
0.060	0.044	0.045
0.070	-0.013	-0.013
0.080	-0.050	-0.052
0.090	-0.061	-0.063
0.100	-0.073	-0.075
0.119	-0.093	-0.095
0.140	-0.107	-0.109
0.160	-0.114	-0.117
0.180	-0.124	-0.126
0.200	-0.141	-0.144
0.220	-0.148	-0.151
0.240	-0.161	-0.164
0.260	-0.170	-0.174
0.280	-0.183	-0.187
0.299	-0.186	-0.191
0.320	-0.198	-0.203
0.340	-0.206	-0.211
0.360	-0.214	-0.219
0.380	-0.224	-0.229
0.399	-0.228	-0.233
0.420	-0.238	-0.244
0.439	-0.247	-0.253
0.460	-0.254	-0.260
0.480	-0.260	-0.266
0.500	-0.272	-0.278
0.519	-0.278	-0.284
0.539	-0.290	-0.297
0.560	-0.295	-0.301
0.580	-0.302	-0.310
0.599	-0.306	-0.314
0.619	-0.306	-0.313
0.639	-0.308	-0.315
0.659	-0.301	-0.308
0.679	-0.295	-0.302
0.699	-0.305	-0.312
0.719	-0.283	-0.290
0.739	-0.262	-0.268
0.759	-0.236	-0.241
0.779	-0.213	-0.218
0.799	-0.181	-0.185
0.819	-0.160	-0.164
0.839	-0.129	-0.132
0.859	-0.103	-0.106
0.879	-0.055	-0.056
0.899	-0.022	-0.022
0.919	0.044	0.045
0.939	0.082	0.084
0.960	0.104	0.106

Spanwise
(upper surface, x/c=.9)

y/b	Cp	C_{p_c}
-0.434	-0.010	-0.010
-0.367	-0.012	-0.012
-0.300	-0.014	-0.015
-0.234	-0.009	-0.009
-0.167	-0.009	-0.009
-0.017	-0.022	-0.022
0.166	-0.015	-0.015
0.232	-0.023	-0.024
0.299	-0.017	-0.017
0.366	-0.023	-0.023
0.432	-0.027	-0.028

Lower surface

x/c	Cp	C_{p_c}
0.950	0.244	0.249
0.850	0.248	0.254
0.750	0.158	0.162
0.650	-0.016	-0.016
0.550	-0.198	-0.203
0.450	-0.346	-0.354
0.350	-0.464	-0.475
0.250	-0.608	-0.623
0.200	-0.666	-0.682
0.150	-0.734	-0.751
0.100	-0.845	-0.865
0.075	-0.835	-0.854
0.050	-0.903	-0.924
0.030	-0.943	-0.965
0.020	-1.027	-1.051
0.010	-1.064	-1.089
0.008	-0.998	-1.021
0.006	-0.932	-0.954
0.004	-0.749	-0.766
0.002	-0.215	-0.220

Figure C − 1 The NAL data corrected for the four wall effects.

Run	Scan	M_s	M_c	α_g(deg)	Re	C_{l_u}	C_{l_c}	$C_{d_{wake}}$
7134	3	0.500	0.483	-0.10	20.9×10^6	0.236	0.241	0.0067

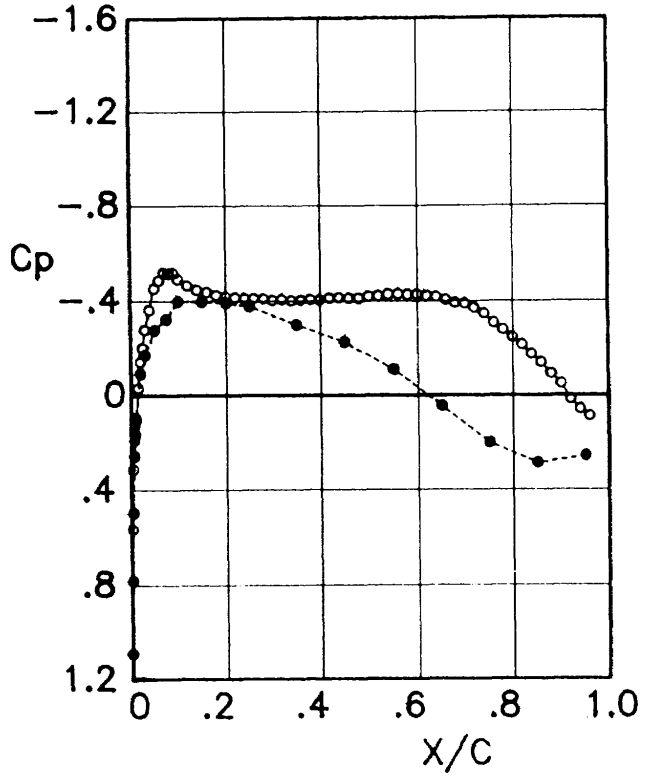

Corrected pressure distribution

Upper surface

x/c	Cp	C_{p_c}
0.000	1.066	1.090
0.002	0.553	0.566
0.004	0.305	0.312
0.006	0.186	0.190
0.008	0.125	0.128
0.010	0.092	0.094
0.015	-0.031	-0.031
0.020	-0.140	-0.143
0.025	-0.197	-0.201
0.030	-0.272	-0.278
0.040	-0.354	-0.362
0.050	-0.443	-0.453
0.060	-0.476	-0.487
0.070	-0.508	-0.519
0.080	-0.506	-0.517
0.090	-0.508	-0.520
0.100	-0.481	-0.492
0.119	-0.455	-0.466
0.140	-0.437	-0.448
0.160	-0.428	-0.438
0.180	-0.416	-0.425
0.200	-0.409	-0.419
0.220	-0.405	-0.414
0.240	-0.401	-0.411
0.260	-0.402	-0.412
0.280	-0.401	-0.410
0.299	-0.394	-0.403
0.320	-0.397	-0.407
0.340	-0.393	-0.402
0.360	-0.395	-0.404
0.380	-0.397	-0.406
0.399	-0.395	-0.404
0.420	-0.403	-0.412
0.439	-0.404	-0.413
0.460	-0.402	-0.412
0.480	-0.402	-0.411
0.500	-0.410	-0.420
0.519	-0.413	-0.422
0.539	-0.419	-0.428
0.560	-0.420	-0.430
0.580	-0.418	-0.427
0.599	-0.418	-0.428
0.619	-0.413	-0.423
0.639	-0.409	-0.418
0.659	-0.396	-0.405
0.679	-0.384	-0.393
0.699	-0.380	-0.389
0.719	-0.362	-0.370
0.739	-0.339	-0.347
0.759	-0.301	-0.308
0.779	-0.273	-0.279
0.799	-0.242	-0.247
0.819	-0.210	-0.215
0.839	-0.171	-0.175
0.859	-0.136	-0.140
0.879	-0.090	-0.092
0.899	-0.049	-0.050
0.919	0.017	0.017
0.939	0.058	0.060
0.960	0.087	0.089

Spanwise
(upper surface, x/c=.9)

y/b	Cp	C_{p_c}
-0.434	-0.040	-0.041
-0.367	-0.037	-0.038
-0.300	-0.041	-0.042
-0.234	-0.036	-0.037
-0.167	-0.037	-0.038
-0.017	-0.049	-0.050
0.166	-0.045	-0.046
0.232	-0.048	-0.049
0.299	-0.046	-0.047
0.366	-0.049	-0.050
0.432	-0.060	-0.061

Lower surface

x/c	Cp	C_{p_c}
0.950	0.252	0.258
0.850	0.282	0.288
0.750	0.198	0.202
0.650	0.045	0.046
0.550	-0.107	-0.110
0.450	-0.220	-0.225
0.350	-0.292	-0.299
0.250	-0.369	-0.378
0.200	-0.383	-0.392
0.150	-0.388	-0.397
0.100	-0.389	-0.397
0.075	-0.315	-0.323
0.050	-0.270	-0.276
0.030	-0.166	-0.170
0.020	-0.089	-0.091
0.010	0.105	0.107
0.008	0.163	0.167
0.006	0.254	0.260
0.004	0.487	0.498
0.002	0.764	0.782

Figure C − 2 The NAL data corrected for the four wall effects.

Run	Scan	M_s	M_c	α_g(deg)	Re	C_{l_u}	C_{l_c}	$C_{d_{wake}}$
7135	1	0.498	0.481	2.62	20.8×10^6	0.545	0.557	0.0070

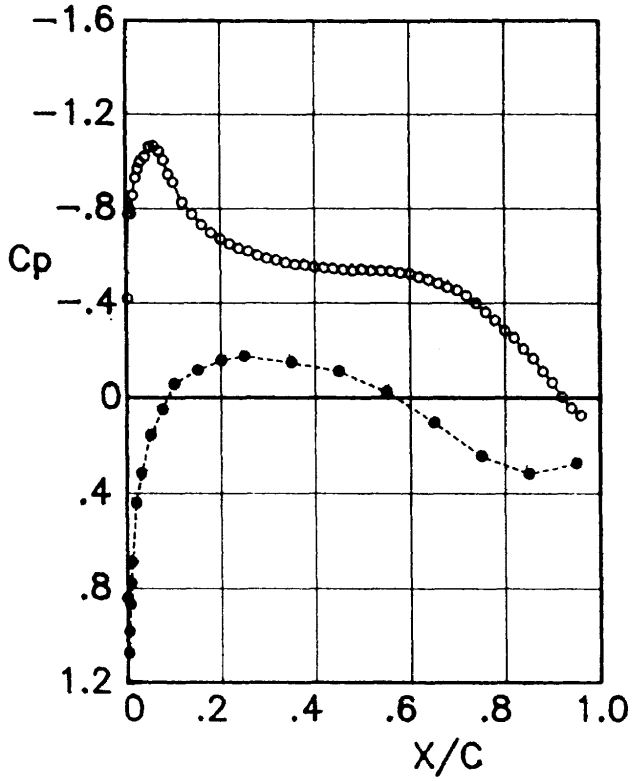

Corrected pressure distribution

Upper surface

x/c	Cp	C_{p_c}
0.000	0.821	0.840
0.002	-0.410	-0.420
0.004	-0.759	-0.777
0.006	-0.765	-0.783
0.008	-0.783	-0.801
0.010	-0.760	-0.778
0.015	-0.837	-0.857
0.020	-0.909	-0.930
0.025	-0.946	-0.968
0.030	-0.974	-0.996
0.040	-0.996	-1.019
0.050	-1.036	-1.060
0.060	-1.041	-1.065
0.070	-1.019	-1.043
0.080	-0.982	-1.005
0.090	-0.924	-0.945
0.100	-0.892	-0.913
0.119	-0.808	-0.826
0.140	-0.757	-0.775
0.160	-0.715	-0.731
0.180	-0.681	-0.697
0.200	-0.655	-0.670
0.220	-0.634	-0.649
0.240	-0.616	-0.630
0.260	-0.604	-0.618
0.280	-0.587	-0.601
0.299	-0.576	-0.589
0.320	-0.568	-0.582
0.340	-0.557	-0.570
0.360	-0.549	-0.562
0.380	-0.547	-0.560
0.399	-0.538	-0.551
0.420	-0.536	-0.548
0.439	-0.532	-0.545
0.460	-0.528	-0.540
0.480	-0.523	-0.535
0.500	-0.529	-0.542
0.519	-0.523	-0.536
0.539	-0.523	-0.535
0.560	-0.521	-0.533
0.580	-0.514	-0.526
0.599	-0.511	-0.523
0.619	-0.498	-0.509
0.639	-0.487	-0.498
0.659	-0.470	-0.481
0.679	-0.454	-0.465
0.699	-0.442	-0.453
0.719	-0.420	-0.429
0.739	-0.389	-0.398
0.759	-0.353	-0.361
0.779	-0.318	-0.326
0.799	-0.276	-0.282
0.819	-0.245	-0.251
0.839	-0.199	-0.204
0.859	-0.160	-0.164
0.879	-0.107	-0.110
0.899	-0.061	-0.063
0.919	-0.001	-0.001
0.939	0.045	0.046
0.960	0.075	0.077

Spanwise
(upper surface, x/c=.9)

y/b	Cp	C_{p_c}
-0.434	-0.062	-0.064
-0.367	-0.059	-0.061
-0.300	-0.060	-0.061
-0.234	-0.054	-0.055
-0.167	-0.055	-0.057
-0.017	-0.061	-0.063
0.166	-0.060	-0.061
0.232	-0.064	-0.065
0.299	-0.062	-0.063
0.366	-0.064	-0.066
0.432	-0.080	-0.082

Lower surface

x/c	Cp	C_{p_c}
0.950	0.270	0.276
0.850	0.312	0.319
0.750	0.240	0.246
0.650	0.103	0.105
0.550	-0.023	-0.023
0.450	-0.109	-0.112
0.350	-0.145	-0.148
0.250	-0.171	-0.175
0.200	-0.153	-0.156
0.150	-0.113	-0.115
0.100	-0.057	-0.058
0.075	0.050	0.051
0.050	0.155	0.158
0.030	0.311	0.319
0.020	0.432	0.442
0.010	0.674	0.689
0.008	0.761	0.778
0.006	0.849	0.869
0.004	0.961	0.983
0.002	1.050	1.075

Figure C − 3 The NAL data corrected for the four wall effects.

Run	Scan	M_s	M_c	α_g(deg)	Re	C_{l_u}	C_{l_c}	$C_{d_{wake}}$
7340	2	0.496	0.481	5.73	20.7×10^6	0.917	0.937	0.0079

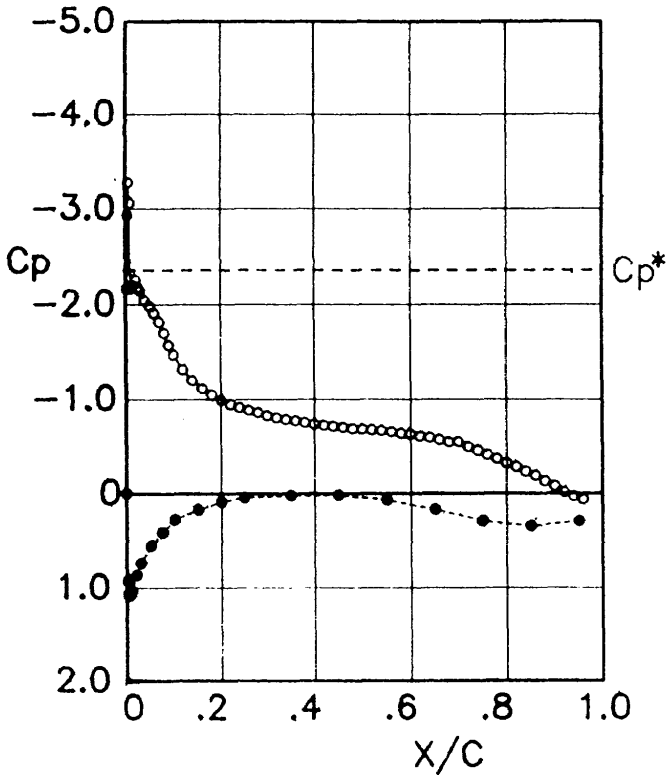

Corrected pressure distribution

Spanwise
(upper surface, x/c=.9)

y/b	C_p	C_{p_c}
-0.434	-0.075	-0.076
-0.367	-0.078	-0.079
-0.300	-0.077	-0.079
-0.234	-0.069	-0.070
-0.167	-0.069	-0.071
-0.017	-0.076	-0.077
0.166	-0.076	-0.077
0.232	-0.083	-0.085
0.299	-0.081	-0.083
0.366	-0.090	-0.092
0.432	-0.093	-0.095

Lower surface

x/c	C_p	C_{p_c}
0.950	0.291	0.297
0.850	0.343	0.350
0.750	0.287	0.293
0.650	0.168	0.171
0.550	0.069	0.070
0.450	0.019	0.020
0.350	0.021	0.021
0.250	0.045	0.046
0.200	0.089	0.091
0.150	0.169	0.173
0.100	0.273	0.279
0.075	0.407	0.415
0.050	0.544	0.556
0.030	0.723	0.738
0.020	0.850	0.867
0.010	1.018	1.039
0.008	1.050	1.072
0.006	1.059	1.081
0.004	1.046	1.068
0.002	0.912	0.931

Upper surface

x/c	C_p	C_{p_c}
0.000	0.000	0.000
0.002	-2.123	-2.168
0.004	-2.872	-2.932
0.006	-3.213	-3.280
0.008	-3.000	-3.063
0.010	-2.117	-2.162
0.015	-2.154	-2.199
0.020	-2.212	-2.258
0.025	-2.135	-2.179
0.030	-2.103	-2.146
0.040	-1.998	-2.040
0.050	-1.944	-1.985
0.060	-1.867	-1.906
0.070	-1.777	-1.814
0.080	-1.661	-1.696
0.090	-1.536	-1.568
0.100	-1.434	-1.464
0.119	-1.284	-1.311
0.140	-1.172	-1.196
0.160	-1.086	-1.108
0.180	-1.021	-1.042
0.200	-0.967	-0.987
0.220	-0.919	-0.939
0.240	-0.886	-0.904
0.260	-0.859	-0.877
0.280	-0.834	-0.851
0.299	-0.802	-0.819
0.320	-0.779	-0.796
0.340	-0.763	-0.778
0.360	-0.750	-0.766
0.380	-0.731	-0.746
0.399	-0.712	-0.727
0.420	-0.702	-0.717
0.439	-0.690	-0.704
0.460	-0.681	-0.695
0.480	-0.666	-0.680
0.500	-0.661	-0.675
0.519	-0.654	-0.668
0.539	-0.647	-0.660
0.560	-0.632	-0.646
0.580	-0.616	-0.629
0.599	-0.610	-0.622
0.619	-0.588	-0.600
0.639	-0.575	-0.587
0.659	-0.550	-0.562
0.679	-0.528	-0.539
0.699	-0.529	-0.540
0.719	-0.478	-0.488
0.739	-0.440	-0.449
0.759	-0.395	-0.404
0.779	-0.357	-0.364
0.799	-0.311	-0.317
0.819	-0.273	-0.278
0.839	-0.225	-0.229
0.859	-0.182	-0.186
0.879	-0.124	-0.127
0.899	-0.076	-0.077
0.919	-0.010	-0.010
0.939	0.032	0.032
0.960	0.065	0.066

Figure C − 4 The NAL data corrected for the four wall effects.

Run	Scan	M_s	M_c	α_g(deg)	Re	C_{l_u}	C_{l_c}	$C_{d_{wake}}$
7341	1	0.494	0.481	8.53	20.5×10^6	1.174	1.195	0.0155

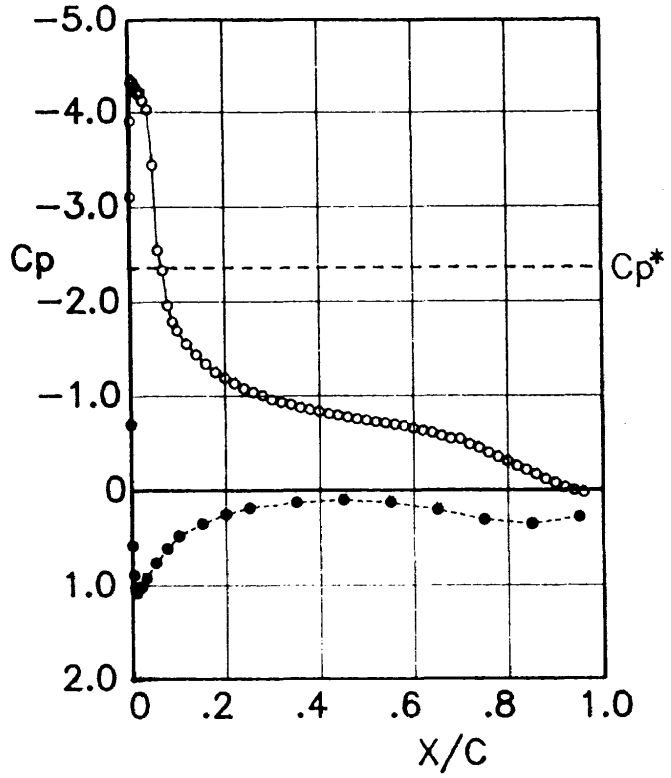

Corrected pressure distribution

Upper surface

x/c	Cp	C_{p_c}
0.000	-0.682	-0.694
0.002	-3.055	-3.110
0.004	-3.838	-3.907
0.006	-4.238	-4.315
0.008	-4.270	-4.346
0.010	-4.243	-4.319
0.015	-4.201	-4.276
0.020	-4.125	-4.199
0.025	-4.148	-4.222
0.030	-4.051	-4.123
0.040	-3.955	-4.026
0.050	-3.378	-3.439
0.060	-2.494	-2.539
0.070	-2.288	-2.329
0.080	-1.921	-1.955
0.090	-1.749	-1.781
0.100	-1.656	-1.686
0.119	-1.516	-1.544
0.140	-1.406	-1.431
0.160	-1.308	-1.332
0.180	-1.222	-1.244
0.200	-1.161	-1.182
0.220	-1.105	-1.125
0.240	-1.054	-1.073
0.260	-1.012	-1.030
0.280	-0.980	-0.997
0.299	-0.934	-0.951
0.320	-0.907	-0.923
0.340	-0.884	-0.899
0.360	-0.851	-0.867
0.380	-0.830	-0.845
0.399	-0.811	-0.825
0.420	-0.787	-0.801
0.439	-0.773	-0.787
0.460	-0.752	-0.765
0.480	-0.734	-0.747
0.500	-0.719	-0.732
0.519	-0.702	-0.715
0.539	-0.690	-0.702
0.560	-0.674	-0.687
0.580	-0.659	-0.671
0.599	-0.635	-0.646
0.619	-0.612	-0.623
0.639	-0.591	-0.602
0.659	-0.557	-0.567
0.679	-0.528	-0.537
0.699	-0.526	-0.535
0.719	-0.468	-0.476
0.739	-0.433	-0.441
0.759	-0.383	-0.390
0.779	-0.341	-0.347
0.799	-0.298	-0.303
0.819	-0.249	-0.253
0.839	-0.207	-0.211
0.859	-0.162	-0.165
0.879	-0.112	-0.114
0.899	-0.073	-0.074
0.919	-0.028	-0.028
0.939	0.003	0.003
0.960	0.025	0.025

Spanwise
(upper surface, x/c=.9)

y/b	Cp	C_{p_c}
-0.434	-0.162	-0.165
-0.367	-0.100	-0.102
-0.300	-0.086	-0.087
-0.234	-0.079	-0.080
-0.167	-0.071	-0.073
-0.017	-0.073	-0.074
0.166	-0.077	-0.078
0.232	-0.089	-0.090
0.299	-0.103	-0.105
0.366	-0.112	-0.114
0.432	-0.187	-0.190

Lower surface

x/c	Cp	C_{p_c}
0.950	0.282	0.287
0.850	0.352	0.359
0.750	0.307	0.312
0.650	0.205	0.209
0.550	0.128	0.130
0.450	0.103	0.104
0.350	0.129	0.132
0.250	0.185	0.188
0.200	0.253	0.257
0.150	0.348	0.354
0.100	0.477	0.486
0.075	0.603	0.614
0.050	0.750	0.763
0.030	0.911	0.928
0.020	1.000	1.018
0.010	1.060	1.079
0.008	1.043	1.062
0.006	1.003	1.021
0.004	0.870	0.886
0.002	0.567	0.577

Figure C − 5 The NAL data corrected for the four wall effects.

Run	Scan	M_s	M_c	α_g(deg)	Re	C_{l_u}	C_{l_c}	$C_{d_{wake}}$
7342	1	0.494	0.482	11.53	21.3×10^6	1.174	1.194	0.0596

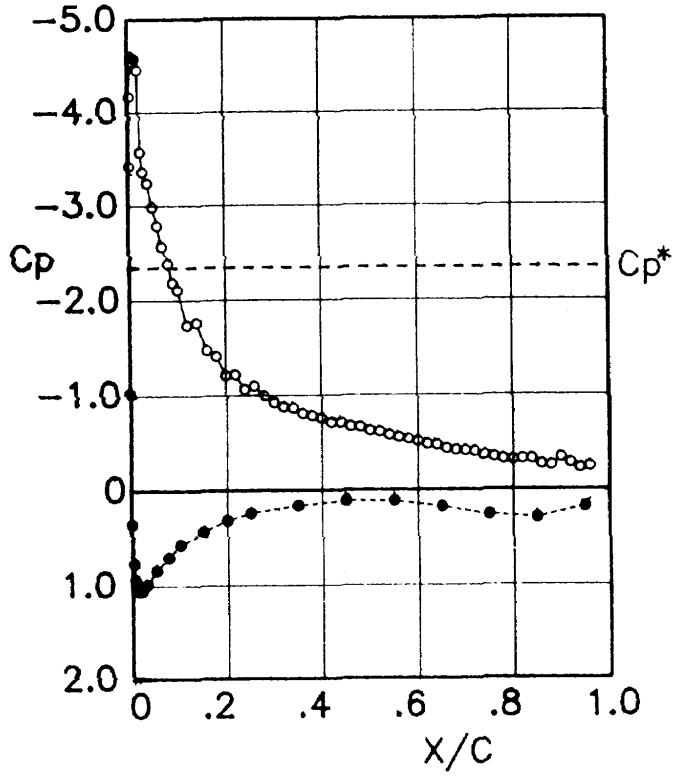

Corrected pressure distribution

Upper surface

x/c	Cp	C_{p_c}
0.000	-1.002	-1.018
0.002	-3.367	-3.423
0.004	-4.103	-4.171
0.006	-4.477	-4.551
0.008	-4.528	-4.604
0.010	-4.520	-4.595
0.015	-4.503	-4.577
0.020	-4.384	-4.457
0.025	-3.514	-3.572
0.030	-3.306	-3.361
0.040	-3.186	-3.239
0.050	-2.935	-2.984
0.060	-2.741	-2.786
0.070	-2.523	-2.565
0.080	-2.347	-2.386
0.090	-2.146	-2.181
0.100	-2.071	-2.105
0.119	-1.707	-1.735
0.140	-1.731	-1.760
0.160	-1.448	-1.472
0.180	-1.385	-1.408
0.200	-1.185	-1.205
0.220	-1.193	-1.213
0.240	-1.041	-1.058
0.260	-1.075	-1.093
0.280	-0.976	-0.992
0.299	-0.902	-0.917
0.320	-0.858	-0.873
0.340	-0.846	-0.860
0.360	-0.788	-0.801
0.380	-0.765	-0.778
0.399	-0.741	-0.753
0.420	-0.696	-0.707
0.439	-0.695	-0.706
0.460	-0.655	-0.665
0.480	-0.649	-0.660
0.500	-0.608	-0.618
0.519	-0.599	-0.608
0.539	-0.562	-0.571
0.560	-0.540	-0.549
0.580	-0.523	-0.532
0.599	-0.499	-0.508
0.619	-0.468	-0.475
0.639	-0.460	-0.467
0.659	-0.423	-0.430
0.679	-0.406	-0.412
0.699	-0.400	-0.407
0.719	-0.390	-0.397
0.739	-0.354	-0.359
0.759	-0.334	-0.339
0.779	-0.312	-0.318
0.799	-0.304	-0.309
0.819	-0.314	-0.319
0.839	-0.313	-0.318
0.859	-0.259	-0.263
0.879	-0.249	-0.253
0.899	-0.330	-0.336
0.919	-0.271	-0.276
0.939	-0.219	-0.223
0.960	-0.236	-0.239

Spanwise
(upper surface, x/c=.9)

y/b	Cp	C_{p_c}
-0.434	-0.289	-0.293
-0.367	-0.293	-0.298
-0.300	-0.321	-0.326
-0.234	-0.403	-0.410
-0.167	-0.281	-0.286
-0.017	-0.330	-0.336
0.166	-0.262	-0.266
0.232	-0.284	-0.288
0.299	-0.274	-0.278
0.366	-0.282	-0.286
0.432	-0.277	-0.282

Lower surface

x/c	Cp	C_{p_c}
0.950	0.176	0.178
0.850	0.291	0.296
0.750	0.257	0.262
0.650	0.172	0.175
0.550	0.113	0.115
0.450	0.108	0.110
0.350	0.158	0.161
0.250	0.235	0.239
0.200	0.309	0.315
0.150	0.425	0.432
0.100	0.558	0.567
0.075	0.689	0.701
0.050	0.825	0.839
0.030	0.969	0.985
0.020	1.042	1.059
0.010	1.040	1.058
0.008	0.989	1.006
0.006	0.918	0.934
0.004	0.754	0.766
0.002	0.343	0.349

Figure C－6 The NAL data corrected for the four wall effects.

Run	Scan	M_s	M_c	α_g(deg)	Re	C_{l_u}	C_{l_c}	$C_{d_{wake}}$
7343	2	0.701	0.678	-3.72	21.3×10^6	-0.184	-0.188	0.0074

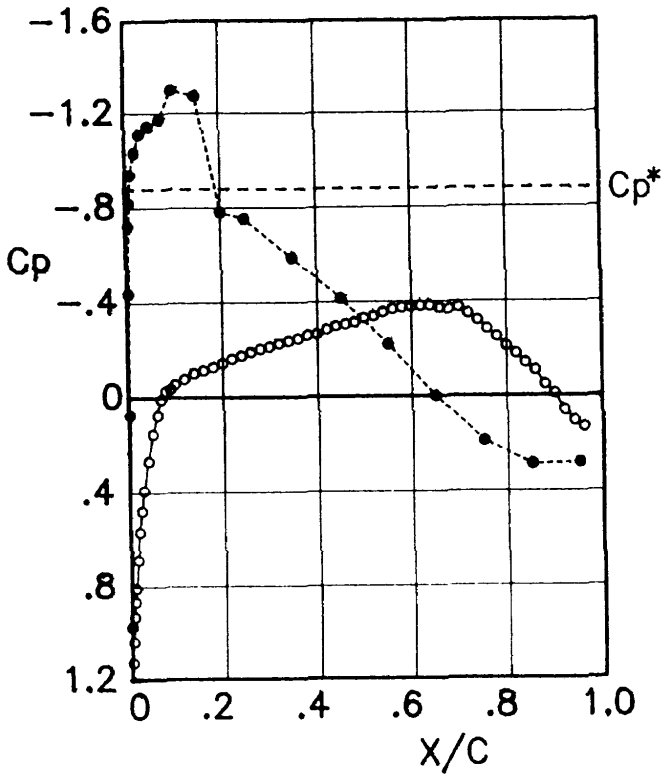

Corrected pressure distribution

Upper surface

x/c	Cp	C_{p_c}
0.000	0.954	0.976
0.002	1.104	1.129
0.004	1.016	1.039
0.006	0.911	0.932
0.008	0.846	0.865
0.010	0.789	0.807
0.015	0.671	0.686
0.020	0.557	0.569
0.025	0.468	0.479
0.030	0.383	0.392
0.040	0.261	0.267
0.050	0.150	0.153
0.060	0.072	0.074
0.070	0.008	0.008
0.080	-0.029	-0.029
0.090	-0.036	-0.037
0.100	-0.055	-0.057
0.119	-0.076	-0.078
0.140	-0.099	-0.102
0.160	-0.111	-0.114
0.180	-0.124	-0.127
0.200	-0.140	-0.144
0.220	-0.158	-0.162
0.240	-0.172	-0.175
0.260	-0.186	-0.191
0.280	-0.199	-0.203
0.299	-0.208	-0.213
0.320	-0.220	-0.225
0.340	-0.230	-0.235
0.360	-0.240	-0.245
0.380	-0.255	-0.260
0.399	-0.258	-0.264
0.420	-0.277	-0.283
0.439	-0.291	-0.297
0.460	-0.298	-0.304
0.480	-0.306	-0.313
0.500	-0.323	-0.331
0.519	-0.331	-0.338
0.539	-0.347	-0.355
0.560	-0.361	-0.369
0.580	-0.367	-0.375
0.599	-0.370	-0.379
0.619	-0.373	-0.381
0.639	-0.374	-0.382
0.659	-0.365	-0.373
0.679	-0.358	-0.366
0.699	-0.367	-0.376
0.719	-0.341	-0.349
0.739	-0.312	-0.319
0.759	-0.276	-0.283
0.779	-0.244	-0.249
0.799	-0.206	-0.210
0.819	-0.175	-0.178
0.839	-0.136	-0.139
0.859	-0.105	-0.107
0.879	-0.046	-0.047
0.899	-0.008	-0.008
0.919	0.061	0.063
0.939	0.104	0.106
0.960	0.129	0.132

Spanwise
(upper surface, x/c=.9)

y/b	Cp	C_{p_c}
-0.434	-0.001	-0.001
-0.367	-0.001	-0.001
-0.300	-0.003	-0.003
-0.234	0.002	0.002
-0.167	0.004	0.004
-0.017	-0.008	-0.008
0.166	-0.004	-0.004
0.232	-0.013	-0.013
0.299	-0.007	-0.007
0.366	-0.014	-0.014
0.432	-0.018	-0.018

Lower surface

x/c	Cp	C_{p_c}
0.950	0.275	0.282
0.850	0.281	0.288
0.750	0.185	0.189
0.650	0.000	0.000
0.550	-0.214	-0.219
0.450	-0.405	-0.414
0.350	-0.574	-0.587
0.250	-0.736	-0.752
0.200	-0.762	-0.779
0.150	-1.246	-1.273
0.100	-1.270	-1.298
0.075	-1.146	-1.172
0.050	-1.117	-1.142
0.030	-1.086	-1.110
0.020	-1.007	-1.030
0.010	-0.917	-0.937
0.008	-0.800	-0.818
0.006	-0.704	-0.720
0.004	-0.426	-0.435
0.002	0.075	0.076

Figure C − 7 The NAL data corrected for the four wall effects.

Run	Scan	M_s	M_c	α_g(deg)	Re	C_{l_u}	C_{l_c}	$C_{d_{wake}}$
7132	3	0.700	0.677	-0.20	21.1×10^6	0.252	0.258	0.0068

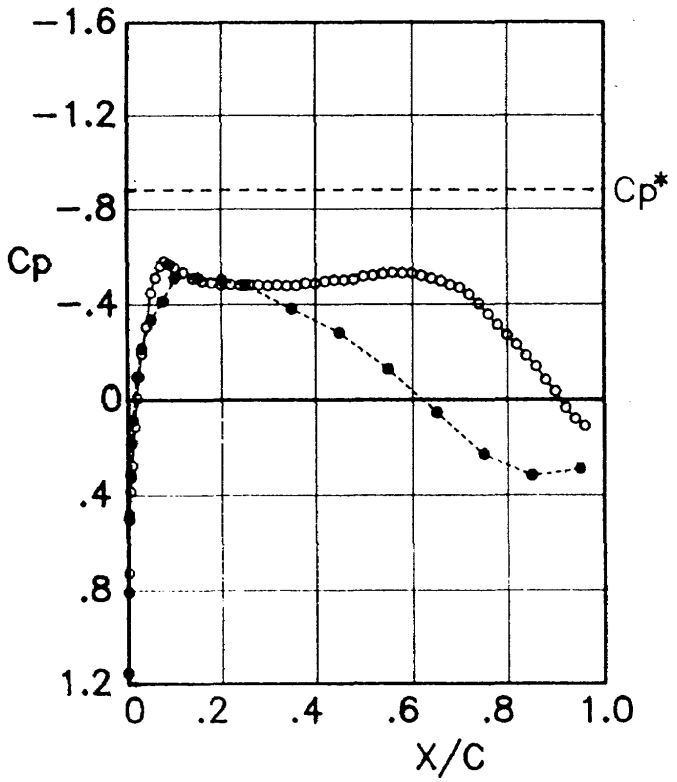

Corrected pressure distribution

Spanwise
(upper surface, x/c=.9)

y/b	Cp	C_{p_c}
-0.434	-0.037	-0.038
-0.367	-0.032	-0.033
-0.300	-0.033	-0.033
-0.234	-0.027	-0.028
-0.167	-0.025	-0.026
-0.017	-0.034	-0.035
0.166	-0.032	-0.033
0.232	-0.034	-0.034
0.299	-0.036	-0.037
0.366	-0.044	-0.045
0.432	-0.051	-0.052

Lower surface

x/c	Cp	C_{p_c}
0.950	0.284	0.290
0.850	0.311	0.318
0.750	0.225	0.230
0.650	0.053	0.055
0.550	-0.126	-0.129
0.450	-0.275	-0.281
0.350	-0.374	-0.383
0.250	-0.471	-0.482
0.200	-0.492	-0.503
0.150	-0.500	-0.511
0.100	-0.500	-0.511
0.075	-0.405	-0.414
0.050	-0.329	-0.336
0.030	-0.210	-0.215
0.020	-0.093	-0.095
0.010	0.085	0.087
0.008	0.181	0.185
0.006	0.307	0.314
0.004	0.492	0.503
0.002	0.790	0.808

Upper surface

x/c	Cp	C_{p_c}
0.000	1.128	1.154
0.002	0.710	0.726
0.004	0.468	0.479
0.006	0.375	0.384
0.008	0.316	0.323
0.010	0.269	0.275
0.015	0.110	0.112
0.020	-0.009	-0.009
0.025	-0.096	-0.098
0.030	-0.188	-0.192
0.040	-0.299	-0.306
0.050	-0.440	-0.450
0.060	-0.500	-0.512
0.070	-0.550	-0.562
0.080	-0.569	-0.582
0.090	-0.557	-0.569
0.100	-0.544	-0.556
0.119	-0.524	-0.536
0.140	-0.498	-0.509
0.160	-0.487	-0.498
0.180	-0.481	-0.492
0.200	-0.472	-0.483
0.220	-0.475	-0.485
0.240	-0.470	-0.481
0.260	-0.473	-0.483
0.280	-0.472	-0.483
0.299	-0.469	-0.479
0.320	-0.471	-0.482
0.340	-0.469	-0.479
0.360	-0.470	-0.481
0.380	-0.479	-0.489
0.399	-0.478	-0.488
0.420	-0.486	-0.497
0.439	-0.491	-0.502
0.460	-0.491	-0.502
0.480	-0.495	-0.506
0.500	-0.507	-0.518
0.519	-0.510	-0.522
0.539	-0.517	-0.529
0.560	-0.522	-0.533
0.580	-0.520	-0.531
0.599	-0.519	-0.530
0.619	-0.509	-0.521
0.639	-0.498	-0.509
0.659	-0.488	-0.499
0.679	-0.471	-0.482
0.699	-0.460	-0.470
0.719	-0.432	-0.441
0.739	-0.394	-0.403
0.759	-0.350	-0.358
0.779	-0.307	-0.314
0.799	-0.265	-0.271
0.819	-0.226	-0.232
0.839	-0.181	-0.185
0.859	-0.137	-0.140
0.879	-0.081	-0.083
0.899	-0.034	-0.035
0.919	0.034	0.035
0.939	0.078	0.080
0.960	0.108	0.111

Figure C − 8 The NAL data corrected for the four wall effects.

Run	Scan	M_s	M_c	α_g(deg)	Re	C_{l_u}	C_{l_c}	$C_{d_{wake}}$
7133	3	0.695	0.675	2.73	20.9×10^6	0.659	0.672	0.0093

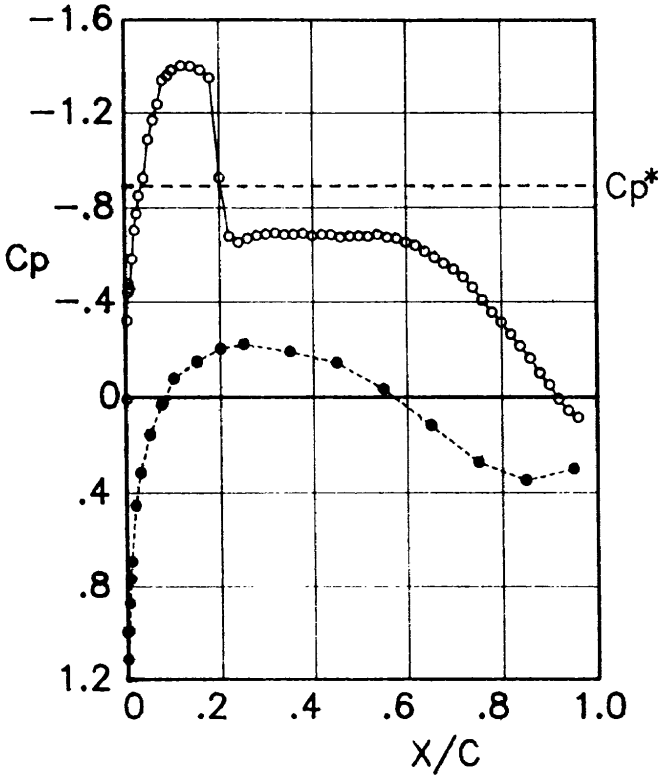

Corrected pressure distribution

Upper surface

x/c	Cp	C_{pc}
0.000	0.979	0.999
0.002	0.007	0.007
0.004	-0.316	-0.322
0.006	-0.434	-0.442
0.008	-0.469	-0.478
0.010	-0.449	-0.458
0.015	-0.572	-0.583
0.020	-0.692	-0.705
0.025	-0.760	-0.775
0.030	-0.834	-0.850
0.040	-0.907	-0.925
0.050	-1.066	-1.087
0.060	-1.146	-1.168
0.070	-1.213	-1.237
0.080	-1.314	-1.339
0.090	-1.333	-1.359
0.100	-1.357	-1.383
0.119	-1.374	-1.401
0.140	-1.372	-1.399
0.160	-1.357	-1.383
0.180	-1.324	-1.350
0.200	-0.908	-0.926
0.220	-0.665	-0.678
0.240	-0.639	-0.652
0.260	-0.655	-0.667
0.280	-0.667	-0.680
0.299	-0.673	-0.686
0.320	-0.678	-0.691
0.340	-0.671	-0.684
0.360	-0.672	-0.685
0.380	-0.676	-0.689
0.399	-0.666	-0.679
0.420	-0.671	-0.684
0.439	-0.670	-0.684
0.460	-0.660	-0.673
0.480	-0.664	-0.677
0.500	-0.665	-0.678
0.519	-0.663	-0.676
0.539	-0.671	-0.684
0.560	-0.658	-0.671
0.580	-0.654	-0.667
0.599	-0.637	-0.650
0.619	-0.625	-0.637
0.639	-0.600	-0.612
0.659	-0.575	-0.586
0.679	-0.551	-0.562
0.699	-0.526	-0.536
0.719	-0.494	-0.504
0.739	-0.451	-0.460
0.759	-0.397	-0.405
0.779	-0.347	-0.354
0.799	-0.306	-0.312
0.819	-0.256	-0.261
0.839	-0.207	-0.211
0.859	-0.157	-0.160
0.879	-0.097	-0.099
0.899	-0.048	-0.049
0.919	0.011	0.011
0.939	0.057	0.058
0.960	0.086	0.088

Spanwise
(upper surface, x/c=.9)

y/b	Cp	C_{pc}
-0.434	-0.059	-0.060
-0.367	-0.053	-0.054
-0.300	-0.051	-0.052
-0.234	-0.046	-0.047
-0.167	-0.037	-0.038
-0.017	-0.048	-0.049
0.166	-0.047	-0.048
0.232	-0.054	-0.055
0.299	-0.058	-0.059
0.366	-0.062	-0.063
0.432	-0.076	-0.078

Lower surface

x/c	Cp	C_{pc}
0.950	0.295	0.301
0.850	0.342	0.349
0.750	0.268	0.273
0.650	0.117	0.119
0.550	-0.033	-0.034
0.450	-0.140	-0.143
0.350	-0.185	-0.189
0.250	-0.216	-0.220
0.200	-0.198	-0.202
0.150	-0.146	-0.149
0.100	-0.076	-0.077
0.075	0.032	0.032
0.050	0.155	0.158
0.030	0.311	0.317
0.020	0.447	0.456
0.010	0.680	0.693
0.008	0.753	0.768
0.006	0.857	0.874
0.004	0.974	0.993
0.002	1.093	1.115

Figure C − 9 The NAL data corrected for the four wall effects.

Run	Scan	M_s	M_c	α_g(deg)	Re	C_{l_u}	C_{l_c}	$C_{d_{wake}}$
7344	1	0.689	0.673	4.52	21.0×10^6	0.954	0.969	0.0222

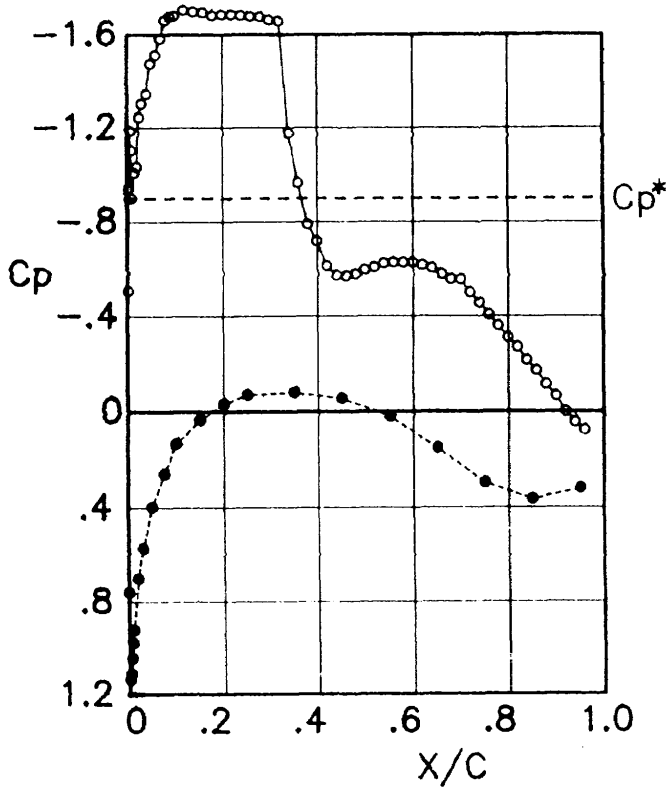

Corrected pressure distribution

Upper surface

x/c	Cp	C_{p_c}
0.000	0.747	0.759
0.002	-0.502	-0.510
0.004	-0.927	-0.942
0.006	-1.171	-1.189
0.008	-1.089	-1.106
0.010	-0.887	-0.901
0.015	-0.993	-1.008
0.020	-1.019	-1.034
0.025	-1.225	-1.244
0.030	-1.283	-1.303
0.040	-1.324	-1.344
0.050	-1.451	-1.474
0.060	-1.487	-1.510
0.070	-1.558	-1.582
0.080	-1.637	-1.663
0.090	-1.653	-1.679
0.100	-1.656	-1.681
0.119	-1.682	-1.708
0.140	-1.675	-1.701
0.160	-1.671	-1.697
0.180	-1.658	-1.683
0.200	-1.662	-1.687
0.220	-1.661	-1.687
0.240	-1.658	-1.684
0.260	-1.655	-1.680
0.280	-1.653	-1.678
0.299	-1.639	-1.664
0.320	-1.634	-1.659
0.340	-1.158	-1.176
0.360	-0.949	-0.964
0.380	-0.776	-0.788
0.399	-0.705	-0.716
0.420	-0.601	-0.610
0.439	-0.562	-0.570
0.460	-0.559	-0.568
0.480	-0.567	-0.576
0.500	-0.586	-0.595
0.519	-0.596	-0.605
0.539	-0.613	-0.622
0.560	-0.616	-0.626
0.580	-0.616	-0.625
0.599	-0.617	-0.626
0.619	-0.605	-0.614
0.639	-0.593	-0.602
0.659	-0.567	-0.576
0.679	-0.546	-0.554
0.699	-0.545	-0.554
0.719	-0.491	-0.498
0.739	-0.448	-0.455
0.759	-0.398	-0.404
0.779	-0.352	-0.357
0.799	-0.303	-0.308
0.819	-0.264	-0.268
0.839	-0.210	-0.214
0.859	-0.168	-0.171
0.879	-0.111	-0.113
0.899	-0.063	-0.064
0.919	0.002	0.002
0.939	0.045	0.046
0.960	0.077	0.079

Spanwise
(upper surface, x/c=.9)

y/b	Cp	C_{p_c}
-0.434	-0.068	-0.069
-0.367	-0.069	-0.070
-0.300	-0.065	-0.066
-0.234	-0.057	-0.058
-0.167	-0.054	-0.055
-0.017	-0.063	-0.064
0.166	-0.057	-0.058
0.232	-0.067	-0.068
0.299	-0.070	-0.071
0.366	-0.075	-0.076
0.432	-0.087	-0.089

Lower surface

x/c	Cp	C_{p_c}
0.950	0.315	0.320
0.850	0.359	0.365
0.750	0.291	0.296
0.650	0.150	0.152
0.550	0.020	0.020
0.450	-0.055	-0.055
0.350	-0.079	-0.080
0.250	-0.069	-0.070
0.200	-0.032	-0.032
0.150	0.035	0.035
0.100	0.131	0.133
0.075	0.256	0.260
0.050	0.391	0.397
0.030	0.563	0.572
0.020	0.690	0.700
0.010	0.907	0.921
0.008	0.963	0.978
0.006	1.029	1.045
0.004	1.096	1.113
0.002	1.119	1.137

Figure C−10 The NAL data corrected for the four wall effects.

Run	Scan	M_s	M_c	α_g(deg)	Re	C_{l_u}	C_{l_c}	$C_{d_{wake}}$
7346	2	0.689	0.676	5.32	20.8×10^6	1.087	1.100	0.0350

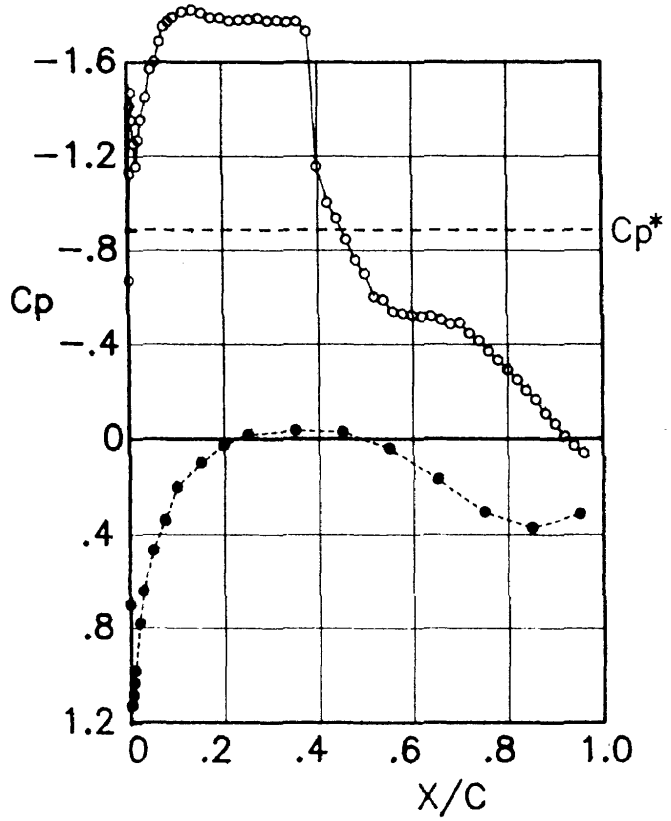

Corrected pressure distribution

Upper surface

x/c	Cp	C_{p_c}
0.000	0.689	0.698
0.002	-0.663	-0.671
0.004	-1.112	-1.126
0.006	-1.395	-1.413
0.008	-1.452	-1.470
0.010	-1.336	-1.353
0.015	-1.237	-1.252
0.020	-1.142	-1.157
0.025	-1.253	-1.268
0.030	-1.338	-1.355
0.040	-1.433	-1.451
0.050	-1.551	-1.570
0.060	-1.582	-1.602
0.070	-1.668	-1.689
0.080	-1.731	-1.753
0.090	-1.751	-1.773
0.100	-1.769	-1.791
0.119	-1.792	-1.815
0.140	-1.800	-1.823
0.160	-1.788	-1.810
0.180	-1.768	-1.790
0.200	-1.767	-1.789
0.220	-1.754	-1.776
0.240	-1.758	-1.780
0.260	-1.760	-1.782
0.280	-1.765	-1.787
0.299	-1.755	-1.777
0.320	-1.757	-1.779
0.340	-1.750	-1.772
0.360	-1.753	-1.776
0.380	-1.711	-1.733
0.399	-1.140	-1.154
0.420	-0.988	-1.000
0.439	-0.922	-0.934
0.460	-0.832	-0.843
0.480	-0.745	-0.754
0.500	-0.688	-0.697
0.519	-0.592	-0.599
0.539	-0.579	-0.586
0.560	-0.530	-0.537
0.580	-0.522	-0.529
0.599	-0.515	-0.521
0.619	-0.509	-0.515
0.639	-0.511	-0.517
0.659	-0.495	-0.502
0.679	-0.478	-0.484
0.699	-0.482	-0.489
0.719	-0.439	-0.444
0.739	-0.408	-0.413
0.759	-0.363	-0.368
0.779	-0.325	-0.329
0.799	-0.286	-0.289
0.819	-0.242	-0.245
0.839	-0.197	-0.199
0.859	-0.159	-0.161
0.879	-0.103	-0.104
0.899	-0.060	-0.061
0.919	-0.007	-0.007
0.939	0.032	0.032
0.960	0.063	0.064

Spanwise
(upper surface, x/c=.9)

y/b	Cp	C_{p_c}
-0.434	-0.076	-0.077
-0.367	-0.070	-0.071
-0.300	-0.067	-0.068
-0.234	-0.060	-0.060
-0.167	-0.056	-0.057
-0.017	-0.060	-0.061
0.166	-0.063	-0.064
0.232	-0.067	-0.068
0.299	-0.069	-0.070
0.366	-0.079	-0.080
0.432	-0.097	-0.099

Lower surface

x/c	Cp	C_{p_c}
0.950	0.310	0.314
0.850	0.367	0.372
0.750	0.302	0.306
0.650	0.168	0.170
0.550	0.041	0.042
0.450	-0.029	-0.029
0.350	-0.035	-0.035
0.250	-0.016	-0.016
0.200	0.027	0.028
0.150	0.099	0.101
0.100	0.201	0.203
0.075	0.337	0.341
0.050	0.462	0.468
0.030	0.632	0.640
0.020	0.770	0.779
0.010	0.971	0.983
0.008	1.022	1.035
0.006	1.072	1.086
0.004	1.114	1.128
0.002	1.115	1.129

Figure C −11 The NAL data corrected for the four wall effects.

Run	Scan	M_s	M_c	α_g(deg)	Re	C_{l_u}	C_{l_c}	$C_{d_{wake}}$
7346	1	0.689	0.678	6.53	20.7×10^6	1.100	1.112	0.0624

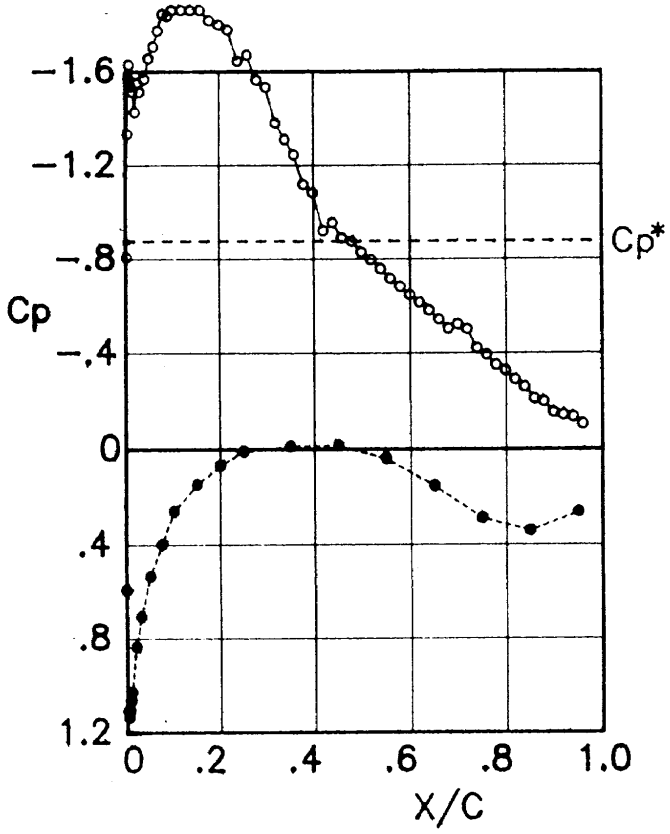

Corrected pressure distribution

Upper surface

x/c	Cp	C_{p_c}
0.000	0.587	0.593
0.002	-0.800	-0.809
0.004	-1.321	-1.335
0.006	-1.557	-1.573
0.008	-1.614	-1.630
0.010	-1.527	-1.542
0.015	-1.499	-1.515
0.020	-1.412	-1.427
0.025	-1.536	-1.552
0.030	-1.497	-1.512
0.040	-1.552	-1.569
0.050	-1.639	-1.656
0.060	-1.690	-1.708
0.070	-1.757	-1.775
0.080	-1.826	-1.845
0.090	-1.819	-1.838
0.100	-1.843	-1.862
0.119	-1.843	-1.862
0.140	-1.843	-1.862
0.160	-1.843	-1.862
0.180	-1.800	-1.819
0.200	-1.781	-1.800
0.220	-1.761	-1.779
0.240	-1.628	-1.645
0.260	-1.655	-1.672
0.280	-1.547	-1.563
0.299	-1.517	-1.533
0.320	-1.366	-1.380
0.340	-1.296	-1.310
0.360	-1.232	-1.245
0.380	-1.105	-1.117
0.399	-1.071	-1.082
0.420	-0.909	-0.919
0.439	-0.944	-0.954
0.460	-0.879	-0.888
0.480	-0.865	-0.874
0.500	-0.819	-0.827
0.519	-0.787	-0.795
0.539	-0.747	-0.755
0.560	-0.706	-0.714
0.580	-0.673	-0.680
0.599	-0.638	-0.645
0.619	-0.607	-0.613
0.639	-0.574	-0.580
0.659	-0.535	-0.541
0.679	-0.496	-0.501
0.699	-0.514	-0.519
0.719	-0.494	-0.499
0.739	-0.415	-0.420
0.759	-0.388	-0.392
0.779	-0.345	-0.349
0.799	-0.322	-0.325
0.819	-0.285	-0.288
0.839	-0.255	-0.257
0.859	-0.206	-0.208
0.879	-0.194	-0.196
0.899	-0.151	-0.152
0.919	-0.139	-0.141
0.939	-0.132	-0.133
0.960	-0.103	-0.104

Spanwise
(upper surface, x/c=.9)

y/b	Cp	C_{p_c}
-0.434	-0.148	-0.149
-0.367	-0.151	-0.153
-0.300	-0.140	-0.141
-0.234	-0.153	-0.154
-0.167	-0.156	-0.158
-0.017	-0.151	-0.152
0.166	-0.149	-0.151
0.232	-0.136	-0.137
0.299	-0.154	-0.155
0.366	-0.129	-0.130
0.432	-0.142	-0.143

Lower surface

x/c	Cp	C_{p_c}
0.950	0.259	0.262
0.850	0.337	0.341
0.750	0.284	0.287
0.650	0.152	0.154
0.550	0.039	0.039
0.450	-0.016	-0.016
0.350	-0.012	-0.012
0.250	0.010	0.010
0.200	0.067	0.068
0.150	0.146	0.148
0.100	0.256	0.258
0.075	0.395	0.399
0.050	0.528	0.534
0.030	0.700	0.707
0.020	0.827	0.836
0.010	1.017	1.028
0.008	1.052	1.063
0.006	1.096	1.108
0.004	1.122	1.134
0.002	1.096	1.107

Figure C－12 The NAL data corrected for the four wall effects.

Run	Scan	M_s	M_c	α_g(deg)	Re	C_{l_u}	C_{l_c}	$C_{d_{wake}}$
7120	2	0.751	0.727	-3.82	21.0×10^6	-0.201	-0.206	0.0124

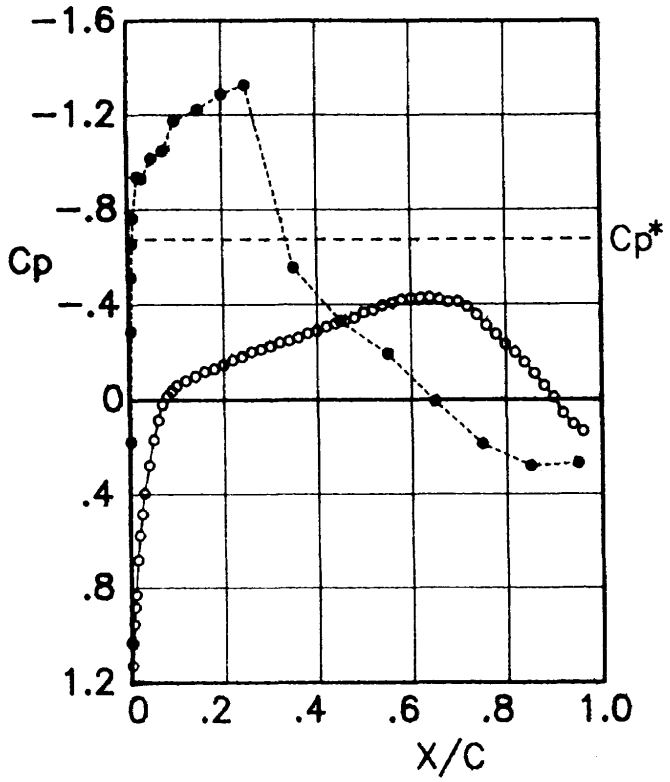

Corrected pressure distribution

Upper surface

x/c	Cp	C_{p_c}
0.000	1.010	1.031
0.002	1.104	1.127
0.004	1.013	1.035
0.006	0.934	0.954
0.008	0.865	0.884
0.010	0.813	0.831
0.015	0.668	0.682
0.020	0.566	0.578
0.025	0.476	0.486
0.030	0.388	0.396
0.040	0.271	0.277
0.050	0.165	0.168
0.060	0.084	0.086
0.070	0.021	0.021
0.080	-0.015	-0.015
0.090	-0.036	-0.037
0.100	-0.058	-0.059
0.119	-0.078	-0.080
0.140	-0.096	-0.098
0.160	-0.116	-0.118
0.180	-0.127	-0.130
0.200	-0.143	-0.146
0.220	-0.163	-0.166
0.240	-0.176	-0.180
0.260	-0.196	-0.201
0.280	-0.207	-0.211
0.299	-0.219	-0.224
0.320	-0.234	-0.239
0.340	-0.242	-0.247
0.360	-0.255	-0.261
0.380	-0.273	-0.279
0.399	-0.281	-0.287
0.420	-0.300	-0.306
0.439	-0.312	-0.318
0.460	-0.323	-0.330
0.480	-0.336	-0.344
0.500	-0.359	-0.366
0.519	-0.370	-0.377
0.539	-0.388	-0.396
0.560	-0.398	-0.406
0.580	-0.411	-0.420
0.599	-0.417	-0.426
0.619	-0.418	-0.427
0.639	-0.421	-0.430
0.659	-0.414	-0.423
0.679	-0.402	-0.411
0.699	-0.404	-0.413
0.719	-0.383	-0.391
0.739	-0.348	-0.356
0.759	-0.305	-0.311
0.779	-0.267	-0.273
0.799	-0.226	-0.231
0.819	-0.193	-0.197
0.839	-0.152	-0.155
0.859	-0.106	-0.109
0.879	-0.057	-0.059
0.899	-0.010	-0.010
0.919	0.057	0.059
0.939	0.102	0.105
0.960	0.131	0.134

Spanwise
(upper surface, x/c=.9)

y/b	Cp	C_{p_c}
-0.434	-0.003	-0.003
-0.367	-0.001	-0.001
-0.300	-0.004	-0.004
-0.234	0.002	0.002
-0.167	0.002	0.002
-0.017	-0.010	-0.010
0.166	-0.014	-0.014
0.232	-0.022	-0.023
0.299	-0.018	-0.018
0.366	-0.027	-0.027
0.432	-0.044	-0.044

Lower surface

x/c	Cp	C_{p_c}
0.950	0.263	0.269
0.850	0.275	0.281
0.750	0.183	0.187
0.650	0.007	0.007
0.550	-0.187	-0.191
0.450	-0.323	-0.330
0.350	-0.544	-0.556
0.250	-1.298	-1.326
0.200	-1.259	-1.286
0.150	-1.196	-1.221
0.100	-1.149	-1.173
0.075	-1.025	-1.047
0.050	-0.993	-1.015
0.030	-0.909	-0.928
0.020	-0.918	-0.937
0.010	-0.745	-0.761
0.008	-0.640	-0.654
0.006	-0.503	-0.513
0.004	-0.278	-0.284
0.002	0.176	0.179

Figure C −13 The NAL data corrected for the four wall effects.

Run	Scan	M_s	M_c	α_g(deg)	Re	C_{l_u}	C_{l_c}	$C_{d_{wake}}$
7119	3	0.748	0.725	0.00	21.1×10^6	0.289	0.295	0.0071

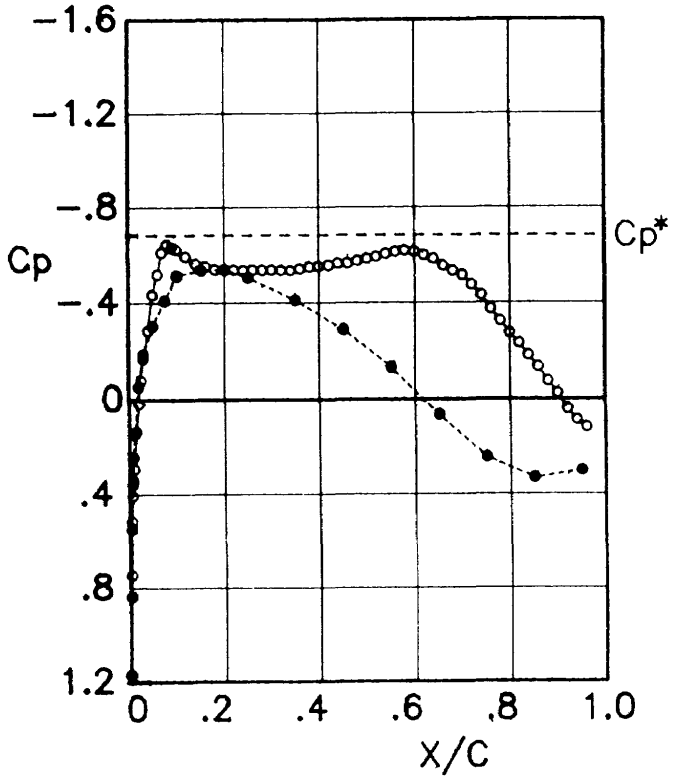

Corrected pressure distribution

Spanwise
(upper surface, x/c=.9)

y/b	Cp	C_{p_c}
-0.434	-0.028	-0.028
-0.367	-0.025	-0.026
-0.300	-0.024	-0.025
-0.234	-0.018	-0.019
-0.167	-0.014	-0.015
-0.017	-0.024	-0.024
0.166	-0.023	-0.024
0.232	-0.030	-0.031
0.299	-0.032	-0.032
0.366	-0.038	-0.039
0.432	-0.050	-0.051

Lower surface

x/c	Cp	C_{p_c}
0.950	0.295	0.301
0.850	0.324	0.331
0.750	0.238	0.243
0.650	0.064	0.066
0.550	-0.129	-0.132
0.450	-0.284	-0.290
0.350	-0.403	-0.411
0.250	-0.495	-0.506
0.200	-0.527	-0.538
0.150	-0.524	-0.535
0.100	-0.502	-0.513
0.075	-0.401	-0.410
0.050	-0.298	-0.304
0.030	-0.181	-0.185
0.020	-0.051	-0.052
0.010	0.140	0.143
0.008	0.240	0.245
0.006	0.350	0.358
0.004	0.539	0.550
0.002	0.821	0.838

Upper surface

x/c	Cp	C_{p_c}
0.000	1.145	1.169
0.002	0.729	0.745
0.004	0.506	0.516
0.006	0.398	0.406
0.008	0.332	0.339
0.010	0.285	0.291
0.015	0.130	0.133
0.020	0.016	0.017
0.025	-0.079	-0.080
0.030	-0.167	-0.170
0.040	-0.280	-0.286
0.050	-0.426	-0.435
0.060	-0.508	-0.519
0.070	-0.598	-0.610
0.080	-0.630	-0.643
0.090	-0.618	-0.631
0.100	-0.610	-0.623
0.119	-0.581	-0.593
0.140	-0.551	-0.563
0.160	-0.540	-0.552
0.180	-0.527	-0.538
0.200	-0.527	-0.539
0.220	-0.526	-0.538
0.240	-0.524	-0.535
0.260	-0.526	-0.537
0.280	-0.525	-0.536
0.299	-0.526	-0.537
0.320	-0.525	-0.536
0.340	-0.524	-0.535
0.360	-0.530	-0.541
0.380	-0.537	-0.549
0.399	-0.540	-0.551
0.420	-0.544	-0.556
0.439	-0.553	-0.564
0.460	-0.554	-0.566
0.480	-0.563	-0.575
0.500	-0.572	-0.585
0.519	-0.579	-0.592
0.539	-0.591	-0.603
0.560	-0.600	-0.613
0.580	-0.605	-0.618
0.599	-0.601	-0.614
0.619	-0.586	-0.599
0.639	-0.571	-0.583
0.659	-0.542	-0.553
0.679	-0.521	-0.533
0.699	-0.504	-0.514
0.719	-0.465	-0.475
0.739	-0.424	-0.433
0.759	-0.366	-0.374
0.779	-0.318	-0.325
0.799	-0.269	-0.275
0.819	-0.227	-0.232
0.839	-0.178	-0.181
0.859	-0.131	-0.134
0.879	-0.073	-0.075
0.899	-0.024	-0.024
0.919	0.041	0.042
0.939	0.086	0.088
0.960	0.116	0.119

Figure C−14 The NAL data corrected for the four wall effects.

Run	Scan	M_s	M_c	α_g(deg)	Re	C_{l_u}	C_{l_c}	$C_{d_{wake}}$
7129	1	0.746	0.723	1.72	20.9×10^6	0.564	0.575	0.0084

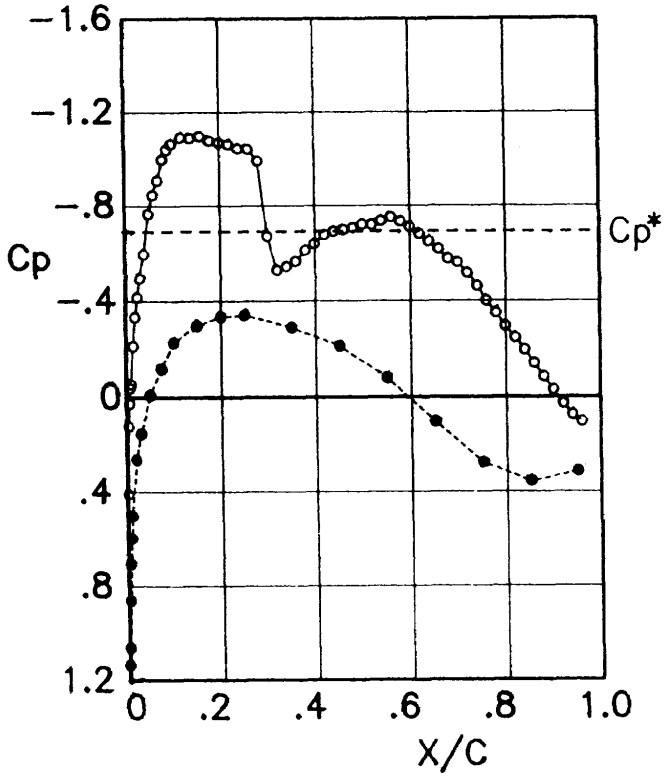

Corrected pressure distribution

Spanwise
(upper surface, x/c=.9)

y/b	C_p	C_{p_c}
-0.434	-0.051	-0.052
-0.367	-0.042	-0.043
-0.300	-0.036	-0.037
-0.234	-0.028	-0.029
-0.167	-0.026	-0.026
-0.017	-0.029	-0.029
0.166	-0.034	-0.035
0.232	-0.040	-0.040
0.299	-0.041	-0.041
0.366	-0.046	-0.047
0.432	-0.058	-0.060

Lower surface

x/c	C_p	C_{p_c}
0.950	0.307	0.314
0.850	0.349	0.356
0.750	0.270	0.276
0.650	0.101	0.103
0.550	-0.078	-0.080
0.450	-0.208	-0.212
0.350	-0.284	-0.290
0.250	-0.336	-0.343
0.200	-0.328	-0.334
0.150	-0.291	-0.297
0.100	-0.223	-0.227
0.075	-0.116	-0.118
0.050	-0.008	-0.008
0.030	0.151	0.154
0.020	0.258	0.263
0.010	0.494	0.504
0.008	0.587	0.599
0.006	0.691	0.706
0.004	0.844	0.861
0.002	1.040	1.061

Upper surface

x/c	C_p	C_{p_c}
0.000	1.112	1.135
0.002	0.400	0.408
0.004	0.117	0.119
0.006	0.026	0.026
0.008	-0.038	-0.039
0.010	-0.055	-0.056
0.015	-0.209	-0.214
0.020	-0.328	-0.334
0.025	-0.409	-0.418
0.030	-0.486	-0.496
0.040	-0.585	-0.597
0.050	-0.750	-0.766
0.060	-0.829	-0.846
0.070	-0.890	-0.909
0.080	-0.978	-0.998
0.090	-1.018	-1.039
0.100	-1.042	-1.064
0.119	-1.070	-1.092
0.140	-1.068	-1.090
0.160	-1.076	-1.098
0.180	-1.056	-1.078
0.200	-1.049	-1.071
0.220	-1.041	-1.062
0.240	-1.024	-1.045
0.260	-1.021	-1.042
0.280	-0.971	-0.991
0.299	-0.657	-0.670
0.320	-0.516	-0.527
0.340	-0.532	-0.543
0.360	-0.554	-0.566
0.380	-0.599	-0.611
0.399	-0.626	-0.639
0.420	-0.662	-0.676
0.439	-0.676	-0.690
0.460	-0.683	-0.697
0.480	-0.691	-0.706
0.500	-0.706	-0.720
0.519	-0.704	-0.719
0.539	-0.720	-0.735
0.560	-0.735	-0.750
0.580	-0.718	-0.733
0.599	-0.695	-0.709
0.619	-0.667	-0.680
0.639	-0.635	-0.648
0.659	-0.603	-0.616
0.679	-0.564	-0.575
0.699	-0.549	-0.560
0.719	-0.505	-0.515
0.739	-0.451	-0.460
0.759	-0.391	-0.400
0.779	-0.342	-0.349
0.799	-0.287	-0.293
0.819	-0.240	-0.245
0.839	-0.190	-0.194
0.859	-0.136	-0.139
0.879	-0.082	-0.083
0.899	-0.029	-0.029
0.919	0.029	0.029
0.939	0.075	0.076
0.960	0.102	0.105

Figure C −15 The NAL data corrected for the four wall effects.

Run	Scan	M_s	M_c	α_g(deg)	Re	C_{l_u}	C_{l_c}	$C_{d_{wake}}$
7102	2	0.744	0.725	2.75	21.2×10^6	0.738	0.751	0.0111

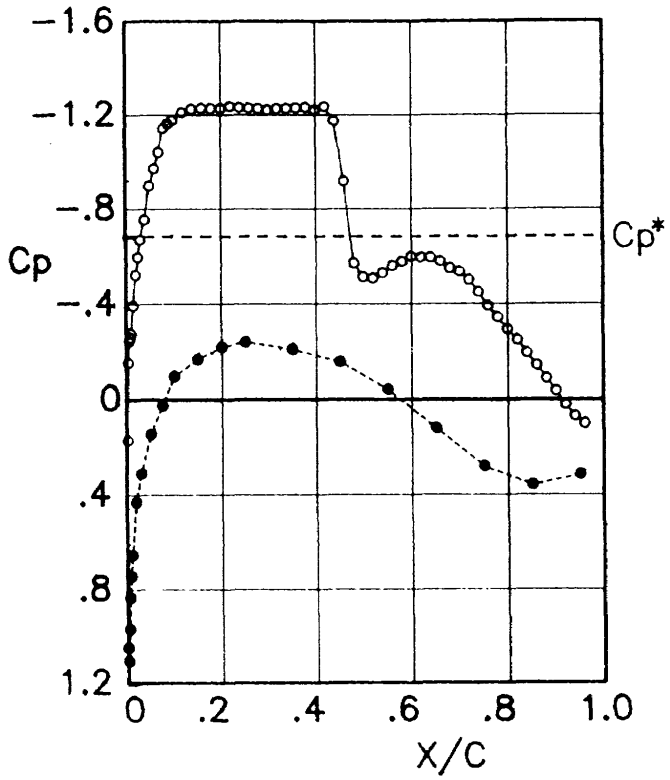

Corrected pressure distribution

Upper surface

x/c	Cp	C_{p_c}
0.000	1.029	1.047
0.002	0.166	0.169
0.004	-0.153	-0.155
0.006	-0.242	-0.246
0.008	-0.256	-0.260
0.010	-0.274	-0.278
0.015	-0.387	-0.394
0.020	-0.514	-0.523
0.025	-0.587	-0.597
0.030	-0.658	-0.669
0.040	-0.742	-0.754
0.050	-0.883	-0.898
0.060	-0.956	-0.972
0.070	-1.023	-1.041
0.080	-1.124	-1.143
0.090	-1.143	-1.162
0.100	-1.159	-1.179
0.119	-1.191	-1.211
0.140	-1.206	-1.226
0.160	-1.209	-1.230
0.180	-1.208	-1.229
0.200	-1.208	-1.228
0.220	-1.217	-1.237
0.240	-1.212	-1.233
0.260	-1.210	-1.230
0.280	-1.207	-1.228
0.299	-1.202	-1.222
0.320	-1.207	-1.228
0.340	-1.208	-1.228
0.360	-1.210	-1.230
0.380	-1.213	-1.233
0.399	-1.201	-1.221
0.420	-1.216	-1.237
0.439	-1.155	-1.175
0.460	-0.902	-0.917
0.480	-0.561	-0.570
0.500	-0.503	-0.512
0.519	-0.498	-0.507
0.539	-0.520	-0.529
0.560	-0.549	-0.558
0.580	-0.567	-0.577
0.599	-0.588	-0.598
0.619	-0.584	-0.594
0.639	-0.584	-0.594
0.659	-0.569	-0.578
0.679	-0.540	-0.549
0.699	-0.526	-0.535
0.719	-0.491	-0.500
0.739	-0.441	-0.448
0.759	-0.384	-0.391
0.779	-0.337	-0.343
0.799	-0.288	-0.293
0.819	-0.243	-0.248
0.839	-0.191	-0.194
0.859	-0.140	-0.142
0.879	-0.086	-0.088
0.899	-0.035	-0.036
0.919	0.022	0.022
0.939	0.070	0.071
0.960	0.100	0.102

Spanwise
(upper surface, x/c=.9)

y/b	Cp	C_{p_c}
-0.434	-0.047	-0.048
-0.367	-0.042	-0.043
-0.300	-0.040	-0.041
-0.234	-0.029	-0.029
-0.167	-0.029	-0.030
-0.017	-0.035	-0.036
0.166	-0.040	-0.041
0.232	-0.043	-0.044
0.299	-0.044	-0.045
0.366	-0.049	-0.050
0.432	-0.064	-0.065

Lower surface

x/c	Cp	C_{p_c}
0.950	0.309	0.314
0.850	0.352	0.358
0.750	0.275	0.280
0.650	0.119	0.121
0.550	-0.042	-0.042
0.450	-0.156	-0.159
0.350	-0.207	-0.211
0.250	-0.238	-0.242
0.200	-0.216	-0.220
0.150	-0.166	-0.169
0.100	-0.096	-0.097
0.075	0.026	0.027
0.050	0.143	0.145
0.030	0.305	0.310
0.020	0.425	0.432
0.010	0.643	0.654
0.008	0.732	0.745
0.006	0.821	0.835
0.004	0.951	0.967
0.002	1.087	1.105

Figure C－16 The NAL data corrected for the four wall effects.

Run	Scan	M_s	M_c	α_g(deg)	Re	C_{l_u}	C_{l_c}	$C_{d_{wake}}$
7127	3	0.738	0.724	3.52	20.8×10^6	0.886	0.897	0.0210

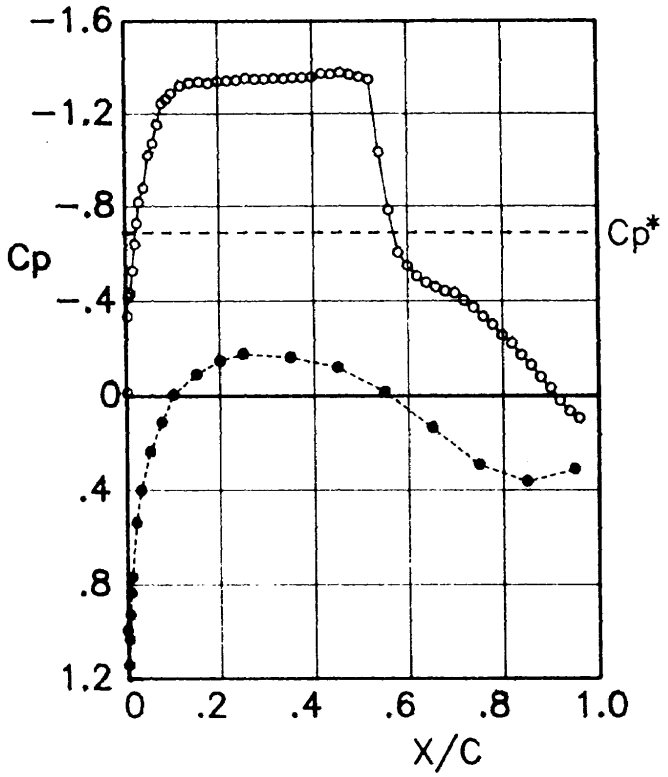

Corrected pressure distribution

Upper surface

x/c	Cp	C_{p_c}
0.000	0.981	0.994
0.002	-0.015	-0.015
0.004	-0.332	-0.337
0.006	-0.413	-0.418
0.008	-0.428	-0.434
0.010	-0.428	-0.433
0.015	-0.520	-0.527
0.020	-0.631	-0.640
0.025	-0.719	-0.728
0.030	-0.807	-0.818
0.040	-0.868	-0.879
0.050	-1.005	-1.019
0.060	-1.055	-1.069
0.070	-1.137	-1.152
0.080	-1.228	-1.245
0.090	-1.247	-1.263
0.100	-1.271	-1.287
0.119	-1.303	-1.320
0.140	-1.315	-1.332
0.160	-1.320	-1.337
0.180	-1.314	-1.331
0.200	-1.322	-1.340
0.220	-1.325	-1.342
0.240	-1.327	-1.345
0.260	-1.334	-1.352
0.280	-1.331	-1.349
0.299	-1.332	-1.349
0.320	-1.335	-1.352
0.340	-1.334	-1.351
0.360	-1.338	-1.355
0.380	-1.338	-1.355
0.399	-1.340	-1.358
0.420	-1.355	-1.373
0.439	-1.353	-1.371
0.460	-1.359	-1.377
0.480	-1.351	-1.368
0.500	-1.341	-1.359
0.519	-1.330	-1.347
0.539	-1.017	-1.031
0.560	-0.771	-0.781
0.580	-0.595	-0.602
0.599	-0.538	-0.545
0.619	-0.495	-0.501
0.639	-0.468	-0.474
0.659	-0.449	-0.455
0.679	-0.433	-0.439
0.699	-0.426	-0.431
0.719	-0.394	-0.399
0.739	-0.365	-0.370
0.759	-0.329	-0.333
0.779	-0.295	-0.299
0.799	-0.249	-0.252
0.819	-0.216	-0.219
0.839	-0.168	-0.170
0.859	-0.127	-0.129
0.879	-0.076	-0.077
0.899	-0.032	-0.032
0.919	0.022	0.023
0.939	0.066	0.067
0.960	0.095	0.096

Spanwise
(upper surface, x/c=.9)

y/b	Cp	C_{p_c}
-0.434	-0.061	-0.061
-0.367	-0.045	-0.046
-0.300	-0.040	-0.040
-0.234	-0.029	-0.029
-0.167	-0.027	-0.028
-0.017	-0.032	-0.032
0.166	-0.034	-0.035
0.232	-0.042	-0.043
0.299	-0.045	-0.045
0.366	-0.058	-0.059
0.432	-0.068	-0.068

Lower surface

x/c	Cp	C_{p_c}
0.950	0.309	0.313
0.850	0.359	0.363
0.750	0.289	0.293
0.650	0.135	0.136
0.550	-0.017	-0.017
0.450	-0.119	-0.121
0.350	-0.160	-0.162
0.250	-0.175	-0.177
0.200	-0.146	-0.148
0.150	-0.089	-0.091
0.100	-0.004	-0.004
0.075	0.112	0.113
0.050	0.235	0.239
0.030	0.397	0.402
0.020	0.531	0.538
0.010	0.759	0.769
0.008	0.825	0.835
0.006	0.916	0.928
0.004	1.020	1.034
0.002	1.127	1.142

Figure C−17 The NAL data corrected for the four wall effects.

Run	Scan	M_s	M_c	α_g(deg)	Re	C_{l_u}	C_{l_c}	$C_{d_{wake}}$
7131	2	0.736	0.725	4.62	21.0×10^6	0.988	0.998	0.0436

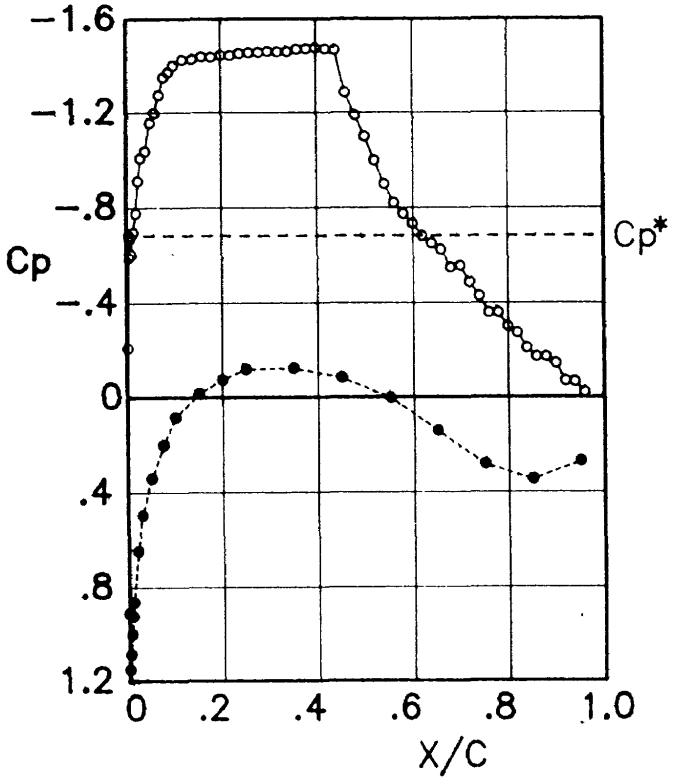

Corrected pressure distribution

Upper surface

x/c	Cp	C_{p_c}
0.000	0.901	0.910
0.002	-0.207	-0.209
0.004	-0.585	-0.592
0.006	-0.677	-0.684
0.008	-0.664	-0.671
0.010	-0.599	-0.605
0.015	-0.689	-0.696
0.020	-0.768	-0.776
0.025	-0.902	-0.912
0.030	-0.997	-1.007
0.040	-1.026	-1.037
0.050	-1.144	-1.156
0.060	-1.186	-1.199
0.070	-1.263	-1.276
0.080	-1.336	-1.350
0.090	-1.358	-1.372
0.100	-1.386	-1.401
0.119	-1.412	-1.426
0.140	-1.414	-1.429
0.160	-1.425	-1.440
0.180	-1.422	-1.437
0.200	-1.430	-1.445
0.220	-1.429	-1.444
0.240	-1.437	-1.452
0.260	-1.440	-1.456
0.280	-1.442	-1.457
0.299	-1.446	-1.462
0.320	-1.445	-1.460
0.340	-1.446	-1.461
0.360	-1.456	-1.471
0.380	-1.458	-1.473
0.399	-1.461	-1.476
0.420	-1.457	-1.472
0.439	-1.453	-1.469
0.460	-1.273	-1.286
0.480	-1.177	-1.190
0.500	-1.086	-1.098
0.519	-0.986	-0.997
0.539	-0.888	-0.897
0.560	-0.810	-0.818
0.580	-0.764	-0.772
0.599	-0.724	-0.732
0.619	-0.673	-0.680
0.639	-0.642	-0.649
0.659	-0.615	-0.622
0.679	-0.542	-0.548
0.699	-0.549	-0.554
0.719	-0.481	-0.486
0.739	-0.423	-0.428
0.759	-0.353	-0.357
0.779	-0.353	-0.357
0.799	-0.295	-0.298
0.819	-0.268	-0.270
0.839	-0.204	-0.206
0.859	-0.167	-0.169
0.879	-0.166	-0.168
0.899	-0.139	-0.141
0.919	-0.066	-0.067
0.939	-0.063	-0.064
0.960	-0.019	-0.019

Spanwise
(upper surface, x/c=.9)

y/b	Cp	C_{p_c}
-0.434	-0.087	-0.088
-0.367	-0.081	-0.082
-0.300	-0.065	-0.066
-0.234	-0.072	-0.073
-0.167	-0.095	-0.096
-0.017	-0.139	-0.141
0.166	-0.128	-0.129
0.232	-0.085	-0.086
0.299	-0.085	-0.086
0.366	-0.081	-0.082
0.432	-0.103	-0.104

Lower surface

x/c	Cp	C_{p_c}
0.950	0.268	0.270
0.850	0.344	0.347
0.750	0.279	0.282
0.650	0.141	0.142
0.550	0.004	0.004
0.450	-0.082	-0.083
0.350	-0.121	-0.123
0.250	-0.117	-0.118
0.200	-0.073	-0.074
0.150	-0.015	-0.015
0.100	0.085	0.086
0.075	0.201	0.203
0.050	0.338	0.342
0.030	0.492	0.498
0.020	0.640	0.647
0.010	0.854	0.863
0.008	0.913	0.922
0.006	0.990	1.000
0.004	1.075	1.086
0.002	1.138	1.150

Figure C−18 The NAL data corrected for the four wall effects.

Run	Scan	M_s	M_c	α_g(deg)	Re	C_{l_u}	C_{l_c}	$C_{d_{wake}}$
7348	2	0.769	0.743	-3.73	20.7×10^6	-0.248	-0.254	0.0199

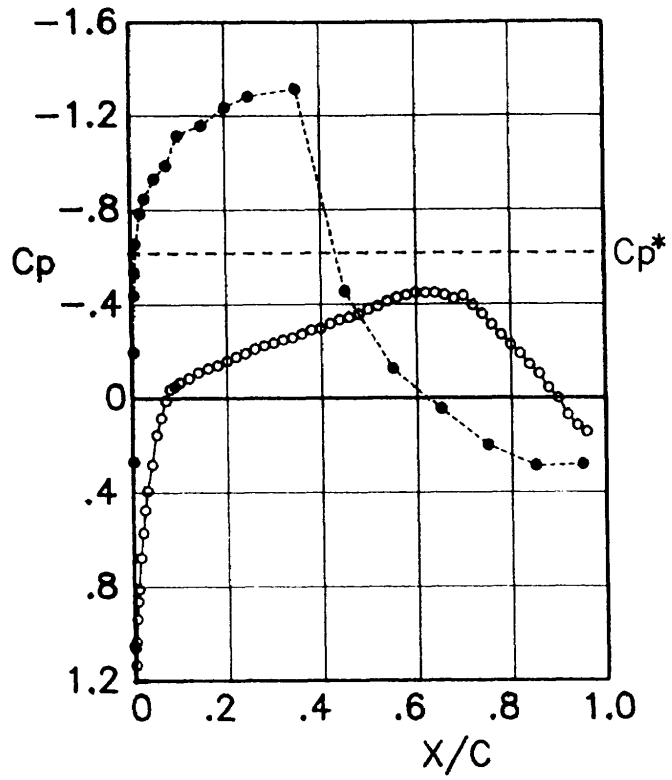

Corrected pressure distribution

Upper surface

x/c	Cp	C_{p_c}
0.000	1.033	1.057
0.002	1.108	1.133
0.004	1.011	1.035
0.006	0.916	0.937
0.008	0.842	0.862
0.010	0.792	0.810
0.015	0.661	0.677
0.020	0.559	0.572
0.025	0.464	0.474
0.030	0.385	0.393
0.040	0.276	0.282
0.050	0.153	0.156
0.060	0.082	0.084
0.070	0.011	0.011
0.080	-0.037	-0.038
0.090	-0.050	-0.051
0.100	-0.065	-0.066
0.119	-0.083	-0.085
0.140	-0.108	-0.111
0.160	-0.125	-0.127
0.180	-0.137	-0.140
0.200	-0.156	-0.160
0.220	-0.173	-0.177
0.240	-0.186	-0.190
0.260	-0.205	-0.210
0.280	-0.219	-0.224
0.299	-0.229	-0.235
0.320	-0.243	-0.249
0.340	-0.252	-0.258
0.360	-0.268	-0.274
0.380	-0.284	-0.291
0.399	-0.290	-0.297
0.420	-0.311	-0.318
0.439	-0.326	-0.334
0.460	-0.337	-0.344
0.480	-0.349	-0.357
0.500	-0.370	-0.378
0.519	-0.384	-0.392
0.539	-0.404	-0.413
0.560	-0.419	-0.429
0.580	-0.430	-0.440
0.599	-0.440	-0.450
0.619	-0.439	-0.449
0.639	-0.438	-0.448
0.659	-0.430	-0.440
0.679	-0.415	-0.424
0.699	-0.427	-0.437
0.719	-0.387	-0.396
0.739	-0.350	-0.358
0.759	-0.305	-0.312
0.779	-0.263	-0.269
0.799	-0.220	-0.225
0.819	-0.185	-0.189
0.839	-0.140	-0.143
0.859	-0.101	-0.104
0.879	-0.043	-0.044
0.899	0.001	0.001
0.919	0.072	0.073
0.939	0.115	0.118
0.960	0.142	0.146

Spanwise
(upper surface, x/c=.9)

y/b	Cp	C_{p_c}
-0.434	0.000	0.000
-0.367	0.005	0.005
-0.300	0.006	0.006
-0.234	0.010	0.011
-0.167	0.013	0.013
-0.017	0.001	0.001
0.166	0.004	0.004
0.232	-0.003	-0.003
0.299	-0.001	-0.001
0.366	-0.006	-0.007
0.432	-0.015	-0.015

Lower surface

x/c	Cp	C_{p_c}
0.950	0.276	0.283
0.850	0.281	0.288
0.750	0.197	0.202
0.650	0.046	0.047
0.550	-0.123	-0.126
0.450	-0.445	-0.455
0.350	-1.285	-1.315
0.250	-1.252	-1.281
0.200	-1.207	-1.235
0.150	-1.129	-1.156
0.100	-1.089	-1.114
0.075	-0.964	-0.987
0.050	-0.908	-0.929
0.030	-0.826	-0.845
0.020	-0.764	-0.782
0.010	-0.640	-0.655
0.008	-0.520	-0.532
0.006	-0.427	-0.437
0.004	-0.189	-0.193
0.002	0.267	0.273

Figure C−19 The NAL data corrected for the four wall effects.

Run	Scan	M_s	M_c	α_g(deg)	Re	C_{l_u}	C_{l_c}	$C_{d_{wake}}$
7115	3	0.767	0.742	0.01	21.2×10^6	0.298	0.305	0.0074

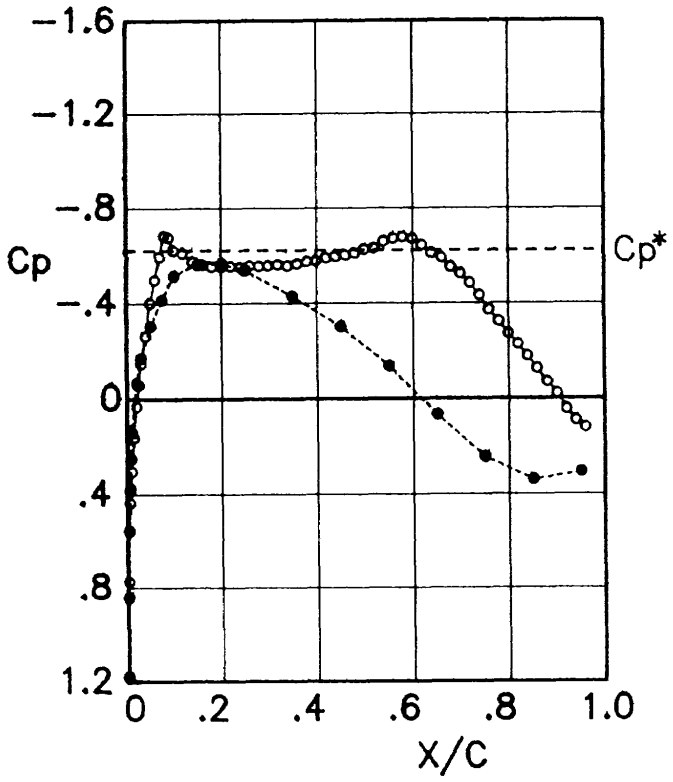

Corrected pressure distribution

Upper surface

x/c	Cp	C_{p_c}
0.000	1.152	1.179
0.002	0.755	0.773
0.004	0.540	0.552
0.006	0.426	0.436
0.008	0.365	0.373
0.010	0.296	0.303
0.015	0.156	0.160
0.020	0.031	0.032
0.025	-0.058	-0.060
0.030	-0.143	-0.146
0.040	-0.257	-0.263
0.050	-0.394	-0.403
0.060	-0.489	-0.500
0.070	-0.583	-0.596
0.080	-0.669	-0.684
0.090	-0.662	-0.677
0.100	-0.609	-0.623
0.119	-0.597	-0.610
0.140	-0.563	-0.576
0.160	-0.551	-0.563
0.180	-0.542	-0.555
0.200	-0.541	-0.554
0.220	-0.543	-0.556
0.240	-0.540	-0.553
0.260	-0.545	-0.557
0.280	-0.543	-0.556
0.299	-0.545	-0.558
0.320	-0.550	-0.562
0.340	-0.544	-0.557
0.360	-0.553	-0.566
0.380	-0.563	-0.575
0.399	-0.565	-0.578
0.420	-0.577	-0.590
0.439	-0.582	-0.596
0.460	-0.588	-0.602
0.480	-0.596	-0.610
0.500	-0.612	-0.626
0.519	-0.617	-0.631
0.539	-0.645	-0.659
0.560	-0.656	-0.671
0.580	-0.662	-0.677
0.599	-0.657	-0.672
0.619	-0.629	-0.644
0.639	-0.597	-0.610
0.659	-0.578	-0.591
0.679	-0.539	-0.551
0.699	-0.512	-0.524
0.719	-0.473	-0.484
0.739	-0.423	-0.433
0.759	-0.363	-0.371
0.779	-0.315	-0.323
0.799	-0.265	-0.271
0.819	-0.221	-0.226
0.839	-0.173	-0.177
0.859	-0.121	-0.123
0.879	-0.067	-0.069
0.899	-0.018	-0.019
0.919	0.045	0.046
0.939	0.091	0.093
0.960	0.120	0.123

Spanwise
(upper surface, x/c=.9)

y/b	Cp	C_{p_c}
-0.434	-0.030	-0.030
-0.367	-0.018	-0.018
-0.300	-0.018	-0.018
-0.234	-0.012	-0.012
-0.167	-0.011	-0.011
-0.017	-0.018	-0.019
0.166	-0.019	-0.019
0.232	-0.022	-0.022
0.299	-0.025	-0.026
0.366	-0.028	-0.029
0.432	-0.044	-0.045

Lower surface

x/c	Cp	C_{p_c}
0.950	0.301	0.308
0.850	0.332	0.339
0.750	0.240	0.245
0.650	0.067	0.069
0.550	-0.131	-0.134
0.450	-0.294	-0.301
0.350	-0.420	-0.429
0.250	-0.526	-0.538
0.200	-0.555	-0.567
0.150	-0.551	-0.563
0.100	-0.504	-0.515
0.075	-0.406	-0.415
0.050	-0.297	-0.304
0.030	-0.165	-0.168
0.020	-0.061	-0.063
0.010	0.138	0.141
0.008	0.247	0.252
0.006	0.379	0.388
0.004	0.546	0.559
0.002	0.825	0.843

Figure C−20 The NAL data corrected for the four wall effects.

Run	Scan	M_s	M_c	α_g(deg)	Re	C_{l_u}	C_{l_c}	$C_{d_{wake}}$
7107	1	0.762	0.742	1.81	20.8×10^6	0.602	0.613	0.0085

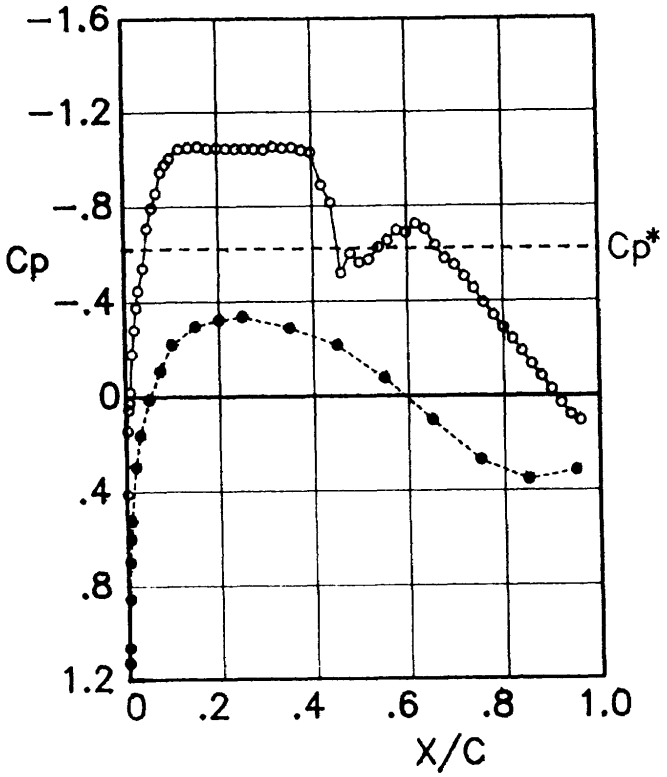

Corrected pressure distribution

Upper surface

x/c	Cp	C_{p_c}
0.000	1.109	1.129
0.002	0.404	0.411
0.004	0.140	0.143
0.006	0.054	0.054
0.008	0.026	0.027
0.010	-0.019	-0.019
0.015	-0.176	-0.179
0.020	-0.277	-0.282
0.025	-0.370	-0.377
0.030	-0.440	-0.448
0.040	-0.533	-0.542
0.050	-0.697	-0.710
0.060	-0.781	-0.795
0.070	-0.842	-0.857
0.080	-0.931	-0.947
0.090	-0.961	-0.978
0.100	-0.986	-1.004
0.119	-1.025	-1.044
0.140	-1.030	-1.048
0.160	-1.034	-1.053
0.180	-1.026	-1.044
0.200	-1.027	-1.046
0.220	-1.026	-1.045
0.240	-1.024	-1.043
0.260	-1.024	-1.043
0.280	-1.023	-1.042
0.299	-1.021	-1.039
0.320	-1.034	-1.053
0.340	-1.027	-1.046
0.360	-1.030	-1.048
0.380	-1.018	-1.036
0.399	-1.008	-1.026
0.420	-0.872	-0.888
0.439	-0.800	-0.814
0.460	-0.508	-0.517
0.480	-0.588	-0.599
0.500	-0.551	-0.561
0.519	-0.563	-0.573
0.539	-0.613	-0.624
0.560	-0.641	-0.652
0.580	-0.683	-0.695
0.599	-0.674	-0.686
0.619	-0.710	-0.723
0.639	-0.688	-0.701
0.659	-0.623	-0.634
0.679	-0.568	-0.578
0.699	-0.539	-0.549
0.719	-0.492	-0.501
0.739	-0.442	-0.450
0.759	-0.384	-0.391
0.779	-0.332	-0.338
0.799	-0.281	-0.286
0.819	-0.232	-0.237
0.839	-0.181	-0.185
0.859	-0.128	-0.130
0.879	-0.078	-0.080
0.899	-0.024	-0.025
0.919	0.033	0.033
0.939	0.080	0.081
0.960	0.105	0.107

Spanwise
(upper surface, x/c=.9)

y/b	Cp	C_{p_c}
-0.434	-0.046	-0.046
-0.367	-0.030	-0.031
-0.300	-0.035	-0.035
-0.234	-0.019	-0.019
-0.167	-0.019	-0.019
-0.017	-0.024	-0.025
0.166	-0.026	-0.026
0.232	-0.031	-0.032
0.299	-0.032	-0.033
0.366	-0.047	-0.048
0.432	-0.056	-0.057

Lower surface

x/c	Cp	C_{p_c}
0.950	0.310	0.316
0.850	0.348	0.354
0.750	0.266	0.271
0.650	0.101	0.102
0.550	-0.073	-0.074
0.450	-0.209	-0.212
0.350	-0.283	-0.288
0.250	-0.329	-0.335
0.200	-0.317	-0.322
0.150	-0.289	-0.295
0.100	-0.213	-0.217
0.075	-0.106	-0.108
0.050	0.013	0.013
0.030	0.160	0.163
0.020	0.292	0.298
0.010	0.516	0.525
0.008	0.591	0.601
0.006	0.687	0.699
0.004	0.840	0.855
0.002	1.047	1.066

Figure C－21 The NAL data corrected for the four wall effects.

Run	Scan	M_s	M_c	α_g(deg)	Re	C_{l_u}	C_{l_c}	$C_{d_{wake}}$
7116	2	0.760	0.744	2.62	21.1×10^6	0.754	0.765	0.0130

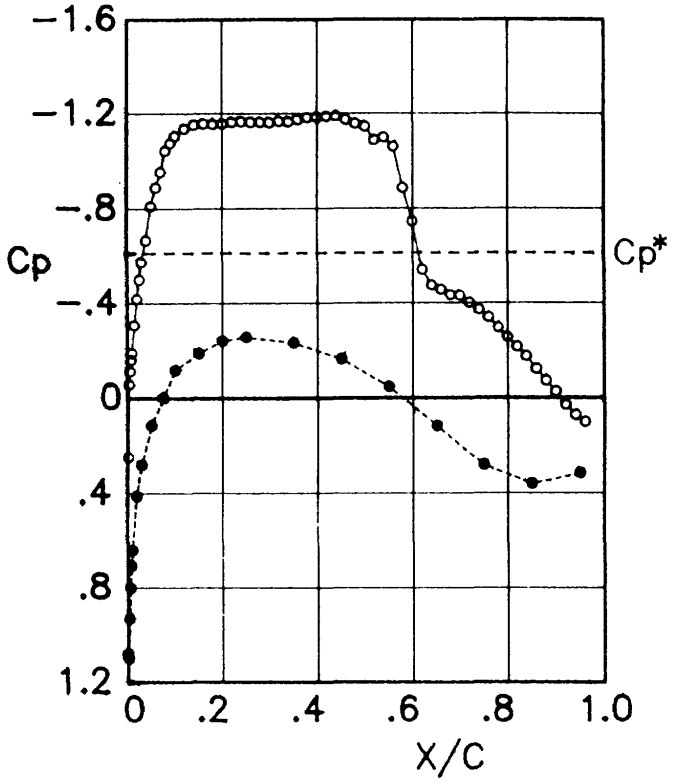

Corrected pressure distribution

Upper surface

x/c	Cp	C_{p_c}
0.000	1.066	1.082
0.002	0.243	0.246
0.004	-0.057	-0.058
0.006	-0.111	-0.113
0.008	-0.158	-0.160
0.010	-0.187	-0.190
0.015	-0.304	-0.308
0.020	-0.414	-0.420
0.025	-0.495	-0.503
0.030	-0.569	-0.577
0.040	-0.658	-0.667
0.050	-0.799	-0.811
0.060	-0.877	-0.889
0.070	-0.941	-0.955
0.080	-1.029	-1.044
0.090	-1.060	-1.076
0.100	-1.090	-1.106
0.119	-1.121	-1.137
0.140	-1.136	-1.153
0.160	-1.140	-1.157
0.180	-1.138	-1.155
0.200	-1.140	-1.157
0.220	-1.147	-1.164
0.240	-1.150	-1.167
0.260	-1.147	-1.163
0.280	-1.147	-1.164
0.299	-1.145	-1.162
0.320	-1.151	-1.168
0.340	-1.150	-1.166
0.360	-1.158	-1.175
0.380	-1.166	-1.183
0.399	-1.167	-1.184
0.420	-1.171	-1.189
0.439	-1.173	-1.190
0.460	-1.158	-1.175
0.480	-1.141	-1.158
0.500	-1.129	-1.145
0.519	-1.072	-1.088
0.539	-1.084	-1.100
0.560	-1.045	-1.061
0.580	-0.873	-0.886
0.599	-0.734	-0.745
0.619	-0.534	-0.542
0.639	-0.468	-0.474
0.659	-0.450	-0.456
0.679	-0.426	-0.433
0.699	-0.425	-0.431
0.719	-0.395	-0.400
0.739	-0.365	-0.371
0.759	-0.333	-0.338
0.779	-0.290	-0.295
0.799	-0.251	-0.254
0.819	-0.210	-0.213
0.839	-0.170	-0.172
0.859	-0.117	-0.119
0.879	-0.069	-0.070
0.899	-0.024	-0.025
0.919	0.031	0.032
0.939	0.074	0.075
0.960	0.103	0.105

Spanwise
(upper surface, x/c=.9)

y/b	Cp	C_{p_c}
-0.434	-0.050	-0.051
-0.367	-0.030	-0.031
-0.300	-0.027	-0.028
-0.234	-0.026	-0.026
-0.167	-0.021	-0.021
-0.017	-0.024	-0.025
0.166	-0.022	-0.022
0.232	-0.029	-0.029
0.299	-0.027	-0.027
0.366	-0.037	-0.037
0.432	-0.056	-0.057

Lower surface

x/c	Cp	C_{p_c}
0.950	0.313	0.317
0.850	0.356	0.361
0.750	0.277	0.281
0.650	0.118	0.119
0.550	-0.045	-0.046
0.450	-0.161	-0.163
0.350	-0.229	-0.232
0.250	-0.253	-0.257
0.200	-0.237	-0.240
0.150	-0.185	-0.188
0.100	-0.115	-0.117
0.075	0.000	0.000
0.050	0.115	0.117
0.030	0.277	0.281
0.020	0.406	0.412
0.010	0.632	0.641
0.008	0.696	0.707
0.006	0.790	0.801
0.004	0.920	0.933
0.002	1.085	1.101

Figure C－22 The NAL data corrected for the four wall effects.

Run	Scan	M_s	M_c	α_g(deg)	Re	C_{l_u}	C_{l_c}	$C_{d_{wake}}$
7117	3	0.758	0.745	3.51	21.1×10^6	0.888	0.898	0.0302

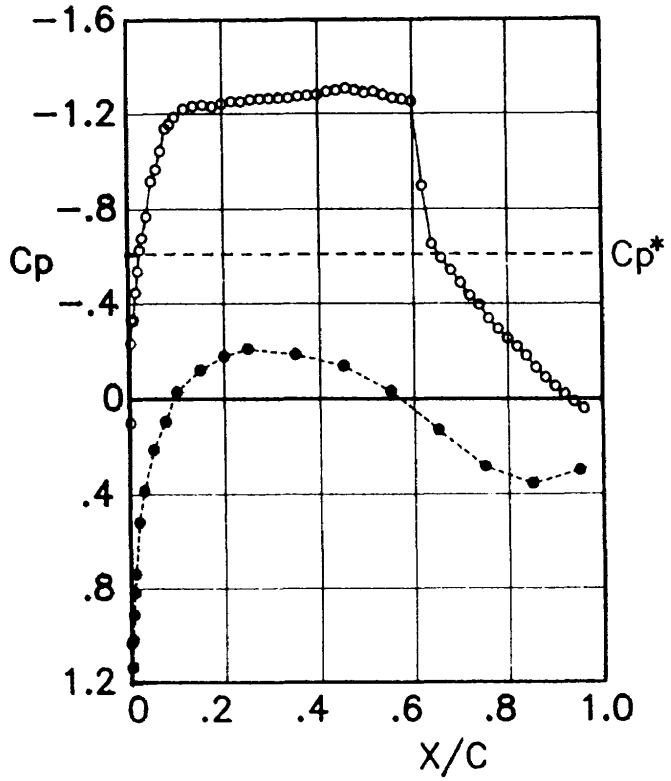

Corrected pressure distribution

Upper surface

x/c	Cp	C_{pc}
0.000	1.021	1.033
0.002	0.098	0.100
0.004	-0.229	-0.232
0.006	-0.329	-0.333
0.008	-0.321	-0.325
0.010	-0.331	-0.335
0.015	-0.443	-0.448
0.020	-0.532	-0.538
0.025	-0.621	-0.629
0.030	-0.669	-0.677
0.040	-0.760	-0.769
0.050	-0.907	-0.918
0.060	-0.955	-0.966
0.070	-1.032	-1.044
0.080	-1.124	-1.137
0.090	-1.142	-1.156
0.100	-1.172	-1.186
0.119	-1.206	-1.221
0.140	-1.218	-1.232
0.160	-1.223	-1.238
0.180	-1.217	-1.232
0.200	-1.229	-1.243
0.220	-1.238	-1.253
0.240	-1.237	-1.252
0.260	-1.245	-1.260
0.280	-1.248	-1.263
0.299	-1.249	-1.264
0.320	-1.252	-1.267
0.340	-1.252	-1.267
0.360	-1.260	-1.274
0.380	-1.263	-1.278
0.399	-1.266	-1.281
0.420	-1.278	-1.293
0.439	-1.284	-1.299
0.460	-1.292	-1.307
0.480	-1.284	-1.299
0.500	-1.273	-1.288
0.519	-1.278	-1.294
0.539	-1.265	-1.280
0.560	-1.251	-1.266
0.580	-1.246	-1.261
0.599	-1.237	-1.252
0.619	-0.887	-0.898
0.639	-0.643	-0.651
0.659	-0.585	-0.592
0.679	-0.535	-0.541
0.699	-0.482	-0.487
0.719	-0.428	-0.433
0.739	-0.389	-0.394
0.759	-0.331	-0.335
0.779	-0.289	-0.292
0.799	-0.248	-0.251
0.819	-0.214	-0.217
0.839	-0.177	-0.179
0.859	-0.128	-0.129
0.879	-0.088	-0.089
0.899	-0.052	-0.052
0.919	-0.018	-0.018
0.939	0.014	0.014
0.960	0.042	0.043

Spanwise
(upper surface, x/c=.9)

y/b	Cp	C_{pc}
-0.434	-0.070	-0.071
-0.367	-0.054	-0.055
-0.300	-0.052	-0.053
-0.234	-0.059	-0.060
-0.167	-0.057	-0.058
-0.017	-0.052	-0.052
0.166	-0.048	-0.049
0.232	-0.072	-0.073
0.299	-0.051	-0.052
0.366	-0.059	-0.059
0.432	-0.081	-0.082

Lower surface

x/c	Cp	C_{pc}
0.950	0.298	0.301
0.850	0.352	0.356
0.750	0.282	0.285
0.650	0.129	0.131
0.550	-0.032	-0.032
0.450	-0.136	-0.137
0.350	-0.183	-0.185
0.250	-0.206	-0.208
0.200	-0.174	-0.176
0.150	-0.118	-0.120
0.100	-0.027	-0.027
0.075	0.095	0.096
0.050	0.212	0.214
0.030	0.381	0.385
0.020	0.514	0.520
0.010	0.730	0.738
0.008	0.808	0.817
0.006	0.901	0.912
0.004	1.006	1.018
0.002	1.123	1.137

Figure C－23 The NAL data corrected for the four wall effects.

Run	Scan	M_s	M_c	α_g(deg)	Re	C_{l_u}	C_{l_c}	$C_{d_{wake}}$
7349	3	0.755	0.742	4.72	20.7×10^6	0.888	0.898	0.0609

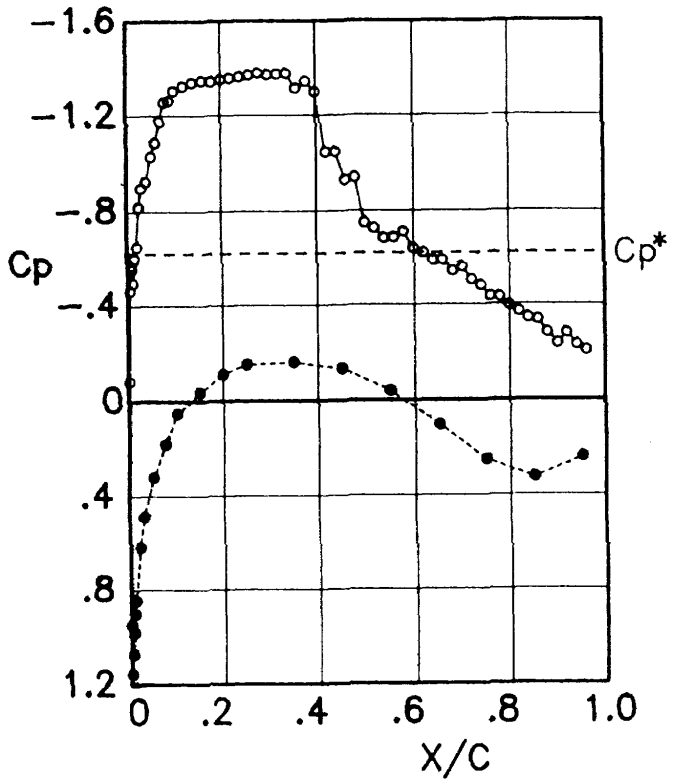

Corrected pressure distribution

Upper surface

x/c	Cp	C_{p_c}
0.000	0.940	0.951
0.002	-0.082	-0.083
0.004	-0.457	-0.462
0.006	-0.566	-0.573
0.008	-0.548	-0.555
0.010	-0.490	-0.496
0.015	-0.595	-0.602
0.020	-0.643	-0.650
0.025	-0.809	-0.819
0.030	-0.888	-0.899
0.040	-0.914	-0.925
0.050	-1.017	-1.029
0.060	-1.074	-1.087
0.070	-1.161	-1.175
0.080	-1.242	-1.257
0.090	-1.247	-1.262
0.100	-1.288	-1.304
0.119	-1.307	-1.323
0.140	-1.323	-1.338
0.160	-1.331	-1.346
0.180	-1.326	-1.342
0.200	-1.335	-1.351
0.220	-1.342	-1.357
0.240	-1.346	-1.362
0.260	-1.354	-1.370
0.280	-1.361	-1.378
0.299	-1.355	-1.371
0.320	-1.357	-1.373
0.340	-1.360	-1.376
0.360	-1.298	-1.314
0.380	-1.327	-1.343
0.399	-1.283	-1.299
0.420	-1.032	-1.045
0.439	-1.034	-1.046
0.460	-0.918	-0.929
0.480	-0.929	-0.940
0.500	-0.739	-0.747
0.519	-0.716	-0.724
0.539	-0.673	-0.681
0.560	-0.676	-0.684
0.580	-0.700	-0.709
0.599	-0.630	-0.638
0.619	-0.611	-0.618
0.639	-0.579	-0.586
0.659	-0.580	-0.587
0.679	-0.534	-0.541
0.699	-0.551	-0.558
0.719	-0.497	-0.502
0.739	-0.472	-0.478
0.759	-0.426	-0.432
0.779	-0.424	-0.429
0.799	-0.389	-0.394
0.819	-0.362	-0.366
0.839	-0.335	-0.339
0.859	-0.328	-0.332
0.879	-0.274	-0.277
0.899	-0.229	-0.232
0.919	-0.272	-0.275
0.939	-0.223	-0.226
0.960	-0.200	-0.203

Spanwise
(upper surface, x/c=.9)

y/b	Cp	C_{p_c}
-0.434	-0.134	-0.136
-0.367	-0.170	-0.172
-0.300	-0.200	-0.202
-0.234	-0.231	-0.234
-0.167	-0.229	-0.232
-0.017	-0.229	-0.232
0.166	-0.259	-0.263
0.232	-0.220	-0.223
0.299	-0.201	-0.203
0.366	-0.150	-0.152
0.432	-0.151	-0.153

Lower surface

x/c	Cp	C_{p_c}
0.950	0.239	0.242
0.850	0.323	0.327
0.750	0.251	0.253
0.650	0.105	0.106
0.550	-0.038	-0.038
0.450	-0.131	-0.132
0.350	-0.159	-0.161
0.250	-0.149	-0.151
0.200	-0.110	-0.111
0.150	-0.035	-0.035
0.100	0.052	0.053
0.075	0.181	0.183
0.050	0.317	0.321
0.030	0.483	0.489
0.020	0.612	0.619
0.010	0.836	0.846
0.008	0.893	0.904
0.006	0.970	0.982
0.004	1.062	1.074
0.002	1.142	1.156

Figure C−24 The NAL data corrected for the four wall effects.

Run	Scan	M_s	M_c	α_g(deg)	Re	C_{l_u}	C_{l_c}	$C_{d_{wake}}$
7353	1	0.778	0.752	-3.52	20.8×10^6	-0.221	-0.226	0.0208

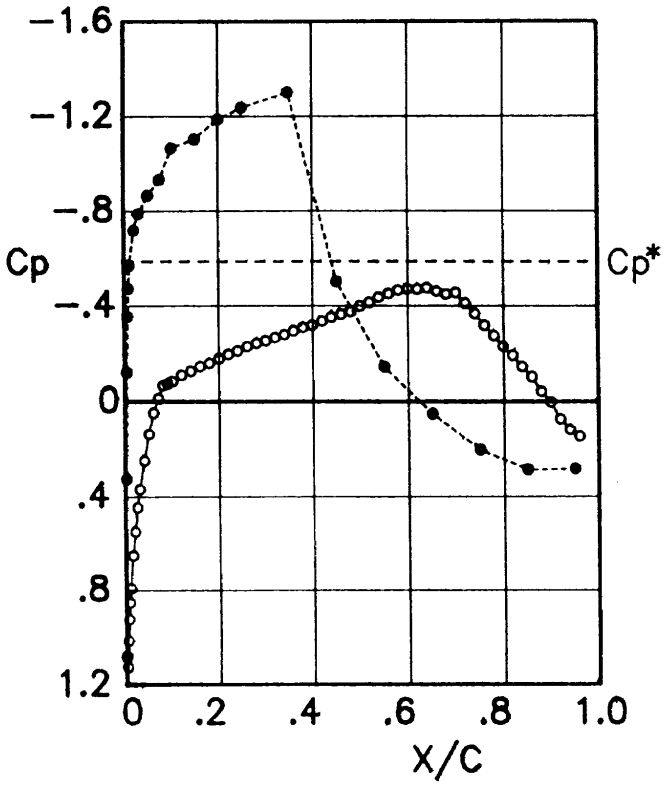

Corrected pressure distribution

Upper surface

x/c	Cp	C_{p_c}
0.000	1.058	1.083
0.002	1.102	1.127
0.004	0.993	1.016
0.006	0.904	0.925
0.008	0.834	0.853
0.010	0.775	0.793
0.015	0.638	0.653
0.020	0.538	0.550
0.025	0.437	0.447
0.030	0.361	0.369
0.040	0.242	0.248
0.050	0.134	0.137
0.060	0.047	0.048
0.070	-0.013	-0.014
0.080	-0.067	-0.068
0.090	-0.074	-0.075
0.100	-0.083	-0.085
0.119	-0.109	-0.112
0.140	-0.125	-0.127
0.160	-0.143	-0.147
0.180	-0.157	-0.160
0.200	-0.175	-0.179
0.220	-0.193	-0.197
0.240	-0.207	-0.212
0.260	-0.224	-0.230
0.280	-0.237	-0.242
0.299	-0.248	-0.254
0.320	-0.261	-0.268
0.340	-0.274	-0.280
0.360	-0.288	-0.295
0.380	-0.303	-0.310
0.399	-0.311	-0.318
0.420	-0.329	-0.336
0.439	-0.344	-0.352
0.460	-0.356	-0.365
0.480	-0.367	-0.376
0.500	-0.390	-0.399
0.519	-0.404	-0.413
0.539	-0.426	-0.436
0.560	-0.441	-0.451
0.580	-0.455	-0.466
0.599	-0.461	-0.472
0.619	-0.460	-0.470
0.639	-0.465	-0.475
0.659	-0.451	-0.462
0.679	-0.439	-0.449
0.699	-0.445	-0.456
0.719	-0.401	-0.410
0.739	-0.360	-0.368
0.759	-0.312	-0.319
0.779	-0.269	-0.275
0.799	-0.225	-0.230
0.819	-0.189	-0.193
0.839	-0.143	-0.146
0.859	-0.101	-0.104
0.879	-0.042	-0.043
0.899	0.003	0.003
0.919	0.073	0.075
0.939	0.116	0.119
0.960	0.144	0.147

Spanwise
(upper surface, x/c=.9)

y/b	Cp	C_{p_c}
-0.434	0.001	0.001
-0.367	0.006	0.006
-0.300	0.005	0.006
-0.234	0.012	0.012
-0.167	0.012	0.013
-0.017	0.003	0.003
0.166	0.004	0.004
0.232	-0.004	-0.004
0.299	-0.002	-0.002
0.366	-0.008	-0.008
0.432	-0.014	-0.015

Lower surface

x/c	Cp	C_{p_c}
0.950	0.276	0.283
0.850	0.281	0.287
0.750	0.198	0.203
0.650	0.052	0.053
0.550	-0.142	-0.145
0.450	-0.490	-0.502
0.350	-1.272	-1.301
0.250	-1.208	-1.235
0.200	-1.159	-1.186
0.150	-1.078	-1.103
0.100	-1.040	-1.064
0.075	-0.912	-0.933
0.050	-0.845	-0.864
0.030	-0.768	-0.786
0.020	-0.700	-0.716
0.010	-0.554	-0.567
0.008	-0.460	-0.470
0.006	-0.345	-0.353
0.004	-0.117	-0.120
0.002	0.320	0.327

Figure C−25 The NAL data corrected for the four wall effects.

Run	Scan	M_s	M_c	α_g(deg)	Re	C_{l_u}	C_{l_c}	$C_{d_{wake}}$
7361	1	0.777	0.753	-0.10	21.3×10^6	0.299	0.305	0.0075

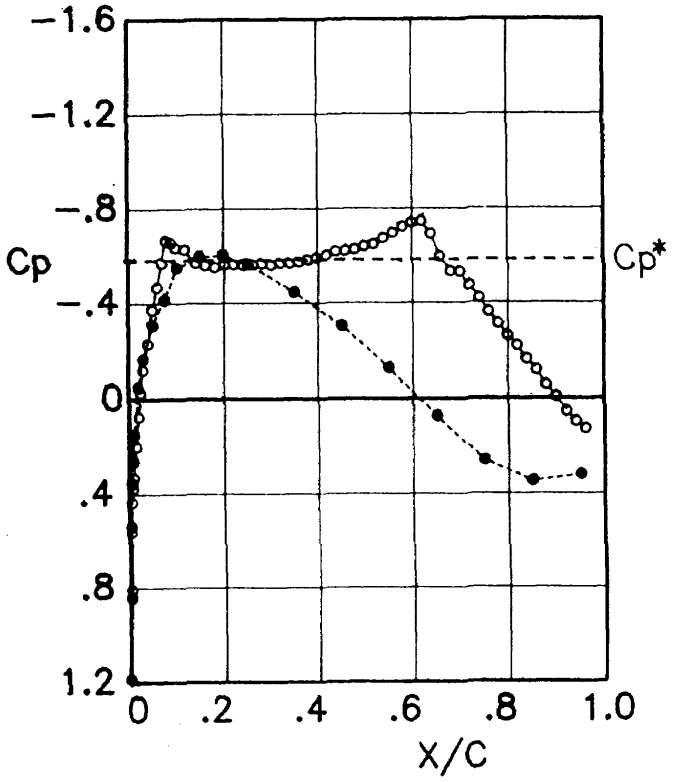

Corrected pressure distribution

Upper surface

x/c	C_p	C_{p_c}
0.000	1.159	1.184
0.002	0.790	0.807
0.004	0.550	0.562
0.006	0.425	0.434
0.008	0.368	0.376
0.010	0.323	0.330
0.015	0.193	0.197
0.020	0.071	0.073
0.025	-0.026	-0.027
0.030	-0.119	-0.122
0.040	-0.226	-0.231
0.050	-0.367	-0.375
0.060	-0.459	-0.469
0.070	-0.559	-0.571
0.080	-0.651	-0.665
0.090	-0.643	-0.657
0.100	-0.622	-0.635
0.119	-0.615	-0.628
0.140	-0.558	-0.570
0.160	-0.549	-0.560
0.180	-0.542	-0.553
0.200	-0.550	-0.561
0.220	-0.552	-0.564
0.240	-0.549	-0.561
0.260	-0.552	-0.564
0.280	-0.555	-0.567
0.299	-0.549	-0.561
0.320	-0.557	-0.569
0.340	-0.557	-0.569
0.360	-0.563	-0.575
0.380	-0.570	-0.583
0.399	-0.578	-0.590
0.420	-0.589	-0.601
0.439	-0.605	-0.618
0.460	-0.607	-0.620
0.480	-0.613	-0.626
0.500	-0.626	-0.639
0.519	-0.634	-0.648
0.539	-0.660	-0.674
0.560	-0.682	-0.696
0.580	-0.708	-0.723
0.599	-0.724	-0.740
0.619	-0.731	-0.746
0.639	-0.678	-0.692
0.659	-0.584	-0.596
0.679	-0.522	-0.533
0.699	-0.520	-0.531
0.719	-0.463	-0.473
0.739	-0.412	-0.421
0.759	-0.355	-0.362
0.779	-0.306	-0.313
0.799	-0.256	-0.261
0.819	-0.214	-0.219
0.839	-0.160	-0.164
0.859	-0.115	-0.118
0.879	-0.055	-0.056
0.899	-0.007	-0.007
0.919	0.053	0.054
0.939	0.095	0.097
0.960	0.125	0.128

Spanwise
(upper surface, x/c=.9)

y/b	C_p	C_{p_c}
-0.434	-0.028	-0.029
-0.367	-0.017	-0.018
-0.300	-0.011	-0.012
-0.234	-0.004	-0.004
-0.167	-0.002	-0.002
-0.017	-0.007	-0.007
0.166	-0.010	-0.010
0.232	-0.017	-0.018
0.299	-0.020	-0.020
0.366	-0.030	-0.030
0.432	-0.040	-0.041

Lower surface

x/c	C_p	C_{p_c}
0.950	0.314	0.320
0.850	0.338	0.346
0.750	0.252	0.258
0.650	0.071	0.073
0.550	-0.126	-0.129
0.450	-0.300-	-0.306
0.350	-0.438	-0.448
0.250	-0.553	-0.565
0.200	-0.591	-0.604
0.150	-0.583	-0.596
0.100	-0.540	-0.551
0.075	-0.405	-0.414
0.050	-0.302	-0.308
0.030	-0.163	-0.166
0.020	-0.046	-0.047
0.010	0.148	0.151
0.008	0.256	0.262
0.006	0.346	0.354
0.004	0.527	0.538
0.002	0.825	0.842

Figure C－26 The NAL data corrected for the four wall effects.

Run	Scan	M_s	M_c	α_g(deg)	Re	C_{l_u}	C_{l_c}	$C_{d_{wake}}$
7108	3	0.772	0.751	1.81	21.1×10^6	0.610	0.621	0.0083

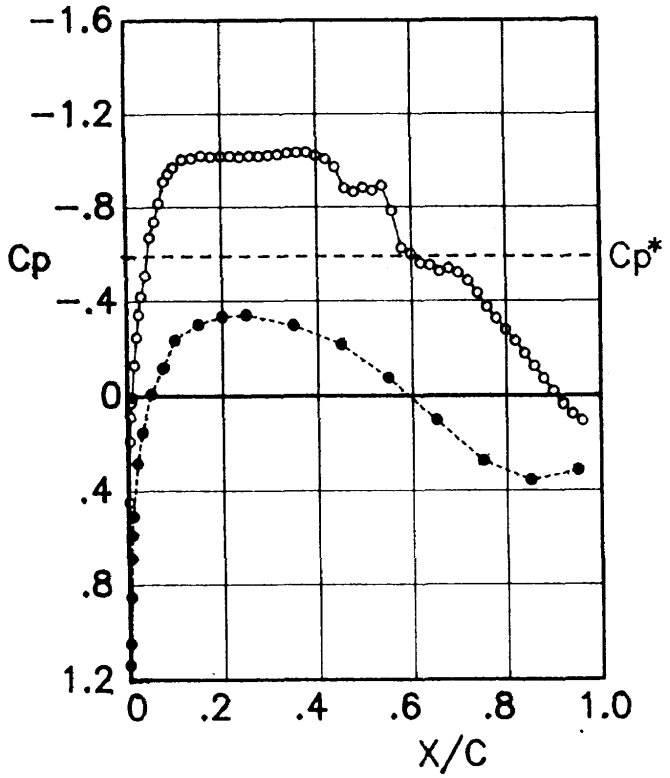

Corrected pressure distribution

Upper surface

x/c	Cp	C_{p_c}
0.000	1.115	1.136
0.002	0.439	0.447
0.004	0.185	0.189
0.006	0.084	0.085
0.008	0.026	0.027
0.010	0.003	0.003
0.015	-0.128	-0.131
0.020	-0.244	-0.249
0.025	-0.337	-0.344
0.030	-0.413	-0.421
0.040	-0.499	-0.508
0.050	-0.657	-0.669
0.060	-0.722	-0.736
0.070	-0.801	-0.816
0.080	-0.892	-0.909
0.090	-0.924	-0.942
0.100	-0.951	-0.969
0.119	-0.985	-1.003
0.140	-0.990	-1.009
0.160	-1.001	-1.020
0.180	-0.997	-1.016
0.200	-0.998	-1.017
0.220	-0.999	-1.018
0.240	-0.995	-1.014
0.260	-1.000	-1.018
0.280	-0.999	-1.017
0.299	-1.003	-1.022
0.320	-1.006	-1.025
0.340	-1.013	-1.032
0.360	-1.015	-1.034
0.380	-1.016	-1.036
0.399	-1.002	-1.021
0.420	-0.988	-1.007
0.439	-0.954	-0.972
0.460	-0.864	-0.880
0.480	-0.848	-0.864
0.500	-0.867	-0.883
0.519	-0.854	-0.870
0.539	-0.874	-0.890
0.560	-0.767	-0.781
0.580	-0.611	-0.623
0.599	-0.586	-0.597
0.619	-0.548	-0.558
0.639	-0.540	-0.550
0.659	-0.514	-0.524
0.679	-0.526	-0.536
0.699	-0.509	-0.518
0.719	-0.475	-0.484
0.739	-0.424	-0.432
0.759	-0.366	-0.373
0.779	-0.318	-0.324
0.799	-0.271	-0.276
0.819	-0.224	-0.228
0.839	-0.172	-0.175
0.859	-0.120	-0.122
0.879	-0.068	-0.069
0.899	-0.016	-0.016
0.919	0.038	0.038
0.939	0.079	0.081
0.960	0.107	0.109

Spanwise
(upper surface, x/c=.9)

y/b	Cp	C_{p_c}
-0.434	-0.039	-0.039
-0.367	-0.030	-0.030
-0.300	-0.025	-0.026
-0.234	-0.016	-0.016
-0.167	-0.019	-0.019
-0.017	-0.016	-0.016
0.166	-0.024	-0.024
0.232	-0.024	-0.025
0.299	-0.028	-0.028
0.366	-0.036	-0.037
0.432	-0.047	-0.048

Lower surface

x/c	Cp	C_{p_c}
0.950	0.310	0.315
0.850	0.351	0.357
0.750	0.270	0.275
0.650	0.102	0.104
0.550	-0.073	-0.075
0.450	-0.211	-0.215
0.350	-0.291	-0.297
0.250	-0.335	-0.341
0.200	-0.327	-0.333
0.150	-0.295	-0.300
0.100	-0.229	-0.233
0.075	-0.114	-0.116
0.050	-0.007	-0.007
0.030	0.153	0.156
0.020	0.279	0.284
0.010	0.500	0.510
0.008	0.579	0.590
0.006	0.674	0.687
0.004	0.836	0.852
0.002	1.028	1.048

Figure C－27 The NAL data corrected for the four wall effects.

Run	Scan	M_s	M_c	α_g(deg)	Re	C_{l_u}	C_{l_c}	$C_{d_{wake}}$
7101	1	0.769	0.752	2.62	21.3×10^6	0.775	0.787	0.0165

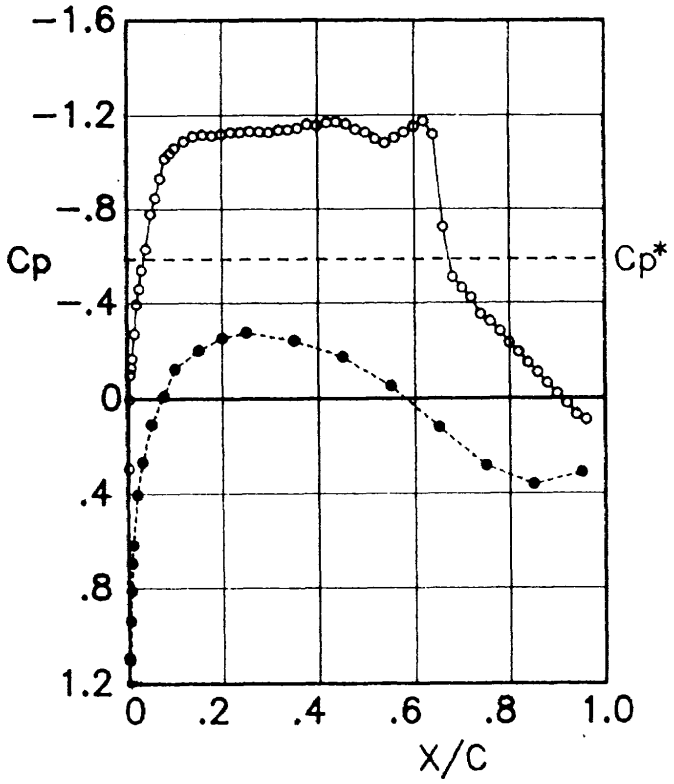

Corrected pressure distribution

Upper surface

x/c	Cp	C_{p_c}
0.000	1.076	1.092
0.002	0.289	0.293
0.004	0.003	0.003
0.006	-0.099	-0.100
0.008	-0.126	-0.128
0.010	-0.164	-0.166
0.015	-0.266	-0.270
0.020	-0.389	-0.395
0.025	-0.453	-0.460
0.030	-0.532	-0.540
0.040	-0.620	-0.630
0.050	-0.768	-0.779
0.060	-0.835	-0.848
0.070	-0.918	-0.932
0.080	-1.002	-1.017
0.090	-1.023	-1.038
0.100	-1.045	-1.061
0.119	-1.072	-1.089
0.140	-1.094	-1.111
0.160	-1.100	-1.117
0.180	-1.097	-1.113
0.200	-1.103	-1.120
0.220	-1.110	-1.127
0.240	-1.110	-1.127
0.260	-1.114	-1.131
0.280	-1.112	-1.129
0.299	-1.110	-1.127
0.320	-1.120	-1.137
0.340	-1.121	-1.138
0.360	-1.128	-1.145
0.380	-1.144	-1.161
0.399	-1.139	-1.156
0.420	-1.151	-1.169
0.439	-1.155	-1.172
0.460	-1.146	-1.163
0.480	-1.123	-1.140
0.500	-1.110	-1.127
0.519	-1.083	-1.100
0.539	-1.066	-1.082
0.560	-1.089	-1.105
0.580	-1.111	-1.128
0.599	-1.134	-1.152
0.619	-1.158	-1.175
0.639	-1.101	-1.118
0.659	-0.711	-0.722
0.679	-0.500	-0.508
0.699	-0.455	-0.462
0.719	-0.415	-0.421
0.739	-0.346	-0.351
0.759	-0.316	-0.320
0.779	-0.275	-0.279
0.799	-0.226	-0.230
0.819	-0.189	-0.192
0.839	-0.145	-0.147
0.859	-0.105	-0.107
0.879	-0.062	-0.062
0.899	-0.017	-0.017
0.919	0.023	0.024
0.939	0.069	0.070
0.960	0.090	0.091

Spanwise
(upper surface, x/c=.9)

y/b	Cp	C_{p_c}
-0.434	-0.055	-0.055
-0.367	-0.032	-0.032
-0.300	-0.027	-0.027
-0.234	-0.015	-0.016
-0.167	-0.015	-0.016
-0.017	-0.017	-0.017
0.166	-0.021	-0.021
0.232	-0.029	-0.030
0.299	-0.032	-0.032
0.366	-0.043	-0.044
0.432	-0.063	-0.064

Lower surface

x/c	Cp	C_{p_c}
0.950	0.308	0.312
0.850	0.355	0.361
0.750	0.278	0.282
0.650	0.120	0.121
0.550	-0.051	-0.052
0.450	-0.171	-0.173
0.350	-0.238	-0.241
0.250	-0.272	-0.276
0.200	-0.248	-0.252
0.150	-0.197	-0.200
0.100	-0.121	-0.123
0.075	-0.008	-0.008
0.050	0.108	0.110
0.030	0.264	0.268
0.020	0.400	0.406
0.010	0.611	0.620
0.008	0.685	0.696
0.006	0.800	0.812
0.004	0.925	0.939
0.002	1.086	1.103

Figure C－28 The NAL data corrected for the four wall effects.

Run	Scan	M_s	M_c	α_g(deg)	Re	C_{l_u}	C_{l_c}	$C_{d_{wake}}$
7351	2	0.768	0.753	3.11	21.0×10^6	0.831	0.842	0.0286

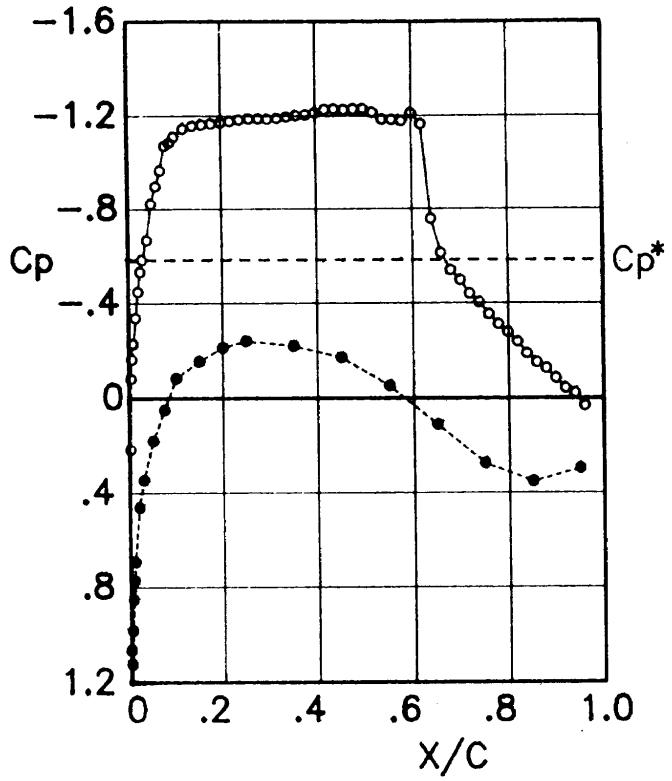

Corrected pressure distribution

Upper surface

x/c	Cp	C_{p_c}
0.000	1.051	1.065
0.002	0.215	0.218
0.004	-0.082	-0.083
0.006	-0.161	-0.163
0.008	-0.227	-0.230
0.010	-0.226	-0.229
0.015	-0.334	-0.338
0.020	-0.443	-0.448
0.025	-0.525	-0.532
0.030	-0.576	-0.584
0.040	-0.658	-0.667
0.050	-0.812	-0.823
0.060	-0.886	-0.898
0.070	-0.954	-0.966
0.080	-1.058	-1.072
0.090	-1.070	-1.084
0.100	-1.096	-1.110
0.119	-1.129	-1.144
0.140	-1.141	-1.157
0.160	-1.147	-1.162
0.180	-1.151	-1.167
0.200	-1.155	-1.171
0.220	-1.161	-1.177
0.240	-1.167	-1.183
0.260	-1.172	-1.188
0.280	-1.173	-1.189
0.299	-1.171	-1.187
0.320	-1.175	-1.190
0.340	-1.180	-1.196
0.360	-1.186	-1.202
0.380	-1.189	-1.205
0.399	-1.197	-1.213
0.420	-1.211	-1.228
0.439	-1.213	-1.230
0.460	-1.211	-1.227
0.480	-1.213	-1.229
0.500	-1.214	-1.230
0.519	-1.200	-1.216
0.539	-1.170	-1.185
0.560	-1.168	-1.183
0.580	-1.163	-1.179
0.599	-1.196	-1.212
0.619	-1.148	-1.163
0.639	-0.746	-0.756
0.659	-0.603	-0.611
0.679	-0.530	-0.537
0.699	-0.489	-0.496
0.719	-0.432	-0.438
0.739	-0.397	-0.403
0.759	-0.347	-0.351
0.779	-0.305	-0.309
0.799	-0.272	-0.276
0.819	-0.232	-0.235
0.839	-0.183	-0.185
0.859	-0.146	-0.148
0.879	-0.122	-0.123
0.899	-0.081	-0.082
0.919	-0.039	-0.040
0.939	-0.020	-0.020
0.960	0.034	0.035

Spanwise
(upper surface, x/c=.9)

y/b	Cp	C_{p_c}
-0.434	-0.071	-0.071
-0.367	-0.062	-0.063
-0.300	-0.063	-0.064
-0.234	-0.056	-0.056
-0.167	-0.063	-0.064
-0.017	-0.081	-0.082
0.166	-0.096	-0.097
0.232	-0.072	-0.073
0.299	-0.066	-0.067
0.366	-0.057	-0.058
0.432	-0.077	-0.078

Lower surface

x/c	Cp	C_{p_c}
0.950	0.294	0.298
0.850	0.348	0.353
0.750	0.273	0.276
0.650	0.113	0.114
0.550	-0.051	-0.051
0.450	-0.168	-0.171
0.350	-0.216	-0.219
0.250	-0.237	-0.240
0.200	-0.208	-0.211
0.150	-0.152	-0.154
0.100	-0.081	-0.083
0.075	0.051	0.052
0.050	0.181	0.183
0.030	0.342	0.347
0.020	0.458	0.464
0.010	0.685	0.694
0.008	0.763	0.773
0.006	0.841	0.852
0.004	0.970	0.983
0.002	1.108	1.123

Figure C－29 The NAL data corrected for the four wall effects.

Run	Scan	M_s	M_c	α_g(deg)	Re	C_{l_u}	C_{l_c}	$C_{d_{wake}}$
7351	3	0.768	0.754	4.52	21.1×10^6	0.829	0.840	0.0654

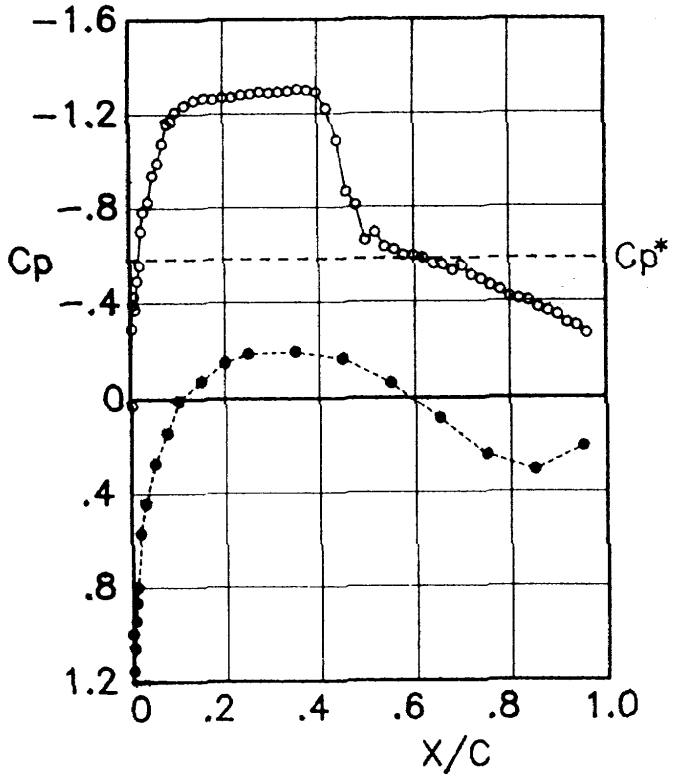

Corrected pressure distribution

Upper surface

x/c	C_p	C_{p_c}
0.000	0.985	0.998
0.002	0.024	0.024
0.004	-0.291	-0.294
0.006	-0.388	-0.393
0.008	-0.423	-0.428
0.010	-0.369	-0.373
0.015	-0.487	-0.493
0.020	-0.551	-0.558
0.025	-0.692	-0.700
0.030	-0.774	-0.784
0.040	-0.818	-0.828
0.050	-0.929	-0.941
0.060	-0.981	-0.993
0.070	-1.063	-1.076
0.080	-1.146	-1.160
0.090	-1.158	-1.172
0.100	-1.195	-1.210
0.119	-1.222	-1.238
0.140	-1.243	-1.259
0.160	-1.253	-1.268
0.180	-1.246	-1.261
0.200	-1.255	-1.271
0.220	-1.255	-1.271
0.240	-1.265	-1.281
0.260	-1.269	-1.284
0.280	-1.277	-1.293
0.299	-1.272	-1.288
0.320	-1.277	-1.292
0.340	-1.280	-1.296
0.360	-1.288	-1.304
0.380	-1.284	-1.300
0.399	-1.276	-1.292
0.420	-1.207	-1.222
0.439	-1.073	-1.086
0.460	-0.856	-0.867
0.480	-0.799	-0.809
0.500	-0.649	-0.657
0.519	-0.682	-0.690
0.539	-0.621	-0.629
0.560	-0.609	-0.617
0.580	-0.585	-0.592
0.599	-0.584	-0.591
0.619	-0.573	-0.581
0.639	-0.550	-0.557
0.659	-0.546	-0.553
0.679	-0.522	-0.528
0.699	-0.541	-0.547
0.719	-0.502	-0.508
0.739	-0.484	-0.490
0.759	-0.457	-0.463
0.779	-0.440	-0.445
0.799	-0.411	-0.416
0.819	-0.403	-0.408
0.839	-0.396	-0.401
0.859	-0.368	-0.372
0.879	-0.352	-0.356
0.899	-0.336	-0.340
0.919	-0.304	-0.307
0.939	-0.292	-0.295
0.960	-0.260	-0.264

Spanwise
(upper surface, x/c=.9)

y/b	C_p	C_{p_c}
-0.434	-0.148	-0.150
-0.367	-0.180	-0.182
-0.300	-0.244	-0.247
-0.234	-0.285	-0.289
-0.167	-0.329	-0.333
-0.017	-0.336	-0.340
0.166	-0.311	-0.314
0.232	-0.276	-0.279
0.299	-0.251	-0.254
0.366	-0.196	-0.198
0.432	-0.142	-0.144

Lower surface

x/c	C_p	C_{p_c}
0.950	0.205	0.208
0.850	0.304	0.307
0.750	0.241	0.244
0.650	0.086	0.087
0.550	-0.061	-0.061
0.450	-0.163	-0.165
0.350	-0.192	-0.195
0.250	-0.185	-0.187
0.200	-0.149	-0.151
0.150	-0.073	-0.074
0.100	0.009	0.009
0.075	0.143	0.145
0.050	0.270	0.273
0.030	0.439	0.444
0.020	0.564	0.571
0.010	0.790	0.800
0.008	0.856	0.867
0.006	0.932	0.944
0.004	1.046	1.059
0.002	1.138	1.152

Figure C－30 The NAL data corrected for the four wall effects.

Run	Scan	M_s	M_c	α_g(deg)	Re	C_{l_u}	C_{l_c}	$C_{d_{wake}}$
7357	1	0.795	0.769	-3.43	20.4×10^6	-0.195	-0.199	0.0344

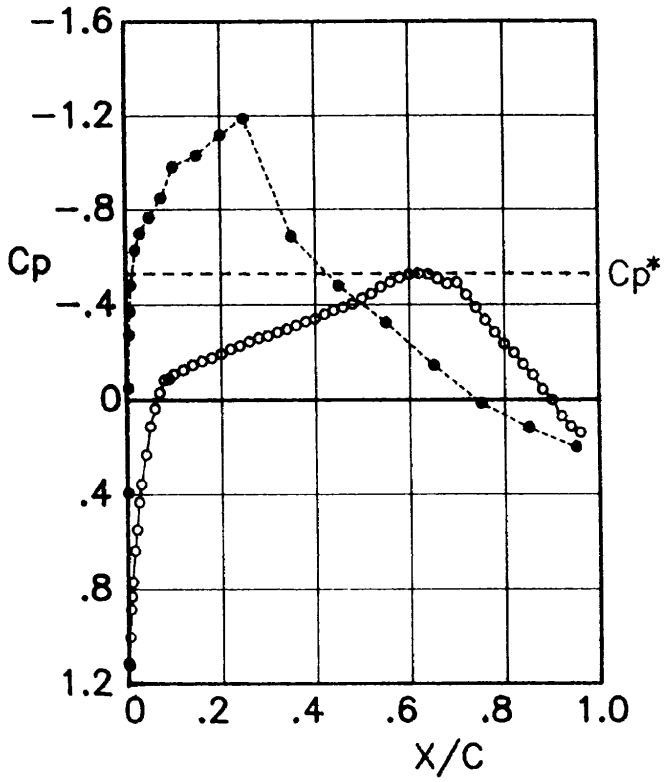

Corrected pressure distribution

Upper surface

x/c	Cp	C_{p_c}
0.000	1.087	1.111
0.002	1.098	1.123
0.004	0.980	1.002
0.006	0.865	0.885
0.008	0.812	0.830
0.010	0.753	0.770
0.015	0.624	0.637
0.020	0.537	0.549
0.025	0.424	0.433
0.030	0.349	0.357
0.040	0.227	0.232
0.050	0.110	0.112
0.060	0.036	0.036
0.070	-0.032	-0.032
0.080	-0.084	-0.086
0.090	-0.088	-0.090
0.100	-0.107	-0.109
0.119	-0.124	-0.127
0.140	-0.145	-0.148
0.160	-0.160	-0.164
0.180	-0.174	-0.178
0.200	-0.190	-0.194
0.220	-0.209	-0.214
0.240	-0.223	-0.228
0.260	-0.241	-0.246
0.280	-0.255	-0.261
0.299	-0.263	-0.269
0.320	-0.279	-0.285
0.340	-0.292	-0.298
0.360	-0.307	-0.313
0.380	-0.322	-0.329
0.399	-0.333	-0.340
0.420	-0.352	-0.360
0.439	-0.368	-0.376
0.460	-0.381	-0.389
0.480	-0.394	-0.403
0.500	-0.419	-0.428
0.519	-0.437	-0.446
0.539	-0.464	-0.475
0.560	-0.484	-0.495
0.580	-0.502	-0.513
0.599	-0.515	-0.527
0.619	-0.520	-0.531
0.639	-0.516	-0.528
0.659	-0.499	-0.510
0.679	-0.477	-0.488
0.699	-0.482	-0.493
0.719	-0.432	-0.442
0.739	-0.379	-0.387
0.759	-0.327	-0.334
0.779	-0.277	-0.284
0.799	-0.230	-0.235
0.819	-0.194	-0.198
0.839	-0.146	-0.150
0.859	-0.103	-0.105
0.879	-0.043	-0.044
0.899	0.001	0.001
0.919	0.070	0.071
0.939	0.112	0.115
0.960	0.138	0.141

Spanwise
(upper surface, x/c=.9)

y/b	Cp	C_{p_c}
-0.434	-0.002	-0.002
-0.367	0.002	0.002
-0.300	0.005	0.005
-0.234	0.010	0.010
-0.167	0.012	0.012
-0.017	0.001	0.001
0.166	0.003	0.003
0.232	-0.003	-0.003
0.299	-0.003	-0.003
0.366	-0.010	-0.011
0.432	-0.022	-0.023

Lower surface

x/c	Cp	C_{p_c}
0.950	0.198	0.203
0.850	0.117	0.120
0.750	0.014	0.015
0.650	-0.143	-0.146
0.550	-0.317	-0.324
0.450	-0.470	-0.480
0.350	-0.671	-0.686
0.250	-1.162	-1.188
0.200	-1.092	-1.116
0.150	-1.006	-1.029
0.100	-0.959	-0.980
0.075	-0.830	-0.849
0.050	-0.748	-0.764
0.030	-0.684	-0.699
0.020	-0.614	-0.628
0.010	-0.471	-0.482
0.008	-0.361	-0.369
0.006	-0.265	-0.271
0.004	-0.047	-0.048
0.002	0.385	0.394

Figure C－31 The NAL data corrected for the four wall effects.

Run	Scan	M_s	M_c	α_g(deg)	Re	C_{l_u}	C_{l_c}	$C_{d_{wake}}$
7359	1	0.798	0.774	0.00	20.4×10^6	0.320	0.327	0.0091

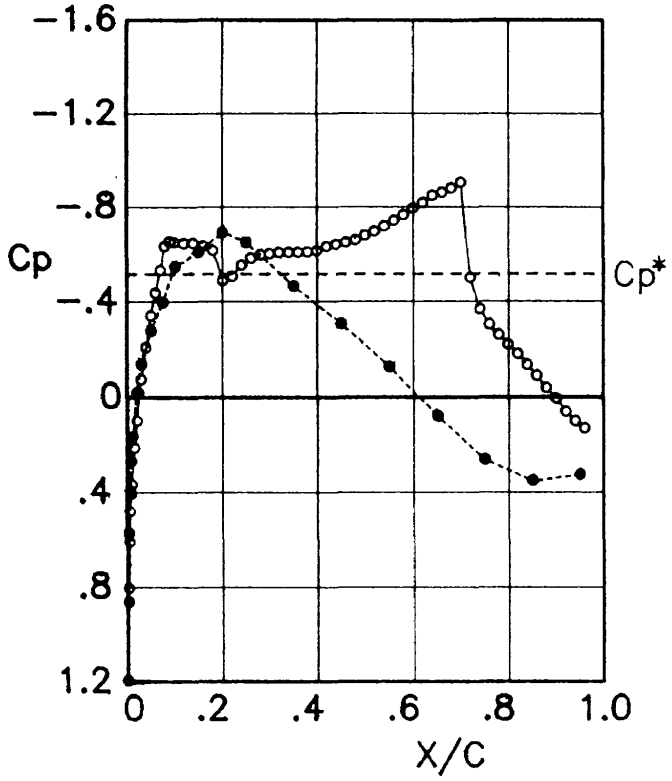

Corrected pressure distribution

Upper surface

x/c	Cp	C_{p_c}
0.000	1.169	1.192
0.002	0.787	0.803
0.004	0.597	0.609
0.006	0.470	0.479
0.008	0.399	0.407
0.010	0.359	0.366
0.015	0.208	0.212
0.020	0.095	0.097
0.025	-0.020	-0.020
0.030	-0.075	-0.077
0.040	-0.205	-0.209
0.050	-0.336	-0.343
0.060	-0.429	-0.438
0.070	-0.522	-0.532
0.080	-0.621	-0.633
0.090	-0.641	-0.654
0.100	-0.638	-0.651
0.119	-0.633	-0.646
0.140	-0.635	-0.648
0.160	-0.623	-0.635
0.180	-0.604	-0.616
0.200	-0.479	-0.489
0.220	-0.496	-0.506
0.240	-0.543	-0.554
0.260	-0.572	-0.583
0.280	-0.586	-0.597
0.299	-0.590	-0.602
0.320	-0.595	-0.607
0.340	-0.595	-0.607
0.360	-0.596	-0.608
0.380	-0.597	-0.609
0.399	-0.602	-0.614
0.420	-0.620	-0.633
0.439	-0.629	-0.641
0.460	-0.638	-0.651
0.480	-0.648	-0.661
0.500	-0.666	-0.680
0.519	-0.684	-0.697
0.539	-0.705	-0.719
0.560	-0.728	-0.742
0.580	-0.751	-0.766
0.599	-0.779	-0.795
0.619	-0.802	-0.818
0.639	-0.832	-0.849
0.659	-0.844	-0.861
0.679	-0.862	-0.880
0.699	-0.887	-0.905
0.719	-0.490	-0.500
0.739	-0.360	-0.368
0.759	-0.298	-0.304
0.779	-0.255	-0.260
0.799	-0.214	-0.218
0.819	-0.176	-0.180
0.839	-0.132	-0.134
0.859	-0.088	-0.090
0.879	-0.038	-0.039
0.899	0.007	0.007
0.919	0.061	0.062
0.939	0.099	0.101
0.960	0.129	0.131

Spanwise
(upper surface, x/c=.9)

y/b	Cp	C_{p_c}
-0.434	-0.019	-0.019
-0.367	-0.005	-0.005
-0.300	-0.002	-0.002
-0.234	0.005	0.005
-0.167	0.008	0.008
-0.017	0.007	0.007
0.166	0.001	0.001
0.232	-0.006	-0.006
0.299	-0.009	-0.009
0.366	-0.021	-0.022
0.432	-0.035	-0.035

Lower surface

x/c	Cp	C_{p_c}
0.950	0.319	0.326
0.850	0.344	0.351
0.750	0.257	0.262
0.650	0.078	0.079
0.550	-0.124	-0.127
0.450	-0.303	-0.309
0.350	-0.456	-0.465
0.250	-0.637	-0.650
0.200	-0.679	-0.693
0.150	-0.597	-0.609
0.100	-0.535	-0.546
0.075	-0.390	-0.398
0.050	-0.272	-0.278
0.030	-0.134	-0.137
0.020	-0.019	-0.019
0.010	0.164	0.167
0.008	0.265	0.270
0.006	0.388	0.396
0.004	0.563	0.574
0.002	0.844	0.862

Figure C－32 The NAL data corrected for the four wall effects.

Run	Scan	M_s	M_c	α_g(deg)	Re	C_{l_u}	C_{l_c}	$C_{d_{wake}}$
7144	1	0.790	0.770	1.73	21.1×10^6	0.622	0.633	0.0151

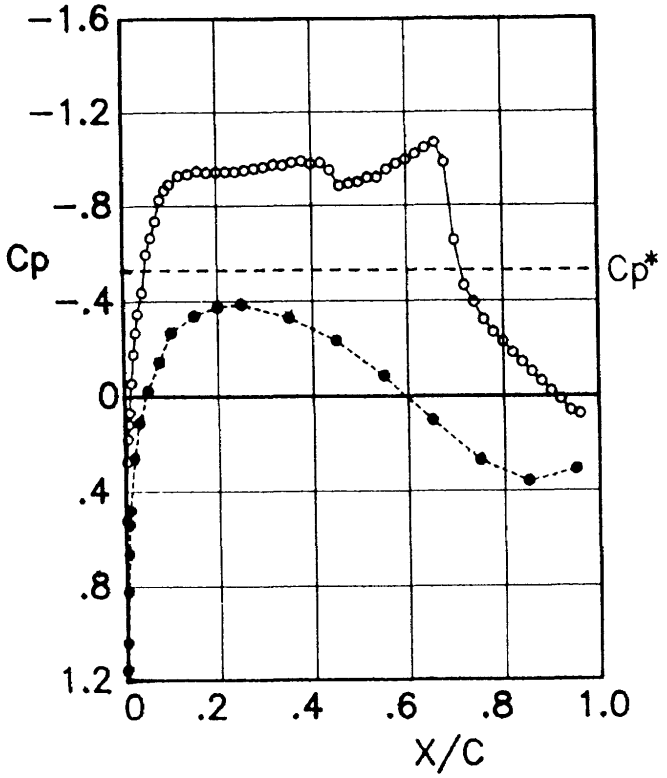

Corrected pressure distribution

Upper surface

x/c	Cp	C_{p_c}
0.000	1.136	1.155
0.002	0.512	0.521
0.004	0.269	0.273
0.006	0.176	0.179
0.008	0.115	0.117
0.010	0.066	0.067
0.015	-0.055	-0.056
0.020	-0.174	-0.177
0.025	-0.263	-0.267
0.030	-0.341	-0.346
0.040	-0.428	-0.436
0.050	-0.585	-0.595
0.060	-0.653	-0.664
0.070	-0.723	-0.735
0.080	-0.811	-0.825
0.090	-0.851	-0.865
0.100	-0.875	-0.890
0.119	-0.911	-0.927
0.140	-0.918	-0.934
0.160	-0.931	-0.947
0.180	-0.924	-0.940
0.200	-0.926	-0.942
0.220	-0.928	-0.944
0.240	-0.928	-0.943
0.260	-0.934	-0.950
0.280	-0.940	-0.957
0.299	-0.946	-0.962
0.320	-0.956	-0.973
0.340	-0.954	-0.970
0.360	-0.966	-0.983
0.380	-0.972	-0.989
0.399	-0.960	-0.976
0.420	-0.964	-0.981
0.439	-0.933	-0.949
0.460	-0.869	-0.884
0.480	-0.877	-0.892
0.500	-0.884	-0.899
0.519	-0.903	-0.918
0.539	-0.903	-0.919
0.560	-0.936	-0.952
0.580	-0.960	-0.976
0.599	-0.978	-0.995
0.619	-1.002	-1.019
0.639	-1.027	-1.044
0.659	-1.049	-1.067
0.679	-0.965	-0.981
0.699	-0.641	-0.652
0.719	-0.454	-0.462
0.739	-0.385	-0.392
0.759	-0.315	-0.320
0.779	-0.262	-0.267
0.799	-0.223	-0.227
0.819	-0.178	-0.181
0.839	-0.138	-0.141
0.859	-0.098	-0.100
0.879	-0.060	-0.061
0.899	-0.019	-0.019
0.919	0.015	0.015
0.939	0.062	0.063
0.960	0.076	0.077

Spanwise
(upper surface, x/c=.9)

y/b	Cp	C_{p_c}
-0.434	-0.050	-0.051
-0.367	-0.025	-0.025
-0.300	-0.019	-0.020
-0.234	-0.011	-0.011
-0.167	-0.019	-0.019
-0.017	-0.019	-0.019
0.166	-0.014	-0.015
0.232	-0.023	-0.024
0.299	-0.018	-0.018
0.366	-0.031	-0.031
0.432	-0.045	-0.046

Lower surface

x/c	Cp	C_{p_c}
0.950	0.306	0.311
0.850	0.354	0.360
0.750	0.268	0.272
0.650	0.101	0.103
0.550	-0.082	-0.084
0.450	-0.228	-0.232
0.350	-0.323	-0.329
0.250	-0.379	-0.386
0.200	-0.368	-0.374
0.150	-0.332	-0.338
0.100	-0.261	-0.266
0.075	-0.140	-0.143
0.050	-0.020	-0.020
0.030	0.113	0.115
0.020	0.258	0.262
0.010	0.474	0.482
0.008	0.532	0.542
0.006	0.652	0.663
0.004	0.808	0.822
0.002	1.022	1.039

Figure C－33 The NAL data corrected for the four wall effects.

Run	Scan	M_s	M_c	α_g(deg)	Re	C_{l_u}	C_{l_c}	$C_{d_{wake}}$
7113	2	0.787	0.770	2.52	21.0×10^6	0.709	0.719	0.0244

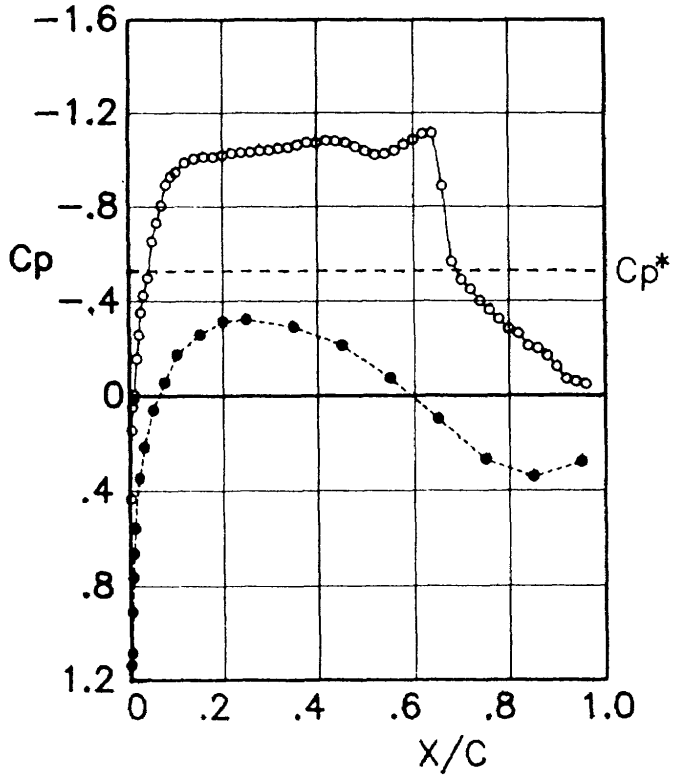

Corrected pressure distribution

Upper surface

x/c	Cp	C_{p_c}
0.000	1.120	1.137
0.002	0.427	0.433
0.004	0.143	0.145
0.006	0.046	0.047
0.008	0.015	0.015
0.010	-0.005	-0.005
0.015	-0.153	-0.156
0.020	-0.253	-0.256
0.025	-0.347	-0.352
0.030	-0.420	-0.426
0.040	-0.491	-0.499
0.050	-0.643	-0.653
0.060	-0.721	-0.732
0.070	-0.793	-0.805
0.080	-0.880	-0.893
0.090	-0.915	-0.928
0.100	-0.932	-0.946
0.119	-0.972	-0.987
0.140	-0.989	-1.004
0.160	-0.997	-1.012
0.180	-0.996	-1.011
0.200	-1.004	-1.019
0.220	-1.012	-1.027
0.240	-1.014	-1.029
0.260	-1.017	-1.032
0.280	-1.023	-1.038
0.299	-1.025	-1.040
0.320	-1.033	-1.048
0.340	-1.036	-1.052
0.360	-1.047	-1.062
0.380	-1.057	-1.073
0.399	-1.056	-1.072
0.420	-1.065	-1.081
0.439	-1.063	-1.079
0.460	-1.057	-1.073
0.480	-1.038	-1.054
0.500	-1.020	-1.035
0.519	-1.004	-1.019
0.539	-1.009	-1.024
0.560	-1.022	-1.038
0.580	-1.049	-1.065
0.599	-1.070	-1.086
0.619	-1.094	-1.111
0.639	-1.098	-1.114
0.659	-0.874	-0.887
0.679	-0.556	-0.565
0.699	-0.481	-0.488
0.719	-0.442	-0.448
0.739	-0.393	-0.399
0.759	-0.354	-0.360
0.779	-0.317	-0.322
0.799	-0.276	-0.280
0.819	-0.256	-0.259
0.839	-0.204	-0.207
0.859	-0.194	-0.197
0.879	-0.163	-0.165
0.899	-0.117	-0.119
0.919	-0.067	-0.068
0.939	-0.056	-0.057
0.960	-0.046	-0.046

Spanwise
(upper surface, x/c=.9)

y/b	Cp	C_{p_c}
-0.434	-0.067	-0.068
-0.367	-0.078	-0.079
-0.300	-0.089	-0.091
-0.234	-0.072	-0.073
-0.167	-0.116	-0.118
-0.017	-0.117	-0.119
0.166	-0.126	-0.128
0.232	-0.143	-0.145
0.299	-0.100	-0.101
0.366	-0.092	-0.093
0.432	-0.097	-0.098

Lower surface

x/c	Cp	C_{p_c}
0.950	0.276	0.280
0.850	0.337	0.343
0.750	0.265	0.269
0.650	0.098	0.099
0.550	-0.073	-0.074
0.450	-0.208	-0.211
0.350	-0.287	-0.291
0.250	-0.317	-0.322
0.200	-0.308	-0.313
0.150	-0.252	-0.256
0.100	-0.171	-0.173
0.075	-0.055	-0.056
0.050	0.060	0.061
0.030	0.215	0.218
0.020	0.344	0.349
0.010	0.550	0.558
0.008	0.654	0.664
0.006	0.752	0.763
0.004	0.896	0.909
0.002	1.068	1.084

Figure C－34 The NAL data corrected for the four wall effects.

Run	Scan	M_s	M_c	α_g(deg)	Re	C_{l_u}	C_{l_c}	$C_{d_{wake}}$
7364	2	0.786	0.770	2.91	21.2×10^6	0.755	0.766	0.0312

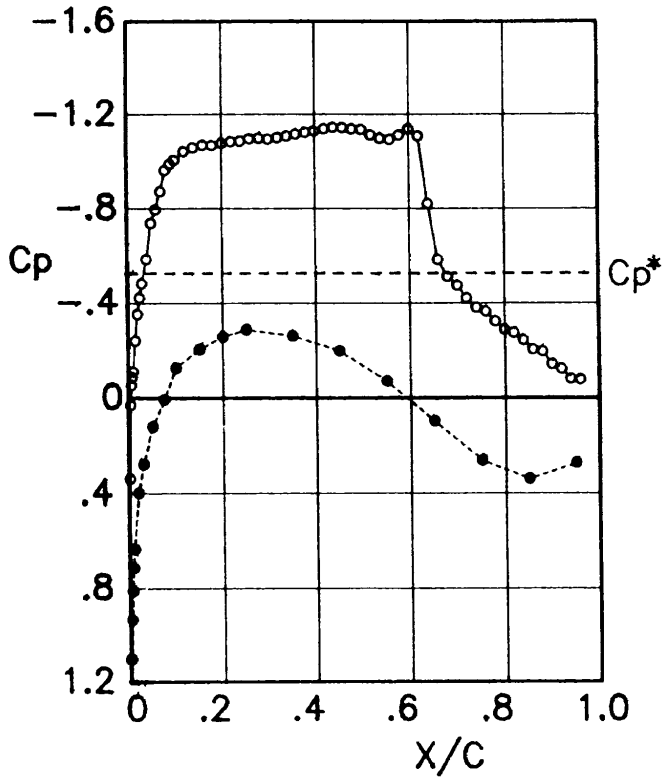

Corrected pressure distribution

Upper surface

x/c	C_p	C_{p_c}
0.000	1.087	1.103
0.002	0.333	0.338
0.004	0.029	0.029
0.006	-0.054	-0.055
0.008	-0.087	-0.088
0.010	-0.111	-0.113
0.015	-0.239	-0.242
0.020	-0.349	-0.354
0.025	-0.418	-0.424
0.030	-0.478	-0.485
0.040	-0.579	-0.587
0.050	-0.728	-0.738
0.060	-0.785	-0.796
0.070	-0.861	-0.873
0.080	-0.949	-0.962
0.090	-0.974	-0.988
0.100	-0.991	-1.005
0.119	-1.028	-1.042
0.140	-1.044	-1.058
0.160	-1.054	-1.069
0.180	-1.053	-1.068
0.200	-1.062	-1.077
0.220	-1.069	-1.084
0.240	-1.071	-1.086
0.260	-1.080	-1.096
0.280	-1.083	-1.098
0.299	-1.079	-1.095
0.320	-1.085	-1.100
0.340	-1.092	-1.107
0.360	-1.100	-1.116
0.380	-1.107	-1.123
0.399	-1.112	-1.128
0.420	-1.122	-1.138
0.439	-1.128	-1.144
0.460	-1.127	-1.143
0.480	-1.121	-1.137
0.500	-1.120	-1.136
0.519	-1.096	-1.112
0.539	-1.082	-1.098
0.560	-1.078	-1.093
0.580	-1.096	-1.112
0.599	-1.122	-1.138
0.619	-1.093	-1.108
0.639	-0.809	-0.820
0.659	-0.575	-0.584
0.679	-0.505	-0.512
0.699	-0.468	-0.474
0.719	-0.415	-0.421
0.739	-0.375	-0.380
0.759	-0.359	-0.364
0.779	-0.318	-0.322
0.799	-0.284	-0.288
0.819	-0.270	-0.274
0.839	-0.239	-0.242
0.859	-0.200	-0.203
0.879	-0.192	-0.195
0.899	-0.139	-0.141
0.919	-0.120	-0.122
0.939	-0.079	-0.080
0.960	-0.076	-0.077

Spanwise
(upper surface, x/c=.9)

y/b	C_p	C_{p_c}
-0.434	-0.084	-0.085
-0.367	-0.100	-0.102
-0.300	-0.120	-0.121
-0.234	-0.118	-0.119
-0.167	-0.101	-0.102
-0.017	-0.139	-0.141
0.166	-0.165	-0.167
0.232	-0.162	-0.164
0.299	-0.174	-0.177
0.366	-0.142	-0.144
0.432	-0.094	-0.096

Lower surface

x/c	C_p	C_{p_c}
0.950	0.270	0.274
0.850	0.335	0.340
0.750	0.259	0.263
0.650	0.096	0.098
0.550	-0.070	-0.071
0.450	-0.196	-0.199
0.350	-0.259	-0.263
0.250	-0.285	-0.289
0.200	-0.255	-0.258
0.150	-0.202	-0.205
0.100	-0.125	-0.127
0.075	0.008	0.008
0.050	0.120	0.121
0.030	0.276	0.279
0.020	0.393	0.399
0.010	0.624	0.633
0.008	0.703	0.713
0.006	0.798	0.810
0.004	0.921	0.934
0.002	1.087	1.102

Figure C－35 The NAL data corrected for the four wall effects.

Run	Scan	M_s	M_c	α_g(deg)	Re	C_{l_u}	C_{l_c}	$C_{d_{wake}}$
7363	2	0.786	0.772	4.42	21.2×10^6	0.766	0.776	0.0672

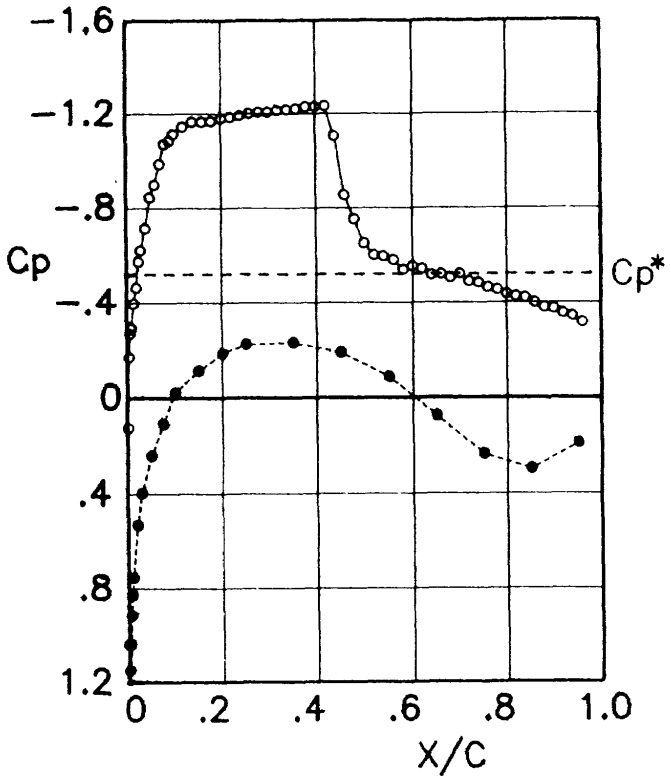

Corrected pressure distribution

Upper surface

x/c	Cp	C_{p_c}
0.000	1.024	1.037
0.002	0.122	0.123
0.004	-0.170	-0.172
0.006	-0.267	-0.270
0.008	-0.288	-0.292
0.010	-0.291	-0.295
0.015	-0.393	-0.398
0.020	-0.459	-0.465
0.025	-0.568	-0.575
0.030	-0.616	-0.623
0.040	-0.706	-0.715
0.050	-0.836	-0.846
0.060	-0.888	-0.899
0.070	-0.975	-0.987
0.080	-1.059	-1.072
0.090	-1.072	-1.085
0.100	-1.101	-1.114
0.119	-1.131	-1.145
0.140	-1.151	-1.165
0.160	-1.152	-1.166
0.180	-1.154	-1.168
0.200	-1.165	-1.179
0.220	-1.170	-1.185
0.240	-1.178	-1.192
0.260	-1.187	-1.201
0.280	-1.192	-1.206
0.299	-1.192	-1.206
0.320	-1.199	-1.213
0.340	-1.203	-1.217
0.360	-1.206	-1.221
0.380	-1.214	-1.229
0.399	-1.216	-1.230
0.420	-1.219	-1.233
0.439	-1.093	-1.106
0.460	-0.844	-0.855
0.480	-0.744	-0.753
0.500	-0.643	-0.651
0.519	-0.594	-0.601
0.539	-0.588	-0.595
0.560	-0.573	-0.580
0.580	-0.531	-0.538
0.599	-0.546	-0.553
0.619	-0.536	-0.542
0.639	-0.509	-0.516
0.659	-0.513	-0.519
0.679	-0.498	-0.504
0.699	-0.514	-0.521
0.719	-0.482	-0.488
0.739	-0.477	-0.483
0.759	-0.457	-0.462
0.779	-0.448	-0.453
0.799	-0.430	-0.435
0.819	-0.420	-0.425
0.839	-0.415	-0.420
0.859	-0.394	-0.398
0.879	-0.374	-0.378
0.899	-0.368	-0.373
0.919	-0.349	-0.353
0.939	-0.338	-0.342
0.960	-0.311	-0.314

Spanwise
(upper surface, x/c=.9)

y/b	Cp	C_{p_c}
-0.434	-0.195	-0.197
-0.367	-0.250	-0.253
-0.300	-0.278	-0.282
-0.234	-0.324	-0.328
-0.167	-0.379	-0.383
-0.017	-0.368	-0.373
0.166	-0.371	-0.376
0.232	-0.336	-0.340
0.299	-0.291	-0.295
0.366	-0.248	-0.251
0.432	-0.186	-0.188

Lower surface

x/c	Cp	C_{p_c}
0.950	0.188	0.190
0.850	0.293	0.297
0.750	0.233	0.236
0.650	0.076	0.077
0.550	-0.086	-0.087
0.450	-0.188	-0.190
0.350	-0.227	-0.230
0.250	-0.221	-0.223
0.200	-0.183	-0.185
0.150	-0.112	-0.113
0.100	-0.022	-0.023
0.075	0.108	0.109
0.050	0.238	0.240
0.030	0.393	0.398
0.020	0.526	0.532
0.010	0.744	0.753
0.008	0.819	0.829
0.006	0.902	0.913
0.004	1.025	1.037
0.002	1.134	1.147

Figure C－36 The NAL data corrected for the four wall effects.

Run	Scan	M_s	M_c	α_g(deg)	Re	C_{l_u}	C_{l_c}	$C_{d_{wake}}$
7137	2	0.762	0.742	1.81	15.3×10^6	0.595	0.606	0.0088

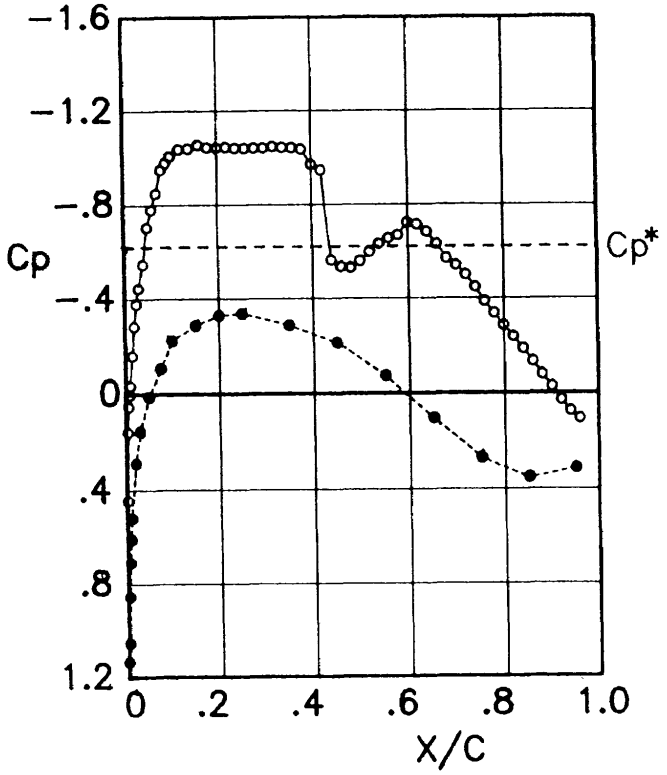

Corrected pressure distribution

Upper surface

x/c	Cp	C_{p_c}
0.000	1.115	1.135
0.002	0.436	0.443
0.004	0.155	0.158
0.006	0.051	0.052
0.008	0.004	0.004
0.010	-0.034	-0.035
0.015	-0.156	-0.159
0.020	-0.279	-0.284
0.025	-0.372	-0.379
0.030	-0.438	-0.446
0.040	-0.538	-0.547
0.050	-0.693	-0.706
0.060	-0.767	-0.780
0.070	-0.835	-0.850
0.080	-0.933	-0.950
0.090	-0.962	-0.979
0.100	-0.990	-1.008
0.119	-1.019	-1.037
0.140	-1.021	-1.039
0.160	-1.037	-1.056
0.180	-1.026	-1.044
0.200	-1.025	-1.043
0.220	-1.027	-1.045
0.240	-1.023	-1.041
0.260	-1.023	-1.041
0.280	-1.023	-1.041
0.299	-1.023	-1.042
0.320	-1.029	-1.047
0.340	-1.025	-1.043
0.360	-1.024	-1.042
0.380	-1.018	-1.036
0.399	-0.954	-0.971
0.420	-0.930	-0.946
0.439	-0.552	-0.562
0.460	-0.525	-0.534
0.480	-0.521	-0.530
0.500	-0.548	-0.558
0.519	-0.586	-0.597
0.539	-0.620	-0.631
0.560	-0.644	-0.655
0.580	-0.657	-0.668
0.599	-0.710	-0.723
0.619	-0.702	-0.715
0.639	-0.671	-0.683
0.659	-0.619	-0.630
0.679	-0.560	-0.570
0.699	-0.531	-0.540
0.719	-0.491	-0.499
0.739	-0.439	-0.447
0.759	-0.379	-0.386
0.779	-0.329	-0.335
0.799	-0.278	-0.283
0.819	-0.231	-0.235
0.839	-0.180	-0.184
0.859	-0.127	-0.130
0.879	-0.074	-0.075
0.899	-0.024	-0.025
0.919	0.031	0.031
0.939	0.076	0.077
0.960	0.107	0.109

Spanwise
(upper surface, x/c=.9)

y/b	Cp	C_{p_c}
-0.434	-0.045	-0.046
-0.367	-0.031	-0.032
-0.300	-0.028	-0.029
-0.234	-0.022	-0.022
-0.167	-0.021	-0.021
-0.017	-0.024	-0.025
0.166	-0.026	-0.027
0.232	-0.036	-0.036
0.299	-0.036	-0.037
0.366	-0.042	-0.042
0.432	-0.055	-0.056

Lower surface

x/c	Cp	C_{p_c}
0.950	0.308	0.313
0.850	0.346	0.352
0.750	0.265	0.270
0.650	0.103	0.105
0.550	-0.071	-0.072
0.450	-0.207	-0.211
0.350	-0.282	-0.287
0.250	-0.331	-0.337
0.200	-0.323	-0.329
0.150	-0.281	-0.286
0.100	-0.218	-0.222
0.075	-0.103	-0.104
0.050	0.013	0.013
0.030	0.154	0.157
0.020	0.284	0.289
0.010	0.511	0.520
0.008	0.599	0.610
0.006	0.696	0.709
0.004	0.839	0.854
0.002	1.036	1.054

Figure C－37 The NAL data corrected for the four wall effects.

Run	Scan	M_s	M_c	α_g(deg)	Re	C_{l_u}	C_{l_c}	$C_{d_{wake}}$
7141	1	0.760	0.740	1.75	30.0×10^6	0.577	0.587	0.0081

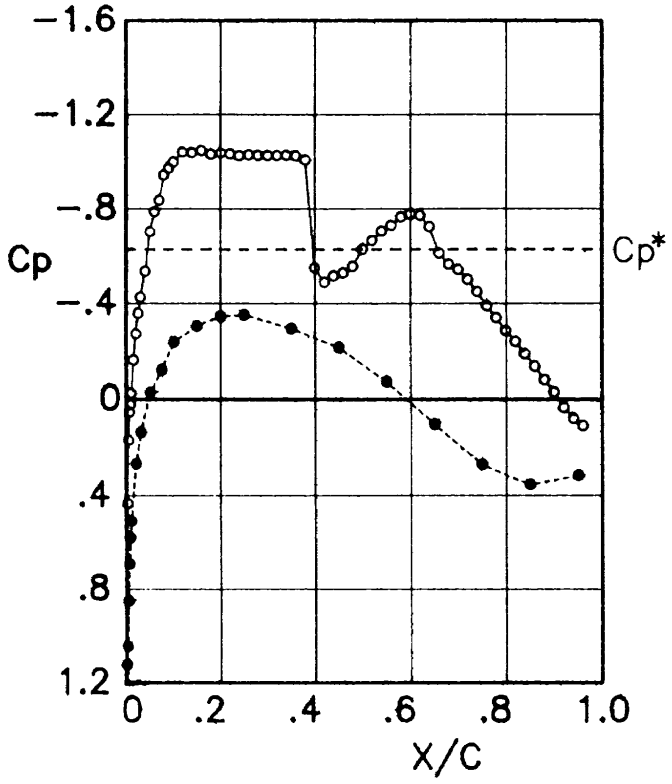

Corrected pressure distribution

Upper surface

x/c	C_p	C_{p_c}
0.000	1.103	1.123
0.002	0.425	0.433
0.004	0.165	0.168
0.006	0.052	0.052
0.008	0.021	0.021
0.010	-0.027	-0.028
0.015	-0.161	-0.164
0.020	-0.269	-0.274
0.025	-0.353	-0.359
0.030	-0.420	-0.428
0.040	-0.527	-0.537
0.050	-0.692	-0.704
0.060	-0.775	-0.789
0.070	-0.822	-0.837
0.080	-0.928	-0.945
0.090	-0.956	-0.973
0.100	-0.981	-0.999
0.119	-1.023	-1.041
0.140	-1.020	-1.038
0.160	-1.029	-1.047
0.180	-1.013	-1.031
0.200	-1.018	-1.037
0.220	-1.015	-1.033
0.240	-1.008	-1.026
0.260	-1.011	-1.029
0.280	-1.008	-1.026
0.299	-1.008	-1.026
0.320	-1.008	-1.026
0.340	-1.009	-1.027
0.360	-1.007	-1.025
0.380	-0.990	-1.007
0.399	-0.540	-0.549
0.420	-0.481	-0.489
0.439	-0.507	-0.516
0.460	-0.519	-0.529
0.480	-0.546	-0.556
0.500	-0.617	-0.628
0.519	-0.654	-0.665
0.539	-0.693	-0.705
0.560	-0.716	-0.729
0.580	-0.752	-0.765
0.599	-0.763	-0.777
0.619	-0.758	-0.772
0.639	-0.712	-0.724
0.659	-0.601	-0.612
0.679	-0.555	-0.565
0.699	-0.533	-0.542
0.719	-0.492	-0.501
0.739	-0.442	-0.449
0.759	-0.382	-0.389
0.779	-0.333	-0.339
0.799	-0.280	-0.285
0.819	-0.236	-0.240
0.839	-0.184	-0.187
0.859	-0.134	-0.136
0.879	-0.079	-0.081
0.899	-0.029	-0.030
0.919	0.036	0.036
0.939	0.080	0.082
0.960	0.110	0.112

Spanwise
(upper surface, x/c=.9)

y/b	C_p	C_{p_c}
-0.434	-0.038	-0.038
-0.367	-0.035	-0.036
-0.300	-0.029	-0.030
-0.234	-0.022	-0.023
-0.167	-0.018	-0.019
-0.017	-0.029	-0.030
0.166	-0.027	-0.027
0.232	-0.031	-0.032
0.299	-0.034	-0.035
0.366	-0.044	-0.045
0.432	-0.060	-0.061

Lower surface

x/c	C_p	C_{p_c}
0.950	0.310	0.316
0.850	0.349	0.355
0.750	0.266	0.271
0.650	0.102	0.104
0.550	-0.072	-0.073
0.450	-0.213	-0.217
0.350	-0.291	-0.296
0.250	-0.347	-0.353
0.200	-0.341	-0.347
0.150	-0.301	-0.306
0.100	-0.234	-0.238
0.075	-0.121	-0.123
0.050	-0.028	-0.029
0.030	0.135	0.137
0.020	0.263	0.268
0.010	0.499	0.508
0.008	0.568	0.578
0.006	0.678	0.690
0.004	0.835	0.850
0.002	1.025	1.044

Figure C－38 The NAL data corrected for the four wall effects.

TECHNICAL REPORT OF NATIONAL
AEROSPACE LABORATORY
TR-1191T

航空宇宙技術研究所報告1191T号(欧文)

平成5年1月発行

発行所 航空宇宙技術研究所
東京都調布市深大寺東町7丁目44番地1
電話三鷹(0422)47-5911(大代表)〒182
印刷所 株式会社 三興印刷
東京都新宿区西早稲田2-1-18

Published by
NATIONAL AEROSPACE LABORATORY
7-44-1 Jindaijihigashi-Machi, Chōfu, Tokyo
JAPAN